Analysis of the effects of amyloid-β on astrocytes

Rodrigo Esteban González-Reyes

A thesis submitted to

Trinity College Dublin

For the degree of

Doctor in Philosophy

Supervisor: Professor Marina Lynch

Trinity College Institute of Neuroscience

Department of Physiology

TCD
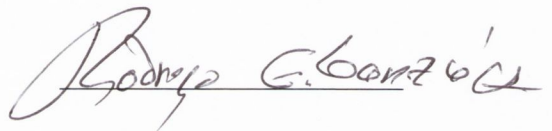
2011

Thesis 9769

Declaration of Authorship

This thesis is the sole work of the author and has not been submitted in whole or in part to this or any other university for any other degree. I agree to deposit this thesis in the University's open access institutional repository or allow the library to do so on my behalf, subject to Irish Copyright Legislation and Trinity College Library conditions of use and acknowledgement. The author gives permission for the library to lend or copy this work upon request.

Rodrigo E. González Reyes

Abstract

Alzheimer's disease (AD) is a neurodegenerative pathology characterized by the presence of extracellular plaques composed of amyloid-β (Aβ) protein and intracellular neurofibrillary tangles composed of tau protein. Aβ, in particular $A\beta_{1-42}$, has been shown to be neurotoxic and to induce functional and morphological changes in astrocytes and microglia. Despite the extensive research in AD, the precise cellular and molecular alterations associated with the development of the disease are unknown. The aims of this study were to determine, *in vivo*, the effects chronic intracerebroventricular (icv) treatment with Aβ has in the brains of aged and young Wistar rats and to explore age-related changes, and, *in vitro*, to examine the effects Aβ treatment has on cytokine production and release and to investigate the signalling pathways and membrane receptors involved in this process, in rat isolated astrocytes.

The data showed that icv treatment with Aβ induced the appearance of immunoreactive structures accompanied by an increase in the astrocytic marker GFAP, and a decrease in the microglial marker CD11b in the brains of aged, but not young rats; no changes were observed in other markers of microglial activation, spatial learning or in pro-inflammatory cytokines. The data obtained *in vitro* showed that Aβ induced a time-related increase in pro-inflammatory cytokines paralleled with IκBα phosphorylation, which indicates activation of NFκB signalling pathway and this process was mediated by RAGE. Incubation of astrocytes with anti-CD36 or anti-CD47 antibodies induced a pro-inflammatory response and augmented the Aβ-induced increase in pro-inflammatory cytokines.

The results obtained in this study provide further evidence of the association between astrocytes and Aβ. Astrocytic interaction with Aβ induces the activation of diverse signalling cascades but the pathophysiological meaning of these responses remains unknown. However, glial cells may also offer protective effects and a greater understanding of their function may identify potential therapeutic targets in the future.

Acknowledgements

List of Abbreviations

The following abbreviations have been used:

5-HT	5-hydroxytryptamine (serotonin)
α1-ACT	α1-antichymotripsin
α7nAChR	α7 nicotinic acetylcholine receptor
Aβ	Amyloid-beta
ABCA7	ATP-binding cassette, sub-family A, member 7
AD	Alzheimer's disease
ACT	α-1-antichymotrypsin
ACTH	Adrenocorticotropic hormone
AGE	Advanced glycation end products
AICD	Amyloid intracellular domain
Aldh1L1	Aldehyde dehydrogenase 1 family, member L1
AMPA	α-amino-3-hydroxy-5-methylisoxazole-4-propionic acid
ANOVA	Analysis of variance
AP-1	Activator protein 1
Aph-1	Anterior pharynx defective 1
ApoE	Apolipoprotein E
ApoE4	Apolipoprotein E 4
ApoJ	Apolipoprotein J
APP	Amyloid precursor protein
APS	Ammonium persulfate
ATF2	Activating transcription factor 2
ATP	Adenosine triphosphate
BACE-1	β-secretase beta-site amyloid precursor protein-cleaving enzyme 1
BBB	Blood brain barrier
BCA	Bicinchoninic acid
BDNF	Brain-derived neurotrophic factor
BIN1	Bridging integrator 1
BSA	Bovine serum albumin
C1q	Complement component 1q
CA1	Cornu ammonis 1
cAMP	Cyclic adenosine monophosphate
CCR2	CC Chemokine receptor 2
CCR3	CC Chemokine receptor 3
CCR5	CC Chemokine receptor 5
CD11b	Cluster of differentiation molecule 11b (also ITGAM)
CD14	Cluster of differentiation 14
CD2AP	CD2-associated protein
CD33	Cluster of differentiation 33
CD36	Cluster of differentiation 36
CD40	Cluster of differentiation 40
CD40L	Cluster of differentiation 40 Ligand

CD47	Cluster of differentiation 47
CD68	Cluster of differentiation 68
cDNA	Complementary deoxyribonucleic acid
cGMP	Cyclic guanosine monophosphate
ClC-7	Chloride channel 7
CLU	Clusterin
CNS	Central nervous system
COX-2	Ciclooxigenase 2
CR1	Complement receptor gene 1
CREB	cAMP-responsive element binding protein
CSF	Cerebrospinal fluid
CTF83	Carboxy-terminal fragment
CXCR2	CXC Chemokine receptor 2 (also Interleukin 8 receptor beta)
CXCR3	CXC Chemokine receptor 3 (also CD183)
DAPI	4,6-diamidino-2-phenylindole
dH$_2$O	Distilled water
D-JNKi1	c-Jun N-terminal kinase peptide inhibitor 1, D-stereoisomer
DMEM	Dulbecco's modified eagle medium
DMSO	Dimethyl sulphoxide
DNA	Deoxyribonucleic Acid
dNTP's	Deoxynucleotide triphosphates
DPX	Dinbutyl phthalate in xylene
EAAT2	Excitatory amino acid transporter 2
EAE	Experimental autoimmune encephalomyelitis
EDTA	Ethylenediaminetetraacetic acid solution
ELISA	Enzyme linked immunosorbent assay
EPHA1	Ephrin receptor A1
epsp	Excitatory postsynaptic potential
ERK	Extracellular signal regulated kinase
esRAGE	Endogenous secretory RAGE
FBS	Fetal bovine serum
FDA	Food and drug administration
FDH	10-formyltetrahydrofolate dehydrogenase
FITC	Fluorescein isothiocyanate
g	grams
GC	Guanylate cyclase
GFAP	Glial fibrillary acidic protein
GLAST	Glutamate-aspartate transporter
GLT-1	Glutamate transporter 1
GSK-3	Glycogen synthase kinase-3
GSK-3β	Glycogen synthase kinase-3β
HEPES	4-(2-Hydroxyethyl)piperazine-1-ethanesulfonic acid
HIV	Human immunodeficiency virus
HMGB1	High-mobility group box chromosomal protein 1
HRP	Horseradish peroxidase
HSD	Honestly significant difference

i.p.	Intraperitoneal
IAP	Integrin associated protein
Iba1	Ionized calcium binding adaptor molecule 1
icv	Intracerebroventricular
IDE	insulin degrading enzyme
IgE	Immunoglobulin E
IgG	Immunoglobulin G
IGEPAL	α-[(1,1,3,3-Tetramethylbutyl)phenyl]-ω-hydroxy-poly(oxy-1,2-ethanediyl) (also NP-40)
IκBα	Nuclear factor of kappa light polypeptide gene enhancer in B-cells inhibitor, alpha
IKK	I-kappa-B-kinase
IL-1β	Interleukin 1-beta
IL-1R1	Interleukin 1 receptor type I
IL-1R2	Interleukin 1 receptor type II
IL-1Ra	Interleukin 1 receptor antagonist
IL-6	Interleukin 6
IL-6R	Interleukin 6 receptor
INF-γ	Interferon-gamma
iNOS	Inducible nitric oxide synthase
IP-10	Interferon inducible protein 10 (also CXCL10)
IRAK1	IL-1 receptor-associated serine/threonine kinase 1
JAK	Janus kinase
JNK	c-Jun N-terminal kinase
JPEG	Joint photographic experts group
kDa	KiloDalton
KO	Knock out
LDL	Low-density lipoprotein
LDLR	Low-density lipoprotein receptor
LPS	Lipopolysaccharide
LRP	Low-density lipoprotein receptor-related protein
LTD	Long term depression
LTP	Long term potentiation
MALT1	Mucosa-associated lymphoid tissue lymphoma translocation protein 1
MAPK	Mitogen-activated protein kinase
MAVS	Mitochondrial antiviral signaling protein
MCI	Mild cognitive impairment
MCP-1	Monocyte chemoattractant protein 1
MCSF	Macrophage colony-stimulating factor
MEF2C	Myocyte enhancer factor 2C
MEK	Mitogen activated protein kinase kinase
MHC II	Major histocompatibility complex class II (also OX6)
min	minutes
MRI	Magnetic resonance imaging
mRNA	Messenger ribonucleic acid

MS4A	Membrane spanning 4A
MS	Multiple sclerosis
MTS	(3-(4,5-dimethylthiazol-2-yl)-5-(3-carboxymethoxyphenyl)-2-(4-sulfophenyl)-2H-tetrazolium)
NCAM	Neural cell adhesion molecule
NEMO	NFκB essential modulator
NFAT1	Nuclear factor of activated T-cells 1
NF-κB	Nuclear factor kappa-light-chain-enhancer of activated B cells
NG2	Neuron-glial antigen 2
Nct	Nicastrin
NICD	Notch intracellular domain
NMDA	N-methyl-D-aspartate
NR2B	NMDA receptor 2B
O.C.T.	Optimal cutting temperature
P2X$_7$	Purinergic receptor P2 subtype X7
p-Akt	Phosphorylated form of Akt
PBS	Phosphate buffered saline
p-c-Jun	Phosphorylated form of c-Jun
PDTC	Pyrrolidine dithiocarbamate
Pen2	Presenilin enhancer 2
PES	Phenazine ethosulphate
PET	Positron emission tomography
PHEM	buffer (PIPES, HEPES, EDTA. MgSO$_4$)
PI3K	Phosphatidylinositol 3-kinase
PIC	Protease inhibitor cocktail
PICALM	Phosphatidylinositol-binding clathrin assembly protein gene
p-IκBα	Phosphorylated form of IκBα
PIPES	Piperazine-1,4-bis(2-ethanesulfonic acid)
p-JNK	Phosphorylated form of JNK
PKG	GC-cGMP- activated protein kinase
PMSF	Phenylmethylsulfonyl fluoride
PSA-NCAM	Polysialylated form of NCAM
PSB-TCEP	Protein solving buffer-BisTris(Bis-(2-hydroxyethyl)-imino-tris(hydroxymethyl)-methane)
PSEN1	Presenilin 1
PSEN2	Presenilin 2
Q-PCR	Quantitative-polymerase chain reaction
RAGE	Receptor for advanced glycation end products
RANTES	Regulated upon activation, normal T-cell expressed, and secreted (also CCL5)
RGB	Red green blue
RHD	Rel homology domain
RIP	Receptor interacting protein
RNA	Ribonucleic acid
RNAse	Ribonuclease
ROS	Reactive oxygen species

rpm	revolutions per minute
RT-PCR	Real time PCR
s	seconds
S100β	S100 calcium binding protein B
sAPPα	Soluble fragment of amyloid precursor protein (also secreted amyloid precursor protein alpha)
SAPK	Stress-activated protein kinase
SD	Standard deviation
SDS	Sodium dodecyl sulfate (also sodium lauryl sulphate)
SEM	Standard error of the mean
SHP	Src-homology-2-domain-containing protein tyrosine phosphatase
SIRPα	Signal-regulatory protein alpha
SOCS	Suppressor of cytokine signalling
SORL1	Sortilin-related receptor 1
SPF	Specific-pathogen free
SRA	Scavenger receptor class A
SRB1	Scavenger receptor class B 1
SR-MARCO	Scavenger receptor class A - macrophage receptor with collagenous structure
STAT	Signal transducer and activator of transcription
Strep-HP	Horseradish peroxidase-conjugated streptavidin
T1	Time 1
T2	Time 2
TACE	TNFα converting enzyme (also referred to as ADAM17)
Taq	*Thermus aquaticus*
TBS	Tris-buffered saline
TBS-T	Tris-buffered saline with 0.05% Tween-20
TEMED	Tetramethylethylenediamine
Th	T helper cell
THF	Tetrahydrofolate
TLR2	Toll-like receptor 2
TLR3	Toll-like receptor 3
TLR4	Toll-like receptor 4
TLR9	Toll-like receptor 9
TMB	Tetramethylbenzidine
TNFα	Tumor necrosis factor-alpha
TRAF	TNF receptor-associated factor
Tris	Tris(hydroxymethyl)aminomethane
TSP-1	Thrombospondin-1
TWB	Tris wash buffer
UK	United Kingdom
US	United States of America
UV	Ultra violet

Table of Contents

List of Figures

List of Tables

Chapter 1: Introduction

1.1. Overview

Alzheimer's disease (AD) is the most frequent type of dementia in humans and one of the most devastating pathologies affecting the central nervous system (CNS). The prevalence of AD increases as the population ages and represents around two-thirds of all the cases of progressive cognitive impairment in adults. AD is clinically characterized by deterioration in memory and cognition and reduced ability to cope with daily living activities (Cummings, 2004). Brains of individuals affected by AD are characterized by two specific types of pathological changes, the presence of extracellular plaques laden with amyloid-β (Aβ) peptide and intracellular neurofibrillary tangles mainly composed of aggregated and hyperphosphorylated tau, a cytoskeletal protein. Currently, there is no treatment available to cure or stop the progression of the disease. Although many advances have increased our understanding of the cause and risk factors associated with AD, the mechanisms that lead to the pathological changes, the selective pattern of neurodegeneration and the precise cellular and molecular alterations associated with the development of the disease are unknown.

1.2. Alzheimer's Disease

Alois Alzheimer, in 1907, was the first to provide a clinical description of AD when he was studying the case of Auguste D., a 51 year old woman who had suffered from progressive dementia (Alzheimer et al., 1995). AD was originally named presenile dementia but this was changed to AD in 1910 because Emil Kraepelin wanted to honour Alzheimer for his description of the pathology (Small and Cappai, 2006). Although the description of AD is just about a century old, historical documentation about dementia have been found in ancient Egypt, Greece and Rome (Boller and Forbes, 1998).

It is estimated that 35.6 million people around the world suffer from AD with prevalence for individuals aged 60 years or more ranging worldwide from 1.2% of western sub-Saharan Africa to 7.2% of western Europe (Wimo and Prince, 2010). The median annual incidence of AD in US was calculated at 1275 per 100,000 at 65 years of age and this doubles every 5 years after 65 years of age (Hirtz et al., 2007). AD has no sex preference

similarly affecting both women and men as opposed to vascular dementia which has a higher incidence in men (Ruitenberg et al., 2001). A higher educational level is associated with decreased risk of both AD and non-AD dementia and it has been calculated that for each additional year of education over 11 years, the relative risk for AD decreases by approximately 9% (Kukull et al., 2002). AD diagnosed at 65 years of age is associated with a mean survival time of 8.3 years implying a 67% reduction in the prospective life expectancy (Brookmeyer et al., 2002). The total cost of dementia worldwide has been calculated in US$ 604 billion, representing approximately 1% of the total world gross domestic product, including direct (medical and social care) as well as indirect (family and caregivers) costs (Wimo and Prince, 2010).

1.2.1. *AD pathophysiology*

The brains of individuals with AD are characterized by the presence of cortical atrophy, affecting principally the frontal, temporal and parietal lobes, with compensatory ventricular enlargement and subsequent reduced brain volume (Stark et al., 2005). Extracellular neuritic plaques containing Aβ protein and intracellular neurofibrillary tangles composed of tau protein represent the principal histological findings of AD. Progressive loss of synapses and neurons accompanied by reactive gliosis and inflammation follow the appearance of Aβ plaques and neurofibrillary tangles (Duyckaerts et al., 2009, Thompson et al., 2003).

Sporadic cases of AD explain around 90-95% of the total cases while genetics account for the remaining 5-10% (Zawia et al., 2009). Mutations of the genes encoding for amyloid precursor protein (APP), presenilin 1 (PSEN1), presenilin 2 (PSEN2) and sortilin-related receptor 1 (SORL1) are implicated in the development of AD; noteworthy, all these genes are involved in production, clearance or uptake of Aβ (Ballard et al., 2011). AD is a human-specific disorder which means all animal models have to be induced mainly by genetic modification or through Aβ injection. Mice carrying the human APP gene mutation were the first transgenic animal model for AD (Wirak et al., 1991). Now more than 18 different transgenic mouse models, as well as

several non-transgenic models in different species, have been developed for the study of AD (Philipson et al., 2010).

To date, 10 loci identified through genome-wide association studies have been found to increase the risk to develop AD. These include: clusterin (CLU), complement receptor gene 1 (CR1), encoding ATP-binding cassette, sub-family A, member 7 (ABCA7), cluster of differentiation 33 (CD33) and encoding ephrin receptor A1 (EPHA1) which have immune functions; phosphatidylinositol-binding clathrin assembly protein gene (PICALM), bridging integrator 1 gene (BIN1), CD33 and CD2-associated protein (CD2AP) which are involved in cell membrane processes; apolipoprotein E (ApoE), CLU and ABCA7 which are involved in lipid processing; and encoding membrane spanning 4A (MS4A) which is a member of a family of cell-surface proteins with high affinity for IgE receptors (Hollingworth et al., 2011). The presence of a single ε4 ApoE allele increases the risk factor of developing AD by 4 and if the two ε4 alleles are present, the risk increases by a factor of 19 (Strittmatter and Roses, 1996).

The precise cause of the pathological changes observed in AD is not known but among the many theories proposed to explain the disease is the amyloid cascade hypothesis which has been the most studied. The amyloid cascade hypothesis suggests that APP is processed into Aβ which accumulates intracellularly and extracellularly in amyloid plaques, forming toxic aggregates that cause neuronal dysfunction, and changes in tau resulting in formation of neurofibrillary tangles and eventually cell death (Ballard et al., 2011). Synaptic failure and disproportionate loss of synapses relative to neurons is observed in individuals with AD and correlates with cognitive decline (Querfurth and LaFerla, 2010). Disruption in the expression of N-methyl-D-aspartate (NMDA) (Snyder et al., 2005) and α-amino-3-hydroxy-5-methylisoxazole-4-propionic acid (AMPA) receptors (Hsieh et al., 2006), as well as reduced levels of brain-derived neurotrophic factor (BDNF) (Garzon and Fahnestock, 2007) and a decreased number of cholinergic projections has also been described in AD (Wang et al., 2000). Mitochondria have been proposed to play a role in the pathophysiology of AD. Aβ has been observed to enter mitochondria and proteins from the PSEN complex were found in this organelle (Coskun et al., 2011). Described Aβ effects on mitochondria include an increase in membrane viscosity, a decrease in ATP/O ratio, reduction in the activity of electron transport chain,

4

increased reactive oxygen species (ROS) production and augmented cytochrome c release; these changes are considered to provide support for the proposal that mitochondrial dysfunction plays a role in the pathophysiology of AD (Aleardi et al., 2005). Glucose levels and alterations in components of the insulin-induced signalling pathway are reported to be altered in AD (Messier and Teutenberg, 2005).

1.2.2. *AD clinical presentation*

AD is the most common type of dementia accounting for up to 80% of all cases (Abbott, 2011). The most frequent symptoms patients with AD manifest are impaired memory, depression, poor judgement and confusion but several behavioural symptoms such as agitation, dysphoria, apathy, and aberrant motor behaviour have been correlated with cognitive impairment (Mega et al., 1996). Seizures, gait and severe motor abnormalities usually manifest only at late stages of the disease (Cummings, 2004). The neurodegenerative nature of AD progresses to a point where the patient is unresponsive and unaware of its environment and incontinent. In the final stages of the disease paraplegia in flexion becomes evident with sufferers adopting the foetal position and entering in a persistent vegetative state (Ropper et al., 2005). According to the progression of the disease, AD can be classified as mild, moderate or severe. See Table 1.1. for a summary of clinical symptoms present in AD.

1.2.3. *AD Diagnosis*

Currently, confirmation of AD diagnosis can only be achieved by post-mortem examination of the affected brain revealing the presence of amyloid plaques and neurofibrillary tangles. Differential diagnoses and the lack of a characteristic biomarker make clinical diagnosis of AD a challenge. Patients with mild cognitive impairment (MCI) are considered to be in a prodromic early stages of AD, but not all individuals with MCI progress to AD (Emery, 2011). Recently, the National Institute on Aging-Alzheimer's Association of the US published a revised version of diagnostic guidelines for AD which includes biomarkers (McKhann et al., 2011). Several biomarkers have

been investigated but only the following provided enough evidence to recommend their use in the clinical setting: biomarkers of Aβ accumulation, which include abnormal tracer retention on amyloid positron emission tomography (PET) imaging and low $Aβ_{1-42}$ in cerebrospinal fluid (CSF), and biomarkers of neuronal degeneration or injury, which include elevated tau in CSF, decreased fluorodeoxyglucose uptake on PET in temporoparietal cortex and atrophy on structural magnetic resonance imaging (MRI) involving medial, basal, and lateral temporal lobes and medial and lateral parietal cortices (Jack et al., 2011).

1.2.4. *AD Treatment*

AD is currently an irreversible, non-preventable neurodegenerative condition. Efforts have been made to develop an effective therapeutic solution but, so far, the best medications can offer only a slight delay in the progression of the disease with limited cognitive improvement. The food and drug administration (FDA) of US has approved several drugs to be used in AD. Of these, galantamine, rivastigmine, donepezil and tacrine target mild to moderate AD while only memantine is approved to treat moderate to severe AD. The first 4 are all cholinesterase inhibitors while memantine is an NMDA receptor antagonist. All these medications treat the symptoms rather than the disease. Several new drugs have completed or are being tested in phase III clinical trials with many designed to reduce the production of Aβ, prevent the aggregation or increase the clearance of Aβ, although, anti-inflammatory agents, serotonin agonists, anti-oxidants, $GABA_A$ agonists and inhibitors of the HMG CoA-reductase are also under investigation. So far the results have not been encouraging with 13 out of 16 phase III clinical trials showing no efficacy (Palmer, 2011). Drugs, such as dimebon (latrepirdine), that generated great expectations in phase I and II trials have failed to provide significant evidence of benefit compared to placebo in phase III clinical trials (Doody et al., 2008, Jones, 2010). Other, less conventional, treatment options still in experimental phases include vaccination with amyloid species, administration of monoclonal anti-amyloid antibodies or intravenous immunoglobulins, vitamin E therapy, oestrogen therapy or delivery of neurotrophic factors (Foster et al., 2009, Golde et al., 2011).

6

1.3. Amyloid-β

Aβ, a 4-5kDa polypeptide, is a normal product of the metabolism of APP with a length that can vary from 36 to 43 amino acids (Haass et al., 1992). The most frequent type of Aβ found under normal conditions in the brain is $A\beta_{1-40}$ but in AD and in Down syndrome, $A\beta_{1-42}$ production is increased and the ratio $A\beta_{1-40}/A\beta_{1-42}$ is reduced (Selkoe, 2001). Aβ can also be found in other tissues and organs where differences in the concentration of the different types of Aβ are present, in blood for example, $A\beta_{1-40}$ constitutes approximately 90% of the total Aβ in plasma (Gravina et al., 1995). See Figure 1.1. for $A\beta_{1-40}$ and $A\beta_{1-42}$ amino-acid sequences.

1.3.1. *Amyloid-β production and degradation*

APP is a ~130kDa polypeptide (Autilio-Gambetti et al., 1988), member of the Type I family of membrane proteins and involved in the production of Aβ. APP is expressed in many tissues and has been implicated in the regulation of synapse formation and neuronal plasticity but its main function remains unknown (Bekris et al., 2011). The APP gene is localized on chromosome 21; individuals with trisomy of chromosome 21 exhibit neuropathological changes similar to those observed in AD, and it has also been shown that inherited mutations in the APP gene alter Aβ production and may precipitate early-onset AD (Walsh and Selkoe, 2007). APP localized in the cellular surface of neurons and astrocytes has been shown to colocalize with cell adhesion proteins such as β1 integrins, clathrin and α-adaptin (Yamazaki et al., 1997).

The enzymatic action of two secretases, α-secretase and β-secretase, dictates the metabolic pathway APP will follow. α-Secretase, which is a collection of metalloproteases, constitutively cleaves 90% of the total cellular APP following the non-amyloidogenic pathway, while β-secretase processes the remaining 10% through the amyloidogenic pathway (Murphy and LeVine, 2010). The non-amyloidogenic pathway starts when α-secretase cleaves APP into an amino-terminal fragment called soluble (sometimes also referred as secreted), APP alpha (sAPPα) and an 83 amino-acids long carboxy-terminal fragment (CTF) named CTF83 (Figure 1.2). CTF83 is subsequently

7

cleaved by γ-secretase releasing extracellular p3 and the amyloid intracellular domain (AICD) (Chow et al., 2010b). On the other hand, the amyloidogenic pathway occurs when APP is cleaved by the β-secretase beta-site amyloid precursor protein-cleaving enzyme 1 (BACE1) into the amino-terminal fragment soluble APP beta (sAPPβ) and the 99-residue carboxi-terminal fragment CTF99. CTF99 is subsequently cleaved by the enzymatic complex γ-secretase into the different types of Aβ and into AICD (Querfurth and LaFerla, 2010).

Stress factors such as hypoxia and ischemia increase the rate of production of BACE1 both *in vivo* and *in vitro* (Guglielmotto et al., 2009). In addition to BACE1, cathepsins have been shown to exert β-secretase activity and may be involved in the production of Aβ (Hook et al., 2005). Increased BACE1 activity in CSF was shown to be related to markers of AD pathology in humans (Mulder et al., 2010).

A multiple protein complex composed of PSEN1 or PSEN2, nicastrin (Nct), presenilin enhancer 2 (Pen2), and anterior pharynx defective 1 (Aph-1) is required for a functional γ-secretase (Kimberly et al., 2003). PSEN forms the active site of the aspartyl protease and, in the brain, PSEN1, not PSEN2, has been found to be the dominant protein (Li et al., 2000). The glycoprotein Nct serves as the γ-secretase substrate receptor as the ectodomain of Nct binds to the amino terminus of APP or Notch and recruits them into the γ-secretase complex (Shah et al., 2005). Notch is a type I transmembrane protein involved in lymphoid cell differentiation and neural development, dysregulation of Notch signal is related with developmental defects and cancer (Nakayama et al., 2011) (Figure 1.3.). The γ-secretase complex is unusual in that it cleaves within the lipid bilayer of the cellular membrane and that it can only process substrates that were previously cleaved by another enzyme (Selkoe and Wolfe, 2007).

So far two proteases are known to degrade Aβ, neprilysin and insulin degrading enzyme (IDE; also referred to as insulysin). Neprilysin, is a plasma membrane-anchored zinc endopeptidase, responsible for the extracellular degradation of Aβ monomers and oligomers (Kanemitsu et al., 2003). IDE is a thiol metalloendopeptidase with intracellular and extracellular activity that degrades mainly insulin but also Aβ monomers (Qiu and Folstein, 2006).

The characteristic β-sheet structure of Aβ peptides facilitates self-assembly into different conformations including dimers, trimers, oligomers (2 to 6 peptides), protofibrils and the fibrillar forms observed in brains of individuals with AD (Reinke and Gestwicki, 2011). Neurotoxicity in AD is currently considered to be caused by the abnormal production and aggregation of $Aβ_{1-42}$ peptide, which form amyloid fibrils more easily than other types of Aβ and are the main constituents of Aβ plaques (Luhrs et al., 2005). $Aβ_{1-42}$ possess higher rigidity in the C-terminal part of its structure compared with $Aβ_{1-40}$, this characteristic has been associated with increased propensity to fibrillar aggregation (Rezaei-Ghaleh et al., 2011). Moreover, synthetic Aβ peptides have been shown to be neurotoxic in different brain regions such as cortex and hippocampus, to impair long-term memory and to exhibit β-sheet mediated fibrillogenesis identified by Congo red staining in the same way as amyloid fibrils (Balducci et al., 2010).

Soluble Aβ, in particular oligomeric forms, has been proposed as the most toxic presentation of all the configurations of Aβ (Cerpa et al., 2008). An increase in the concentration of soluble Aβ correlates with synaptic loss and is a good predictor of synaptic change in AD (Lue et al., 1999). Soluble oligomers have been reported to cause alterations in the cellular membrane. Kayed and colleagues (2004) reported that amyloid oligomers and protofibrils increase membrane conductivity by means of a non-channel mechanism (Kayed et al., 2004). Furthermore, it has been shown that soluble oligomers increase the area per molecule of the lipids involved in membrane formation, thus thinning, lowering the dielectric barrier and increasing the conductance of the membrane (Sokolov et al., 2006). In addition, Aβ soluble dimers obtained from the brains of individuals with AD alter glutamatergic synaptic transmission (Shankar et al., 2008). Aβ soluble oligomers have been shown to disrupt axonal transport by causing dysregulation of intracellular signalling cascades via an NMDA receptor mechanism mediated by glycogen synthase kinase-3β (GSK-3β) in primary hippocampal neurons (Decker et al., 2010). Aβ fibrils have also been shown to be toxic though they are less toxic than oligomers. Neuronal dystrophy and loss of synaptic connections without cell death have

been described in cultured rat neurons incubated with fibrillar Aβ (Grace et al., 2002). Deposition of fibrillar Aβ caused dendritic spine loss and shaft atrophy which led to permanent disruption of neuronal connections in transgenic mice (Tsai et al., 2004). Picone and colleagues (2009) showed that both oligomers and fibrils are toxic to LAN5 neuroblastoma cells inducing apoptosis through different mechanisms, as oligomers induce activation of the intrinsic pathway principally through activation of caspase 9 while fibrils induce activation of the extrinsic pathway mainly through caspase 8 (Picone et al., 2009). Despite these findings, the precise cytotoxic mechanism of Aβ in AD remains to be determined.

1.4. Tau

Tau is a microtubule-associated protein expressed mainly in neurons and required for the stabilization of neuronal cytoskeleton (Martin et al., 2011). Alternative splicing of tau pre-mRNA results in 6 tau isoforms in the human brain (Iqbal et al., 2010) ranging from 352–441 amino acids and possessing a molecular weight between 60 and 74 kDa (Buee et al., 2000). Tau is composed by a N-terminal region (exons 1-5), a proline-rich domain (exon 7), a microtubule-binding domain with four repeats R1, R2, R3 and R4 (exons 9-12) and a C-terminal region (exon 13) (Mandelkow et al., 1996). Tau has 85 phosphorylatable amino acid residues which include 45 serines, 35 threonines and 5 tyrosines, phosphorylation of these amino acids by diverse kinases regulates tau functions (Hernandez et al., 2010) (Figure 1.4.). Abnormal hyperphosphorylation of tau induces the appearance of neurofibrillary tangles which is one of the main pathological characteristics of AD. Hyperphosphorylated tau sequesters normal microtubule-associated proteins, disrupts microtubules and self-assembles into paired helical filaments (Iqbal et al., 2010), also, it induces neuroinflammation and activation of microglia and astrocytes (Metcalfe and Figueiredo-Pereira, 2010). In a recent study in humans, Desikan and colleagues (2011) found that increased entorhinal cortex atrophy was significantly related to decreased CSF Aβ$_{1-42}$ only when CSF phosphorylated tau was elevated, suggesting that Aβ-associated volume loss occurs only in the presence of phosphorylated-tau in humans at risk for dementia (Desikan et al., 2011).

In addition to AD, other tauopathies include frontotemporal lobar degeneration with tau inclusions such as Pick's disease, progressive supranuclear palsy, and corticobasal degeneration; agyrophillic grain disease; some forms of prion diseases; amyotrophic lateral sclerosis/parkinsonism-dementia complex; chronic traumatic encephalopathy; and some genetic forms of Parkinson's disease (Morris et al., 2011).

1.5. Astrocytes

Astrocytes are members of the family of glial cells, specific non-neuronal cells in the nervous system, which also include the oligodendrocytes, Schwann cells, microglia and ependymal cells. The astrocytes are of ectodermic embryologic origin and it has been shown that neural stem/progenitor cells during adult neurogenesis can differentiate into astrocytes, neurons or oligodendrocytes (Yoneyama et al., 2011). Neuroglia were thought to serve a role only as supporting cells for the neurons; the name, given by Rudolph Virchow in 1856, is directly derived from the word glue. This point of view has been challenged, in particular in the past two decades due to technical advances that have identified important physiological activities that these cells exert in the organism (Somjen, 1988).

Although Michael von Lenhossèk coined the term astrocyte in 1893, it was the Spanish neuropathologist Santiago Ramón y Cajal who, optimizing a silver carbonate staining technique developed by Camilo Golgi, accurately described their characteristic star-like appearance and classified these cells according to their anatomical localization as fibrous astrocytes, residing in the white matter, and protoplasmic astrocytes, residing in the gray matter (Garcia-Marin et al., 2007).

Although astrocytes are commonly considered as the most numerous cell type in the CNS, a recent study in human brains by Acevedo and colleagues (2009), showed that non-neuronal to neuronal cells ratios change across the different regions of the nervous system. The cerebral cortex, including gray and white matter, showed a 3.76:1 ratio of non-neuronal to neuronal cells, the cerebellum a 0.23:1 ratio and the rest of the brain (basal ganglia, diencephalon, mesencephalon and pons) an 11.35:1 ratio, for an overall

ratio of 0.99:1, differing from the previous studies based usually on only one brain region that calculated a 10:1 ratio in the whole brain (Azevedo et al., 2009).

Until relatively recently, astrocytes were considered as cells which provided only nutritional and structural support for neurons, largely due to the lack of recordable electrical excitability. They were also thought to lack the mechanisms to communicate with astrocytes or any other cells or to be directly involved with synapses until it was shown that they possess different biochemical messengers, called "gliotransmitters" to do so (Volterra and Meldolesi, 2005). Since then, numerous investigations have led to a series of discoveries revealing the increasing range of functions and the roles astrocytes play in physiology and pathology.

1.5.1. *Characterization of astrocytes*

Astrocytes represent a diverse population of cells with regional and physiological variability in function and morphology. Astrocytes are commonly characterized by the expression of the glial fibrillary acidic protein (GFAP). Although this definition is practical it may not be sufficient, as the family of astrocytes is large and some cells that possess the morphological characteristics of astrocytes, do not always express GFAP (Walz and Lang, 1998). For example, astrocytic end-feet around larger blood vessels (> 8μm in diameter) are predominantly GFAP-positive while end-feet around smaller blood vessels (< 8μm in diameter) are uniformly GFAP-negative, suggesting a relationship of GFAP with the dynamics of vessels and blood-brain barrier (Simard et al., 2003). Furthermore, other types of glial cells such as ependymal glia and radial glia, because of their close embryological origin with astrocytes, have the capacity to express GFAP (Liu et al., 2006).

Other markers can be used to help facilitate the identification of astrocytes from a functional and structural point of view but none is without limitations. S100β is a calcium-binding protein considered to be glial-specific although it seems to be mainly expressed by a subtype of mature astrocytes ensheathing blood vessels, the oligodendrocytes-precursor cells or neuron-glial antigen 2 (NG2)-expressing cells as well as by some endothelial cells (Steiner et al., 2007). The glutamate transporter 1 (GLT-1),

also known as excitatory amino acid transporter 2 (EAAT2) in humans, is also expressed in astrocytes but it has a regional-specific localization so it is not useful to identify the totality of the cells (Wang and Bordey, 2008). Glutamine synthase has also been used as a marker of astrogliosis; this is the enzyme responsible for the conversion of glutamate to glutamine, but this enzyme is not astrocyte-specific, as it has also been identified in grey and white matter oligodendrocytes. Inward-rectifying potassium channels like the Kir4.1 are only expressed in some subtypes of astrocytes and the aquaeporin channel 4 is localized specifically in the processes of the astrocytes. In addition, the enzyme aldehyde dehydrogenase 1 family, member L1 (Aldh1L1), also known as 10-formyltetrahydrofolate dehydrogenase (FDH), has been shown to be a more specific marker of astrocytes than GFAP, identifying both the cell body and the processes and it is more widely expressed on the brain (Cahoy et al., 2008). Another marker is the protein bystin which has been proposed as a marker of astrogliosis and has been shown to be a more sensitive marker in activated astrocytes induced by ischemia and hypoxia compared with GFAP (Fang et al., 2008). Finally, glycogen granules have also been used as markers of astrocytic function. Despite the alternative markers, GFAP continues to be used as the primary astrocytic indicator *in vivo* and *in vitro*.

1.5.2. *Astrocyte functions*

Astrocytes carry out numerous important functions in the nervous system (Cotrina and Nedergaard, 2002). They regulate the ionic environment, especially extracellular K^+ concentration. Their end-feet make contact with capillaries and arterioles contributing to the maintenance of the blood-brain barrier and modulating transport of substances from the blood to the astrocyte and *vice versa*. Astrocytes respond to the metabolic needs of neurons by activating glycogen metabolism and releasing lactate, and are responsible for the uptake of glutamate in the synaptic cleft. They also respond directly to calcium and adenosine signals from neurons as well as from other glial cells (Ni et al., 2007). Astrocytes are in physical contact with adjacent cells through gap junctions and hemichannels, creating an extensive syncitium of cells which facilitates communication and signalling. A recent finding in adult mouse hippocampus confirmed that astrocytes

13

are intimately integrated into synaptic signalling as they detect and modulate synaptic calcium release (Di Castro et al., 2011).

An indication of their wide-ranging reactivity is highlighted by the fact that astrocytes express numerous receptors including G protein-coupled receptors and ionotropic receptors, receptors for growth factors, chemokines, steroids and receptors which are involved in innate immunity like toll-like receptors; interestingly, astroglia display heterogeneity in their pattern of receptor expression and adjust the pattern according to their microenvironment (Wang and Bordey, 2008). Recent evidence indicates that they may be involved in processes such as learning and memory (Gibbs et al., 2008).

1.5.3. *Astrocytes pathophysiology*

Whenever the CNS sustains an insult, for example physical trauma, chemical injury or exposure to pathogens, astrocytes become reactive. This astrogliosis characterized by cellular hypertrophy and proliferation, is identified by rapid GFAP synthesis (Eng et al., 2000). Reactive astrocytes surround and isolate dying neurons, impeding their regrowth or contact with fully functional cells (Ridet et al., 1997). As such, astrogliosis has been classified in two forms, anisomorphic, when the hypertrophic astrocytes surrounding a lesion form a permanent glial scar and isomorphic, when astrocytes distal to an injury site promote the growth of neurites and synaptogenesis facilitating the recovery of neuronal networks instead of replacing the tissue with a scar (Rodriguez et al., 2009). Although the main role of astrogliosis is protective, a failure or disruption in any of its related processes such as attenuation of neurotoxicity due to excess glutamate or regulation of inflammatory reactions induced by trauma or infection can increase the negative impact of a disease in the CNS. It has been shown that under specific circumstances astrogliosis can exert detrimental effects such as impeding axon regrowth while it can also exacerbate inflammation through cytokine production, increasing the production of ROS, releasing glutamate, altering blood brain barrier (BBB) or causing cytotoxic edema during trauma and stroke (Sofroniew and Vinters, 2010).

There is evidence that altered astrocytic function occurs in certain types of epilepsy. In mesial temporal lobe epilepsy, a decrease in the aquaporin 4 channels and in dystrophin

leads to altered water flux and impaired K^+ buffering reducing the threshold for developing seizures (Eid et al., 2005). Connexin 43 is considered to be the main gap junction protein of astrocytes, and its expression is altered under pathological conditions; for example, it is downregulated by inflammatory reactions in multiple sclerosis (Brand-Schieber et al., 2005).

Alexander disease is a potentially lethal neurodegenerative type of leukodystrophy of genetic origin characterized by seizures, spasticity and developmental delays, in which the regulation of GFAP expression is compromised leading to the apparition of excessive accumulations of toxic GFAP, called Rosenthal fibres (Sawaishi, 2009).

1.5.4. *Astrocytes, Aβ and AD*

The observed functional and structural changes present in astrocytes during aging pointed to a possible link between astroglia and AD (Duffy et al., 1980). More recent discoveries involving the numerous physiological properties of astrocytes, together with the development of animal models, have offered new perspectives on the participation of astrocytes in the development of AD (Rodriguez et al., 2009). A complex neuroinflammatory reaction has been related to the development of AD and astrocytes seem to be involved in this process being part of a pro-inflammatory reaction shared with microglia and neurons, characterised by the secretion of cytokines, chemokines, neurotoxic molecules, and complement activation (Sastre et al., 2006).

Astrocytes are directly associated with amyloid plaques and neurofibrillary tangles. Abundant activated astrocytes have been observed in the cortical molecular layer and near amyloid plaques in pyramidal cell layers in brains from individuals with AD; those close to the molecular layer show a gradient of GFAP immunoreactivity labelling that increases in intensity the closer it is to the subpial cortical surface and this appears to be proportional to the stage of the disease (Nagele et al., 2003). *In vitro* studies with rodent brains have also shown a close interaction between astrocytes and Aβ peptides. Cultured rat cortical astrocytes become reactive when in contact with $Aβ_{1-42}$ peptide and have the ability to degrade it; moreover, when microglia were added to the culture, astrocytes, through the release of glycosaminonglycase-sensitive molecules, impeded the removal of

Aβ_{1-42} by microglia (Shaffer et al., 1995). It seems that microglia adopt a position within and adjacent to the central amyloid core of the neuritic plaque, whereas the astrocytes often surround the outside of the plaque with some of the processes directed to the amyloid core (Farfara et al., 2008).

Astrocytes have the capacity to bind and degrade Aβ_{1-42}. Wyss-Coray and colleagues (2003) used astrocytes from adult mice brains and incubated them with Aβ_{1-42} to quantitate the degradation of Aβ. The Aβ content of the cell fraction and cell-culture supernatant was determined by western blot and ELISA analysis. Within 3 hours, Aβ_{1-42} levels decreased in the supernatant and increased in the cell-associated fraction. After 3 hours, the levels of Aβ in the cell fraction began to decrease, and by 24–48 hours there was no Aβ detectable in the supernatant or in the cell fraction (Wyss-Coray et al., 2003). This was corroborated by the finding that transplanted astrocytes from adult, but not neonate mouse brain, were able to degrade and internalize Aβ from slices of human AD brains, although cells from both adult and neonates were able to internalize Aβ *in vivo* (Pihlaja et al., 2008).

Activated astrocytes, like neurons, accumulate Aβ in the brains of individuals with AD, although the predominant type of Aβ varies depending on the anatomical localization; astrocytes within the cortical molecular layer contain the highest amount of Aβ_{1-42} with a lower immunoreactivity for Aβ_{1-40} and Aβ_{1-43} (Nagele et al., 2003).

The same researchers reported that death and lysis of Aβ_{1-42}-overburdened astrocytes may give rise to GFAP-positive plaques in the molecular layer. Additionally, it was reported that astrocytes are recruited to the sites of Aβ deposition by localized release of the chemoattractant, monocyte chemoattractant protein 1 (MCP-1). As soon as the astrocytes contact the Aβ in the extracellular matrix, they become immobilized. This adhesion mechanism is calcium- and magnesium-independent, suggesting possible involvement of molecules which share characteristics with scavenger receptors such as receptor for advanced glycation end products (RAGE), low-density lipoprotein receptor-related protein (LRP) or membrane-associated proteoglycans (Wyss-Coray et al., 2003).

In this context is important to note that astrocytes express numerous receptors that interact with Aβ in addition to RAGE, these include Toll-like receptors (TLR), TLR2,

16

TLR3, TLR4 and TLR9, scavenger receptors SRA, SRB1, SR-MACRO and CD36, glycoprotein receptor lactadherin and CD47, lipoprotein receptors ApoE, LRP and CD14, complement C1q receptor, chemokine receptors CCR2, CCR3, CCR5, CXCR2 and CXCR3, T-cell receptors CD40L and major histocompatibility complex class II (MHC-II), and manose receptor (Farfara et al., 2008). Table 1.2. gives a detailed list of proposed astrocytic Aβ receptors.

Some types of Aβ-containing plaques represent a transient deposit of Aβ which contain the N-terminal truncated Aβ; these have been observed in the internal layers of human entorhinal cortex, where they are considered to be associated with astrocytes as intracytoplasmic inclusions (Thal et al., 2000). The N-truncated Aβ, as opposed to the full length Aβ$_{1-42}$, can be easily internalized and cleared by astrocytes suggesting a potential therapeutic role in AD.

ApoE4, an isoform of the major lipid carrier in the brain apolipoprotein E, is synthesized mainly in astrocytes and mutations in its gene have been considered as a risk factor for the development of AD (Fagan and Holtzman, 2000). Cultured astrocytes prepared from ApoE-deficient mice, compared with wild-type mice, failed to clear Aβ; astrocyte viability was not modified and this suggested that ApoE expressed and secreted by astrocytes was essential for the response. It is believed that a receptor-mediated mechanism involving a member of the LDL receptor family is responsible (Koistinaho et al., 2004). Aβ induces an increase in endogenous levels of ApoE and ApoJ in activated astrocytes and treatment with an ApoE receptor inhibitor abolishes the Aβ-induced changes and reduces the ApoE levels but fails to alter the ApoJ levels; this suggests that the extracellular stimuli generated by Aβ induces an immunomodulatory response in the ApoE receptor (LaDu et al., 2000). In the same study it was proposed LRP mediates Aβ-induced astrocyte activation while low-density lipoprotein receptor (LDLR) mediates the Aβ-induced changes in ApoE.

Post mortem tissue prepared from individuals with AD demonstrated elevated immunolabeling for connexin 43 in Aβ plaques suggesting an infiltration of astrocytic processes into plaques and an increase in the expression of gap junctions proteins (Nagy et al., 1996). Activated astrocytes in AD exhibit elevated levels of the lysosome-specific

17

protein cathepsin D, suggesting an increase in the activity of this cellular compartment (Nagele et al., 2003). In the presence of untreated astrocytes, synapses were protected from Aβ$_{25-35}$, with synaptophysin immunolabeling regaining the classical dot-like appearance characteristic of normal synapses; this pattern of immunostaining was lost when the neurons were co-cultured with Aβ-treated astrocytes (Paradisi et al., 2004). Moreover, glucocorticoids have been shown to reduce the expression of Aβ-degrading proteases decreasing astrocytic Aβ degradation (Wang et al., 2011b).

Astrocytes have also been related to neurofibrillary tangles with a significant association between S100β+ overexpressing cells and free tangles in the neuropil in AD (Sheng et al., 1997). Another study quantified the relationship between neurofibrillary tangles, astrocytes and amyloid plaques in different regions of post-mortem human brains; neurofibrillary tangle density was significantly correlated with GFAP-positive cells in the entorhinal cortex, and amyloid plaques were significantly correlated with GFAP expressed in the cornu ammonis (CA), the subiculum and the entorhinal cortex (Muramori et al., 1998). Tau protein, which aggregates abnormally in AD generating neurofibrillary tangles, possesses a tyrosine residue (Tyr 18) which is the most vulnerable place for disassembly. Nitration in this region prevents or slows tau filament self-assembly; it has been proposed that, in AD, this mechanism is impaired. Reyes and colleagues (2008) showed that in AD brains, nitration at Tyr 18 occurs in GFAP-positive astrocytes which are in contact with Aβ plaques; this was observed before the appearance of neurofibrillary tangles so it is unclear if it represents a protective or an early toxic mechanism (Reyes et al., 2008). In a recent study it was shown that tau significantly increased astrocytic expression of GFAP and S100β and that this was enhanced by co-treatment with Aβ (Lu et al., 2009).

1.5.5. *GFAP*

GFAP is member of a family of intermediate filament proteins, which also include vimentin and nestin, and serves principally cyto-architectural functions (Pekny and Pekna, 2004). GFAP, ranging from 8-9 nm in size, is considered the most important intermediate filament in astrocytes and contributes to the modulation of astrocyte motility

and shape by providing structural stability to astrocytic processes (Eng et al., 2000). Human GFAP is located in the chromosome 17 but no relation has been identified with other pathologies encoded in the same region such as frontotemporal dementia with parkinsonism (Isaacs et al., 1998). GFAP knockout mice exhibit subtle effects on diverse functions like long- and short-term depression and potentiation as well as BBB integrity (Tanaka et al., 2002); the evidence suggests that other intermediate filaments like vimentin can functionally replace the missing GFAP (Eng et al., 2000). On the other hand, an overexpression of GFAP in transgenic mice leads to a fatal encephalopathy and is directly related to the rare leukodystrophy of Alexander disease (Messing et al., 1998, Hagemann et al., 2006). As mentioned previously, astrogliosis is correlated with redistribution and increase in the expression of GFAP and this process is observed in brains of individuals with AD (Li et al., 2011a).

1.5.6. *RAGE*

RAGE was first cloned and described in 1992 (Neeper et al., 1992). RAGE is a 45kDa multifunctional cell surface protein with immunoglobulin characteristics that binds to different structures such as advanced glycation end products (AGE), S100 proteins, amyloid β and High Mobility Group Box Protein 1 (HMGB1) (Park and Boyington, 2010). The structure of RAGE consists of an extracellular variable V-domain (residues 24–127), two extracellular constant C type domains (C1 residues 132–230 and C2 residues 239–320), a single transmembrane region (residues 321-360) and a short C-terminal cytoplasmic tail (residues 361-404) (Leclerc et al., 2010). So far, 20 RAGE isoforms have been identified in a diverse range of tissues and organs including rat liver and kidney and human lung, aortic smooth muscle cells, vascular endothelial cells, pericytes and widespread in the brain (Leclerc et al., 2009). The most prevalent isoform in the brain is endogenous secretory RAGE (esRAGE), which lacks both the transmembranal and intracellular domains (Park et al., 2004).

RAGE is a multifunctional receptor as its effects are dependent on the ligand but is known to induce pro-inflammatory signals in a diverse range of cells and to induce activation of NFκB pathway (Li and Schmidt, 1997). RAGE has been shown to interact

with S100β activating the NFκB pathway (Hofmann et al., 1999). Different pathologies such as diabetes, cancer, rheumatoid arthritis, stroke, multiple sclerosis (MS), amyotrophic lateral sclerosis and AD are associated with an increase in the presence of ligands for RAGE, such as AGE's, HMGB1 or Aβ, which activate RAGE leading to inflammatory signalling (Lue et al., 2009). RAGE was shown to specifically bind to Aβ and mediate Aβ-induced oxidative stress more than a decade ago and since then it has been suspected to play a role in the pathophysiology of AD (Yan et al., 1996). Recently, a study by Li and colleagues (2011) in rats showed that blocking RAGE with an antibody attenuated the AGE-induced glycogen synthase kinase-3 (GSK-3) activation, tau hyperphosphorylation, and memory deficits with restoration of synaptic functions (Li et al., 2011b).

1.5.7. *S100β*

S100β is a 21kDa protein, member of the S100 calcium-binding family of proteins mainly expressed in the CNS (Vives et al., 2003). S100β consists of a pair of distinct EF-hand motifs connected by a hinge region, a C-terminal calcium-binding site and an N-terminal calcium-binding site (Ostendorp et al., 2005). S100β can adopt different configurations forming dimers, tetramers, hexamers or octamers (Ostendorp et al., 2007). Human S100β gene is the only member of the S100 family to be localized on chromosome 21q (Reston et al., 1995). The precise role of S100β is still not clear as this protein interacts with many targets including microtubules and other cytoskeleton components, enzymes from the glycolytic pathway, tumour suppressor p53, zinc and copper (Donato et al., 2009, Ostendorp et al., 2011). It is also involved in cell growth, cell cycle control and cell differentiation (Scotto et al., 1998). S100β is considered a biomarker of brain damage as its expression is increased after traumatic brain injury, encephalitis or in neurodegenerative pathologies such as AD (Ostendorp et al., 2007). Furthermore, Roltsch and colleagues (2010) reported that ablation of S100β decreases amyloid plaque load in the cortex, reduces gliosis and attenuates neuronal dysfunction in PSEN-APP double transgenic mice (Roltsch et al., 2010). Activated astrocytes present in AD amyloid plaques have been shown to overexpress S100β protein (Mrak and

Griffinbc, 2001). S100A6 is another member of the S100 protein family present in astrocytes which shows upregulation in both animal models and patients with AD (Boom et al., 2004).

1.5.8. *EAAT2*

EAAT2, also referred to as GLT-1 in rodents, is the major glutamate transporter in human astroglia (Lauriat and McInnes, 2007). Its molecular weight is 66kDa and the structural model reported consists of 8 transmembrane domains in addition to a pair of less well-defined re-entrant loops near the C-terminal region, the N-terminal domain and the C-terminal domain (Ye et al., 2010). The principal function of EAAT2 is to transport glutamate from the extracellular fluid into astrocytes thus preventing the possibility of excitotoxicity and it is responsible for more than 90% of the glutamate clearance (Haugeto et al., 1996). Amyotrophic lateral sclerosis and AD have been linked with altered expression and function of EAAT2 (Li et al., 1997). Rat astrocytes incubated with a subtoxic concentration of $A\beta_{1-42}$ showed an increase in glutamate uptake and expression of GLT-1 mediated in part by activation of the NFκB signalling pathway (Rodriguez-Kern et al., 2003).

1.5.9. *Aldh1L1*

Aldh1L1, also referred to as FDH, is a member of the family of aldehyde dehydrogenases present in many organs but primarily in cortical astrocytes in the brain (Yang et al., 2011). This enzyme is formed by a tetramer composed of four identical units of 100kDa (Tsybovsky and Krupenko, 2011). Aldh1L1 structure includes an N-terminal folate-binding domain (residues 1–310), an intermediate domain of unknown nature (residues 311–419) and an aldehyde dehydrogenase-like C-terminal domain (residues 420–902) (Cook et al., 1991). The main function of Aldh1L1 is to convert 10-formyltetrahydrofolate to tetrahydrofolate (THF) and CO_2 in a NADP$^+$-dependent reaction, serving a major role in *de novo* nucleotide biosynthesis and regeneration of methionine which involves cell division and growth (Krupenko, 2009). There is no

reported link between changes in Aldh1L1 and AD or any other neurodegenerative condition, although it has been suggested that overexpression of Aldh1L1 may reduce cellular proliferation in the embryonic dorsal midline causing neural tube defects (Anthony and Heintz, 2007).

1.6. Microglia

The word microglia was first used by the Spanish neuropathologist Pío del Río-Hortega, a student of Ramón y Cajal. Río-Hortega described the morphology of microglia using the silver carbonate staining technique (Kaur et al., 2001). Microglia are unique among glial cells in that they have a different embryological origin. All cells in the CNS are derived from the neuroectoderm with the exception of microglial cells which are stemmed from the mesoderm, sharing the same embryological origin as immune cells. It is considered that microglia migrate and localize within the CNS during development although the specific cell precursor is still a matter of debate; the hypothesis that microglia are derived from circulating blood monocytes before migrating to the CNS has been challenged by evidence that points to a non-monocytic original cell that colonises the nervous system through extravascular routes (Chan et al., 2007). This embryological difference makes microglial cells functionally distinct from all the other nervous system cells as it is accepted that microglia work as the main immunological regulators within the nervous system.

1.6.1. *Characterization of microglia*

Many markers have been found to help study microglial activation; among them are, clusters of differentiation proteins such as CD11b and CD68, MHC II, TLR2 and TLR4, Iba1, lectin and nestin (Graeber and Streit, 2010). Expression of MHC II, a cell-surface marker that interacts with CD4 Th cells, is increased when microglial cells become activated (Vidyadaran et al., 2009). CD40 is a member of the tumor necrosis factor-alpha (TNFα) receptor superfamily that mediates immune reactions including T-cells and is expressed by microglia among other cells; it has been found that the expression of CD40

is increased in microglia in the presence of harmful stimuli (Qin et al., 2005). CD68 is frequently used as an indicator of phagocytosis and related to microglia as microglial cells are the main phagocytic cells in the nervous system. Despite the large number of microglial markers none of them is specific for microglia as all of them are shared either with macrophages or with other cells of the nervous system (Schmid et al., 2009).

1.6.2. *Microglial functions*

Many functions have been attributed to microglia during and after development of the nervous system. Microglia phagocytose and remove cellular debris and apoptotic cells, sense damaged synapses and maintain CNS circuitry, combat infectious agents, perform neuroimmunological regulation, are involved in pain mechanisms and in the re-establishment of physiological conditions in the brain and spinal cord after injury (Graeber and Streit, 2010). Microglial cells possesses numerous types of receptors; some, like AMPA and metabotropic glutamate receptors, are considered to mediate chemotaxis (Liu et al., 2009). Microglia act as initial sensors of potentially dangerous signals which are recognized by TLR4 and, in response, secrete pro-inflammatory mediators such as TNFα and IL-1β that can act on astrocytes inducing secondary inflammatory responses (Saijo et al., 2009). Microglia can detect astrocytic calcium-waves and they express K^+, Cl^- and H^+ channels (Farber and Kettenmann, 2005). It has been suggested that microglial cells are not a homogeneous population of cells representing a diverse range of functions (Parkhurst and Gan, 2010).

1.6.3. *Microglial pathophysiology*

Microglial cells modify their morphology according to environmental conditions with two major characteristic shapes, amoeboid, which exists transiently in the developing brain and later when the cell is phagocytic or motile and, ramified, which is the predominant form in the adult form; ramified cells are involved in the surveillance of the brain and the spinal cord (Kaur et al., 2001). In response to any insult that alters or threatens the physiological balance in the environment of the nervous system, microglia

change morphology and adopt an activated state which can be acute (seconds to minutes) or chronic (hours to weeks) (Parkhurst and Gan, 2010). Additionally, it has been reported that microglial activation during stress differs from activation due to infection or inflammation suggesting different mechanisms of activation (Sugama et al., 2009). Evidence indicates that microglia and astrocytes share cellular communication signals that regulate their activity. It has been shown that astrocytes are capable of activating microglia through chemokine expression (MCP-1 and IP-10) in individuals with MS and in the presence of an infection (Ovanesov et al., 2008, Tanuma et al., 2006).

Altered microglial function has been associated with numerous brain pathologies. For example microglia are the primary target in the CNS following infection with human immunodeficiency virus (HIV), as HIV binds to the CD4, CCR3 and CCR5 expressed by these cells (He et al., 1997). Microglia also have been linked to the pathophysiology of MS as activated microglia have the ability to stimulate Th1 and Th2 CD4$^+$ T-cell lines and present antigens (Aloisi, 2001). Additionally, activation of microglial cells has also been observed in the brains of children with Rasmussen's encephalitis (Wirenfeldt et al., 2011), and in other neurodegenerative conditions including Parkinson's disease (Tansey and Goldberg, 2010) and AD (Combs, 2009).

1.6.4. *Microglia, Aβ and AD*

A link between AD and alterations in the brain immune system has been consistently demonstrated and, considering that microglia are the natural immune regulators of the nervous system, a connection between microglia and AD is intuitive. Although there is an extensive literature on the subject, the role that these cells play in the pathophysiology of AD is unclear (Graeber and Streit, 2010). There is evidence that reactive microglia are present in the brains of individuals with AD, frequently within or around compact Aβ peptide-containing plaques although they have also been observed, to a lesser extent, close to diffuse plaques (Combs, 2009). The proximity of microglia to Aβ plaques led to the belief that microglia were involved in the formation and maintenance of the plaques but this suggestion was challenged by a recent study which showed that complete ablation of microglia failed to alter the development of plaques and that the amyloid-

associated neuritic dystrophy was unaffected (Grathwohl et al., 2009). Despite this, there is evidence that the reactive load of microglial cells increases in AD and directly correlates with the degree of cognitive deficit suggesting a role in an early pathological event (Cagnin et al., 2001). In addition, Aβ has been shown to potently activate microglia and, at least some evidence suggests that this requires the expression of the purinergic receptor P2X$_7$ (Sanz et al., 2009). On the other hand, Streit and colleagues (2009) suggested that degenerating neuronal tau-positive structures were colocalized with severely dystrophic, rather than with activated, microglial cells and that microglial dystrophy precedes the spread of tau pathology. This group demonstrated that deposits of Aβ lacking tau-positive structures were colocalized with non-activated, ramified microglia, suggesting that Aβ may not trigger microglial activation (Streit et al., 2009).

Microglia internalize fibrillar and soluble Aβ and segregate them into separate subcellular vesicular compartments; the proposed mechanism of fibrillar Aβ internalization is through receptor-mediated phagocytosis while the soluble Aβ is through a process of fluid-phase micropinocytosis (Mandrekar et al., 2009). Fibrillar Aβ has been shown to be partially digested by the lysosomes in microglia (Majumdar et al., 2007). Recently, Majumdar and colleagues (2011) showed that in primary mouse microglia the specific chloride transporter, chloride channel 7 (ClC-7), is not delivered efficiently to lysosomes causing incomplete lysosomal acidification and reduced fibrillar Aβ degradation; activation of microglia with macrophage colony-stimulating factor (MCSF) increased lysosomal acidification and augmented fibrillar Aβ degradation (Majumdar et al., 2011).

1.6.5. *MHC II*

MHC II is a member of the histocompatibility family of surface glycoproteins and responsible for binding and presenting peptides to CD4 T cells. MHC II consists of a heterodimer formed by two homologous peptides and α and β chains (Stern et al., 1994). Three isotypes of MHC II genes are present in humans, HLA-DR, HLA-DP, and HLA-DQ, these genes are characteristically highly polymorphic with many alleles existing at each gene locus, which could potentially generate more than 4000 combinations of HLA

class II α and β subunits (Nielsen et al., 2010). In the nervous system MHC II is expressed mainly in microglial cells although it has been reported that astrocytes can express MHC II under particular circumstances such as during viral infections (Hamo et al., 2007). MHC II upregulation has been associated with a number of brain pathologies, in MS, aberrant expression of MHC II antigens are considered to be involved in the autoimmune aspect of this disorder (Raddassi et al., 2011). HLA-DQ and HLA-DR appear to be risk factors for developing narcolepsy and cataplexy (Mignot et al., 2001). Recently, Shi and colleagues (2011) showed that short Aβ immunogens (Aβ$_{1-15}$ and Aβ$_{1-15}$ plus the addition of Arg-Gly-Asp motif) increased MHC II expression and T cell activation in TNFα matured-dendritic cells without stimulating pro-inflammatory pathways, suggesting the potential use of these immunogens in AD immunotherapy (Shi et al., 2011).

1.6.6. CD11b

CD11b (also referred to as α$_M$ subunit) is a 165kDa protein, member of the integrin family and part of the CD11b/CD18 complex (also known as Mac-1,CR3 or α$_M$β$_2$ integrin) which is involved in phagocytosis, cell-mediated cytotoxicity, chemotaxis and cellular activation (Ross, 2002). CD11b contains seven repeating motifs of approximately 60 amino acids each that form the N-terminal region, three of the N-terminal repeats contain Ca^{2+}-binding sites and are localized under a seven-bladed β-propeller integrin structure which serves as the backbone of the protein. It also possesses a 200 amino acid region near the N-terminus region termed the I-domain and a C-terminal domain (Springer, 1997). CD11b has been found to be increased during microglial activation (Roy et al., 2008). In addition to microglia, CD11b is also used as a marker in the diagnosis of myeloid leukemia (Paietta et al., 1998) and a marker of neutrophils and other granulocytes (Mobberley-Schuman and Weiss, 2005). Choucair-Jaafar and colleagues (2010) reported that antibodies against CD11b or CD18 decreased the uptake of either Aβ$_{1-40}$ or Aβ$_{1-42}$ in microglia and that concomitant inhibition of LRP and the CD11b/CD18 complex completely blocked the ingestion of Aβ, suggesting that these are the microglial receptors involved in this process (Choucair-Jaafar et al., 2011).

1.6.7. *CD68*

CD68 (macrosialin in mice) is an 110kDa transmembrane protein, member of the scavenger receptor family and used as marker of lysosomal and endosomal activation as well as phagocytosis (Boer et al., 2006). CD68 is composed of two extracellular domains separated by a proline-rich hinge region and a small intracellular tail of 10 residues long which contains an amino acid motif homologous to low-density lipoprotein and transferrin receptors (Jiang et al., 1998b). CD68 expression is increased in activated microglia in different conditions such as thiamine deficiency (Wang and Hazell, 2010) or hepatitis C infection (Wilkinson et al., 2010). Additionally, CD68 has been reported to increase with physiological brain aging (Wong et al., 2005).

1.7. Inflammation

The immune system is functionally classified in terms of innate and adaptive immunity. Innate immunity is carried on mainly by monocytes and macrophages and occurs when these cells release cytokines in response to the presence of pathogens or damaged cells. Adaptive immunity involves mainly lymphocytes and its responses are based on the immunological memory from previous exposure to antigens. Inflammation is a complex cytokine-induced response to harmful stimuli including injury, allergens or infectious agents. The inflammatory response can be acute (minutes to days), characterized by fluid and plasma protein exudation with a predominant accumulation of neutrophils or chronic (days to years), described by the presence of lymphocytes and macrophages associated with vascular proliferation and fibrosis (Kumar and Robbins, 2007). Clinically, inflammation is accompanied by erythema, fever, pain and swelling.

Although inflammation is a physiological protective mechanism it has been observed that under certain circumstances an excessive inflammatory response becomes harmful to the organism. This led to the proposal of the "cytokine theory of disease" in which overproduction of cytokines by the immune system can cause signs, symptoms, and damaging effects of a disease, stating the paradigm that cytokines are necessary and sufficient for disease pathogenesis (Rosas-Ballina and Tracey, 2009, Tracey, 2007). Brain

pathologies, in particular neurodegenerative disorders, have been associated with altered immunologic responses (Glass et al., 2010). Inflammation has been shown to cause alterations in the metabolism of $A\beta_{1-42}$ and to reduce $A\beta$ levels in the CSF of patients with MS (Mori et al., 2011). Pro-inflammatory cytokines such as IL-1β alter $A\beta$ metabolism in the cerebral cortex and increase APP in the brains of rats (Fan et al., 2009). Moreover, treatment with interferon-gamma (INF-γ) increases the protein expression of BACE and the production of sAPPβ in astrocytes (Hong et al., 2003).

1.7.1 *Cytokines*

Cytokines encompass a large number of soluble molecules characterized by intercellular communication and signalling and secreted by cells from the immune system as well as glial cells in the brain. Cytokines bind to cell surface receptors initiating signalling cascades that result in nuclear gene transcription. Functional pleiotropy is a well-described characteristic of cytokines, revealed by the numerous and diverse physiological and cellular actions these molecules exert on the organism (Kumanogoh and Ogata, 2010). Cytokines are pro- or anti- inflammatory determined by the cellular receptor to which they bind. Traditional pro-inflammatory cytokines such as IL-1β, IL-6 and TNFα have been reported to increase in the brain with age and also in neurodegenerative conditions such as AD (Bodles and Barger, 2004).

1.7.1.1. *Interleukin-1β*

IL-1β (also known as IL-1F2) is one of the 11 described members of the IL-1 family of cytokines which also include IL-1α, IL-1 receptor antagonist (IL-1Ra), IL-18, IL-33 and IL-1F5. IL-1β genes, as well as all the encoding genes of the IL-1 family members with the exception of IL-18 and IL-33, are present in human chromosome 2 (Sims and Smith, 2010). The primary sources of IL-1β are monocytes, tissue macrophages, and dendritic cells and microglia and astrocytes in the brain. Different signals can induce the expression of IL-1β including hypoxia, complement activation, blood clotting and microbial products (Dinarello, 2009). IL-1β can also induce its own expression both *in*

vivo and *in vitro* (Dinarello et al., 1987). Pro-domains present at the amino termini are cleaved by the inflammasome assembly to secrete and to generate the active form of IL-1β (Martinon et al., 2009). The signalling pathways involved in the production of IL-1β include the NFκB and the mitogen-activated protein kinase (MAPK) pathways (O'Neill, 2008).

Release of IL-1β is regulated by the IL-1Ra which impedes the binding of IL-1β to interleukin 1 receptor, type I (IL-1R1) (Greenfeder et al., 1995) and IL-1 receptor type II (IL-1R2) which prevents excessive autocrine activation of the IL-1 signalling pathway (Colotta et al., 1993).

IL-1β plays an important role in the induction of fever and alterations in the inflammasome allow the spontaneous release of IL-1β, causing the development of rare hereditary diseases characterized by fever, rash and arthritis (Sims and Smith, 2010). In the brain, IL-1β is involved in the pathogenesis of MS, as mice lacking either IL-1 or IL-1R1 do not develop experimental autoimmune encephalomyelitis (EAE) which is the mouse model of MS (Sutton et al., 2006). IL-1β overexpression is present in the brain of individuals with AD and it has been proposed that IL-1β may be associated with amyloid plaque development (Griffin et al., 1995). It has been shown that IL-1β activates astrocytes inducing the expression of different proteins such as α1-antichymotripsin (α1-ACT), ApoE and complement component C3, all of which are increased in AD amyloid plaques (Akiyama et al., 2000).

1.7.1.2. *Interleukin-6*

IL-6 is involved in numerous physiological processes such as immune regulation, hematopoiesis, inflammation, cell growth and differentiation and has been related to pathological responses including oncogenesis, acute phase responses, chronic inflammation, autoimmunity, endothelial cell dysfunction and fibrogenesis (Barnes et al., 2011). Additionally, IL-6 has been shown to be essential for the differentiation of Th17 cells (Bettelli et al., 2006).

Microglia, astroglia, neurons, and endothelial cells are all capable of synthesizing IL-6 in the CNS (Akiyama et al., 2000). In astrocytes, TNFα and IL-1β induce the expression of

IL-6, but this is not the case for IL-6 as it was unable to induce its own expression (Van Wagoner and Benveniste, 1999). In macrophages, activation of Stat1 and NFκB induces the expression of IL-6 (Kimura et al., 2009).Two proteins act as functional receptors for IL-6, the specific IL-6 receptor (IL-6R) (Yamasaki et al., 1988) and gp130, which is a common signal transducer of cytokines related to IL-6 (Hibi et al., 1990); JAK-signal transducer and activator of transcription (JAK-STAT) and Ras-MAPK pathways mediate IL-6 signal transduction through gp130 (Kishimoto, 2010). Production of IL-6 is negatively regulated by the suppressor of cytokine signals (SOCS) (Starr et al., 1997).

A meta-analysis performed by Swardfager and colleagues (2010) revealed significantly higher peripheral blood cytokine concentrations for IL-6, TNFα, IL-1β, IL-12 and IL-18 in AD subjects compared with healthy control subjects with the strongest evidence values for IL-6, IL-12 and IL-18 (Swardfager et al., 2010). Additionally, astrocytic expression of IL-6, IL-6R, and gp130 has been detected in frontal, temporal, parietal, and occipital cortex samples from rapid autopsies of individuals with AD subjects (Akiyama et al., 2000). In mice treated with LPS an increased brain influx and decreased brain efflux of Aβ was observed and levels of IL-6 mirrored the Aβ changes (Jaeger et al., 2009).

IL-6 also has been attributed with direct and indirect anti-inflammatory properties. It has been shown that IL-6 can inhibit INF-γ, IL-1β and LPS-induced production of TNFα in glial cells (Xing et al., 1998, Di Santo et al., 1997). Furthermore, IL-6 can act as an indirect immunosuppressant as it stimulates the hypothalamic-pituitary-adrenal axis in humans inducing the release of adrenocorticotropic hormone (ACTH) which in turn increases the synthesis of glucocorticoids (Akiyama et al., 2000).

1.7.1.3. *TNFα*

TNFα is synthesized as a monomeric type-2 transmembrane protein which is inserted as a homotrimer into the membrane and then cleaved by the matrix metalloprotease TNFα converting enzyme (TACE, also known as ADAM17) to produce a 51 kDa soluble circulating trimer (McCoy and Tansey, 2008). Macrophages are the main source of TNFα but it has been reported that, in the brain, microglia, astrocytes and some populations of neurons can produce it (Lieberman et al., 1989, Morganti-Kossman et al., 1997). TNFα

binds to two different receptors TNFR1, which is expressed in most cell types, and TNFR2 which is expressed primarily in cells of the immune system including microglia and in endothelial cells (Chan et al., 2000). TNFα activates different signalling pathways including NFκB, p38, ERK and JNK (Croft, 2009). Interestingly, rat astrocytes incubated with TNFα showed an increase in the expression of GFAP and S100β but without compromise of astrocytic viability (Edwards and Robinson, 2006).

TNFα signalling in the brain is involved in many physiological processes such as injury-mediated microglial and astrocytic activation, regulation of BBB permeability, febrile responses, glutamatergic transmission, and synaptic plasticity (McCoy and Tansey, 2008).

Altered expression and release of TNFα is associated with several neurological disorders. In the brains of individuals with MS, increased TNFα expression is found colocalized with active lesions (Hofman et al., 1989). Also, in Parkinson's disease, TNFα levels are increased in CSF and in the *substantia nigra*, in the areas presenting greater loss of dopaminergic neurons (Mogi et al., 2000). In APP transgenic mice, amyloid plaques displayed increased levels of TNFα (Munch et al., 2003) a similar increase in brains of individuals with AD has also been observed (Zhao et al., 2003).

1.7.2. *Chemokines*

Chemokines (the name is derived from *chemo*tactic cyto*kines*) are a group of molecules, members of the cytokine family, which serve as chemoattractants and activators of different immune and non-immune cells and which characteristically act on G-protein-coupled serpentine receptors (Proudfoot, 2002). More than 50 members of the chemokine family have been described and these are further classified into four subfamilies (CXC, CC, C, and CX3C) based on the relative positions of conserved cysteine residues (Streit et al., 2001). Chemokine receptors are also numerous and 20 have been discovered so far (Allen et al., 2007). Chemokines are also classified according to their function as constitutive (developmentally regulated) or inducible (inflammatory) (Proudfoot, 2002). Constitutive chemokines act as homeostatic regulators of the immune system involving immune surveillance and developmental processes while inducible chemokines are

temporarily expressed in response to inflammatory mediators such as TNFα, INFγ, microbial products or trauma (Allen et al., 2007). Chemokines such as regulated upon activation, normal T-cell expressed, and secreted (RANTES) or MCP-1 have been associated with CNS pathologies and conditions including MS, AD, HIV, ischemia and trauma (Banisadr et al., 2005).

1.7.2.1 *RANTES*

RANTES (CCL5) is a 8kDa pro-inflammatory chemokine mainly responsible for the chemoattration of T cells, dendritic cells, eosinophils, NK cells, mast cells and basophils to sites of inflammation and infection (Levy, 2009). RANTES is secreted by a diverse range of cells including activated leukocytes, platelets, epithelial cells, endothelial cells and astrocytes (Murooka et al., 2006, Avdoshina et al., 2010). It has been shown that pro-inflammatory cytokines IL-1β and TNFα stimulate the production of RANTES from astrocytes (Chen et al., 2011). Additionally, RANTES is prone to aggregation and can be found at monomeric, dimeric or oligomeric functional assemblies (Wang et al., 2011a). The main binding receptor for RANTES is the inducible chemokine receptor CCR5 although it can also ligate CCR1 and CCR3 (Proudfoot, 2002).

The potential of RANTES to exert detrimental effects in the organism occurs through excessive recruitment of immune cells that enhance inflammatory processes which happens in conditions such as arthritis, atopic dermatitis, nephritis and possibly AD, also, RANTES can be angiogenic and this may be related to the development of cancer (Levy, 2009). Aβ-activated rat astrocytes showed an increase in the production of chemokines MCP-1 and RANTES (Johnstone et al., 1999). Tripathy and colleagues (2010) showed that RANTES is upregulated in the brains of individuals with AD but they suggest that this increase is protective rather than harmful as, in the same paper, is reported that *in vitro*, RANTES increases cell survival and exerts neuroprotective effects on neurons exposed to toxic stimuli such as thrombin or sodium nitroprusside (Tripathy et al., 2010).

1.7.2.2. *MCP-1*

MCP-1 (CCL2) is a 13 kDa protein, member of the CC family of chemokines and a potent chemotactic factor for monocytes, T-cells and dendritic cells to sites of injury or infection (Yadav et al., 2010). The human gene for MCP-1 was identified in the chromosome 17 (Naruse et al., 1996). MCP-1 was the first CC chemokine identified and is the most representative monocyte chemoatractant protein of the four described so far (CCL7, CCL8 and CCL13) (Deshmane et al., 2009).

MCP-1 expression can be induced by many factors including IL-1, IL-4, TNFα, platelet-derived growth factor, vascular endothelial growth factor, LPS and INFγ (Sheikine and Hansson, 2004). The main sources of MCP-1 are monocytes and macrophages but it can also be produced in numerous cell types including endothelial, epithelial, smooth muscle, fibroblasts, astrocytes and microglia (Yadav et al., 2010). MCP-1 binds principally to CCR2 chemokine receptor and to a lesser extent to CCR11 (Schweickart et al., 2000). A diverse range of signalling pathways including MAPK, JAK2, JNK, p38 and PI3-kinase have been associated with MCP-1 (Yen et al., 1997, Cambien et al., 2001).

MCP-1 has been related to a vast number of physiological and pathological processes such as regulation of infection and inflammation, allergies, HIV, transplant rejection, bone remodelling, BBB permeability, atherosclerosis and cancer (Yadav et al., 2010). As mentioned previously Aβ increases the production of MCP-1 in astrocytes (Johnstone et al., 1999). Furthermore, MCP-1 overexpression was found to significantly increase the formation of Aβ plaques in the hippocampus of APP transgenic mice (Yamamoto et al., 2005). Sokolova and colleagues (2009) reported upregulation of MCP-1, IL-6 and IL-18 in the brains of individuals with AD and determined through logistic linear regression modelling that MCP-1 was the most reliable predictor of the disease (Sokolova et al., 2009).

1.7.3. *Signalling pathways*

1.7.3.1. The NFκB pathway

The NFκB pathway is a signalling pathway mainly involved in the regulation of innate and adaptive immunity and inflammatory responses. The NFκB family of transcription factors consists of NFκB1 (p50 and its precursor p105), NFκB2 (p52 and its precursor p100), RelA (also known as p65), c-Rel, and RelB; all NFκB factors characteristically possess an N-terminal Rel homology domain (RHD) responsible for dimerization and for sequence-specific DNA binding (Vallabhapurapu and Karin, 2009).

NFκB signalling is inhibited by a family of interacting proteins called IκB proteins (IκBα, IκBβ and IκBε) which retain the inactive dimers of NFκB in the cytoplasm of the cell (Hayden and Ghosh, 2008). The activation of NFκB dimers can be accomplished through either the type 1 or canonical pathway, which is induced by numerous stimuli including proinflammatory cytokines, bacteria, viruses, radiation and oxidative stress, or the type 2 or non-canonical pathway, which is induced by receptors involved in lymphoid tissue organogenesis and in lymphocyte development (Pasparakis, 2009). In the type 1 pathway, p50:RelA and p50:c-Rel heterodimers are activated, this requires a sequential phosphorylation, ubiquitylation and proteosome-degradation of the associated IκB in order to release the NFκB dimer and allow it to translocate in the nucleus. In the type 2 pathway, p52:RelB dimers are activated, this requires inducible proteolytic removal of the ankryin-repeat domain of the p100:RelB heterodimer, releasing the p52:RelB NFκB dimer allowing it to translocate in the nucleus (Smale, 2010). IκB actions are controlled by the IκB kinase (IKK) complex which is composed of two catalytic subunits, IKKα (also known as IKK1) and IKKβ (also known as IKK2), and the regulatory subunit NFκB essential modulator (NEMO). Following cell activation, the IKK complex proceeds to phosphorylate IκB proteins thus inducing the ubiquitylation and proteasomal degradation required for the release of the dimers and therefore, allowing NFκB to activate gene transcription (Pasparakis, 2009). Upstream activators of the IKK complex are numerous and seem to be shared with other signalling pathways, these include receptor-interacting protein (RIP), TNF receptor-associated factor (TRAF), MyD88, mitochondrial antiviral signaling protein (MAVS), IL-1 receptor-associated serine/threonine kinase 1 (IRAK1) and mucosa-associated lymphoid tissue lymphoma translocation protein 1 (MALT1)

(Hayden and Ghosh, 2008). IκBα is resynthesized in a NFκB-dependent manner to constitute a regulatory negative feedback loop in which newly synthesized IκBα associates with deacetylated RelA:p50 heterodimers in order to terminate their transcriptional activity and shuttle them back to the cytoplasm (Vallabhapurapu and Karin, 2009). Figure 1.5. illustrates the main components of the NFκB pathway.

NFκB transcription is a rapid event important for the physiological responses of cells. NFκB promotes the expression of pro-inflammatory genes encoding for cytokines, chemokines, enzymes and adhesion molecules fundamental for the development of immune responses (Pasparakis, 2009). NFκB can also activate protective signals that induce the expression of inhibitors of apoptosis (Wang et al., 1998) and enzymes with antioxidant functions (Pham et al., 2004). The pro-inflammatory cytokines IL-1β and TNFα are known strong activators of the NFκB pathway (Hayden et al., 2006).

Aberrant activation of the NFκB pathway has been related to the pathophysiology of numerous conditions including AD. In the brains of individuals with AD activated NFκB has been observed in neurons and glial cells close to Aβ plaques (Terai et al., 1996). Furthermore, it has been shown that both tau and Aβ are able to induce the activation of the NFκB pathway and this is mainly mediated through activation of the RAGE signalling pathway (Granic et al., 2009).

A number of inhibitors of the NFκB pathway have been described. In this study wedelolactone was used. Wedelolactone is an organic compound, identified as a coumestan, derived from the herb *Eclipta prostata*. Wedelolactone has demonstrated anti-inflammatory effects as it has been shown to inhibit the expression of IL-1β by irreversibly inhibiting IKK and thus impeding the phosphorylation of IκBα and NFκB pathway activation (Kobori et al., 2004).

1.7.3.2. *The JNK Pathway*

There are four described subfamilies of MAPK, all of which are serine/threonine kinases, these are JNK, ERK1/2, p38 and ERK5; JNK and p38 are the only members that can be activated by cellular stress and are collectively known as stress-activated MAPKs (Huang et al., 2009). Three mammalian genes for JNK isoforms have been described so far,

JNK1 (also referred to as stress-activated protein kinase-gamma (SAPKγ)), JNK2 (SAPKα) and JNK3 (SAPKβ) (Bogoyevitch et al., 2010). Each JNK protein is expressed in two forms, a short form of 46kDa and a long form of 56kDa (Pulverer et al., 1991). JNK1 (four isoforms) and JNK2 (four isoforms) are constitutively expressed in numerous tissues while JNK3 (two isoforms) seems to be primarily localized in neurons, cardiac myocytes and in the testis (Johnson and Nakamura, 2007). The most important substrates of JNK are c-Jun, Elk-1 and activating transcription factor 2 (ATF2). Activation of the JNK pathway can be induced by several factors such as diverse cellular and oxidative stressors, cytokines, DNA and protein synthesis inhibitors, growth factors, GPCR ligands, and serum (Bogoyevitch et al., 2010).

Activation of the JNK pathway involves numerous elements before starting nuclear transcription. The signalling pathway starts when an extracellular stimuli activates small GTP-binding proteins of the Ras/Rho family which, in turn, interact with and activate through phosphorylation one of the 20 described MAPKKKs (MAP3K) (Cargnello and Roux, 2011). Phosphorylated MAPKKK proceeds to phosphorylate and activate one of the many MAPKKs (MAP2K); MKK4 (also known as SEK1) and MKK7 are the principal MAPKKs involved in JNK activation, which is accomplished through phosphorylation of the threonine and tyrosine loop TXY motif of JNK. Once JNK is activated it proceeds to phosphorylate c-Jun, JunD or ATF2 which in turn, will start the nuclear transcription (Huang et al., 2009, Johnson and Nakamura, 2007). JNK activation of c-Jun involves a mechanism of double phosphorylation (in ser63 and ser73) before c-Jun can form, in combination with c-Fos, the transcription factor activator protein 1 (AP-1) (Weston and Davis, 2002). Furthermore, c-Jun possesses a cis-element for the myocyte enhancer factor 2C (MEF2C) localized in the c-Jun promoter that permits activated p38 and ERK5 to contribute to the induction of c-jun expression (Kyriakis and Avruch, 2001). In addition, JNKs also are regulated by many scaffold proteins which induce conformational changes in bound kinases or their substrates, localize activated MAPK, or terminate MAPK activity through the recruitment of phosphatases or ubiquitin ligases (Vallerie and Hotamisligil, 2010, Engstrom et al., 2010). Figure 1.6. illustrates the main components of the JNK pathway.

JNK participates in a wide range of physiological responses in the organism. In the brain, JNK signalling is involved in development and in regenerative responses to injury but also in apoptosis, other functions including specific isoforms of JNK, such as JNK1, have been associated with microtubule stability and microtubule-associated protein phosphorylation (Mehan et al., 2011). JNK1 has also been shown to regulate the hypothalamic-pituitary-thyroid axis, and obesity-induced JNK activation has been observed in mice (Vallerie and Hotamisligil, 2010).

There is evidence that supports a role of JNK signalling in AD, as JNK activation has been associated with tau induced neurodegeneration (Dias-Santagata et al., 2007) and with Aβ pathology (Colombo et al., 2007). Additionally, Aβ-induced down regulation of the anti-apoptotic factor Bcl-w and activation of TLR4, involved activation of JNK signalling pathway (Mehan et al., 2011).

Several JNK pathway inhibitors have been developed (Bogoyevitch et al., 2010). The inhibitor c-Jun N-terminal kinase peptide inhibitor 1, D-stereoisomer (D-JNKi1) is one of the most frequently used and is used in this study. D-JNKi1 acts preventing the interaction of JNK with its substrates thus impeding the activation of the JNK pathway. Treatment with D-JNKi1 has shown protective effects against cell death, excitotoxicity and cerebral ischemia (Hirt et al., 2004, Borsello et al., 2003).

1.7.4. *Receptors in signal transduction*

1.7.4.1. *CD36*

CD36 is an 88kDa protein, originally described in platelets as glycoprotein IV, and member of the class B scavenger receptor family (Febbraio and Silverstein, 2007). CD36 is a multiligand membrane-bound glycoprotein of 471 amino acids composed of a large extracellular loop and two transmembrane α-helices, one at the amino and the other at the carboxy termini (Martin et al., 2007). CD36 gene was found to be encoded on chromosome 7q11.2 (Fernandez-Ruiz et al., 1993). CD36 is expressed in numerous cell types including endothelial cells, platelets, macrophages, microglia, dendritic cells,

hepatocytes, adipocytes, myocytes and astrocytes (Silverstein and Febbraio, 2009, Wilhelmus et al., 2007).

The main physiological role of CD36 is still not clear as it has been associated with a diverse range of processes including uptake of lipids and apoptotic cells, long-chain fatty acid transport, adhesion and angiogenesis (Martin et al., 2007). In addition, CD36 is a multiligand receptor reported to bind with oxidized LDL, thrombospondin-1 (TSP-1), apoptotic cells, type I and type IV collagen, long chain fatty acids, erythrocytes infected with *Plasmodium* parasites and Aβ (Parsons et al., 2008). CD36 is frequently localized within lipid rafts in the plasma membrane and this seems to be fundamental for its involvement in signal transduction (Thorne et al., 2006). Several signalling pathways such as caspase-3, NFκB, p38 and JNK have been associated with CD36 activation (Silverstein and Febbraio, 2009). CD36 forms functional complexes such as the CD36/CD47/$\alpha_6\beta_1$ integrin which interacts with Aβ (Koenigsknecht and Landreth, 2004), and the CD36/TLR4/TLR6 which signals through NFκB in the presence of Aβ (Stewart et al., 2010). Is precisely these reported interactions with Aβ that have suggested a relation between CD36 and AD (Husemann et al., 2002).

1.7.4.2. *CD47*

CD47 is a 47-52kDa protein which was discovered originally in the placenta as a membrane molecule associated to $\alpha_v\beta_3$ integrin, hence its initial name of integrin associated protein (IAP) (Brown et al., 1990). CD47 is also a member of the Ig superfamily of membrane proteins and possess a structure composed of a single IgV-like domain at its N-terminus, a hydrophobic stretch with five membrane-spanning segments (known as the multiply membrane-spanning domain) and an alternatively-spliced cytoplasmic C-terminus ranging from 3-36 amino acids (Brown and Frazier, 2001). CD47 can bind to many ligands including SIRPα and SIRPγ, in cis to integrins ($\alpha_v\beta_3$, $\alpha_{IIb}\beta_3$ and $\alpha_2\beta_1$) and in trans to TSP (Barclay, 2009). Additionally, as previously mentioned, CD47 forms a functional complex with CD36 and $\alpha_6\beta_1$ integrin which interacts with Aβ (Koenigsknecht and Landreth, 2004).

CD47 is present in essentially all tissues and most cell types which underscore its physiological importance (Reinhold et al., 1995). Binding of SIRPα on macrophages by CD47 on red blood cells or platelets promotes tyrosine phosphorylation of SIRPα which, in turn, associates with the phosphatase SHP-1 resulting in inhibition of phagocytosis ("do not eat me signal") of red blood cells or platelets by macrophages (Matozaki et al., 2009). When CD47, present in T cells, binds to SIRPα, on immature dendritic cells, the phenotypic and functional maturation of dendritic cells is suppressed thus preventing their activation (Latour et al., 2001). Additionally, TSP-1 acts via CD47 to inhibit NO signalling in the vascular system (Isenberg et al., 2008). Similarly, a study by Lamy and colleagues (2007) revealed that CD47 plays a fundamental role in the regulation of the inflammatory response by eliminating activated lymphocytes (Lamy et al., 2007). CD47 has been implicated in synaptic plasticity and memory formation as forced expression of CD47 in cultured hippocampal neurons was reported to promote neurite formation and branching and, furthermore, the binding of CD47 to SIRPα significantly increased the formation of filopodium and spines in cultured neurons (Matozaki et al., 2009).

CD47 may play a role in AD as, in addition to the previously mentioned CD36/CD47/ $\alpha_6\beta_1$ integrin complex link to Aβ, fibrillar $A\beta_{1-40}$- and $A\beta_{1-42}$- induced mast cell activation operating through a CD47/β1-integrin membrane complex coupled with G_i-proteins (Niederhoffer et al., 2009).

1.7.4.2.1. *SIRPα*

The signal regulatory proteins constitute a family of transmembrane glycoproteins and are included in the "paired receptor" group of receptors which are represented by closely related extracellular regions but different cytoplasmic regions inducing contrasting types of signals (van Beek et al., 2005). The SIRP family consists of three members, SIRPα (also known as SHPS-1, BIT, MFR, CD172a or p84), SIRPβ (CD172b) and SIRPγ (CD172g). CD47 is the principal binding partner for SIRPα but it has been reported that surfactant proteins A and D as well as TSP can bind to SIRPα (Barclay, 2009). SIRPα structure contains three Ig-like domains in its extracellular region and four putative tyrosine phosphorylation sites in its cytoplasmic region (Matozaki et al., 2009). SIRPα is

expressed mainly by myeloid cells and neurons but it can also be present in other cell types (Barclay and Brown, 2006).

In addition to the previously described inhibitory interactions of SIRPα with CD47, SIRPα has been involved in production of NO via JAK2 which suggests SIRPα can also act as an activator of effector functions (Alblas et al., 2005). The scope of SIRPα functions can be even larger as other components such as tyrosine kynases CSK and PYK2 as well as the adaptor molecules Grb2, FyB/SLAP-130, and SKAP55hom have been proposed to regulate its signalling (van Beek et al., 2005).

1.8. Objective

The objectives of this study are to determine, *in vivo*, the effects chronic icv treatment with Aβ has in the brains of aged and young rats and to explore age-related changes, and, *in vitro*, to examine the effects Aβ treatment has on cytokine production and release and to investigate the signalling pathways and membrane receptors involved in this process, in rat isolated astrocytes.

COGNITIVE	BEHAVIOURAL	MOTOR
Impaired memory	Apathy/Depression	Abnormal reflexes
Impaired judgement	Agitation	Paratonia
Confusion	Anxiety	Abnormal mouth movements
Agnosia	Irritability	Rigidity
Apraxia	Dysphoria	Bradykinesia
Aphasia and Paraphasia	Disinhibition	Abnormal gait
Dysarthria	Delusions	Seizures
Echolalia	Hallucinations	
Palilalia		

Table 1.1. Clinical signs and symptoms of AD.

	N-terminus	C-terminus
Aβ₁₋₄₀	DAEFRHDSGYEVHHQKLVFFAEDVGSNKGAIIGLMVGGVV	

Aβ₁₋₄₀   DAEFRHDSGYEVHHQKLVFFAEDVGSNKGAIIGLMVGGVV

Aβ₁₋₄₂   DAEFRHDSGYEVHHQKLVFFAEDVGSNKGAIIGLMVGGVVIA
          1   10   20   30   40

Figure 1.1. Amino-acid sequence of Aβ peptides Aβ₁₋₄₀ and Aβ₁₋₄₂. In red the additional isoleucine and alanine present in Aβ₁₋₄₂ at the C-terminus.

RECEPTOR FAMILY	RECEPTORS	Aβ PRESENTATION
Advanced glycation end products receptor	RAGE	Monomers Fibrils
Toll-like receptor	TLR2, TLR3, TLR4, TLR9	————
Scavenger receptor	CD36, SRA, SRBI, SR-MACRO	Fibrils
Glycoprotein receptor	Lactadherin, CD47	Fibrils
Lipoprotein receptor	ApoE receptor, LRE, CD14	Monomers Fibrils
Complement receptor	C1q receptor	————
Chemokine receptor	CCR2, CCR3, CCR5, CXCR2, CXCR3	————
T-Cell receptor	CD40L	————
Mannose receptor	MR	————
Insulin Receptor	IR	Monomers
Acetylcholine receptors	α7nAChR	Monomers Fibrils
Information extracted from (Farfara et al., 2008) and (Verdier et al., 2004)		

Table 1.2. List of receptors proposed to mediate interaction of Aβ with astrocytes.
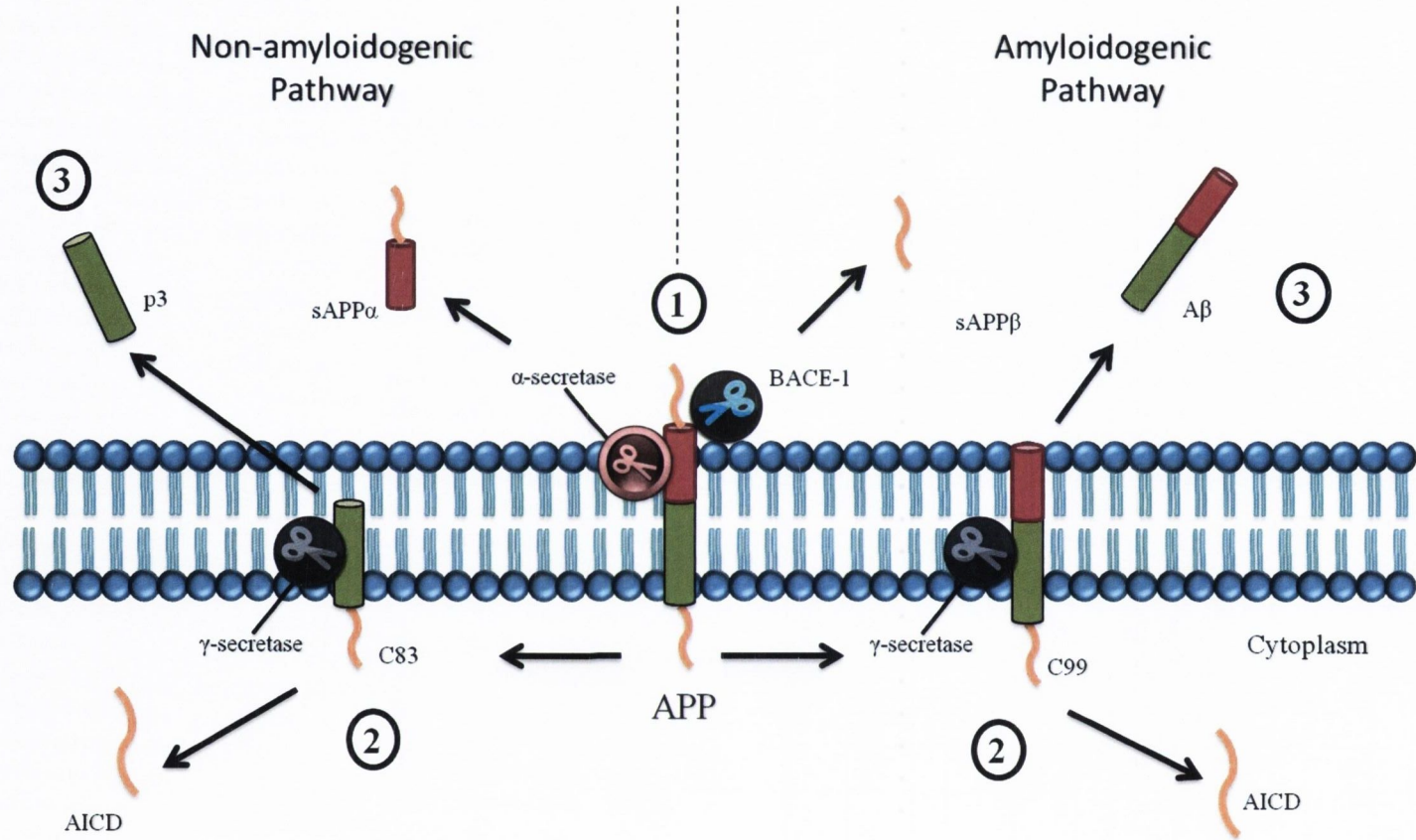
Figure 1.2. Schematic representation of Aβ production.
1 APP can be cleaved by α-secretase initiating the non-amyloidogenic pathway or BACE-1 initiating the amyloidogenic pathway. α-Secretase enzymatic action produces sAPPβ and C83 while BACE-1 produces sAPPβ and C99. **2** The γ-secretase complex cleaves C83 into p3 and AICD or C99 into Aβ and AICD. **3** p3 and Aβ are the final products of the non-amyloidogenic and the amyloidogenic pathway, respectively.
Modified from Querfurth and LaFerla (2010).
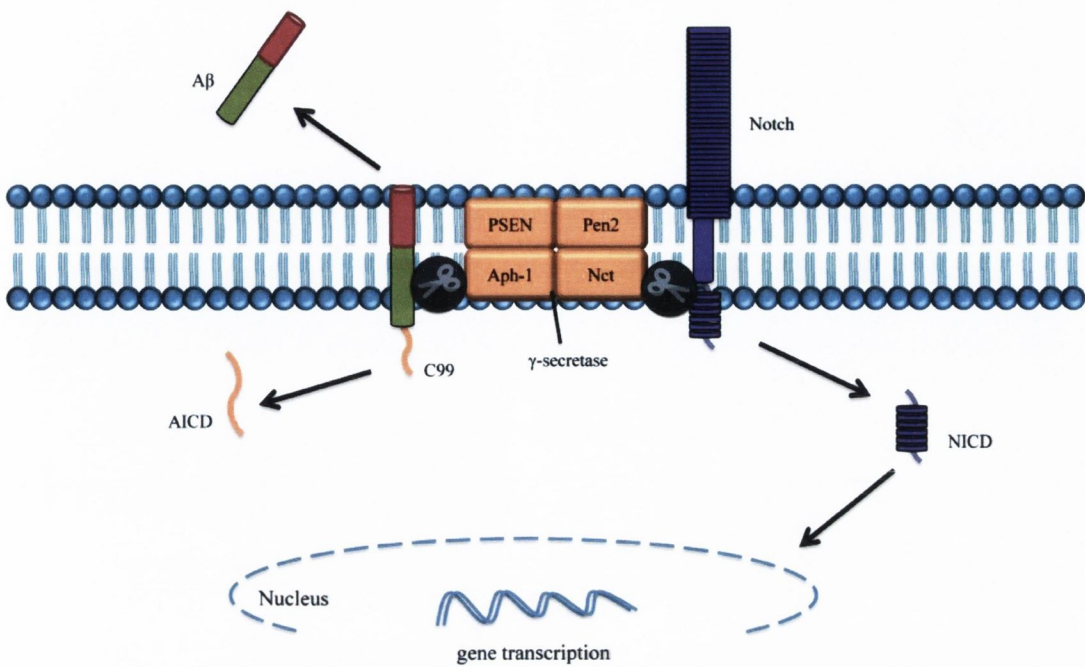
Figure 1.3. Schematic representation of γ-secretase activity.

The γ-secretase complex, composed of presenilin 1 or 2 (PSEN), Nicastrin (Nct), Pen2 and Aph-1, can cleave different Type I transmembrane proteins including APP, Notch or Delta. γ-secretase cleaves the APP C99 fragment into amyloid intracellular domain (AICD) and Aβ. Notch is cleaved by γ-secretase at the S3 site releasing Notch intracellular domain (NICD), which will migrate to the nucleus and bind to transcription factors.
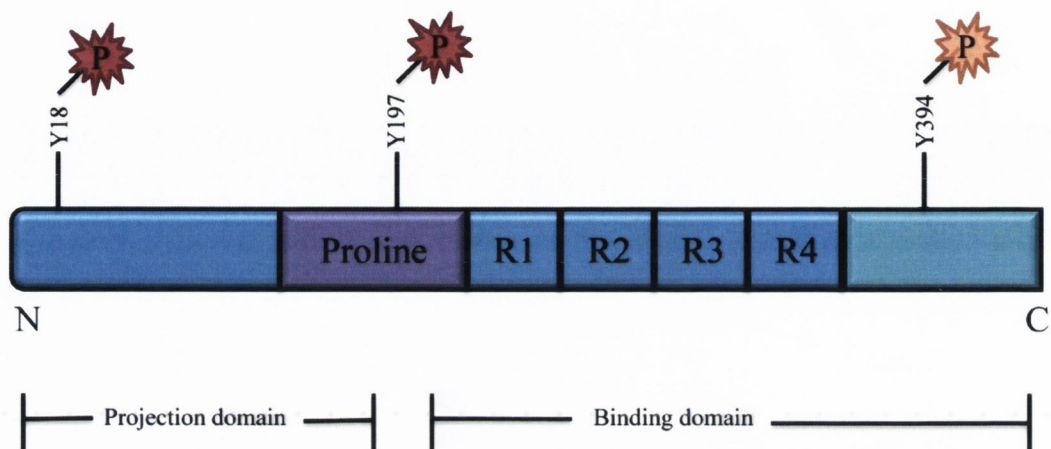
Figure 1.4. Tau protein structure.

Tau protein is composed of an N-terminal region, a proline-rich domain, a microtubule-binding domain with repeats R1, R2, R3 and R4 and a C-terminal region. The tyrosine kinases 18 and 197 have been shown to be phosphorylated in the brains of individuals with AD while tyrosine 394 is phosphorylated both in physiological conditions and in AD. P represents phosphorylation.
Modified from (Lebouvier et al., 2009).
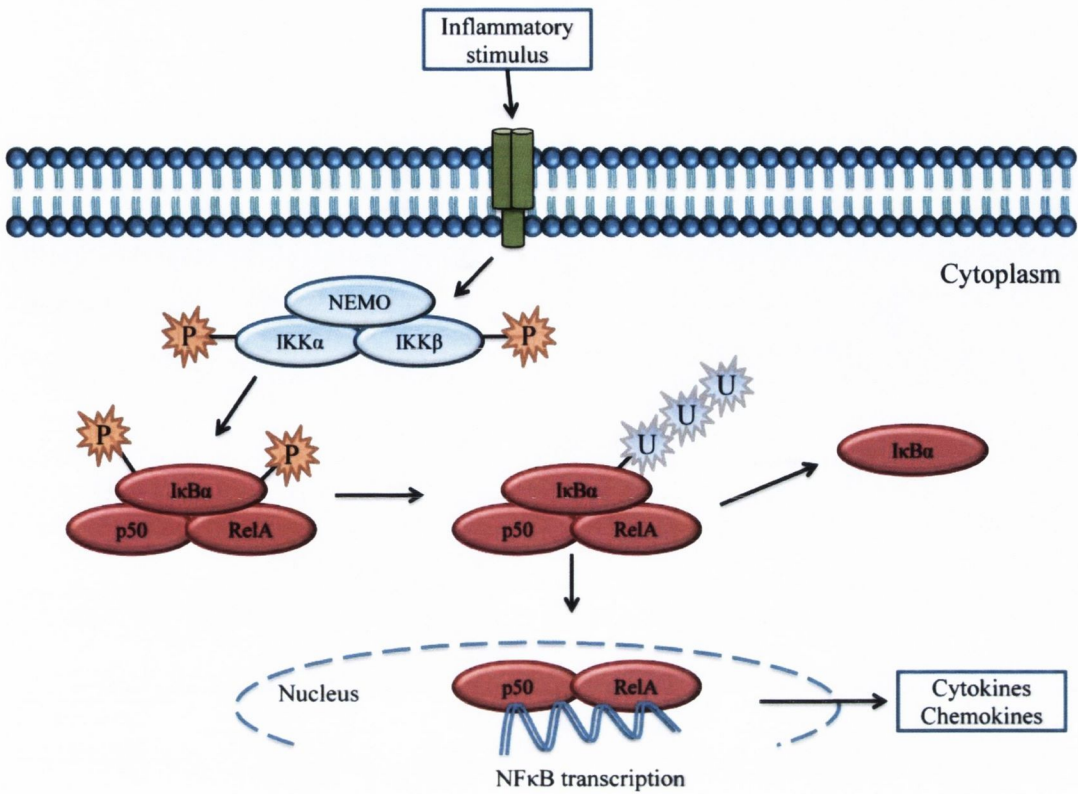
Figure 1.5. NFκB canonical pathway

A pro-inflammatory stimulus induces cell-surface receptors to activate the IKK complex (IKKα, IKKβ and NEMO). The activated IKK complex phosphorylates and triggers the ubiquitylation and degradation of the inhibitory IκBα, allowing p50 and RelA to initiate the transcription of genes for cytokines and chemokines. P represents phosphorylation and U represents ubiquitylation.
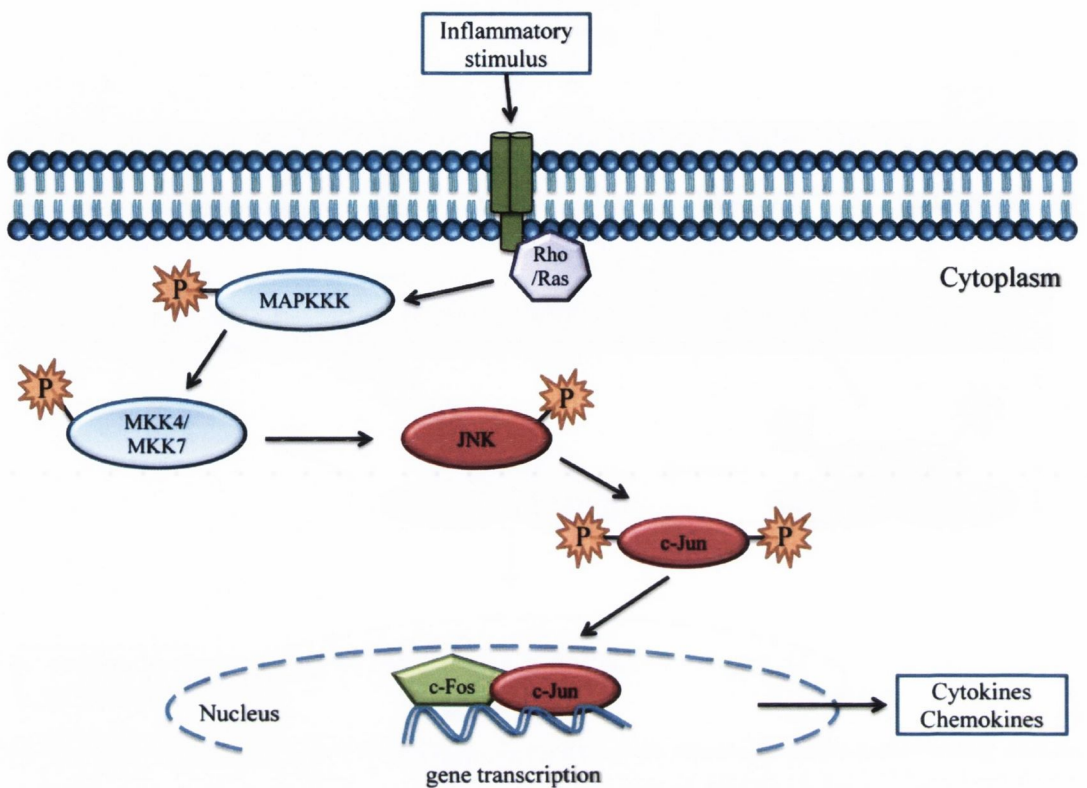
Figure 1.6. JNK signalling pathway.

A pro-inflammatory stimulus induces cell-surface receptors coupled to Rho/Ras to activate MAPKKK. Activated MAPKKK phosphorylates and activates MKK4/MKK7 which in turn phosphorylates and activates JNK. Activated JNK proceeds to phosphorylate c-Jun, thus allowing c-Jun to associate with c-Fos and form the transcription factor AP-1, which subsequently induce the gene transcription of different proteins including cytokines and chemokines.
P represents phosphorylation.

Chapter 2: Materials and Methods

2.1. Animals

2.1.1. *Animals*

Aged (18-22 months; 550-800g) and young (2-4 months; 200-360g) male Wistar rats were used in this study. The animals were supplied by Bantham and Kingham, UK. All animals were housed in a specific-pathogen free (SPF) environment at the BioResources Unit (BioResources Unit, Trinity College Dublin, Dublin 2, Ireland). Young rats were housed in groups of 3-4 per cage and aged rats were housed in groups of 2-3 per cage. All animals were maintained under veterinary supervision at an ambient temperature of 22-23°C and under a 12-hour light-dark cycle, food (standard laboratory chow) and water were provided *ad libitum*. Food and liquid intake were monitored for the duration of the experiment. All animal experimentation was performed under a license granted by the Minister for Health and Children, Ireland, with approval from the local ethical committee and in compliance with the Cruelty to Animals Act, 1876 and the European Community Directive, 86/609/EC, and every effort was made to minimize stress to the animals.

2.2. Animal Treatments

2.2.1. *Preparation of Amyloid-β_{40-1} and Amyloid-$\beta_{1-40/1-42}$ peptides*

Artificial CSF (composition: NaCl 296mM; K^+ 3mM; Ca^{2+} 1.4mM; Mg^{2+} 0.8mM and P 1mM) was used to prepare the mix of amyloid-β_{1-40} and amyloid-β_{1-42} (hereafter referred to as Aβ) and the control reverse peptide amyloid-β_{40-1} (hereafter referred to as Aβ_{40-1}). Aβ_{1-40} and Aβ_{1-42} (Invitrogen, US) and reverse control peptide (Aβ_{40-1}, Invitrogen, US) were aggregated according to the manufacturer's instructions. The Aβ_{1-42} lyophilised peptide was dissolved in sterile distilled water to a concentration of 6mg/ml and then further diluted to a 1mg/ml stock solution with phosphate buffered saline (PBS; Sigma, UK). The Aβ_{1-40} peptide and the reverse Aβ_{40-1} peptide were dissolved in PBS to a concentration of 1mg/ml. Aβ_{1-40} peptide was aggregated for 24 hours at 25°C and the Aβ_{1-42} peptide for 48 hours at 37°C. All stock solutions were aliquoted and stored at -

50

20°C until required. $A\beta_{1-40}$ and $A\beta_{1-42}$ were diluted in artificial CSF to a final concentration of 26.9µM and 36.9µM respectively. Pumps were loaded with a mix composed of 23.3µl of $A\beta_{1-40}$ and 33.3µl of $A\beta_{1-42}$. The control peptide was loaded at a molecular concentration equivalent to the sum of the concentrations of the two active $A\beta$ peptides.

2.2.2. *Priming of Alzet® osmotic pumps*

Alzet® osmotic mini-pumps (Alzet® Osmotic pump model 2004; Alzet, US) were used to deliver control peptide or $A\beta$ to the animals. Handling of the pumps was always carried on under sterile conditions. The empty pump was weighed together with its flow moderator. The head of the cannula was assembled with 3 height-adjustment spacer disks (which were spaced to ensure delivery into the ventricle). A filling tube was attached to a syringe loaded with $A\beta$ or control peptide and transferred into the osmotic mini-pump in an upright position to reduce air bubble formation. The filling tube was inserted through the opening at the top of the pump until the tip of the tube reached the bottom of the pump reservoir. The plunger of the syringe was pushed slowly holding the pump in an upright position. When the solution appeared at the outlet, the filling was stopped and the tube carefully removed. The excess solution was wiped off and the flow moderator was inserted until the cap was flush with the top of the pump. The flow moderator was fully inserted into the body of the pump. After the osmotic pump was filled, it was transferred to a 37°C incubator and primed by placing the pump into a 50ml falcon tube loaded with sterile 0.9% saline solution; the delivery gauge was not in contact with the saline solution. The pumps were primed for a minimum of 40 hours before use. Each pump, including the cannulae, was loaded with 250µl of $A\beta$ or control peptide for a calculated rate of delivery of 0.25µl/hour when implanted, sufficient to ensure delivery of solution for 28 days.

2.2.3. *Surgical Description*

Animals were weighed and sedated by intraperitoneal (i.p.) administration of a mix of ketamine (Vetalar; 75mg/kg; Pharmacia, Germany) and xylazine (Rompun; 10mg/kg; Bayer, Germany). Rats were transferred to a transparent anaesthesia box where they received a controlled flow of oxygen (1L/min at 50%) with isoflurane (5% for induction; Abbott, UK.) until deeply anaesthetised which was established through lack of pedal reflex. Rats were placed in a stereotaxic frame with the incisor bar 2mm below the ears to ensure the head was stable. A nasal mask was secured to provide oxygen (1L/min at 50%) and isoflurane (1.5-2% for maintenance) for the duration of the intervention. Eyes were protected with topical application of Bepanthen® eye cream (Bayer, Ireland). The surgical area was shaved and 2 aseptic washes in circular motion, from the centre of the area to the external border of the surgical field, were done using sterile gauzes. The first wash was with povidone-iodine scrub and the second one with povidone-iodine solution. The incision was performed longitudinally with a sterile surgical blade mounted on a scalpel (Tekno Surgical, Germany) from the midline of an imaginary line between the posterior borders of the eyes to approximately 1cm after the posterior border of the skull (*circa* supraoccipital structure). The skin and subcutaneous tissue were clamped with 4 Kelly forceps to open the surgical field in a diamond pattern. Muscular fascia and the temporalis muscle were dissected and scraped with the scalpel from the midline towards the lateral border of the skull until bregma and lambda were clearly identified. Haemostasis was ensured by local pressure with sterile cotton bud or sterile gauze. To remove the remaining tissue from the periosteum and to improve the visual field, a few peroxide drops were applied and left for 10-15 s and the area was cleaned with sterile gauze. The point of craniotomy for the rat right lateral ventricle was identified at +0.9mm posterior to bregma and +1.3mm lateral to the midline. A trepanation of 0.45mm (diameter) was performed with a handpiece dental drill. Mayo scissors were positioned at the caudal end of the surgical wound advancing through the midline for 4-6cm, preserving nerves and vascular structures, until a subcutaneous pocket was dissected. The Alzet® osmotic pump was positioned in the subcutaneous pocket and the cannula tip gauge was carefully inserted without angulation through the meninges and brain tissue

down to the right lateral ventricle. The cannula was affixed to the skull with superfast glue and secured in place with dental cement (Stoelten, US). Blood was cleaned, Kelly forceps removed and the skin was sutured with a skin surgical stapler. Topic 4% lidocaine hydrochloride (Xylocaine 4% w/v topical solution, Astra Zeneca, Ireland) was applied to the wound. A subcutaneous injection of Carprofen (Rimadyl; 5mg/kg; Pfizer, Ireland) was given to provide post-operative analgesia. The rats were closely monitored during recovery and kept under a heat lamp to prevent hypothermia until they were active.

2.3. Behavioural Analysis

2.3.1. *Morris water maze*

Rats from each treatment cohort were assessed for spatial learning in the Morris water maze. The maze was located in a dark room and comprised a black circular pool, 1.5m in diameter, filled with water which was maintained at a constant temperature of $20\pm1°C$; a hidden platform was placed in a quadrant of the pool and submerged 3cm below the water surface, not visible at water level. The location of the platform was kept constant for the entire experiment and was not removed on the last day of the trials. Visual cues were arranged on the curtains surrounding the pool. The position of the cues was constant for the duration of the experiment. Animals were subjected to 8x1-min trials on the first day and 6x1-min trials for the following 4 days when they were required to search for the hidden platform. If the platform was not successfully reached within this time frame, the animal was guided to the platform. Once on the platform, the rats were left alone for 30 s to study the visual cues and remember the location of the platform. A computerized digital tracking system was used to record the swimming paths and the escape latencies for each rat and each trial. The analysis of the data obtained from the Morris water maze experiment was performed with the EthoVision software (EthoVision v3.1; Noldus Information Technology, Netherlands).

2.4. LTP Analysis

2.4.1. *Induction of LTP in vivo*

On the day of the experiment, rats were anaesthetized by an i.p. injection of urethane (1.5 g/kg); the absence of a pedal reflex was considered to be an indicator of deep anaesthesia. The ability of rats to sustain LTP in the perforant path–granule cell synapses, in response to tetanic stimulation of the perforant path, was assessed as previously described (Minogue et al., 2003). In brief, rats were placed in a stereotaxic frame, a bipolar stimulating electrode was positioned in the perforant path (4.4mm lateral to lambda) and a unipolar recording electrode was positioned in the dorsal cell body region of the dentate gyrus (2.5mm lateral and 3.9mm posterior to Bregma). Test shocks were delivered at 30 s intervals, and after a stabilization period, responses were recorded for 15 min before and 45 min after tetanic stimulation (3 trains of stimuli; 250Hz for 200 ms; 30 s intertrain interval). The stimulus intensity required to induce a spike was similar in all treatment groups (0.5–1mA) and the same stimulus strength was used during delivery of the tetanic stimulation. Responses were assessed by measuring the slope of the excitatory postsynaptic potential (epsp) in the middle one-third of the rising phase of the epsp and mean and standard error of the mean (SEM) values for each treatment group in 30 s bins were calculated and presented. LTP experiments were performed by Dr. Thelma Cowley.

2.5. Preparation of Tissue

2.5.1. *Dissections and preparation of tissue*

At the end of the LTP recording, rats were killed by decapitation and brains were rapidly removed and placed on ice. The brain hemispheres were separated and two-thirds of the left hemisphere was placed on a cork disk, covered with optimal cutting temperature compound (O.C.T. Tissue-Tek®; Sakura, Japan) and immersed in liquid nitrogen for later preparation of cryostat sections. The hippocampus was dissected from the right hemisphere and the remaining portion of the left hemisphere was split in 3 portions; the

first was flash-frozen in liquid nitrogen for later analysis of mRNA and the second and third were prepared for protein analysis (ELISA and Meso Scale) in Krebs buffer (composition in mM: NaCl 136; KCl 2.54; KH_2PO_4 1.18; $MgSO_4\cdot 7H_2O$ 1.18; $NaHCO_3$ 16 and glucose 10) with added $CaCl_2$ (1.13mM) and 10% dimethyl sulphoxide (DMSO) and stored at -80°C until required for analysis. The cerebral cortex was also dissected and added to tubes with Krebs buffer containing $CaCl_2$ and 10% DMSO and stored at -80°C until required for analysis. Samples of serum were taken from each animal and stored at -80°C until required for analysis. Osmotic pumps were then removed from the rats, opened, and any remaining solution was stored at -80°C until required for analysis.

2.5.2. *Protein Quantification*

Hippocampal tissue from the animals was thawed on ice and rinsed 3 times in ice-cold Krebs buffer containing $CaCl_2$. The tissue was allowed to settle and then homogenised in Krebs buffer containing $CaCl_2$ using a polytron homogeniser (Kinematica, Germany).

The protein concentration was assessed in the hippocampal homogenates using the bicinchoninic acid protein (BCA) assay kit (Pierce, US). Standards (0-2000µg/ml) were prepared with bovine serum albumin (BSA; 2000µg/ml) diluted in Krebs buffer containing $CaCl_2$. Duplicate standards and samples (25µl) were pipetted into a 96-well plate to which 200µl of diluted working reagent was added; the plate was covered and incubated at 37°C for 30 min. The absorbance was read at 570nm in a 96-well plate reader (Labsystems Multiskan RC, UK). A standard curve was made by plotting the standards against their absorbance. Protein concentrations were calculated from the standard curve and protein concentration in samples were equalised to a concentration of 4ng/µl by dilution in ice-cold Krebs buffer containing $CaCl_2$.

2.6. Preparation of cultured cortical mixed glia, isolated microglia and isolated astrocytes

2.6.1. *Preparation of sterile coverslips*

Glass coverslips (10mm diameter) were sterilized in 70% ethanol for 1 hour and dried overnight under a sterile UV light in a laminar flow hood. The following day, the coverslips were incubated at 37°C in sterile poly-L-lysine (1mg/ml) diluted in sterile PBS (composition in mM: NaCl 137; KCl 2.7; Na_2HPO_4 8.1 and KH_2PO_4 1.5; pH 7.5) for 1 hour in a Petri dish. After incubation, the coverslips were dried in a sterile laminar flow hood and placed in 24-well plates or stored for future use.

2.6.2. *Preparation of cortical mixed glia from Wistar Rats*

Primary cortical glial cells were prepared from neonate Wistar rats (BioResources Unit, Trinity College, Dublin 2, Ireland). Neonates were decapitated using sterile sharp operating scissors and the brains were removed. The cerebral cortices were dissected free and the meninges carefully removed. The cortical tissue was chopped bi-directionally using a sterile scalpel and placed into 15ml falcon tubes containing warm filter-sterilized culture media Dulbecco's Modified Eagle Medium (DMEM; 2ml; DMEM/F12 (Ham) 1x with L-glutamine and HEPES 15mM; Gibco, UK) supplemented with penicillin (100µl/ml; Gibco, UK), streptomycin (100µl/ml; Gibco, UK) and fetal bovine serum (FBS; 10% $^w/_v$; Gibco, UK). The tissue was incubated for 5 min in 5% CO_2 at 37°C, removed from the incubator and triturated using a sterile Pasteur pipette and filtered through a 50µl sterile nylon mesh filter (BD Biosciences, US) into 50ml falcon tubes. The tubes were centrifuged (2,000g for 3 min at 20°C) with the resulting supernatant removed and the pellet reconstituted in 1ml warm filter-sterilized culture media and triturated. Resuspended glia were counted and equalized to a cell density of 1.5×10^5 cells/ml. Equal numbers of cells were plated onto the centre of each of the poly-L-lysine coated coverslips and incubated for 2 hours in 5% CO_2 at 37°C to allow the cells to adhere. After this time the cells were flooded with 400µl warm filter-sterilized culture media and incubated for 3 days in 5% CO_2 at 37°C. Culture media was replaced with fresh culture media every 3 days for 12-16 days until cells were ready for treatments.

2.6.3. Preparation of isolated cortical astrocytes and microglia from Wistar rats

Primary cortical astrocytes were isolated from neonate Wistar rats (BioResources Unit, Trinity College, Dublin 2, Ireland) following the same method as described above for primary cortical glial cells, except that resuspended glia from each neonate were plated into separate T25 flasks (Fisher, UK) using a Pasteur pipette and the glia were left in the incubator for 2 hours to allow the cells to adhere and then flooded with 8ml of DMEM culture media. Culture media was replaced with fresh DMEM culture media every 3 days for 7-10 days until ready for separation into microglia and astrocytes. When ready, the T25 flasks, with the head and neck wrapped in parafilm to make them air tight, were placed on an orbital shaker for 2-4 hours (110rpm at room temperature). Microglial cells were isolated first. The shaken T25 flasks were taken back to the laminar flow hood and each one was tapped for at least 1 min and the contents from all the flasks poured into a new 50ml falcon tube, which was centrifuged at 2,000rpm for 5 min at 20°C. The supernatant was removed and the resulting pellet was resuspended in DMEM culture media. The microglial cells were counted and equalized to a cell density of 1×10^5 cells/ml. The microglial cells were plated onto the centre of poly-L-lysine coated coverslips and incubated for 2 hours in 5% CO_2 at 37°C to allow the cells to adhere, then flooded with 400µl of culture media. After the microglial cells were isolated, the T25 flasks were washed twice with sterile PBS to remove any possible remaining DMEM. The astrocytes were incubated with 1ml Trypsin-EDTA (Sigma, UK) for 15 min at 37°C and tapped thoroughly for 1 min. The cell suspension was poured into new falcon tubes (1 per flask) and spun at 2,000rpm for 5 min at 20°C. The supernatant was removed and the resulting pellet was resuspended in DMEM culture media (1560µl). The cells were counted and equalized to a cell density of 1×10^5 cells/ml and 65µl of the cell suspension was plated onto the centre of poly-L-lysine coated coverslips and incubated for 2 hours in 5% CO_2 at 37°C to allow the cells to adhere, then flooded with 400µl of culture media.

2.6.4 Treatment of cortical mixed glia and isolated astrocytes from neonate Wistar rats
The effects of Aβ were examined on isolated astrocytes prepared from neonatal male Wistar rats. Cells were treated with a mix of Aβ$_{1-40}$ (4.2µM; Invitrogen, US) and Aβ$_{1-42}$

(5.6μM; Invitrogen, US) or DMEM culture media and incubated for 24 hours at which time they were harvested. $A\beta_{40-1}$ (10μM; Invitrogen, US) or DMEM culture media were used as controls.

The effects of Aβ, D-JNKi1 (Enzo Life Sciences, UK), wedelolactone (Enzo Life Sciences, UK), an antibody against RAGE (αRAGE; R&D Systems, UK), S100β peptide (Sino Biological Inc, China), an antibody against CD47 (αCD47; AbD Serotec, UK), an antibody against SIRPα (αSIRPα; Abcam, UK) and an antibody against CD36 (αCD36; Abcam, UK) were examined on isolated astrocytes prepared from neonate male Wistar rats. The cells were pre-treated with D-JNKi1 (2μM), wedelolactone (50μM), αRAGE (2.5μg/ml), S100β (0.001μM), αCD47 (2μg/ml), αSIRPα (2.5μg/ml) and αCD36 (2μg/ml) for 1 hour. After 1 hour, cells were treated with a mix of $A\beta_{1-40}$ (4.2μM) and $A\beta_{1-42}$ (5.6μM) or DMEM culture media and incubated for 24 hours at which time they were harvested.

2.6.5. *Harvesting of mixed glia and isolated astrocytes from male Wistar rats*

The plates with the cultured cells were taken out of the incubator one at a time and left on ice during the harvesting process. The supernatants were removed through aspiration with a pipette and stored in fresh 1.5ml tubes (Sardstedt, Germany) at -20°C until required for cytokine analysis. The wells were washed in ice-cold 1% PBS twice using a Pasteur pipette.

If the cells were prepared for quantitative-polymerase chain reaction (Q-PCR), then RA1 buffer (Macherey-Nagel, Germany) including β-mercaptoethanol (Sigma, UK) was added to each well (65μl/well for 24-well plates). If the cells were prepared directly for western immunoblotting, then complete lysis buffer (composition: Tris-HCl 10mM; NaCl 50mM; $Na_4P_2O_7 \cdot 10H_2O$ 10mM; NaF 50mM; IGEPAL 1%; Na_3VO_4 1mM; PMSF 1mM and PIC $^1/_{1000}$ dilution; Sigma, UK) was added to each well (65μl/well for 24-well plates).

The cells on the poly-L-lysine coated coverslips were scraped using the plunger of a syringe or the tip of a pipette. The supernatant was removed and stored in small sterile RNAse free Eppendorf tubes at a temperature of -20°C until required for analysis.

Some of the cells were used for immunostaining using confocal microscopy. In this case cells were washed twice with ice-cold 1% PBS and fixed by incubating in ice-cold ethanol/methanol (Sigma, UK) for 5 min. After the ice-cold ethanol/methanol was removed, slides were washed twice with PHEM. The cells were flooded with PHEM and stored at 4°C for late staining.

2.6.6. *Analysis of cell viability using MTS assay*

The CellTiter 96® AQueous One Solution Cell Proliferation Assay (Promega, US) was used to determine the viability of cells in culture. This solution is composed of MTS and phenazine ethosulphate (PES), which enhances the chemical stability of MTS. MTS is reduced in metabolically active cells into a formazan product, the quantity of which is directly proportional to the number of living cells in culture. MTS was added directly to the cell supernatant in a 1 in 5 dilution (50μl of MTS into 250μl of supernatant for 24-well plates) and left to incubate for 1-4 hours at 37°C. After incubation, 100μl of MTS-containing supernatant were added into 96-well plates and absorbance was read at 490nm.

2.7. Analysis of mRNA by Q-PCR

2.7.1. *RNA extraction*

Messenger RNA (mRNA) was extracted from the hippocampal and cortical tissue or from cultured cortical astrocytes. Cortical and hippocampal samples from aged and young rats were thawed on ice and cell lysis mastermix (Nucleospin RNA II; Macherey-Nagel, Germany) was added to each tube. These samples were homogenised using a polytron homogeniser (Kinematica, Germany) at high speed. To remove any insoluble tissue and reduce viscosity, the lysate was added to a Nucleospin Filter placed in an Eppendorf collecting tube and centrifuged at 11,000g for 1 min. The Nucleospin Filter column was discarded and ethanol (350μl; 70%, Sigma, UK) was added to the lysate, the ethanol and lysate were mixed and loaded onto Nucleospin RNA II columns (the addition

of ethanol improves binding of the RNA to the column). The new column and lysate were added to new collecting tubes and these were centrifuged at 8,000g for 30 s. The column was removed and added to a new collecting tube; the silica membrane of the column was desalted by adding membrane-desalting buffer (350µl), to allow the subsequent RNAase-free DNAses to digest more effectively. Samples were centrifuged at 11,000g for 1 min to dry the membrane. DNA was digested by adding DNAse reaction mixture (95µl) to the column and samples were incubated at room temperature for 15 min. The silica membrane of the column was sequentially washed with RA2 buffer (200µl), RA3 buffer (600µl) and RA3 buffer (250µl), centrifuged between washes (11,000g for 30 s or 2 min) and placed into labelled nuclease-free collecting 1.5ml Eppendorf tubes. RNA was eluted by adding RNAse free water (60µl or 40µl for a higher concentration) and centrifuged at 11,000g for 1 min and RNA concentration was quantified using a NanoDrop-spectrophotometer (ND-1000 v3.5, Nanodrop Technologies, Inc., US).

2.7.2. *Reverse transcription for cDNA synthesis*

Total mRNA was reverse transcribed into complementary DNA (cDNA) using a high-capacity cDNA archive kit (Applied Biosystems, UK). A 2x mastermix was prepared containing 10x RT buffer (4µl), 25x dNTP's (1.6µl), 10x random primers (4µl), multiscribe reverse transcriptase (2µl) and nuclease-free water (8.4µl) per sample. RNA was added to fresh tubes to make a final volume of 20µl per sample. The mastermix including the nuclease-free water (20µl) was added to the RNA and tubes were spun and incubated for 10 min at 25°C followed by 2 hours on a thermocycler (PTC-200, Peltier Thermal Cycler, MJ Research, Bioscience, Ireland) at 37°C.

2.7.3. *cDNA amplification by Q-PCR*

mRNA expression was assessed in cortical and hippocampal tissue and in cultured astrocytes. For rat cDNA, a PCR mastermix was made up containing Taqman Universal PCR Mastermix (12.5µl/sample; Applied Biosystems, UK), rat β-actin RNA

(1.25µl/sample; Applied Biosystems, UK) as the endogenous control and specific primers (1.25µl/sample) for each target gene probed (TaqMan® Gene Expression Assays, Applied Biosystems, UK) (see Table 2.1). In all cases, cDNA was diluted at a ratio 1:1 (5µl sample and 5µl free-RNAse water) and added to a MicroAmp Optical 96-well reaction plate (Applied Biosystems, US). Mastermix for each target gene (20µl) was added to each well giving a total reaction volume of 25µl/well. Plates were centrifuged at 2,000rpm for 1 min and then Q-PCR was performed. The PCR consisted of 40 cycles with 2 min at 50°C, 10 min at 95°C, 15 s per cycle at 95°C for denaturation and 1 min at 60°C for transcription to ensure complete extension of the PCR product (7300 real-time PCR System, Applied Biosystems, US).

2.7.4. *PCR Quantification*

The expression of each target gene was determined using the efficiency corrected comparative CT method. Target genes in different samples were compared to a reference gene (β-actin). These values were then normalized to an endogenous control and the relative differences between samples were expressed as a ratio. Values are expressed as relative quantities of specific genes (7300 real-time PCR Software, Applied Biosystems, US).

2.8. Analysis of cytokine concentrations

2.8.1. *Preparation of samples*

The concentrations of IL-1β, IL-6 and TNFα were assessed by ELISA in supernatants from cultured astroglial cells and from hippocampal samples obtained from rats treated with Aβ or control peptide. Hippocampal samples were thawed on ice and washed 3 times with ice-cold Krebs buffer containing $CaCl_2$, and homogenised in 400µl ice-cold Krebs containing $CaCl_2$ using a polytron homogeniser (Kinematica, Germany) at

maximum speed for 10 s. Protein concentrations were equalized to 4ng/µl. Details of antibodies and conditions are given in Table 2.2.

2.8.2. General ELISA Protocol

ELISA plates (96-well; NUNC, Denmark) were incubated overnight at room temperature with capture antibody. Plates were washed 3 times with wash buffer (200µl; PBS containing 0.05% Tween-20; Sigma, UK), incubated at room temperature for 1 hour in blocking buffer (200µl/well), washed and incubated at room temperature with samples and standards. Plates were again washed 3 times with wash buffer (200µl), incubated at room temperature with detection antibody, washed and incubated in the dark at room temperature for 20-30 min with horseradish peroxidase-conjugated streptavidin (strep-HP; 1:200 dilution in 1% BSA/PBS). After incubation, samples were washed and incubated with substrate solution (100µl; 1:1 H_2O_2: tetramethylbenzidine (TMB); R&D Systems, US) in the dark at room temperature for 20-30 min or until colour reaction developed. The reaction was stopped using a stop solution (50µl; H_2SO_4 1M) and absorbance was read at 450nm using a 96-well plate reader (Labsystem Multiskan RC, UK). A standard curve was made up by plotting the standards with their absorbance and concentrations were corrected for protein concentration and expressed as pg/mg protein in the case of tissue or pg/ml in the case of supernatants (GraphPad Prism v4.0; GraphPad Software, US).

2.9. Meso Scale assay for Aβ

Hippocampal samples from control or Aβ-treated rats were thawed on ice and washed 3 times with homogenisation buffer (1% SDS containing: NaCl (50nM; Sigma, UK), PIC (10µl/ml; p8340, Sigma, UK), phosphatase inhibitor I cocktail (5µl/ml; p2850, Sigma, UK) and phosphatase inhibitor II cocktail (5µl/ml; p5726, Sigma, UK); solution pH 10). Homogenising buffer was added to the tissue in a 5:1 ratio (250µl buffer; 50g tissue). Samples were homogenised using a polytron homogeniser (Kinematica, Germany) at

maximum speed for 10 s, centrifuged at 15,000rpm for 40 min at 4°C and the supernatant was removed. The pellet was stored at -80°C for later use. Supernatants were assessed for protein using the BCA protein assay. Aliquots (25µl) of the standards and samples were loaded into a 96-well plate and 200µl of the working reagent was added to each well, the plates were incubated for 30 min at 37°C and the absorbance was read at 570nm in a 96-well plate reader (Labsystems Multiskan RC, UK). Supernatants samples were equalised with homogenisation buffer, neutralised by the addition of 10% Tris-HCl ($^v/_v$ 0.5M; pH 6.8; Sigma, UK) and stored at -80°C for later use.

When required for analysis, the samples were diluted in kit buffer (MSD, US) to a final protein concentration of 5µg/well. Blocking solution A was added to the wells (150µl) and the plate was incubated for 1 hour at room temperature on an orbital shaker and washed 3 times with Tris wash buffer (TWB; 150µl). Detection antibody solution (1% Blocking solution A, 2910µl; 50x Sulfo-Tag 468 detection antibody, 60µl; 100x Blocker G, 30µl; MSD, US) standards (in duplicates) and samples were added to each well (25µl); samples were incubated for 2 hours at room temperature on an orbital rocker and then washed 3 times with 1x TWB. After the plate was washed, 2x MSD read buffer T (150µl/well; MSD, US) was added to the wells, the plate was read immediately on a SECTOR® Imager (SECTOR® Imager 2400, MSD, US) and the data analysis was carried out using the discovery workbench software (Discovery Workbench Software, MSD, US).

2.10. Analysis of protein expression by Western immunoblotting

2.10.1. Protein purification from cultured astrocytes using NucleoSpin® TriPrep protocol

To remove any insoluble tissue and reduce viscosity, the lysate collected from the harvested astrocytes was added to a Nucleospin filter placed in an Eppendorf collecting tube and centrifuged at 11,000g for 1 min. The Nucleospin Filter column was discarded and 70% ethanol (350µl) was added to the lysate, the ethanol and lysate were mixed and loaded onto Nucleospin RNA II columns. The Nucleospin RNA II column and the lysate

were added to new collecting tubes and these were centrifuged at 8,000*g* for 30 s to isolate the protein content from the RNA. The flow-through was recovered and the protein was precipitated with 1 volume of protein precipitator (Macherey-Nagel, Germany) in a new collection tube, mixed vigorously and incubated for 10 min at room temperature. The mix was then centrifuged at 11,000*g* for 5 min. Supernatant was removed, the protein was washed with 50% ethanol (500µl) and centrifuged at 11,000*g* for 1 min, and the resultant supernatant was removed avoiding dislodging the protein pellet. The pellet was dried for 10 min at room temperature, PSB-TCEP (100µl; Macherey-Nagel, Germany) was added and samples were incubated (3 min at 95-98°C) to ensure protein denaturation. Samples were centrifuged at 11,000*g* for 1 min to pellet residual insoluble material. Supernatant was recovered and stored at -20°C until required for analysis.

2.10.2. *Preparation of tissue/cerebral cortices for gel electrophoresis*

GFAP, RAGE and phosphorylated forms of c-Jun (p-c-Jun), IκBα (p-IκBα) and JNK (p-JNK) were assessed by western immunoblotting in cultured astrocytes. Samples were prepared for gel electrophoresis in complete lysis buffer or in PSB-TCEP. The protein concentration in the samples was equalized using either complete lysis buffer or PSB-TCEP. Samples prepared with complete lysis buffer were reconstituted in Tris-glycine sample buffer (composition: Tris-HCl 0.03125M; glycerol 12.5%; SDS 1%; β-mercaptoethanol 2.5%; bromophenol blue powder; pH 6.8) and placed in a -20°C freezer until required for further analysis.

2.10.3. *Gel Electrophoresis*

Gels composed of acrylamide (30%; Sigma, UK), distilled water, gel buffer with SDS (Tris base 1.5M; SDS 0.2%; pH 8.8), ammonium persulfate (APS; 10%; Sigma, UK) and TEMED (Sigma; UK) were prepared on the same day of the western blot and mounted between a spacer and short glass plates (Biorad, Ireland). The proportion of acrylamide used to prepare the gel varied between 10-12% according to the size of the target protein

studied. The wells were shaped with the use of a plastic comb (Biorad, Ireland) inserted in the upper portion of the gel which was prepared with acrylamide (30%), distilled water, stacking buffer (Tris base 0.5M; SDS 0.4%; bromophenol blue powder; pH 6.8), APS 10% and Temed. The gels were mounted in an electrophoretic unit (Biorad, Ireland) and the unit was filled with electrode running buffer. Aliquots of samples were heated to 90°C for 3 min to denature the protein and then were loaded onto the wells of the gels along with a pre-stained molecular weight marker (7 μl; SeeBlue® Plus2; Invitrogen, UK) and with MagicMark (2 μl; Invitrogen, UK). A Power Pac Basic (Biorad, Ireland) was used to pass a constant current of 100V across the unit to separate the proteins (for 80 min or until the marker reached the bottom of the gel). Following protein separation, the gel was placed onto a nitrocellulose transfer membrane (Whatman, Germany). Filter paper (Whatman, UK) and sponges (Biorad, Ireland) pre-soaked in transfer buffer, were placed at either side of the gel and membrane forming a sandwich. This sandwich was inserted in a cassette (Biorad, Ireland), placed into a transferring unit filled with transfer buffer and received a constant current of 80V applied for 60 min to complete the protein transfer. Nitrocellulose membranes were removed from the sandwich and placed in plastic blotting recipients. Protein transference was verified using Ponceau S solution (Sigma, UK) for 5 min. After a single wash, nitrocellulose membranes were ready to be immunoblotted with the appropriate antibody.

2.10.4 *General Protocol for Western immunoblotting*

The nitrocellulose transfer membranes were incubated for 1 hour at room temperature with 5% milk (Marvel; Ireland) in Tris-buffered saline (TBS) with 0.05% Tween-20 (TBS-T). The nitrocellulose membranes were incubated overnight at 4°C with a primary antibody raised against the appropriate protein. Membranes were washed with TBS-T (4x10 min), incubated for 1 hour at room temperature with a secondary antibody conjugated to horseradish peroxidase (HRP; Sigma, UK), and washed with TBS-T (4x10 min). The nitrocellulose membranes were incubated with a chemiluminescent detection solution (Immobilon western chemiluminescent HRP substrate; Millipore, US) to visualize protein complexes. Membranes were exposed in a luminescent image analyzer

(Fujifilm, US; Model LAS-4000) and images were processed and taken using image reader software (Image Reader LAS-4000 v2.0; Fujifilm, US). Nitrocellulose membranes were stripped with antibody stripping solution (1:10 dilution in dH_2O; Reblot Plus Strong antibody stripping solution; Millipore, US) and re-probed for another target protein or for β-actin, which was used as loading control. The specific details for the proteins assessed by western immunoblotting are presented in Table 2.3.

2.10.5 *Quantification Analysis*

Protein bands exposed were analyzed and quantified using the ImageJ software (Image processing and analysis in Java v1.45I; National Institutes of Health, US). In all cases, ratios of the phosphorylated target protein/total β-actin or target protein/total β-actin are presented. For a detailed explanation of the method of analysis and quantification using ImageJ software see: (http://lukemiller.org/index.php/2010/11/analyzing-gels-and-western-blots-with-image-j/).

2.11. Immunofluorescent and Immunohistochemical Staining

2.11.1. *Preparation of slides for immunofluorescent and immunohistochemical staining*

The left brain hemisphere of male Wistar rats into which cannulae were implanted was dissected free and covered with O.C.T. and sliced sagittally using a cryostat (Leica, US; Model Leica CM 1900). Microtome carbon steel blades C35 (Feather, Germany) were used for the slicing and the slice thickness was set at 10μm, 10 slides (Glass Superfrost® Plus slides; Thermo Scientific, Germany) with 3 slices per slide were prepared from each brain. The slides were stored in boxes at -20°C for later analysis.

2.11.2. *General Protocol for immunofluorescent staining in Wistar rats*

Tissue sections were brought to room temperature and individual brain sections were contained in a hydrophobic well using a cytomation pen (Dako, UK). Sections were fixed

in ice-cold methanol (Sigma, UK) for 5 min and rinsed 3 times in PHEM buffer (composition in mM: PIPES 60, HEPES 25, EDTA 10, $MgCl_2$ 2). Following fixation, the tissue was permeabilized (except when samples were assessed for MHC II) in 0.1% Triton®X-100 (Sigma, US) diluted in PHEM for 10 min and washed with PHEM. Non-specific interactions were blocked using 10% blocking buffer (10% normal goat serum plus 4% BSA in PHEM buffer) for 2 hours at room temperature. The tissue was incubated with primary antibodies raised against the proteins of interest (300μl/well; diluted in 5% normal goat serum plus 2% BSA in PHEM buffer) and left overnight at 4°C. Negative controls were incubated with an isoform of the primary IgG antibody (300μl/well; diluted in 5% normal goat serum plus 2% BSA in PHEM buffer) or with 5% blocking buffer without the addition of any antibody. Samples were washed with PHEM and incubated with an appropriate secondary antibody conjugated to either ALEXA Fluor®488 or ALEXA®633 (300μl/well diluted in 5% normal goat serum plus 2% BSA in PHEM buffer; Invitrogen, UK) and DAPI (concentration 1/1000; added simultaneously with the secondary antibodies; Invitrogen, UK) for 1.5 hours in the dark at room temperature. Samples were washed with PHEM every 10 min for 2 hours, to remove as much of the fluorescent background as possible, and in the dark to avoid bleaching of the fluorescent label. Slides were mounted with Vectashield® fluorescent mounting media with DAPI (Vector Laboratories, UK), covered with 22x55mm borosilicate glass (VWR International, Ireland) and secured with a thin line of clear nail polish (Rimmel, Ireland) and stored in the dark at 4°C until required for analysis (see Table 2.4 for immunofluorescent staining protocols).

2.11.3. *Confocal Microscopy*

The incorporated fluorophores were viewed using a confocal microscope (Karl Zeiss, UK; Zeiss Model LSM-510-META) with appropriate excitation wavelengths and filter sets. For ALEXA Fluor®488™ the peak excitation/emission wavelengths were 495nm/520nm and the beam splitters were UV 488/543/633nm and band pass 505-530. For ALEXA Fluor®633™ the peak excitation/emission wavelengths were 632nm/647nm and the beam splitters were UV 488/543/633nm and band pass 575-640nm. Images were

acquired and optimised using LSM 510 software (LSM 510 software; Karl Zeiss, UK) and quantified using ImageJ software (Image processing and analysis in Java v1.45I; National Institutes of Health, US).

2.11.4. *Light Microscopy*

The slides were observed under an Olympus IX51 inverted microscope (Olympus, US) and pictures were taken with a colour Olympus microscope camera (Olympus, US). Images were acquired and optimised using analysis D v5.0 software (Soft Imaging System, US).

2.11.5. *Congo Red Staining for amyloid protein aggregates in male Wistar rats*

Congo red staining was used to assess aggregates of Aβ. Tissue sections were brought to room temperature, placed in a slide rack for staining, rehydrated for 30 s in distilled water and incubated for 20 min in alkaline saturated NaCl solution to weaken the native hydrogen bonds in the amyloid fibrils and reveal the binding sites for the Congo red. Slides were incubated for 30 min in filtered alkaline Congo red. After the incubation period, the slides were rinsed 8 times in 95% ethanol, 16 times in 100% ethanol and incubated for 5 min 3 times in xylenes (Sigma, UK). The slides were counterstained with methyl green (Sigma, UK) for 10 min and washed 3 times in distilled water. The outer section on each slide was not counterstained with methyl green. The slides were mounted with DPX (RA Lamb, UK), covered with 22x55mm borosilicate glass (VWR International, Ireland) and stored at 4°C until required for analysis.

2.12. Statistical analysis

Data are expressed as mean $\pm$ SEM. A 2-tailed Student's t-test for paired and unpaired means, 1-way analysis of variance (ANOVA), 1-way repeated measures ANOVA or 2-way ANOVA was performed, where appropriate, to determine whether significant differences existed between conditions. When ANOVA analysis indicated significance

(at the 0.05 level), a post-hoc Tukey honestly significant difference (HSD) or Newmann-Keuls test was used to determine which conditions were significantly different from each other. All statistical analyses were performed with GraphPad Prism software (GraphPad Prism v4.0; GraphPad Software, US).

RAT PRIMERS (APPLIED BIOSYSTEMS)	PRIMER ASSAY NUMBERS
Aldh1L1	Rn00574839_m1
β-actin	Rn00667869_m1
CD11b	Rn00709342_m1
CD47 (Itgp)	Rn01763248_m1
CD68	Rn01495631_g1
EAAT2 (Slcla2)	Rn00568080_m1
GFAP	Rn00566603_m1
IL-1β	Rn00580432_m1
IL-6	Rn00561420_m1
MCP-1 (Cc12)	Rn00580555_m1
MHC II	Rn01768597_m1
RAGE (Ager)	Rn00584249_m1
RANTES (Ccl5)	Rn00579590_m1
S100β	Rn00566139_m1
SIRPα (Ptpns1)	Rn00564609_m1
TLR2	Rn02133647_s1
TNFα	Rn99999017_m1

Table 2.1. Rat PCR primer assay numbers

CYTOKINE STUDIED	SUPPLIER	BLOCK	CAPTURE ANTIBODY	STANDARD ANTIBODY	DETECTION ANTIBODY
IL-1β	BD Biosciences, US	1% BSA in PBS	Monoclonal anti-rat IL-1β (1μg/ml; in PBS)	Rat recombinant IL-1β standards (0-1000pg/ml; 1% BSA in PBS)	Biotinylated anti-rat IL-1β (350ng/ml; 1% BSA and 2% normal goat serum in PBS)
IL-6	BD Biosciences, US	1% BSA in PBS	Monoclonal anti-rat IL-6 (4μg/ml; Na2CO$_3$ in PBS)	Rat recombinant IL-6 standards (0-4000pg/ml; 1% BSA in PBS)	Biotinylated anti-rat IL-6 (4μg/ml; 1% BSA in PBS)
TNFα	BD Biosciences, US	1% BSA in PBS	Monoclonal anti-rat TNFα (4μg/ml; Na2CO$_3$ in PBS)	Rat recombinant TNFα standards (0-4000pg/ml; 1% BSA in PBS)	Biotinylated anti-rat TNFα (4μg/ml; 1% BSA and in PBS)

Table 2.2. Cytokine analysis protocols

PROTEIN TARGET	PROTEIN BAND SIZE (KDA)	ANTIBODY DILUTIONS	BLOCK % IN TBS-T
β-actin[1]	42	1[ry] 1/5000 mouse monoclonal to β-actin 2[ry] anti-mouse 1/5000	5% milk overnight at 4°C 5% milk for 1 hour at RT
GFAP[2]	55	1[ry] 1/1000 rabbit polyclonal to GFAP 2[ry] anti-rabbit 1/5000	5% milk overnight at 4°C 5% milk for 1 hour at RT
p-c-Jun[3]	48	1[ry] 1/1000 rabbit polyclonal to p-c-Jun 2[ry] anti-rabbit 1/5000	5% milk overnight at 4°C 5% milk for 1 hour at RT
p-IκBα[3]	40	1[ry] 1/1000 rabbit polyclonal to p-IκBα 2[ry] anti-rabbit 1/5000	5% milk overnight at 4°C 5% milk for 1 hour at RT
p-JNK[3]	54 (upper) 46 (lower)	1[ry] 1/1000 rabbit polyclonal to p-JNK 2[ry] anti-rabbit 1/5000	5% milk overnight at 4°C 5% milk for 1 hour at RT
RAGE[2]	42	1[ry] 1/1000 rabbit polyclonal to RAGE 2[ry] anti-rabbit 1/5000	5% milk overnight at 4°C 5% milk for 1 hour at RT
1 = Sigma, UK 2 = Abcam, UK; 3 = Cell Signaling, US; RT = Room Temperature			

Table 2.3. Summary of Western immunoblotting protocol

ANTIBODY	HOST	REACTIVITY	STOCK IGG CONCENTRATION (MG/ML)	DILUTION
MHC II (OX6)[1]	mouse	rat	1.0	1/100
GFAP[1]	rabbit	rabbit	0.5	1/4000
CD11b (OX42)[1]	mouse	rat	1.0	1/1000
DAPI[2]	Reagent		1.0	1/1000
1 = Serotec, UK; 2 = Invitrogen, UK				

Table 2.4. Summary of immunofluorescent staining protocols

Chapter 3

3.1. Introduction

Aging is a natural process occurring in all living forms and accompanied by a progressive decline in the performance of physical tasks and neuronal function. The effects of the aging process can be observed in all organs and cells including neurons and neuroglia. Cellular senescence is associated with functional and structural changes in genome maintenance mechanisms, DNA damage signalling and metabolic and immune regulation (Sahin and Depinho, 2010). Aging is considered the principal risk factor for many chronic and neurodegenerative diseases including dementia. As human life expectancy increases due, in part, to improved medical care and diet, so does the prevalence of age-related pathologies such as AD.

AD is the most common type of dementia, affecting almost 35 million people worldwide with an estimated cost of US \$604 billion annually including both direct and indirect costs (Wimo and Prince, 2010). Main clinical symptoms include impaired memory, depression, poor judgement and confusion. Brains from individuals with AD are characterized by the presence of intracellular neurofibrillary tangles composed of hyperphosphorylated tau and extracellular plaques composed of $A\beta$ peptide.

$A\beta$ is a 4kDa naturally-occurring peptide derived from the sequential cleaving of the amyloid precursor protein (APP) by the endoproteases, β-secretase and γ-secretase. This enzymatic process results in the formation of several species of $A\beta$, with those cleaved at position 40 ($A\beta_{1-40}$) found to be the most abundant followed by those cleaved in position 42 ($A\beta_{1-42}$) (Selkoe, 2001). The production of $A\beta_{1-42}$ species is altered in AD and has been shown to be the main component of amyloid plaques (Luhrs et al., 2005). The $A\beta_{1-42}$ peptide is considered to be immunogenic and has been shown to induce oxidative stress and neurotoxicity (Butterfield, 2002). Mounting evidence suggest that oligomeric soluble forms of $A\beta$ are the most toxic and the effectors of synapse loss and neuronal injury (Walsh and Selkoe, 2007).

Different animal models have been developed to explore and help understand the changes related to accumulation of $A\beta$ observed in the brains of individuals with AD. As AD is a human-specific disorder, the animal models developed to study $A\beta$ cytotoxic effects tend to be induced, such as genetic mouse models of the APP mutation or icv injection of $A\beta$

peptides. It has been shown that acute infusion of large amounts of Aβ causes inflammatory reactions, glial activation and transient neurotoxicity (Frautschy et al., 1991), and that chronic infusion also exerts these changes (Frautschy et al., 1996).

Cognitive dysfunction, particularly memory loss, is one of the clinical symptoms of AD that causes most concern in affected individuals and their families. These changes are associated with evidence of impaired synaptic plasticity. Specifically, exogenously administration of Aβ, as well as accumulation of Aβ which occurs in animal models of Aβ, have been shown to be associated with decreased performance in the Morris water maze (Chen et al., 1996) and with impaired LTP (Shankar et al., 2008). Age-related changes have also been observed in spatial learning and in LTP. Aged individuals show a deficit in maintenance of LTP (Griffin et al., 2006) and in spatial learning (Chen et al., 2000a) compared with young animals; it is suggested that deficits in calcium regulation, reduced amplitude of presynaptic fibre potential and reduction in the number of perforant-path synaptic contacts on granule cells all contribute to these differences (Barnes, 2003).

As the brain ages it becomes less effective in overcoming challenges such as those produced by infections, traumas or surgeries, in part due to changes in the immune system which shows a functional decline with age. Microglia seem to be critical in this, as they possess both immune and neuroprotective properties; therefore, any consequence of microglial senescence is likely to be reflected in increased susceptibility to brain infections and neurodegenerative conditions (Streit and Xue, 2010). It has been shown that Aβ fibrils and oligomers stimulate inflammatory microglial signalling compromising neuronal survival (Sondag et al., 2009).

In addition to microglia, astrocytic activation has been observed with age and astrocytes are known to become reactive when in the presence of Aβ initiating an inflammatory response when surrounding extracellular amyloid plaques (Sastre et al., 2006). These findings suggest a poorly-regulated pro-inflammatory profile associated to the established pathological changes observed in AD (or prompted by Aβ) facilitated by a vulnerable immune system in aged individuals.

The aims of the study were to assess Aβ-induced and age-related changes on the brain of aged and young rats which received a chronic icv delivery of Aβ and to explore if this treatment or age exerted an effect on astrocytic and microglial markers.

3.2. Methods

Aged (18-22 months) and young (2-4 months) rats were infused icv for 28 days with Aβ or a control peptide (see section 2.2. for details). Animals were assessed for performance in the Morris water maze in 8x1-min trials on the first day and 6x1-min trials for the following 4 days when they were required to search for the hidden platform (see section 2.3. for details). After a 1 day recovery period rats were anaesthetized by an i.p. injection of urethane (1.5 g/kg) and LTP was recorded on the dorsal cell body region of the DG (see section 2.4. for details). At the end of the LTP recording, rats were killed by decapitation and the cortex and hippocampus were dissected from the right hemisphere. The tissue was prepared for mRNA analysis (see section 2.7. for details) or protein analysis (ELISA and Meso Scale; see sections 2.8. and 2.9. for details). The left hemisphere was used to prepare cryostat sections for immunofluorescent and immunohistochemical staining (see section 2.11. for details).

3.3. Results

3.3. Effects of chronic infusion of amyloid-β in aged and young rats.

3.3.1. *Aβ deposition in the brain parenchyma was observed in rats chronically infused with Aβ peptides.*

This study was undertaken to determine the effects of chronic (28 days) Aβ icv infusion on the brains of aged and young Wistar rats. The concentration of insoluble and soluble $A\beta_{1-38}$, $A\beta_{1-40}$ and $A\beta_{1-42}$ was measured in supernatants prepared from the hippocampus of Aβ-treated aged and young rats and analyzed using Meso Scale technology. Chronic infusion with Aβ significantly increased insoluble $A\beta_{1-42}$ concentration in tissue prepared from the hippocampus of Aβ-treated aged rats (286.1 ± 94.73pg/mg) compared with control-treated aged rats (70.22 ± 30.65pg/mg; $p<0.05$; ANOVA; Figure 3.1A) but not in the hippocampus of Aβ-treated young rats (55.11 ± 21.72pg/mg) compared with control-treated young rats (131.7 ± 43.8pg/mg; Figure 3.1A). Whereas concentrations of insoluble $A\beta_{1-40}$ prepared from the hippocampus of Aβ-treated aged rats (114.4 ± 37.39pg/mg) compared with control-treated aged rats (70.55 ± 25.22pg/mg; Figure 3.1B) and $A\beta_{1-38}$ prepared from the hippocampus of Aβ-treated aged rats (163.4 ± 61.95pg/mg) compared with control-treated aged rats (31.7 ± 13.06pg/mg) were also increased, these changes failed to reach statistical significance. No changes were observed in the concentration of insoluble $A\beta_{1-40}$ prepared from the hippocampus of Aβ-treated young rats (273 ± 148.1pg/mg) compared with control-treated young rats (179.1 ± 83.26pg/mg; Figure 3.1B) or $A\beta_{1-38}$ prepared from the hippocampus of Aβ-treated young rats (37.05 ± 11.47pg/mg) compared with control-treated young rats (86.05 ± 22.22pg/mg). No age-related significant differences in the hippocampal concentrations of insoluble $A\beta_{1-42}$, $A\beta_{1-40}$ and $A\beta_{1-38}$ were found between aged and young controls.

Chronic infusion with Aβ significantly increased soluble $A\beta_{1-40}$ concentration in tissue prepared from the hippocampus of Aβ-treated aged rats (30.29 ± 5.33pg/mg) compared with control-treated aged rats (16.8 ± 5.29pg/mg; $p<0.05$; ANOVA; Figure 3.1C) but not in the hippocampus of Aβ-treated young rats (10.91 ± 3.92pg/mg) compared with control-treated young rats (7.55 ± 2.66pg/mg; Figure 3.1C). Whereas concentrations of soluble $A\beta_{1-42}$ prepared from the hippocampus of Aβ-treated aged rats ($36.53 \pm$

7.42pg/mg) compared with control-treated aged rats (19.21 ± 1.8pg/mg; Figure 3.1D) and Aβ$_{1-38}$ prepared from the hippocampus of Aβ-treated aged rats (35.31 ± 9.03pg/mg) compared with control-treated aged rats (20.52 ± 5.45pg/mg) were also increased, these changes failed to reach statistical significance. No changes were observed in the concentration of soluble Aβ$_{1-42}$ prepared from the hippocampus of Aβ-treated young rats (25.64 ± 3.08pg/mg) compared with control-treated young rats (26.67 ± 4.46pg/mg; Figure 3.1D) and Aβ$_{1-38}$ prepared from the hippocampus of Aβ-treated young rats (21.85 ± 2.26pg/mg) compared with control-treated young rats (20.19 ± 4.16pg/mg). No age-related significant differences in the hippocampal concentrations of soluble Aβ$_{1-42}$, Aβ$_{1-40}$ and Aβ$_{1-38}$ were found between aged and young controls.

Predictably, the hippocampal concentration of insoluble Aβ$_{1-42}$, Aβ$_{1-40}$ and Aβ$_{1-38}$ was greater than the soluble forms.

3.3.2. Identification of immunoreactive structures in the brains of rats chronically infused with icv Aβ peptides through Congo red staining.

Cryostat sections obtained from the brains of aged and young rats infused icv for 28 days with Aβ were stained with Congo red to investigate the presence of fibrillar Aβ structures. Sparse immunoreactive structures suggestive of Aβ deposition were observed in the brains of Aβ-treated aged and young rats, appearing to be more prevalent in the aged animals. There was no evidence of immunoreactive structures in the brains of control-treated aged and young rats (Figure 3.2).

3.3.3. Escape latency in Morris water maze was not affected by chronic administration of Aβ.

Aged and young rats infused icv for 28 days with Aβ or a control peptide, were assessed for spatial memory in the Morris water maze. Rats in all treatment groups showed improvement in learning with time when the mean escape latencies on day 1 and day 5 were compared. A statistically significant reduction in the mean escape latency was observed in control-treated young rats (37.53 ±7.35s on day 1 compared with 12.73

±3.43s on day 5; p<0.01; Student t-test for dependent means), control-treated aged rats (50.71 ±3.53s on day 1 compared with 28.80 ±6.24s on day 5; p<0.05; Student t-test for dependent means) and Aβ-treated young rats (47.21 ±3.07s on day 1 compared with 12.62 ±3.30s on day 5; p<0.001; Student t-test for dependent means), but not in Aβ-treated aged rats (49.19 ±1.14s on day 1 compared with 36.82 ±6.35s on day 5; Student t-test for dependent means). No changes were observed on the mean escape latency from the Morris water maze on day 5 between Aβ-treated rats and control-treated rats for aged and young groups (ANOVA; Figure 3.3A). Similarly, no age-related changes on the mean escape latency from the Morris water maze on day 5 were observed between control-treated rats although a significant difference was found between Aβ-treated rats (p<0.05; ANOVA; Figure 3.3A). The swim speed of the animals was not affected by treatment or age in any of the groups (ANOVA; Figure 3.3B).

3.3.4. *Chronic treatment with Aβ affected LTP in aged and young rats.*

This experiment was undertaken by Dr. Thelma Cowley. The following results are mentioned as LTP was performed in the same experimental animals and provides additional evidence of the effects of treatment with Aβ on the brains of aged and young rats. LTP was recorded in the dorsal cell body region of the dentate gyrus and mean population epsp slope was analysed in order to investigate any effect of chronic icv infusion of Aβ. Mean population epsp slope was increased in all groups immediately after delivery of a high frequency train of stimuli to the perforant path and this increase was maintained for the duration of the experiment except in aged rats where it returned to baseline after about 15 min. Aβ-treated young rats showed a significant reduction of the mean epsp slope in the last 10 min of the experiment compared with control-treated young rats (115.9 ± 0.38% compared with 126.2 ± 0.47%; p<0.001; ANOVA) but the opposite was observed in aged rats, with a significant increase of the mean epsp slope in the last 10 min of the experiment in the Aβ-treated aged rats compared with the control-treated aged rats (121.7 ± 0.47% compared with 96.65 ± 0.62%; p<0.001; ANOVA). The mean epsp slope in the last 10 min of the experiment from the control-treated young rats

was significantly larger than control-treated aged rats (p<0.001; ANOVA) showing an age-related difference in LTP.

3.3.5. *Effects of chronic icv Aβ infusion on rat astrocytes.*

To assess the effects of Aβ on astroglial cells, expression of several astrocytic markers were investigated in tissue prepared from control or Aβ-treated animals. Hippocampal (p<0.01; ANOVA; Figure 3.4A) and cortical (p<0.05; ANOVA; Figure 3.4B) GFAP mRNA was significantly increased in control-treated aged rats compared with control-treated young rats. Treatment with Aβ further increased GFAP mRNA in the hippocampus of aged rats (p<0.05; ANOVA; Figure 3.4A) but not in young rats nor in the cortex.

Immunofluorescent staining intensity for GFAP was increased in the dentate gyrus (p<0.05; ANOVA; Figure 3.5B), hippocampus (p<0.05; ANOVA; Figure 3.6B) and cortex (p<0.05; ANOVA; Figure 3.7B) of Aβ-treated aged rats compared with control-treated aged rats; no difference was found between Aβ-treated young rats and control-treated young rats in any of the three brain regions studied. GFAP staining was slightly increased in the three studied brain regions in control-treated aged rats compared with control-treated young rats but the differences failed to reach statistical significance. No significant difference was found in the staining intensity for DAPI between any of the treatments.

S100β, and RAGE mRNA were also assessed in tissue prepared from these rats but no age- or Aβ-associated changes were observed (Figure 3.8). Aldh1L1, and EAAT2 mRNA were also assessed in tissue prepared from these rats but no age- or Aβ-associated changes were observed (Figure 3.9A and B).

3.3.6. *Effects of chronic icv Aβ infusion on rat microglia.*

To assess the effects of Aβ on microglial cells, mRNA expression of MHC II, CD11b and CD68 (used as markers of microglial activation) and the immunofluorescent staining intensity of MHC II, were measured. No change was observed in Aβ-treated young rats

compared with control-treated young rats but Aβ-treated aged rats showed a significant decrease in hippocampal CD11b mRNA compared with control-treated aged rats (p<0.05; ANOVA; Figure 3.10A). An age-related increase in the mRNA expression of CD11b was observed in the hippocampus of control-treated rats (p<0.01; ANOVA; Figure 3.10A). MHC II mRNA expression was increased in the hippocampus of Aβ-treated aged and young rats compared with control-treated aged and young rats but the differences failed to reach statistical significance (ANOVA; Figure 3.10B). No age-related changes were observed in hippocampal MHC II mRNA. No Aβ-treatment effects were observed in hippocampal CD68 mRNA of aged and young rats but a significant age-related increase was observed in control-treated rats (p<0.05; Student t-test for independent means; Figure 3.10C).

Immunofluorescent staining intensity for MHC II in the dentate gyrus showed no difference between Aβ-treated aged and young rats and control-treated aged and young rats (ANOVA; Figure 3.11B), but a significant age-related increase in mean fluorescence was observed in Aβ-treated aged rats compared with Aβ-treated young rats (p<0.05; ANOVA; Figure 3.11B). An age-related significant increase in mean fluorescence for MHC II in the cortex between control-treated aged rats and control-treated young rats was observed (p<0.01; Student t-test for independent means; Figure 3.12B). No Aβ-induced changes in cortical mean fluorescence for MHC II were observed in aged or young rats. No significant difference was found in the staining intensity for DAPI between any of the treatments.

3.3.7. *Effects of chronic icv Aβ infusion on the brain mRNA expression and protein concentration of pro-inflammatory cytokines.*

To study the inflammatory effects of Aβ, the mRNA expression and protein concentration of pro-inflammatory cytokines IL-1β, IL-6 and TNFα were evaluated in tissue prepared from control- and Aβ- treated aged and young rats.

IL-1β mRNA expression was increased in the hippocampus of Aβ-treated aged and young rats compared with control-treated aged and young rats but the differences failed to reach statistical significance; no age-related changes were observed (ANOVA; Figure

3.13A). IL-1β concentration was slightly increased in the hippocampus of Aβ-treated aged (44.7 ± 6.88pg/mg) and young (46.93 ± 11.4pg/mg) rats compared with control-treated aged (41.9 ± 4.69pg/mg) and young (42.3 ± 10.7pg/mg) rats but the differences failed to reach statistical significance; no age-related changes were observed (ANOVA; Figure 3.13B).

No significant difference in the hippocampal IL-6 mRNA expression of Aβ-treated aged and young rats compared with control-treated aged and young rats was found and no age-related changes were observed (ANOVA; Figure 3.13C). IL-6 concentration was found to be slightly increased in the hippocampus of Aβ-treated aged (436.3 ± 72.52pg/mg) and young (541.7 ± 93.03pg/mg) rats compared with control-treated aged (326.6 ± 54.85pg/mg) and young (453.8 ± 29.53pg/mg) rats but the differences failed to reach statistical significance; no age-related changes were observed (ANOVA; Figure 3.13D).

No significant difference in the hippocampal TNFα mRNA expression of Aβ-treated aged and young rats compared with control-treated aged and young rats was found and no age-related changes were observed (ANOVA; Figure 3.13E). TNFα protein concentration was found to be slightly decreased in the hippocampus of Aβ-treated aged (251.7 ± 28.23pg/mg) and young (257.5 ± 21.56pg/mg) rats compared with control-treated aged (332.5 ± 43.95pg/mg) and young (265.2 ± 35.93pg/mg) rats but the differences failed to reach statistical significance; no age-related changes were observed (ANOVA; Figure 3.13F).

IL-1β, IL-6 and TNFα mRNA was also evaluated in the cortex of control- and Aβ-treated aged and young rats but no treatment- or age-related differences were observed (Figure 3.14).

3.3.8. *Effects of chronic icv Aβ infusion on hippocampal RANTES mRNA expression.*

Hippocampal RANTES mRNA was significantly increased in control-treated aged rats compared with control-treated young rats (p<0.05; ANOVA; Figure 3.15) but no Aβ-associated changes were observed.

3.4. Discussion

The objective of this study was to determine the effects chronic icv treatment with Aβ has in the brains of aged and young rats and to explore age-related changes. The data showed that icv treatment with Aβ induced the appearance of immunoreactive structures accompanied with increased GFAP and decreased CD11b in the brains of aged, but not young rats; no changes were observed in other markers of microglial activation, spatial learning or in pro-inflammatory cytokines (Table 3.1).

Chronic infusion of Aβ led to accumulation of the insoluble form of $Aβ_{1-42}$ in the hippocampus of aged, but not young rats and this was accompanied by Aβ-immunoreactive structures stained with Congo red. Congo red only binds to the β-pleated sheet structure of fibrillar Aβ (Wilcock et al., 2006) and therefore, chronic delivery of Aβ led to formation of these accumulations. These data are similar to a previous finding which reported a similar accumulation of Aβ in brains of Sprague-Dawley female rats chronically infused with Aβ (Frautschy et al., 1996).

It has been shown that Aβ species $Aβ_{1-40}$ and $Aβ_{1-42}$ have distinctive pathways of assembly and oligomerization, with $Aβ_{1-42}$ species forming oligomers more readily than $Aβ_{1-40}$ (Bitan et al., 2003). $Aβ_{1-42}$ has been observed to be more prone to aggregation and plaque formation than $Aβ_{1-40}$ (Riek et al., 2001). These findings could help explain why the concentration of insoluble but not soluble $Aβ_{1-42}$ was significantly increased in Aβ-treated rats and why insoluble $Aβ_{1-40}$ was not increased.

Soluble Aβ concentrations were an order of magnitude lower than the insoluble concentrations in all the treated groups. This difference in concentration may be explained by the possibility that soluble Aβ is drained from the brain tissue into the CSF more easily than insoluble Aβ. Aβ concentration in the CSF has been thoroughly studied as a possible biomarker of AD both for the diagnosis and the prognosis of the disease. Research has consistently shown a reduction in $Aβ_{1-42}$ in the CSF of individuals with AD while the $Aβ_{1-40}$ peptide is normal or increased (Mattsson et al., 2009); one possible explanation for this is that $Aβ_{1-42}$ is deposited in plaques and not removed into the CSF (Grimmer et al., 2009).

Part of the role of the CSF is to maintain metabolic homeostasis through the removal of brain waste products and to maintain biochemical and nutritional balance (Kapoor et al., 2008). The flow of the CSF therefore serves as a drainage system running from the lateral ventricles into the arachnoid granulations and the venous sinus blood or the lymphatic system (Johnston and Papaiconomou, 2002). Ependymal cells are responsible for the production and surveillance of the CSF; bidirectional signalling and transporters have been reported in these cells (Spector, 2010). The CSF barrier seems to be affected with age becoming less functional. An increase in several amino acids measured in the CSF of aged, compared with young, sheep, as well as impaired amino acid transporters found in old animals, indicate an age-related compromise in the CSF barrier system which could increase the risk of neurotoxicity in the brain (Chen and Preston, 2010). This could help understand why no significant changes were found in insoluble or soluble Aβ concentrations in any of the treated groups of young rats, suggesting the CSF barrier in young animals copes better with the Aβ challenge.

The results presented in this study indicate that Aβ can be chronically delivered into the CSF and successfully transported into the brain of aged rats, although it is not clear which transporter or specific mechanism enables Aβ to cross from the CSF into the brain. A significant question is how Aβ moves through the interstitial brain fluids as it may reflect the way Aβ accumulation spreads in AD.

Analysis of spatial learning in the Morris water maze is a useful task to evaluate hippocampal-dependent function (Morris et al., 1982). The number of Aβ plaques and tau neurofibrillary tangles in the entorhinal cortex and hippocampus seem to correlate with impairment in memory performance in individuals with AD (Reitz et al., 2009). In this study, although chronic delivery of Aβ increased the concentration of insoluble $Aβ_{1-42}$ in the hippocampus of aged rats, no significant difference was found in the escape latency from Morris water maze between control and Aβ-treated rats. There are a number of possible explanations for this observation. Cleary and colleagues (2005) showed that natural soluble oligomers of Aβ protein specifically disrupt cognitive function in rats (Cleary et al., 2005); in the present study, all groups showed similar hippocampal concentrations of soluble $Aβ_{1-42}$ as opposed to insoluble $Aβ_{1-42}$ which was notably

elevated in the Aβ-treated animals and present at a much higher concentration. Although Aβ plaques development is one of the pathological features of AD and has been correlated with cognitive deficits (Chen et al., 2000a), it has been reported that about a third of non-demented older adults have Aβ deposition (Aizenstein et al., 2008). Whether these individuals are in a preclinical state of AD, or the Aβ aggregation is less harmful than that in AD patients is still not clear, but it suggests that the presence of Aβ alone may not be enough to cause severe cognitive deficits (Sperling et al., 2009). Aged, as opposed to young, rats in the present study showed a poorer ability to learn the localization of the hidden platform during the 5-day period training and this is consistent with other studies in which an age-related decline in water maze learning has been reported (Wyss et al., 2000, Kelly et al., 2003).

A critical aspect in the study of dementias is to understand the mechanisms that lead to cellular changes that impair the processes related to memory consolidation, formation and retrieval. LTP is a useful tool to evaluate the cellular substrates involved in memory considering that it is readily demonstrable in the hippocampus, that the naturally occurring theta rhythm recorded in the hippocampus during exploratory behavior can induce LTP, that inhibitors of hippocampal LTP also block hippocampal-dependent learning and that numerous biochemical changes that occur after LTP induction occur also during memory acquisition (Lynch, 2004). LTP has been shown to be attenuated with normal aging (Minogue et al., 2007, de Toledo-Morrell and Morrell, 1985), and data obtained from Dr. Cowley in this study, showed a mean percentage change in population epsp at the end of the experiment of 96% in aged controls compared with 126% of young controls. It has been shown in rats that there is an age-related decrease in the Schaffer collateral-evoked epsp which was correlated with poor spatial learning in the Morris water maze (Barnes et al., 2000), similar to the age-related decrease in LTP and spatial learning observed in this study. Surprisingly, the aged rats treated with Aβ were able to sustain LTP with an increase in epsp slope of about 30% compared with aged controls. The opposite was found in young rats, where Aβ treatment caused a significant attenuation in epsp slope of about 10% compared with controls.

LTP is a complex process that depends on several different cellular mechanisms so many possible explanations can be proposed to explain the deficit observed in Aβ-treated

86

young animals. The literature reports that Aβ attenuates LTP, as shown by Walsh and colleagues (2002), where Aβ oligomers inhibited hippocampal LTP *in vivo* at concentrations found in human brain and CSF (Walsh et al., 2002). LTP inhibition caused by treatment with $A\beta_{1-42}$ peptide has been observed both *in vivo* and *in vitro* (Klyubin et al., 2011). Perfusion with $A\beta_{1-40}$ and $A\beta_{1-42}$ has been shown to inhibit LTP induction in the dentate gyrus and CA1 region of rat hippocampal slices (Chen et al., 2000b), although there is evidence that low concentrations of $A\beta_{1-40}$ increase LTP *in vitro* (Wu et al., 1995). $A\beta_{1-42}$ has been shown to block LTP and post-tetanic stimulation induced by high-frequency stimulation but not by theta burst stimulation in mouse hippocampal slices (Smith et al., 2009) and that soluble oligomers of $A\beta_{1-42}$ inhibit LTP in rat hippocampal slices (Wang et al., 2002). It has also been shown that soluble oligomers of Aβ facilitate hippocampal LTD by disrupting neuronal glutamate uptake (Li et al., 2009). It is important, in the context of this study to note that $A\beta_{1-42}$ can impair spatial learning (Nagata et al., 2010).

In the present study, an increase in GFAP mRNA expression in the hippocampus was observed in Aβ-treated aged rats and this was accompanied by an increase in GFAP immunoreactivity in different brain areas. It is known that astrocytes are activated in response to brain injury or toxic stimuli exhibiting an increase in the expression of GFAP, a structural protein used as marker of astrocytic activity (Eng et al., 2000); such astrogliosis has been found in postmortem brains of AD patients where an increase in the phosphorylated and N-glysosylated acidic isoforms of GFAP has been described (Korolainen et al., 2005). Astrocytes, as well as neurons, from patients with AD, have been shown to accumulate $A\beta_{1-42}$ (Nagele et al., 2003), and *in vitro*, astrocytes are able to bind and internalize $A\beta_{1-42}$ (Nielsen et al., 2009); the evidence suggests that this astrocytic response towards $A\beta_{1-42}$ changes with age (Wyss-Coray et al., 2003). An age-related increase in cortical and hippocampal GFAP mRNA was observed in this study, similar to the finding by Amenta and colleagues (1998) which reported an increase in the number and size of GFAP-immunoreactive astrocytes in the frontal cortex and in the CA1 subfield of the hippocampus of aged, compared with adult, rats (Amenta et al., 1998). Astrocytes are evenly distributed in the brain, but GFAP-positive astrocytes are

more numerous in the cortex and hippocampus than in the brain stem (Taft et al., 2005). In AD, GFAP-positive astrocytes or astrocytes laden with Aβ seem to localize in the entorhinal cortex (Thal et al., 2000), and in the hippocampus (Ross et al., 2003). Here, the results were broadly consistent with this, with data showing that there was increased GFAP staining in the dentate gyrus, hippocampus and cortex of Aβ-treated aged, but not young, rats. Xu and colleagues (1999) showed that mouse astrocytes cultured for 9 days exhibited no increase in GFAP when exposed to Aβ, as opposed to astrocytes cultured for 30 days which exhibited GFAP upregulation (Xu et al., 1999). These observations suggest that the astrocytic response to Aβ is altered and depends on different factors including age.

S100β is a cytokine-like calcium-binding protein with neurotrophic functions expressed in astrocytes and used as a biomarker for brain damage and astrocytic activity (Nogueira et al., 2009). In this study, the hippocampal and cortical mRNA expression of S100β were not altered by treatment with Aβ. No age-related changes were observed in the hippocampal or cortical mRNA expression of S100β in this study. This contrasts with a study by Akhisaroglu and colleagues (2003) that showed an S100β age-related increase in the hippocampus of mice and humans (Akhisaroglu et al., 2003). S100β is correlated with dystrophic neurites in amyloid plaques in individuals with AD (Mrak et al., 1996), and it has been shown that overexpression of S100β exacerbates cerebral amyloidosis and gliosis in TG2576 mice (Mori et al., 2010). Aβ has been reported to induce intracellular calcium transients and spontaneous intercellular calcium waves in isolated astrocytes in purified cultures affecting both GFAP and S100β expression (Chow et al., 2010a). It is not clear why S100β is not increased in the aged or in the Aβ-treated animals while GFAP is. However, S100β is expressed in different cell types and is a less astrocyte-specific marker than GFAP (Steiner et al., 2007); this may help explain some of the results observed in this study. RAGE, the receptor for S100β, was not changed by treatment with Aβ consistent with the S100β findings.

RANTES (CCL5), a chemokine that binds to CCR5 receptor, promotes neuronal differentiation and has some neurotrophic properties in neurons, is released by astrocytes (Park et al., 2009). In this study, RANTES mRNA expression in hippocampus was

significantly increased in control-treated aged rats compared with control-treated young rats. Age-related increase in the expression of RANTES has been observed in humans in the thymus (Mello Coelho et al., 2009) but not in plasma, where concentrations remain stable with aging, with the exception of centenarians, where it is increased (Mariani et al., 2006, Gerli et al., 2000). In this study, RANTES mRNA expression was not significantly affected by treatment with Aβ in young and aged animals, this result differs from other reports that have shown Aβ stimulates the production of RANTES (Pellicano et al., 2010).

In this study, no marker of microglial activation was increased in the hippocampus of Aβ-treated rats and no cytokine or chemokine produced any significant variation from the other groups with the exception of CD11b mRNA, which was significantly reduced in hippocampus of aged rats. Although, CD11b, CD68 and MHCII were increased with age, it is not clear why microglia did not show signs of activation in the presence on Aβ as it has been reported that microglial cells become active and produce pro-inflammatory cytokines when in the presence of Aβ (Cameron and Landreth, 2010). One possible explanation may be that microglia reacts different to soluble or insoluble Aβ. Sondag and colleagues (2009) showed that fibrils and oligomers stimulate unique signalling responses in microglia; oligomers offered a differential secretory profile for IL-6, MCP-1 and keratinocyte chemoattractant when compared with fibrils (Sondag et al., 2009). Tau hyperphosphorylation and the formation of intracellular neurofibrillary tangles are also present in the pathology of AD and it has been shown that tau activates and elicits a pro-inflammatory response from microglia (Zilka et al., 2009). Tau was not explored in this study and the absence of neurofibrillary tangles may explain the observed reduction in the inflammatory response. Microglia require the presence of the purinergic receptor $P2X_7$ to become activated when in the presence of Aβ; changes in the dynamics of ATP and the interaction with $P2X_7$ may offer another explanation for the observed results (Sanz et al., 2009).

The reduction in the expression of CD11b mRNA in the presence of Aβ in this study may be related to the decreased pro-inflammatory activity of microglia; it is not clear why this is happening as it has been shown previously that Aβ increases the expression of CD11b in aged animals (Jimenez et al., 2008). A possible explanation involves iNOS as it has

been shown that NO stimulates the expression of CD11b (Roy et al., 2006) and when either NO is scavenged or iNOS inhibited then CD11b is not produced (Roy et al., 2008). It has been reported that $A\beta_{1-42}$ stimulates the expression of iNOS (Szaingurten-Solodkin et al., 2009). A recent study showed that microglial phagocytosis of $A\beta_{1-40}$ and $A\beta_{1-42}$ depends exclusively on the receptors LRP and CR3, of which CD11b is a structural component (Choucair-Jaafar et al., 2011), also, it has been observed that microglia have a diminished ability to phagocytose fibrillar $A\beta$ (Floden and Combs, 2006). These observations may help explain the reduction in the mRNA expression of CD11b and the lack of increased expression in CD68, taking into account that insoluble $A\beta$ was predominant in the hippocampus of $A\beta$-treated animals. An age-related increase in CD11b was reported in mice (Ruan et al., 2009), similar to the one found in this study.

MHC II was not increased in rats treated with $A\beta$, which contrasts with other findings where MHC II-positive microglia are associated with $A\beta$ plaques in patients with AD (Perlmutter et al., 1992) and where MHC II is increased in the hippocampus of young rats which received a single icv injection of $A\beta$ (Lyons et al., 2007). On the other hand, one report showed that activation of microglia by aggregated $A\beta$ or LPS decreases MHC II expression and this was attributed to selective death of MHC II-expressing microglia (Butovsky et al., 2005); although the study used only $A\beta_{1-40}$ and was done in hippocampal slices, as opposed to this study that used both $A\beta_{1-40}$ and $A\beta_{1-42}$, it may offer a possible explanation for the MHC II results. It is not clear why no age-related changes were observed in MHC II mRNA when a significant age-related increase in cortical fluorescence intensity for MHC II was present. An age-related increase in MHC II has been reported before (Sheffield and Berman, 1998).

CD68, a glycoprotein located mainly in endosomes and involved in phagocytosis, has been shown to be increased in physiological brain aging (Wong et al., 2005). In this study, CD68 showed an age-related increase in hippocampal mRNA but no changes were observed in $A\beta$-treated rats. The increase in CD68 with age and the lack of an $A\beta$-induced change parallels the changes in MHC II and CD11b.

Hippocampal concentrations of IL-1β, IL-6 and TNFα were not changed with age or $A\beta$ treatment. The observed lack of activation of microglia in this study could offer an

explanation for these results, as microglia are considered the main produces of pro-inflammatory cytokines in the brain (Aloisi, 2001).

The present findings indicate differences in the functional brain state of aged and young rats. Young rats seem to be able to cope notably better with the challenge of infused Aβ compared with aged rats. Although no major behavioural deficits were observed with Aβ treatment, changes in LTP and astrocytic markers suggest that chronic delivery of Aβ interferes with basic physiological brain processes. The results indicate Aβ treatment affects primarily astrocytes rather than microglia.
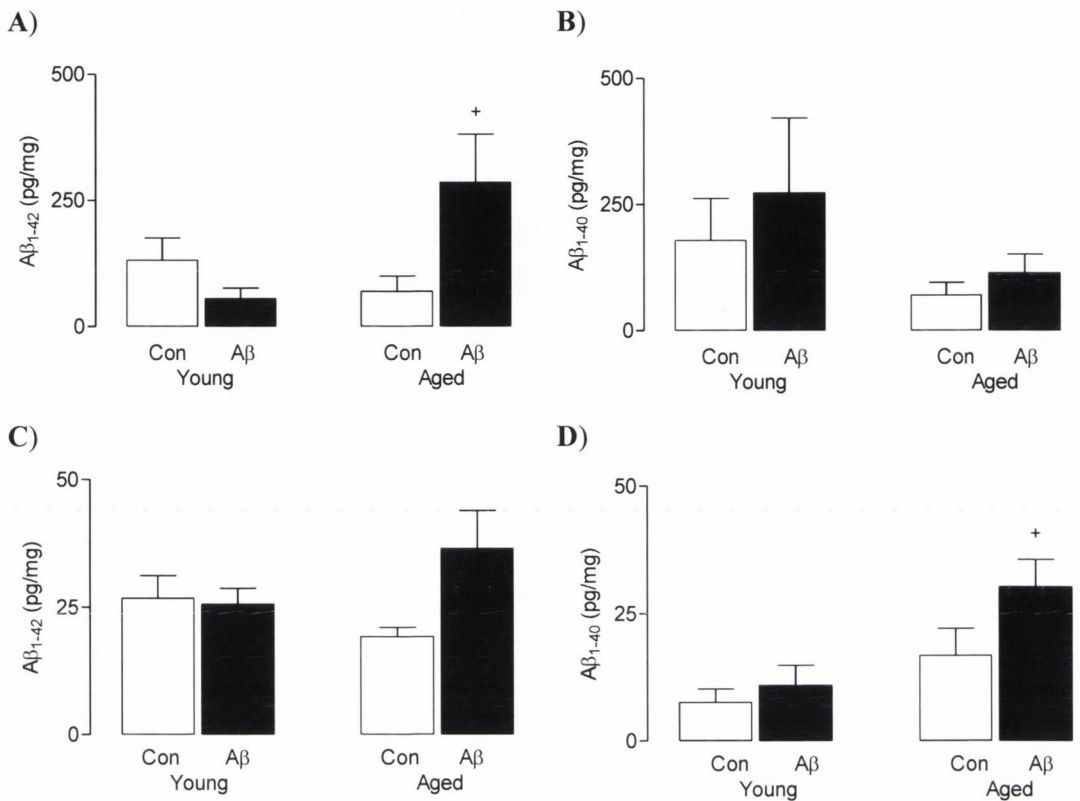
Figure 3.1 Insoluble and soluble Aβ deposition in the hippocampus of Aβ-treated rats

Hippocampal tissue was prepared from aged and young rats infused icv with Aβ or a control peptide for 28 days and assessed for insoluble Aβ. Data are presented as means ± SEM.

A) Insoluble $Aβ_{1-42}$ was significantly increased in the hippocampus of Aβ-treated aged rats compared with control-treated aged rats ($^+p<0.05$ vs. aged control; ANOVA). No significant differences were found between Aβ-treated young rats and control-treated young rats and no significant age-related changes were observed. ANOVA $F_{(3,22)} =3.486$, p=0.032; n=6 (control-treated aged and young rats) and n=7 (Aβ-treated aged and young rats).

B) No Aβ-treatment or age-related changes were observed in the concentration of insoluble $Aβ_{1-40}$ obtained from the hippocampal tissue of aged and young rats; ANOVA $F_{(3,19)} =0.852$, p=0.482; n=5 (control-treated young and Aβ-treated aged rats), n=6 (aged-treated controls) and n=7 (Aβ-treated aged rats).

C) No Aβ-treatment or age-related changes were observed in the concentration of soluble $Aβ_{1-42}$ obtained from the hippocampal tissue of aged and young rats; ANOVA $F_{(3,22)} =2.170$, p=0.120; n=6 (control-treated aged and young rats) and n=7 (Aβ-treated aged and young rats).

D) Soluble $Aβ_{1-40}$ was significantly increased in supernatants prepared from the hippocampus of Aβ-treated aged rats compared with control-treated aged rats ($^+p<0.05$ vs. aged control; ANOVA) No significant differences were found between Aβ-treated young rats and control-treated young rats and no significant age-related changes were observed. ANOVA $F_{(3,22)} =5.135$, p=0.007; n=6 (control-treated aged and young rats) and n=7 (Aβ-treated aged and young rats).

92
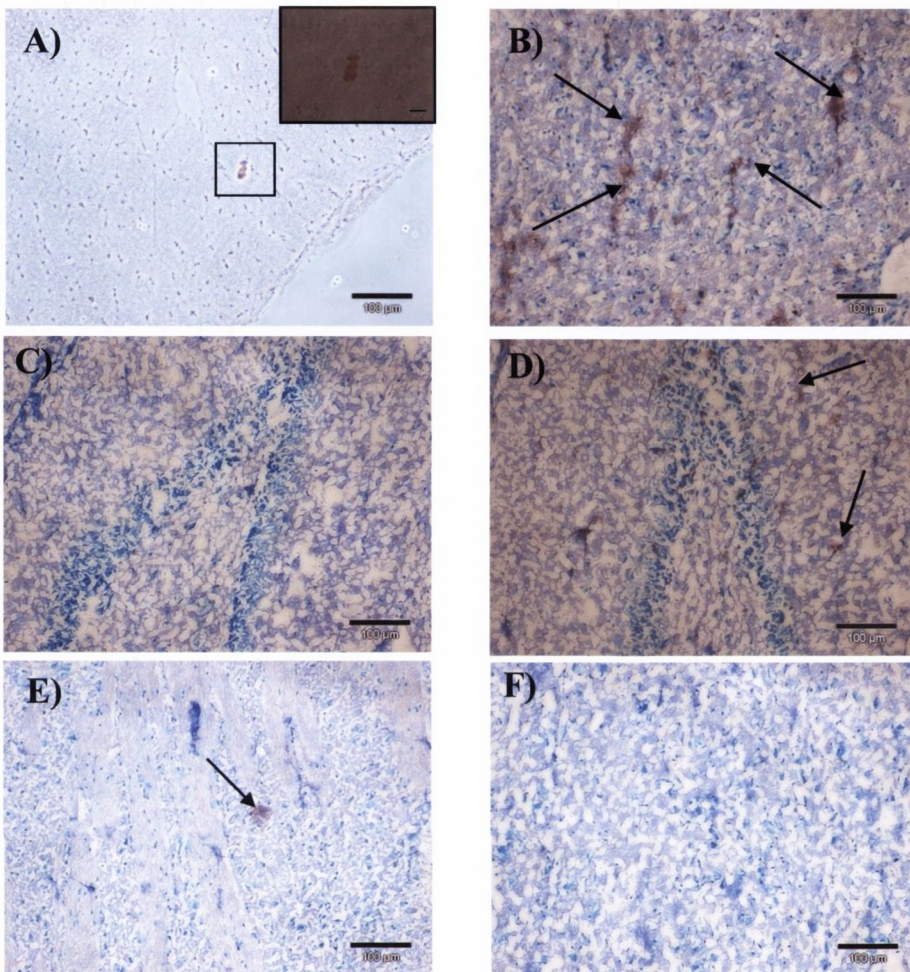
Figure 3.2 Congo red staining identified the presence of immunoreactive structures in the brains of Aβ-treated rats

Hippocampal tissue was prepared from aged and young rats infused icv with Aβ or a control peptide for 28 days and stained with Congo red to observe immunoreactive Aβ structures.

A) Immunoreactive structure in an Aβ-treated aged rat identified by Congo red staining (10X, scale bar 100μm; insert at 40X, scale bar 20μm). **B)** Immunoreactive structures (black arrows) in the cortex of an Aβ-treated aged rat (Congo red counterstained with methyl green; 10X, scale bar 100μm). **C)** Staining in the dentate gyrus of a control-treated aged rat (Congo red counterstained with methyl green; 10X, scale bar 100μm). **D)** Staining in the dentate gyrus of an Aβ-treated aged rat. Black arrows indicate immunoreactive structures (Congo red counterstained with methyl green; 10X, scale bar 100μm). **E)** Immunoreactive structure (black arrow) in the brain of an Aβ-treated young rat (Congo red counterstained with methyl green; 10X, scale bar 100μm). **F)** Staining in the cortex of a control-treated young rat. No immunoreactive structures were apparent (Congo red counterstained with methyl green; 10X, scale bar 100μm).

A)

B)
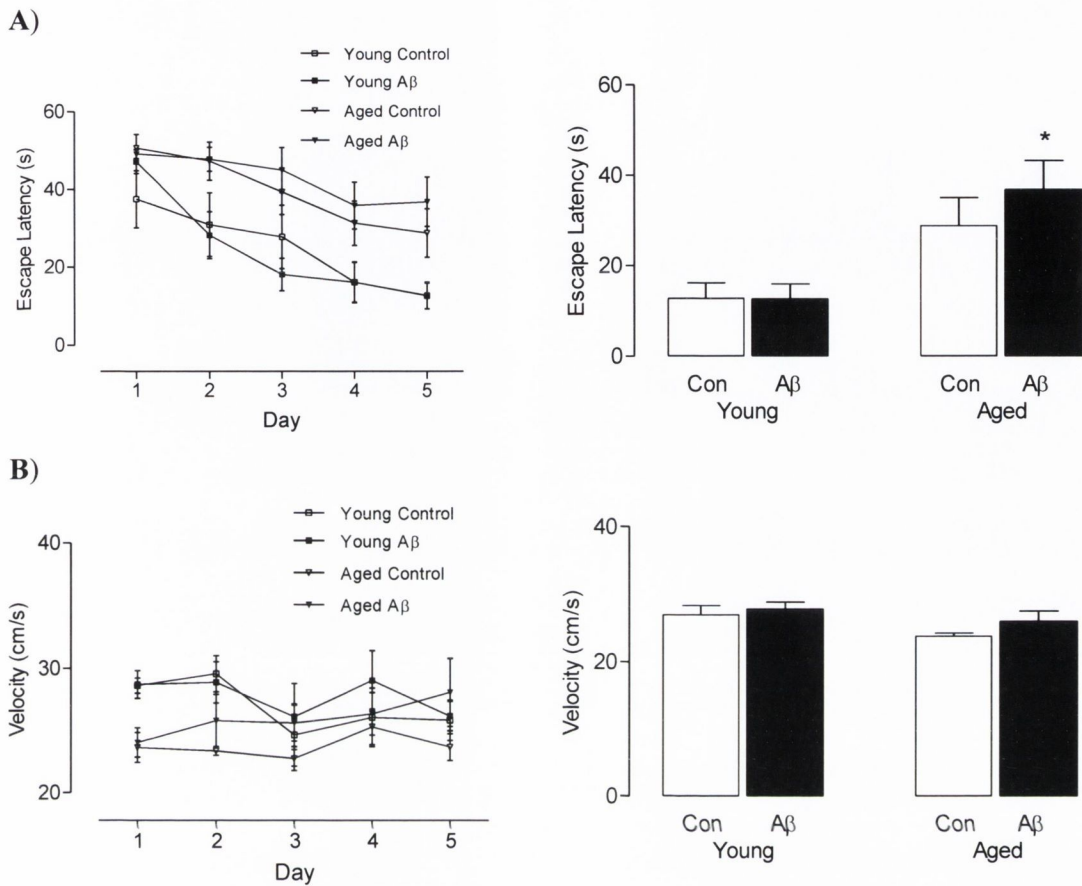
Figure 3.3 Spatial learning in the Morris water maze was not affected by chronic infusion of Aβ

Aged and young rats infused icv with Aβ or a control peptide for 28 days were assessed for spatial memory in the Morris water maze for 1 min. Data are presented as means ± SEM.

A) The mean escape latency was similar in all groups but a significant age-related increase was observed in Aβ-treated aged rats compared with Aβ-treated young rats (*p<0.05 vs. young Aβ; ANOVA $F_{(3,23)}$ =5.465, p=0.005; n=6 (control-treated young rats) and n=7 (control-treated aged rats and Aβ-treated aged and young rats)).

B) The mean swimming velocity was similar in all treatment groups; ANOVA $F_{(3,23)}$ =2.366, p=0.097; n=6 (control-treated young rats) and n=7 (control-treated aged rats and Aβ-treated aged and young rats).

A)
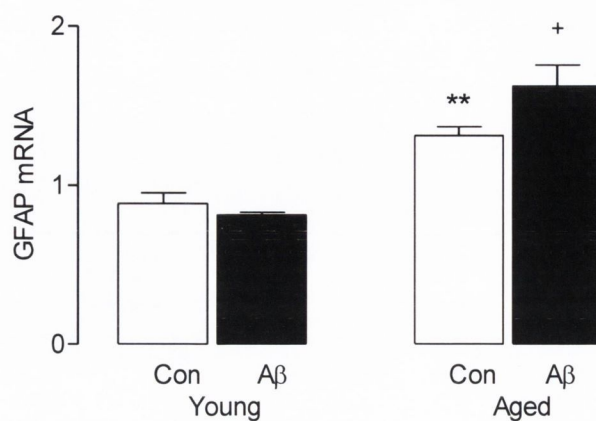
B)
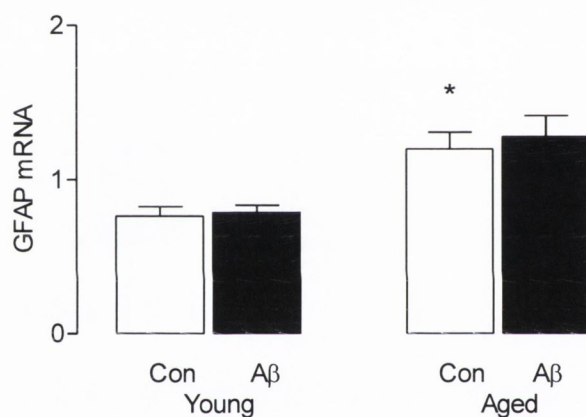
Figure 3.4 Age- and treatment- related changes in GFAP mRNA in rats chronically infused with Aβ

Hippocampal and cortical tissue was prepared from aged and young rats infused icv with Aβ or a control peptide for 28 days and assessed for GFAP mRNA. Data are presented as means ± SEM.

A) GFAP mRNA was significantly increased in hippocampus of control-treated aged rats compared with control-treated young rats (**p<0.01 vs. young controls) and in Aβ-treated aged rats compared with control-treated aged rats ($^{+}$p<0.05 vs. aged control). No Aβ-induced changes were observed in GFAP mRNA in young rats. ANOVA $F_{(3,21)}$ =25.19, p<0.0001; n=6 (control-treated aged and young rats and Aβ-treated aged rats) and n=7 (Aβ-treated young rats).

B) GFAP mRNA was significantly increased in cortex of control-treated aged rats compared with control-treated young rats (*p<0.01 vs. young controls). No Aβ-induced changes were observed in GFAP mRNA in aged or young rats. ANOVA $F_{(3,23)}$ =7.536, p=0.001; n=6 (control-treated young rats) and n=7 (control-treated aged rats and Aβ-treated aged and young rats).

A)
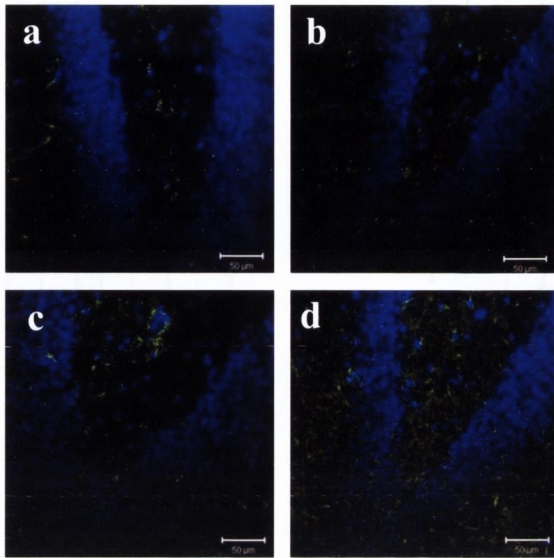
B)

Figure 3.5 GFAP fluorescent intensity was increased in the dentate gyrus of aged rats chronically infused with Aβ

Tissue from the dentate gyrus was prepared from aged and young rats infused icv with Aβ or a control peptide for 28 days and studied for the staining intensity of GFAP using confocal microscopy.

A) Images show immunofluorescence for GFAP (green) and DAPI (blue), used as counterstain, in the dentate gyrus. **a** control-treated young rat; **b** Aβ-treated young rat; **c** control-treated aged rat and **d** Aβ-treated aged rat (40x, scale bar 50μm). Images shown are representative of the replicates from each animal. Data are presented as means ± SEM.

B) Mean fluorescent staining intensity of GFAP in the dentate gyrus was significantly increased in Aβ-treated aged rats compared with control-treated aged rats ($^+$p<0.05 vs. aged control); no Aβ-treatment effects in young animals and no age-related changes were observed. ANOVA $F_{(3,18)}$ =4.415, p=0.017; n=5 (Aβ-treated young rats and control-treated aged rats) and n=6 (control-treated young rats and Aβ-treated aged rats).

96

A)

B)
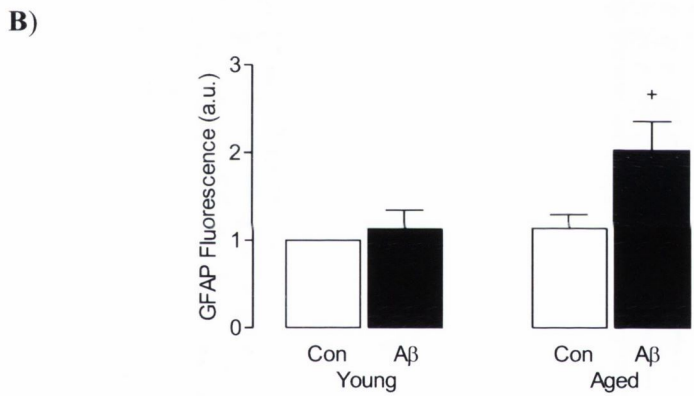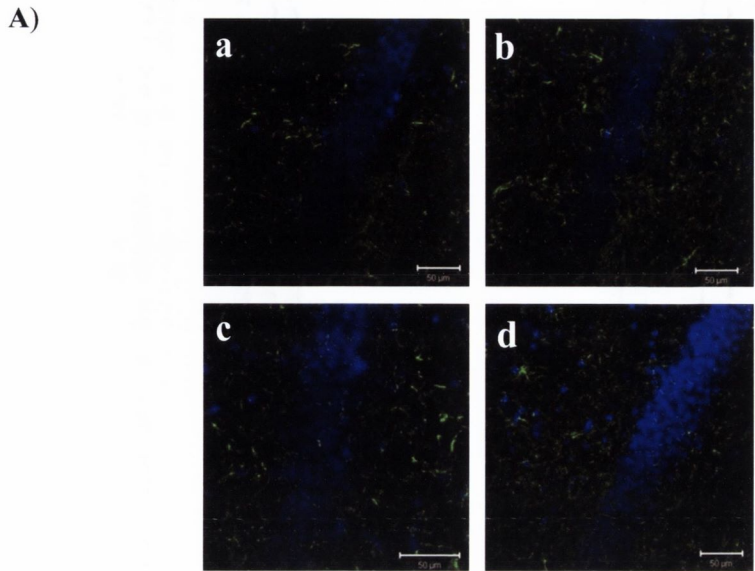
Figure 3.6 GFAP fluorescent intensity was increased in the hippocampus of aged rats chronically infused with Aβ

Hippocampal tissue was prepared from aged and young rats infused icv with Aβ or a control peptide for 28 days and studied for the staining intensity of GFAP using confocal microscopy. Data are presented as means ± SEM.

A) Images show immunofluorescence for GFAP (green) and DAPI (blue), used as counterstain, in the hippocampus. **a** control-treated young rat; **b** Aβ-treated young rat; **c** control-treated aged rat and **d** Aβ-treated aged rat (40x, scale bar 50μm). Images shown are representative of the replicates from each animal.

B) Mean fluorescent staining intensity of GFAP in the hippocampus was significantly increased in Aβ-treated aged rats compared with control-treated aged rats ($^+$p<0.05 vs. aged control); no Aβ-treatment effects in young animals and no age-related changes were observed. ANOVA $F_{(3,18)}$ =5.07, p=0.01; n=5 (Aβ-treated young rats and control-treated aged rats) and n=6 (control-treated young rats and Aβ-treated aged rats).

A)
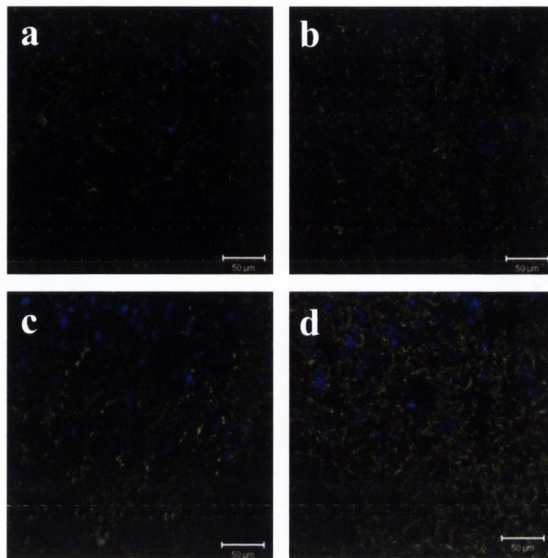
B)
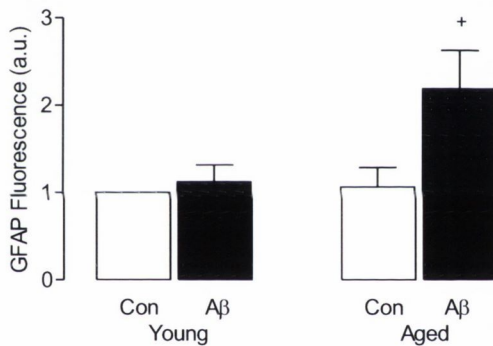
Figure 3.7 GFAP fluorescent intensity was increased in the cortex of aged rats chronically infused with Aβ

Cortical tissue was prepared from aged and young rats infused icv with Aβ or a control peptide for 28 days and studied for the staining intensity of GFAP using confocal microscopy. Data are presented as means ± SEM.

A) Images show immunofluorescence for GFAP (green) and DAPI (blue), used as counterstain, in the cortex. **a** control-treated young rat; **b** Aβ-treated young rat; **c** control-treated aged rat and **d** Aβ-treated aged rat (40x, scale bar 50μm). Images shown are representative of the replicates from each animal.

B) Mean fluorescent staining intensity of GFAP in the cortex was significantly increased in Aβ-treated aged rats compared with control-treated aged rats ([+]p<0.05 vs. aged control); no Aβ-treatment effects in young animals and no age-related changes were observed. ANOVA $F_{(3,18)}$ =4.488, p=0.016; n=5 (Aβ-treated young rats and control-treated aged rats) and n=6 (control-treated young rats and Aβ-treated aged rats).
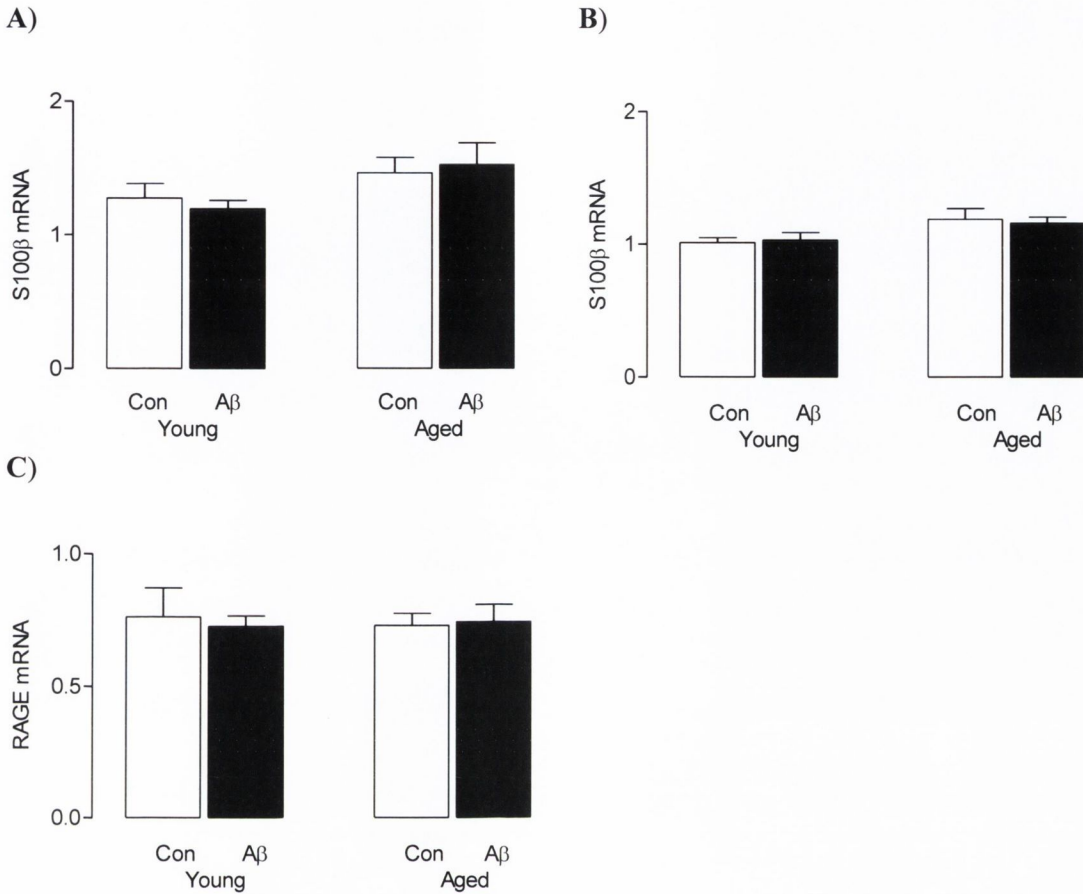
Figure 3.8 No age- or treatment- related changes in S100β or RAGE mRNA were found in rats chronically infused with Aβ

Hippocampal and cortical tissue was prepared from aged and young rats infused icv with Aβ or a control peptide for 28 days and assessed for S100β or RAGE mRNA. Data are presented as means ± SEM.

No age- or Aβ-associated changes were observed in S100β mRNA in hippocampus (**A**) or cortex (**B**) or in RAGE mRNA in hippocampus (**C**).

A)

B)
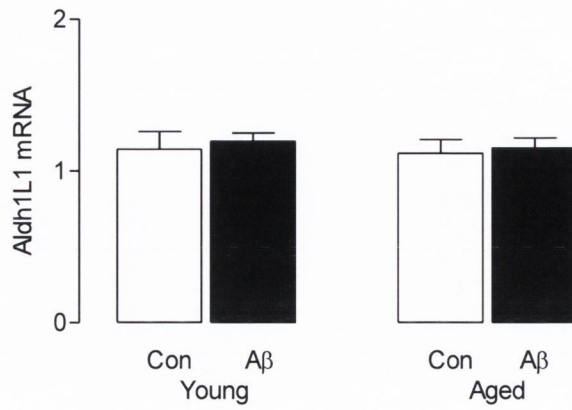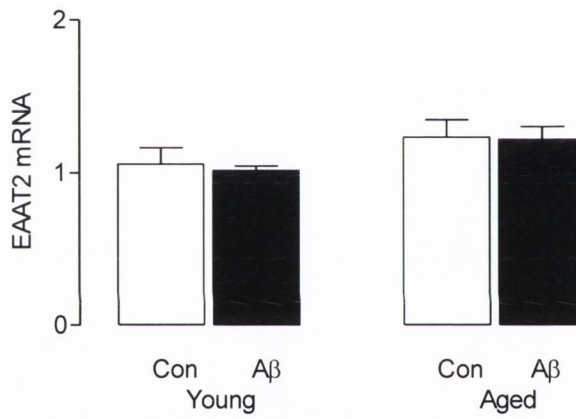
Figure 3.9 No Aβ-treatment related changes in Aldh1L1 or EAAT2 mRNA were found in rats chronically infused with Aβ

Cortical tissue was prepared from aged and young rats infused icv with Aβ or a control peptide for 28 days and assessed for Aldh1L1 and EAAT2 mRNA. Data are presented as means ± SEM.

No age- or Aβ-associated changes were observed in Aldh1L1 mRNA (**A**) or in EAAT2 mRNA (**B**) in cortex.
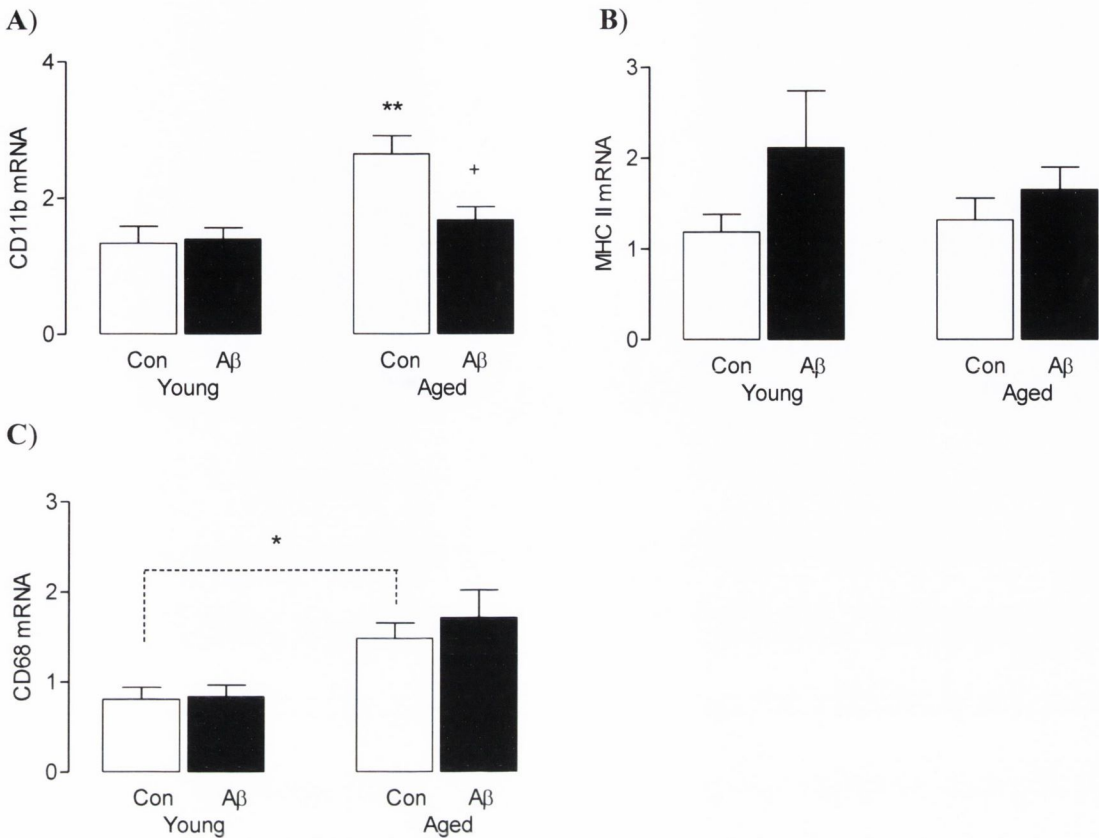
Figure 3.10 Aβ-treatment and age-related effects in mRNA of microglial markers in rats chronically infused with Aβ

Hippocampal tissue was prepared from aged and young rats infused icv with Aβ or a control peptide for 28 days and assessed for CD11b, MHC II or CD68 mRNA. Data are presented as means ± SEM.

A) CD11b mRNA was significantly increased in hippocampus of control-treated aged rats compared with control-treated young rats (**p<0.01 vs. young controls); this was significantly attenuated with Aβ-treatment (⁺p<0.05 vs. aged control). No Aβ-induced changes were observed in CD11b mRNA in young rats. ANOVA $F_{(3,22)}$ =7.787, p=0.001; n=6 (control-treated young rats and Aβ-treated aged rats) and n=7 (Aβ-treated young rats and control-treated aged rats).

B) No age- or Aβ-associated changes were observed in MHC II mRNA in hippocampus.

C) CD68 mRNA was significantly increased in hippocampus of control-treated aged rats compared with control-treated young rats (*p<0.05 vs. young control; Student t-test for independent means; n=6 (control-treated young rats) and n=7 (control-treated aged rats and Aβ-treated aged and young rats)); no Aβ-induced changes were observed in CD68 mRNA in aged or young rats. Dotted line represents the Student t-test analysis.

A)
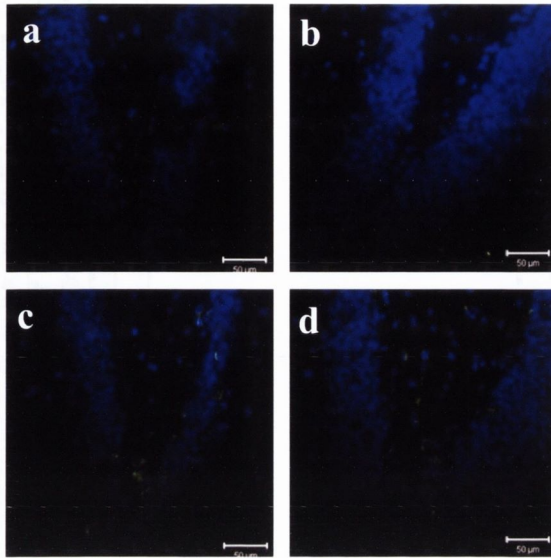
B)

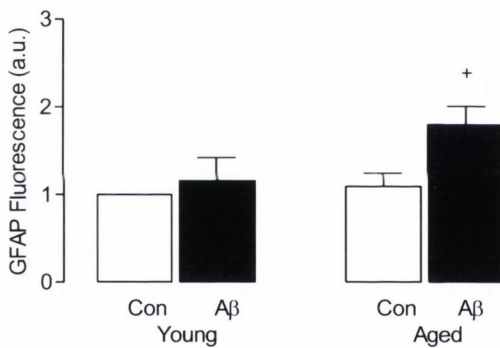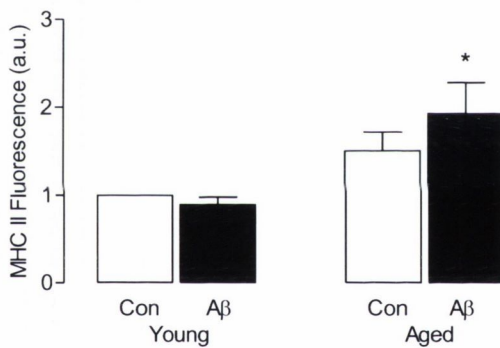**Figure 3.11 MHC II fluorescent intensity in the dentate gyrus of rats chronically infused with Aβ**

Tissue from the dentate gyrus was prepared from aged and young rats infused icv with Aβ or a control peptide for 28 days and studied for the staining intensity of MHC II using confocal microscopy. Data are presented as means ± SEM.

A) Images show immunofluorescence for MHC II (green) and DAPI (blue), used as counterstain, in the dentate gyrus. **a** control-treated young rat; **b** Aβ-treated young rat; **c** control-treated aged rat and **d** Aβ-treated aged rat (40x, scale bar 50 μm). Images shown are representative of the replicates from each animal.

B) Mean fluorescent staining intensity of MHC II in the dentate gyrus was significantly increased in Aβ-treated aged rats compared with Aβ-treated young rats (*p<0.05 vs. young Aβ); no Aβ-induced change was found in young rats. ANOVA $F_{(3,16)}$ =4.26, p=0.320; n=4 (Aβ-treated young rats), n=5 (control-treated young rats and Aβ-treated aged rats) and n=6 (control-treated aged rats).

A)
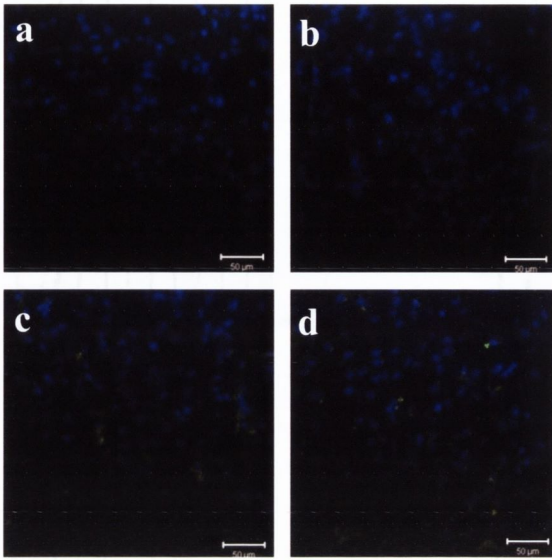
B)
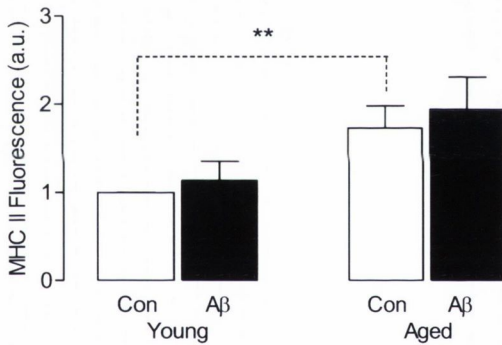
Figure 3.12 MHC II fluorescent intensity in the cortex of rats chronically infused with Aβ

Cortical tissue was prepared from aged and young rats infused icv with Aβ or a control peptide for 28 days and studied for the staining intensity of MHC II using confocal microscopy. Data are presented as means ± SEM.

A) Images show immunofluorescence for MHC II (green) and DAPI (blue), used as counterstain, in the cortex. **a** control-treated young rat; **b** Aβ-treated young rat; **c** control-treated aged rat and **d** Aβ-treated aged rat (40x, scale bar 50µm). Images shown are representative of the replicates from each animal.

B) Mean fluorescent staining intensity of MHC II in the cortex was significantly increased in control-treated aged rats compared with control-treated young rats (**p<0.01 vs. young control; Student t-test for independent means; n=5 (Aβ-treated aged and young rats), n=6 (control-treated aged rats) and n=7 (control-treated young rats)). No Aβ-induced changes were found in aged or young rats. Dotted line represents the Student t-test analysis.
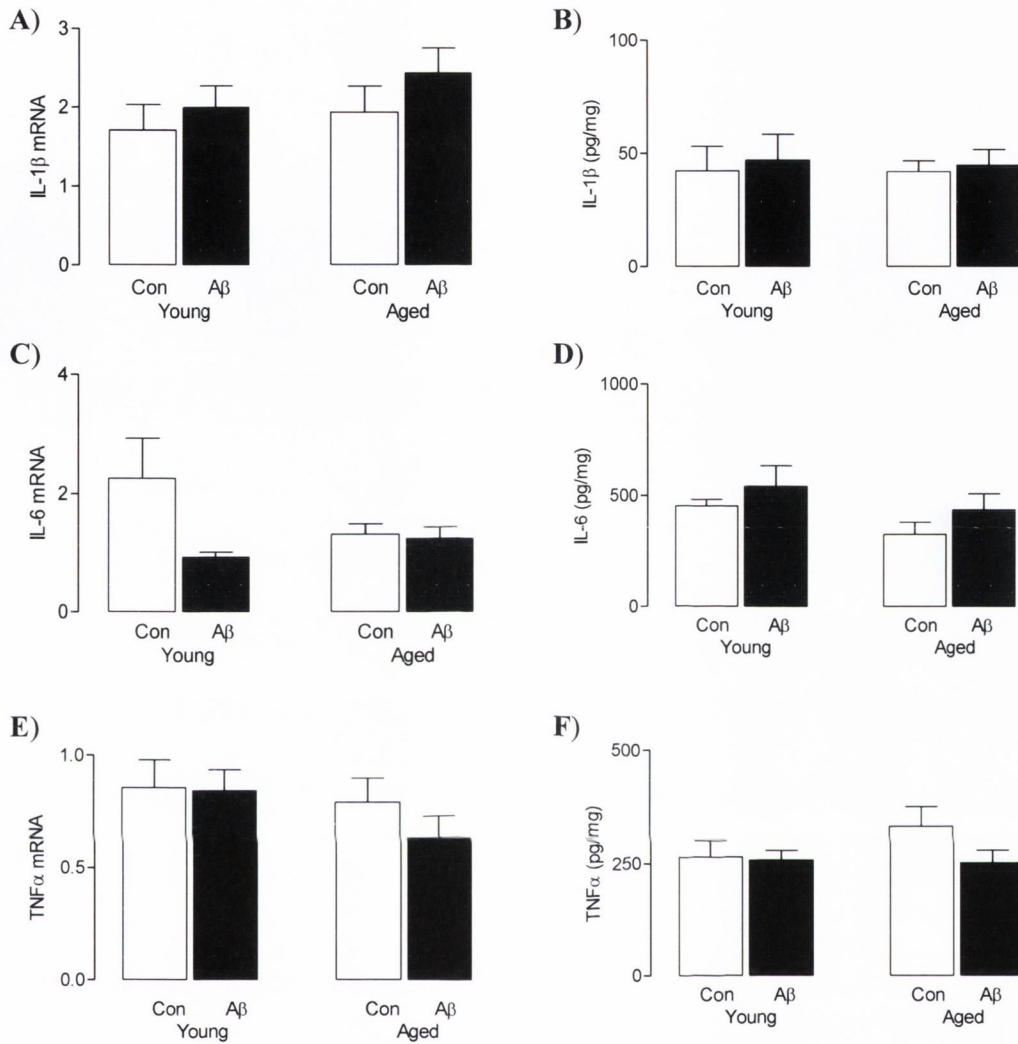
Figure 3.13 Chronic infusion of Aβ did not affect hippocampal mRNA or supernatant concentration of pro-inflammatory cytokines in treated rats.

Hippocampal tissue was prepared from aged and young rats infused icv with Aβ or a control peptide for 28 days and assessed for IL-1β, IL-6 and TNFα mRNA and supernatant concentration. Data are presented as means ± SEM.

No age- or Aβ-associated changes were observed in IL-1β mRNA (**A**) or supernatant concentration (**B**) in hippocampus.

No age- or Aβ-associated changes were observed in IL-6 mRNA (**C**) or supernatant concentration (**D**) in hippocampus.

No age- or Aβ-associated changes were observed in IL-1β mRNA (**E**) or supernatant concentration (**F**) in hippocampus.
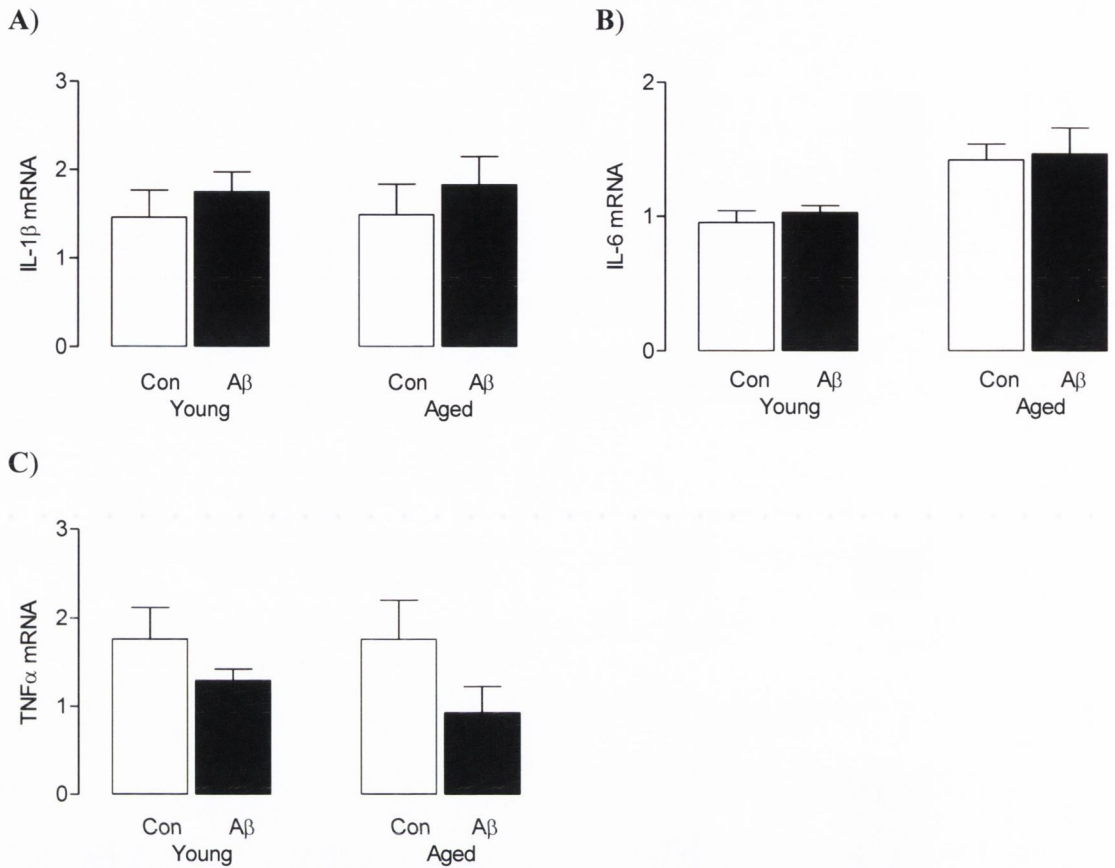
Figure 3.14 Chronic infusion of Aβ did not affect cortical, IL-1β, IL-6 or TNFα mRNA in treated rats.

Cortical tissue was prepared from aged and young rats infused icv with Aβ or a control peptide for 28 days and assessed for IL-1β, IL-6 or TNFα mRNA. Data are presented as means ± SEM.

No age- or Aβ-associated changes were observed in IL-1β (**A**), IL-6 (**B**) or TNFα (**C**) mRNA in cortex.
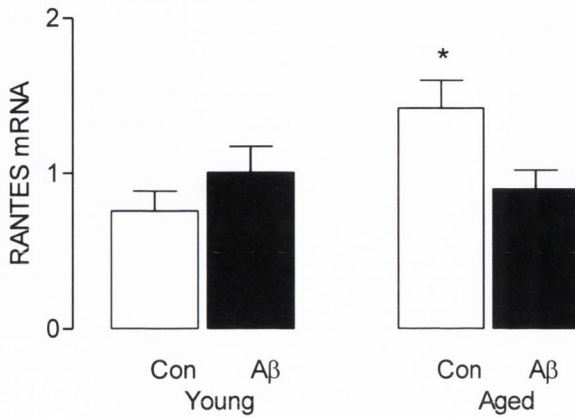
Figure 3.15 An age-related increase in RANTES mRNA was found in rats chronically infused with Aβ

Hippocampal tissue was prepared from aged and young rats infused icv with Aβ or a control peptide for 28 days and assessed for RANTES mRNA. Data are presented as means ± SEM.

RANTES mRNA was significantly increased in the hippocampus of control-treated aged rats compared with control-treated young rats (*p<0.01 vs. young controls). No Aβ-induced changes were observed in RANTES mRNA in aged or young rats. ANOVA $F_{(3,17)}$ =3.403, p=0.041; n=4 (control-treated young rats), n=5 (Aβ-treated young rats) and n=6 (control-treated aged rats and Aβ-treated aged and rats).

	BRAIN REGION	AGE-RELATED CHANGES	$A\beta$	
			YOUNG	AGED
Insoluble $A\beta_{1-42}$	Hippocampus	No changes	No changes	**Increased**
Insoluble $A\beta_{1-40}$	Hippocampus	No changes	No changes	No changes
Soluble $A\beta_{1-42}$	Hippocampus	No changes	No changes	No changes
Soluble $A\beta_{1-40}$	Hippocampus	No changes	No changes	**Increased**
Escape latency Morris water maze	———	No changes	No changes	No changes
Swimming velocity	———	No changes	No changes	No changes
GFAP mRNA	Hippocampus	**Increased**	No changes	**Increased**
GFAP mRNA	Cortex	**Increased**	No changes	No changes
GFAP fluorescence	Dentate gyrus	No changes	No changes	**Increased**
GFAP fluorescence	Hippocampus	No changes	No changes	**Increased**
GFAP fluorescence	Cortex	No changes	No changes	**Increased**
S100β mRNA	Hippocampus	No changes	No changes	No changes
S100β mRNA	Cortex	No changes	No changes	No changes
RAGE mRNA	Hippocampus	No changes	No changes	No changes
Aldh1L1 mRNA	Cortex	No changes	No changes	No changes
EAAT2 mRNA	Cortex	No changes	No changes	No changes
CD11b mRNA	Hippocampus	**Increased**	No changes	**Decreased**
CD68 mRNA	Hippocampus	**Increased**	No changes	No changes
MHC II mRNA	Hippocampus	No changes	No changes	No changes
MHC II fluorescence	Dentate gyrus	No changes	No changes	No changes
MHC II fluorescence	Cortex	**Increased**	No changes	No changes
IL-1β mRNA	Hippocampus	No changes	No changes	No changes
IL-1β protein	Hippocampus	No changes	No changes	No changes
IL-6 mRNA	Hippocampus	No changes	No changes	No changes
IL-6 protein	Hippocampus	No changes	No changes	No changes
TNFα mRNA	Hippocampus	No changes	No changes	No changes
TNFα protein	Hippocampus	No changes	No changes	No changes
IL-1β mRNA	Cortex	No changes	No changes	No changes
IL-6 mRNA	Cortex	No changes	No changes	No changes
TNFα mRNA	Cortex	No changes	No changes	No changes
RANTES mRNA	Hippocampus	**Increased**	No changes	No changes

Table 3.1   Summary of results Chapter 3.

Summary of the data presented in this chapter. Highlighted in bold are results which reached a statistically significant difference.

Chapter 4

4.1. Introduction

In addition to neurons, the cellular universe of the nervous system is populated by a diverse group of glia. Astrocytes (which are the focus of this chapter) are the most abundant type of glial cells, proliferating during brain development or under pathological circumstances when this is described as reactive astrogliosis (Guizzetti et al., 2011). Astrocytes can be found throughout the whole CNS, showing distinctive phenotypes according to the anatomical localization. Gray matter astrocytes, also called protoplasmic astrocytes, are derived from radial glia and possess many branching processes, which envelop synapses and cover blood vessels, as opposed to white matter astrocytes, also called fibrous, which have long unbranched processes that envelop nodes of Ranvier (Wang and Bordey, 2008).

The morphological diversity of astrocytes is also reflected in their numerous functions. Conventionally, astrocytes are considered to be the cells which provide nutritional and structural support for neurons, but in addition to these well-known properties, astrocytes also are known to be involved in regulation of neurotransmitters (particularly glutamate), buffering of K^+, inter and intracellular communication, synapse maintenance, plasticity, neurogenesis and immune regulation, among others (Seth and Koul, 2008).

Because of the fundamental role of astrocytes in brain function their activity is related to many pathological processes including neurodegenerative disorders such as AD. The presence of activated astrocytes surrounding amyloid plaques has been found in human brains with AD (Nagele et al., 2004). In a triple transgenic mouse model for AD (mutant for APP, PSEN 1 and tau), reactive hypertrophic astrocytes surround the neuritic plaques and astroglial cells throughout the brain parenchyma exhibit signs of atrophy (Rodriguez et al., 2009). Astrocytes have also been shown to react in the presence of Aβ internalizing and accumulating $A\beta_{1-42}$ (Nagele et al., 2003).

Microglia are considered to be the principal immune cells and the main producers of cytokines and chemokines within the nervous system, but astrocytes contribute to, and help coordinate, the inflammatory reaction. There is evidence of direct bi-directional communication between astrocytes and microglia including functional regulation that modulates phagocytic activity of Aβ in microglia (Terwel et al., 2011). In addition to microglial production of pro-inflammatory cytokines, cultured astrocytes incubated in the

presence of stimuli such as LPS and Aβ, also produce cytokines (Suzumura et al., 2006, Howlett et al., 2011).

The aims of this study were to assess the production of pro-inflammatory cytokines from isolated astrocytes treated with Aβ and investigate the signalling pathways involved in this process.

4.2. Methods

Isolated astrocytes were obtained from the cortices of neonatal rats and plated into 24-well plates following the protocol detailed in section 2.6.3. Astrocytes were pre-treated with wedelolactone (50μM) (Figure 4.1.) or D-JNKi1 (2μM) (Figure 4.2.) for 1 hour and then incubated in the presence of Aβ (Aβ$_{1-40/1-42}$) or DMEM for 24 hours. To evaluate the time-dependent nature of the response to Aβ, astrocytes were incubated with Aβ for 40 min, 120 min, 240 min, 360 min or 24 hours. IL-1β, IL-6, TNFα, GFAP, Aldh1L1 and EAAT2 mRNA prepared from the cell lysate were measured by PCR (see section 2.7. for details). The supernatant concentration of the cytokines was determined by ELISA (see section 2.8. for details). GFAP, RAGE and the phosphorylated forms of IκBα, JNK, and c-Jun were determined by western immunoblotting (see section 2.10. for details). The MTS assay was used to determine cell viability in astrocytes treated with Aβ (see section 2.6.6. for details). Isolated astrocytes and microglia were plated into coverslips, prepared for confocal microscopy and co-stained with GFAP and CD11b and counterstained with DAPI (see section 2.11 for details).

4.3. Results

4.3. Pro-inflammatory effects of Aβ in isolated rat cortical astrocytes

4.3.1. *Characterization of cultured rat isolated astrocytes*

Primary cortical glial cells were prepared from the cortices of neonatal Wistar rats. Isolated astrocytes and microglia were prepared and plated into coverslips in 24-well plates (see section 2.6. for details). In order to characterize the cells, the coverslips containing the isolated astrocytes were prepared for confocal microscopy and co-stained for GFAP, an specific marker for astrocytes, and CD11b, an specific marker for microglial cells. The confocal images obtained showed a distinctive GFAP staining with a lack of CD11b staining in the isolated astrocytes (Figure 4.3). The blue-fluorescent DAPI nucleic acid stain was used as counterstain to visualize the nuclei of the cells. FACS analysis performed by Dr. Thelma Cowley revealed that this culture protocol yielded a 95% pure population of astrocytes.

4.3.2. *Effect of Aβ on the cell viability of isolated rat cortical astrocytes*

To explore the effects of Aβ on cell viability, isolated astrocytes were incubated for 24 hours in the presence of $A\beta_{1-40}$, $A\beta_{1-42}$, Aβ cocktail or DMEM. The wells containing the astrocytes had the tetrazolium compound, MTS, added to the supernatants and incubated for 2 hours. The absorbance from the colorimetric reaction was measured and the findings indicated that Aβ-treatment had no effect on the cell viability of isolated astrocytes as no significant changes in the relative absorbance were observed between the Aβ-treated groups and the controls (ANOVA; Figure 4.4).

4.3.3. *Effect of Aβ on cytokine release from isolated rat cortical astrocytes*

To explore the role of Aβ as a stimulator of responses in astroglial cells, isolated astrocytes were incubated in the presence of Aβ or DMEM. The Aβ-treated cells were

harvested at different time points (40 min, 120 min, 240 min, 360 min or 24 hours) and the supernatant concentrations of IL-1β, IL-6 and TNFα were measured.

IL-1β concentration was significantly increased in supernatants prepared from Aβ-treated astrocytes at 360 min (37.68 ± 7.03pg/ml; $p<0.05$; ANOVA) and 24 hours (74.28 ± 12.85pg/ml; $p<0.001$; ANOVA) compared with astrocytes which were incubated in medium alone (11.6 ± 8.08pg/ml; Figure 4.5A). IL-6 concentration was significantly increased in supernatants prepared from Aβ-treated astrocytes at 120 min (137.3 ± 38.84pg/ml; $p<0.001$; ANOVA), 360 min (120 ± 27.51pg/ml; $p<0.001$; ANOVA) and 24 hours (137.1 ± 24.66pg/ml; $p<0.001$; ANOVA) compared with controls (24.17 ± 12.58pg/ml; Figure 4.5B). TNFα concentration was significantly increased in supernatants prepared from Aβ-treated astrocytes at 240 min (74.82 ± 16.44pg/ml; $p<0.01$; ANOVA), 360 min (107.6 ± 18.89pg/ml; $p<0.001$; ANOVA) and 24 hours (80.37 ± 26.55pg/ml; $p<0.001$; ANOVA) compared with controls (34.05 ± 19.82pg/ml; Figure 4.5C).

4.3.4. *Effect of Aβ on intracellular signalling pathways in isolated rat cortical astrocytes*

To further explore the inflammatory effects of Aβ, isolated astrocytes were incubated in the presence of Aβ or DMEM for 40 min, 120 min, 240 min, 360 min or 24 hours. Phosphorylated forms of IκBα, JNK and c-Jun as well as GFAP and RAGE were determined by western immunoblotting.

IκBα phosphorylation was significantly increased at 240 min ($p<0.05$; ANOVA), 360 min ($p<0.01$; ANOVA) and 24 hours ($p<0.01$; ANOVA) in Aβ-treated astrocytes compared with controls suggesting that Aβ lead to the activation of NFκB (Figure 4.6B). JNK phosphorylation was significantly increased at 40 min ($p<0.001$; ANOVA) in Aβ-treated isolated astrocytes compared with controls (Figure 4.6D) and c-Jun phosphorylation was also significantly increased at this time point ($p<0.01$; ANOVA) and at 120 min ($p<0.05$; ANOVA) and 240 min ($p<0.05$; ANOVA; Figure 4.7B). GFAP (ANOVA; Figure 4.8B) and RAGE (ANOVA; Figure 4.9B) were not affected by Aβ at any of the time points studied.

4.3.5. Effects of wedelolactone in rat astrocytes treated with Aβ

To further explore the consequences of the effects of Aβ on NF-κB activation, astrocytes were pre-treated with wedelolactone (50μM) for 1 hour and incubated in the presence of Aβ or DMEM for 24 hours. Wedelolactone inhibits IKK, a kinase critical for the activation of NF-κB by triggering phosphorylation of IκBα. Supernatant concentrations and mRNA expression of IL-1β, IL-6 and TNFα were assessed. In addition, Aldh1L1, EAAT2 and GFAP mRNA was assessed in harvested cells. To confirm the action of wedelolactone, the phosphorylated form of IκBα was determined by western immunoblotting in cell lysates.

IL-1β mRNA was significantly increased in Aβ-treated isolated astrocytes compared with controls ($p < 0.01$; ANOVA; Figure 4.10A); pre-treatment with wedelolactone significantly attenuated the Aβ-induced increase in IL-1β mRNA expression ($p < 0.001$; ANOVA; Figure 4.10A). IL-1β concentration was significantly increased in supernatants prepared from Aβ-treated astrocytes (46.35 ± 11.23pg/ml) compared with control astrocytes (16.81 ± 7.15pg/ml; $p < 0.01$; ANOVA; Figure 4.10B); pre-treatment with wedelolactone significantly attenuated the Aβ-induced increase in IL-1β concentration (5.92 ± 1.42pg/ml; $p < 0.001$; ANOVA; Figure 4.10B).

IL-6 mRNA was increased in Aβ-treated isolated astrocytes ($p < 0.05$; Student t-test for dependent means; Figure 4.10C). IL-6 concentration was significantly increased in supernatants prepared from Aβ-treated astrocytes (269.8 ± 46.15pg/ml) compared with control astrocytes (54.43 ± 25.54pg/ml; $p < 0.001$; ANOVA; Figure 4.10D); pre-treatment with wedelolactone significantly attenuated the Aβ-induced increase in IL-6 concentration (69.47 ± 35.3pg/ml; $p < 0.01$; ANOVA; Figure 4.10D).

TNFα mRNA was not affected by Aβ but, pre-treatment with wedelolactone significantly decreased TNFα mRNA in control-treated and Aβ-treated astrocytes ($p < 0.001$; ANOVA; Figure 4.10E). TNFα concentration was significantly increased in supernatants prepared from Aβ-treated astrocytes (18.98 ± 3.61pg/ml) compared with control astrocytes (4.43 ± 3.38pg/ml; $p < 0.05$; ANOVA; Figure 4.10F); pre-treatment with wedelolactone significantly attenuated the Aβ-induced increase in TNFα concentration (5.45 ± 3.37pg/ml; $p < 0.01$; ANOVA; Figure 4.10F).

To confirm that wedelolactone was acting on the NFκB pathway, its effect on IκBα phosphorylation was examined and the data showed that IκBα phosphorylation was significantly increased in Aβ-treated astrocytes compared with controls (p<0.01; ANOVA); pre-treatment with wedelolactone significantly attenuated the Aβ-induced increase in p-IκBα (p<0.05; ANOVA; Figure 4.11B).

Neither Aβ nor wedelolactone affected GFAP mRNA (ANOVA; Figure 4.12A), Aldh1L1 mRNA (ANOVA; Figure 4.12B) or EAAT2 mRNA (ANOVA; Figure 4.12C) in isolated astrocytes.

4.3.6. *Effects of D-JNKi1 in rat astrocytes treated with Aβ*

To explore the consequences of the effects of Aβ on JNK activation, astrocytes were pre-treated with D-JNKi1 (2μM) for 1 hour and incubated in the presence of Aβ cocktail or DMEM for 24 hours. D-JNKi1 is a cell permeable selective inhibitor of the JNK pathway that blocks the access of JNK to c-Jun. IL-1β, IL-6 and TNFα were assessed in the supernatants and IL-1β, IL-6, TNFα, Aldh1L1, EAAT2 and GFAP mRNA was measured in harvested cells.

IL-1β mRNA was significantly increased in Aβ-treated isolated astrocytes compared with controls (p<0.01; ANOVA; Figure 4.13A); pre-treatment with D-JNKi1 did not affect the Aβ-induced change (ANOVA; Figure 4.13A). IL-1β concentration was significantly increased in supernatants prepared from Aβ-treated astrocytes (46.35 ± 11.23pg/ml) compared with control astrocytes (16.81 ± 7.15pg/ml; p<0.01; ANOVA; Figure 4.13B); pre-treatment with D-JNKi1 significantly attenuated the Aβ-induced increase in IL-1β concentration (26.91 ± 6.45pg/ml; p<0.001; ANOVA; Figure 4.13B).

IL-6 mRNA was significantly increased in Aβ-treated isolated astrocytes compared with controls (p<0.01; ANOVA; Figure 4.13C); pre-treatment with D-JNKi1 did not affect the Aβ-induced change (ANOVA; Figure 4.13C). IL-6 concentration was significantly increased in supernatants prepared from Aβ-treated astrocytes (544.1 ± 87.05pg/ml) compared with control astrocytes (203.6 ± 45.49pg/ml; p<0.001; ANOVA; Figure 4.13D); pre-treatment with D-JNKi1 significantly attenuated the Aβ-induced increase in IL-6 concentration (287.7.47 ± 31.32pg/ml; p<0.01; ANOVA; Figure 4.13D).

TNFα mRNA was not affected with Aβ-treatment in isolated astrocytes; although, pre-treatment with D-JNKi1 significantly increased TNFα mRNA ($p < 0.001$; ANOVA; Figure 4.13E). TNFα concentration was increased in supernatants prepared from Aβ-treated astrocytes (18.98 ± 3.61pg/ml) compared with control astrocytes (4.43 ± 3.38pg/ml) but this increase did not reached statistical significance; pre-treatment with D-JNKi1 had no effect in TNFα concentration (11.89 ± 7.38pg/ml; $p < 0.01$; ANOVA; Figure 4.13F).

Neither Aβ nor D-JNKi1 affected GFAP mRNA (ANOVA; Figure 4.14A), Aldh1L1 mRNA (ANOVA; Figure 4.14B) or EAAT2 mRNA (ANOVA; Figure 4.14C) in isolated astrocytes.

4.4. Discussion

The objective of this study was to examine the effects of Aβ treatment on cytokine production and release in isolated astrocytes and to investigate the signalling pathways involved in this process. The data showed that Aβ induced a time-related increase in the production and release of IL-1β, IL-6 and TNFα, and in IκBα phosphorylation. Wedelolactone, an inhibitor of IκBα, significantly attenuated the Aβ-induced increase in IL-1β and IL-6, indicating NFκB signalling pathway as an important component in this activation process (Table 4.1).

The images obtained by confocal microscopy after co-staining isolated glial cells with both GFAP and CD11b showed a clear characterization of astrocytes and microglia in culture. As this study was based on isolated astrocytes, is fundamental to obtain the best possible culture purity. The technique used in this study has proven successful in the isolation of pure population of astrocytes reflecting the degree of purity reported using similar protocols (McCarthy and de Vellis, 1980, Jana et al., 2007). Currently, is not technically possible to obtain 100% pure astrocytic cultures. Although most amoeboid-shaped microglia are detached from the flasks containing mixed glia during the "shaking" step, a population of nonrefringent, more ramified microglia, intermingled with astrocytes, remain (Saura, 2007). It has been shown that when astrocytes are detached with trypsin and re-plated, the number of these ramified microglial cells is greatly reduced, as they are not affected by trypsin and remain in the flask (Saura et al., 2003). It has been suggested that astrocytic cultures which contain less than 10% of microglial cells can be considered as purified astrocytes (Saura, 2007). All astrocyte cultures presented in this work have less than 10% microglial cells. A technical issue related to the astrocytic isolation protocol used in this study (and most other studies) is the mechanical stimulation caused by the "shaking" step; it has been reported this may cause some changes in cellular activity related to astrocytic "activation" (Du et al., 2010) and this may help explain the occasional large variability in responses (reflected by large error bars) and why, in some experiments, non-treated astrocytes under control conditions have increased levels of inflammatory cytokines or markers of activation.

The present data show that incubation of astrocytes in the presence of Aβ did not affect cell viability. This finding concurs with others; it has been shown that while Aβ induces morphological changes in rat isolated astrocytes it does not alter cell viability (Salinero et al., 1997). However, it has also been reported that cultured rat astrocytes treated with Aβ$_{1-42}$ showed a reduction in cell viability, assessed by MTT assay, and altered vesicular trafficking, but without cell death and without affecting ATP levels or lactate release; moreover, the cells were able to proliferate after incubation with Aβ$_{1-42}$ (Kerokoski et al., 2001). Soluble oligomers of Aβ$_{1-42}$ peptide seem to be the most cytotoxic (Lambert et al., 1998), but the present data suggests that aggregated Aβ$_{1-42}$, alone, or in combination with Aβ$_{1-40}$ in astrocytes had no cytotoxic effect. The inherent characteristics and functions of astrocytes and neurons explain their differential physiological and pathological responses. Astrocytes are believed to be more resistant to cytotoxicity and to cope better with harmful challenges than neurons (Dineley et al., 2000, Gurer et al., 2009). Neuronal cell viability is markedly reduced in the presence of Aβ, these cytotoxic actions involve intracellular reactions including, among others, the production of free radicals and lipid peroxidation (Behl et al., 1994).

Aβ has been shown to induce numerous functional and morphological changes in astrocytes including the production and release of cytokines and chemokines. In brains of individuals with AD, astrocytes react to the presence of Aβ and increase the expression of GFAP changing their morphology, this process termed astrogliosis has been proposed to be involved in the neuropathology of AD (Olabarria et al., 2010, Nagele et al., 2004). Astrogliosis has been reported to be accompanied by signs of neuroinflammation and to contribute to an increase in pro-inflammatory cytokines (Cowley et al., 2010). The release of IL-1β, IL-6 and TNFα from astrocytes has been reported previously; Hu and colleagues (1994), treated murine astrocytes with LPS inducing the release of these cytokines (Hu et al., 1994). Also, astrocytes are known to release pro-inflammatory cytokines under different experimental and pathological conditions, such as in the presence of coronavirus (Yu and Zhang, 2006), in bacterial meningoencephalitis (Wen et al., 2007) and during traumatic brain injury (Szmydynger-Chodobska et al., 2010) among others.

In this study, a time-dependent increase in the supernatant concentration of cytokines was observed, peaking between 360 min and 24 hours. A significant increase in IL-1β was observed at 6 hours which further increased at 24 hours. These findings, although using $A\beta_{1-40}$ + $A\beta_{1-42}$ to stimulate cells are similar to previous observations. Rat cortical astrocytes treated with aggregated $A\beta_{1-42}$ for 24 hours showed a significant increase in IL-1β mRNA compared with control or $A\beta_{17-42}$-treated cells (Hu et al., 1998). Similarly, cultured rat astrocytes treated with fibrillar $A\beta_{1-42}$ showed an increase in IL-1β compared with controls reaching highest levels between 24 and 48 hours (White et al., 2005). The Aβ-induced increase in IL-6 was evident after 2 hours and persisted for at least 24 hours. This response is earlier than previously described where cultured astrocytes stimulated with $A\beta_{25-35}$ reached peak concentration for IL-6 at 24 hours which was sustained up to 48 hours (Kim et al., 2002). It is possible that the early increase in IL-6 might be explained by effects of physical manipulation of the cells during the "shaking" step but, if this was the case, a parallel change in others cytokines might be expected. TNFα supernatant concentration peaked at 360 min and persisted until 24 hours, consistent with the previous results of Kim and colleagues (2002). As 24 hours seemed the period at which cytokine production in Aβ-stimulated astrocytes peaked, all the culture work involving Aβ-treatments in this study and the next one (see Chapter 5) were done at this time point.

Activation of the NFκB pathway was assessed in Aβ-treated isolated astrocytes. Phosphorylation of IκBα increased in Aβ-stimulated astrocytes in a time-dependent manner with significant increases observed at 240 min, 360 min and 24. This resembled the Aβ-induced time-dependent change in cytokine production. The NFκB pathway is known to be present in astrocytes and to be involved in the production of chemokines and cytokines. Cultured rat astrocytes stimulated with $A\beta_{1-42}$ showed activation of the NFκB pathway with increased production of NO (Akama et al., 1998). Bradykinin, an inflammatory mediator produced during stroke or brain trauma, was shown to stimulate the expression and release of IL-6 through NFκB activation in cultured mice astrocytes (Schwaninger et al., 1999) and it has been reported that chloroquine induced the expression of IL-1β, IL-6 and TNFα in human astrocytes through activation of the NFκB pathway (Park et al., 2003). In contrast, chloroquine suppressed LPS-induced microglial

expression of cytokines in an NFκB-independent manner (Park et al., 2003), suggesting that NFκB activation could work different in astrocytes and microglia. Interestingly, brain tissue from scrapie-infected mice, showed an increase in IL-1β, IL-6 and TNFα and also NFκB immunoreactivity co-localized with GFAP(+) astrocytes, providing indirect evidence that activation of astroglial NFκB is responsible for the production of these cytokines (Kim et al., 1999).

In this study, pre-treatment with wedelolactone attenuated the Aβ-induced increase in p-IκBα as expected. However, it also reduced the expression of IL-1β and the supernatant concentration of IL-1β, IL-6 and TNFα; these results suggest that astrocytes stimulated with Aβ increase the production of inflammatory cytokines through activation of the NFκB pathway. NFκB can also be activated by cytokines, as shown by Stanimirovic and colleagues (2001) in human astrocytes, where IL-1β mediated autocrine activation of NFκB pathway induced by hypoxia/reoxygenation (Stanimirovic et al., 2001). Cultured rat astrocytes have been shown to respond to IL-1β and TNFα with the production of chemokines MCP-1 (CCL2) and MCP-7 (CCL7) and this is reported to be dependent on activation of the NFκB pathway (Thompson and Van Eldik, 2009). It has been proposed that NFκB mediates neuroinflammation to facilitate the removal of Aβ; APPswe/PS1dE9 mice treated with pyrrolidine dithiocarbamate (PDTC), an inhibitor of NFκB activation, showed abolishment of COX-2 and TNFα induction, attenuated astrogliosis in both cortex and hippocampus and increased cerebral burden of $Aβ_{1-42}$ but not $Aβ_{1-40}$ (Zhang et al., 2009).

Activation of JNK and c-Jun in human astrocytes has been reported during neurodegenerative processes. Double-labelling immunohistochemistry in brains of individuals with different tauopathies, demonstrated abnormal tau deposition in astrocytes stained with SAPK/JNK-p (Ferrer et al., 2001). In human brains of individuals with AD, Jun immunoreactivity was co-localized with GFAP surrounding amyloid plaques identified with thioflavine (Anderson et al., 1994). In this study, both p-JNK and p-c-Jun were increased in the presence of Aβ in isolated astrocytes, but the time relationship of the activation did not paralleled the time-related change in cytokine production. However, this pathway may still play a role in initiating the mechanism that triggers the Aβ-induced increase in cytokine production. Matos and colleagues (2008)

treated isolated rat astrocytes with $A\beta_{1-40}$ and reported a significant increase in JNK phosphorylation at 3 hours but not later, where levels returned to values similar to those of the controls (Matos et al., 2008). Here there was no evidence that the increase in JNK activation persisted for 3 hours but the increase in c-Jun phosphorylation, which, like JNK, was evident at 40 min, still exhibited a 2-fold increase over control levels at 3 hours. These results contrast with the activation pattern of p-IκBα, which peaked at 24 hours when stimulated with Aβ. JNK pathway in astrocytes has been involved in pro-inflammatory signalling cascades. Cultured mice astrocytes treated with IL-17 and IL-6 binding subunit (IL-6R), showed increased JNK activation at 30 and 60 min, inducing an increase in IL-6 gene expression; inhibition of JNK or p38, partially blocked the IL-6 increase, while inhibition of NFκB showed a most robust decrease, suggesting that IL-6 gene expression occurs by a transcriptional mechanism that involves NFκB, p38, and JNK signalling (Ma et al., 2010). IL-1 treatment induced phosphorylation of JNK in human foetal astrocytes indicating that JNK is activated by stress and inflammatory signals (Hua et al., 2002).

In the present study, as expected, p-JNK was not affected by treatment with Aβ or D-JNKi1 after 24 hours. D-JNKi1 showed no effect on IL-1β or IL-6 expression but significantly decreased the supernatant concentration of both cytokines; these results suggest that JNK may be more involved in astrocytic regulation of cytokine release than in production. D-JNKi1 showed no effect on TNFα supernatant concentration but unexpectedly, TNFα mRNA was significantly increased in Aβ-treated astrocytes pre-treated with D-JNKi1 compared with Aβ-treated astrocytes. It is not clear why the JNK inhibitor caused this effect on TNFα expression, as production of TNF-α was shown to be increased in LPS-treated astrocytes through activation of ERK, p38, and JNK pathways (Shao et al., 2011). JNK pathway has been shown to be involved in the regulation of astrocytic glutamate transporter activity, through downregulation of GLT-1 in Aβ-treated rat astrocytes (Matos et al., 2008). In a different study, Jayakumar and colleagues (2006) reported JNK activation upregulates glutamate-aspartate transporter (GLAST) in ammonia-treated rat astrocytes (Jayakumar et al., 2006). These results indicate that in astrocytes, JNK pathway activation is not exclusively inflammatory and may possess other regulatory functions.

An increase in GFAP is a common finding in brains of individuals with AD (Pike et al., 1995). GFAP increase has been shown to be correlated with age in APP/PS1KI mice, showing no changes at 2 months and marked increase in aged animals (Wirths et al., 2010). In the present study, Aβ, wedelolactone or D-JNKi1 exerted no effect on GFAP in rat neonatal astrocytes. This suggests that GFAP production is independent of inflammatory activation pathways such as NFκB. Brahmachari and colleagues (2006) showed that NO used the GC-cGMP-PKG signalling pathway but not NFκB to induce expression of GFAP in LPS-treated astrocytes, suggesting that activation of NFκB is upstream of NO production and that NO increases expression of GFAP in astrocytes independent of NFκB activation (Brahmachari et al., 2006). It has also been reported that GFAP expression is dependent on changes in calcium homoeostasis induced by Aβ, rather than by a direct effect of Aβ (Chow et al., 2010a). GFAP mRNA and protein levels were not changed in $Aβ_{1-42}$-treated cortical rat astrocytes when compared with controls, although Aβ-treated astrocytes showed a reorganization of GFAP indicative of activated morphology, suggesting that changes in GFAP are related to increased antigen density due to cell shape change, epitope redistribution or filament rearrangement (Hu et al., 1998). Aβ, wedelolactone or D-JNKi1 had no effect on other markers of astrocytic function such as Aldh1L1 and EAAT2 and, similarly, Aβ didn't alter RAGE production in the present study. The lack of effect on EAAT2 is consistent with the finding that EAAT1 and EAAT2 were unchanged in cultured rat astrocytes treated with $Aβ_{1-40}$ for 24 hours. (Dallas et al., 2007). These results suggest that Aβ can induce an inflammatory response in astrocytes without affecting other main astrocytic functional aspects.

The data described here suggest that although JNK and NFκB pathways can be activated by Aβ in astrocytes, NFκB appears to be the main signalling mediator in the production of pro-inflammatory cytokines. The JNK pathway, which showed a faster activation, seems to be involved in other astrocytic processes induced by the presence of Aβ although it may be able to complement the NFκB slower and more sustained inflammatory response (Figure 4.15). An interesting question to be addressed is which receptors are activated by Aβ in order to produce the effects observed in this study.
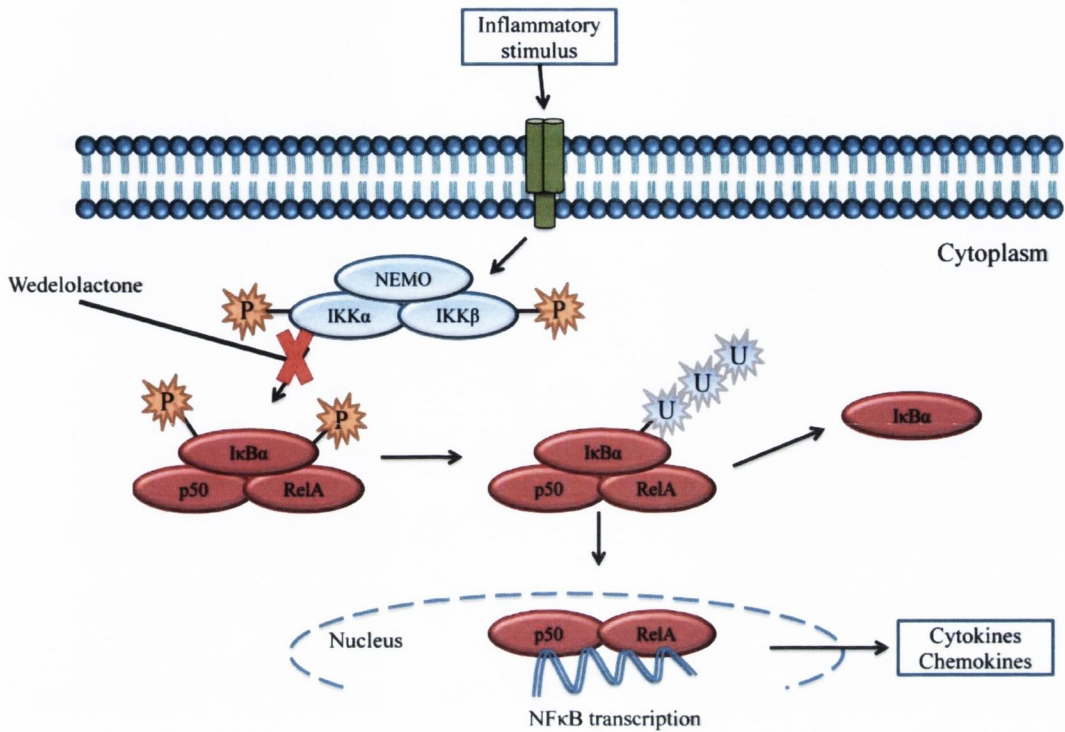
Figure 4.1. Wedelolactone effect on NFκB pathway.

Wedelolactone is an irreversible inhibitor of the NFκB signalling pathway which impedes the phosphorylation of IκBα by IKK thus preventing the transcription of pro-inflammatory cytokines and chemokines.
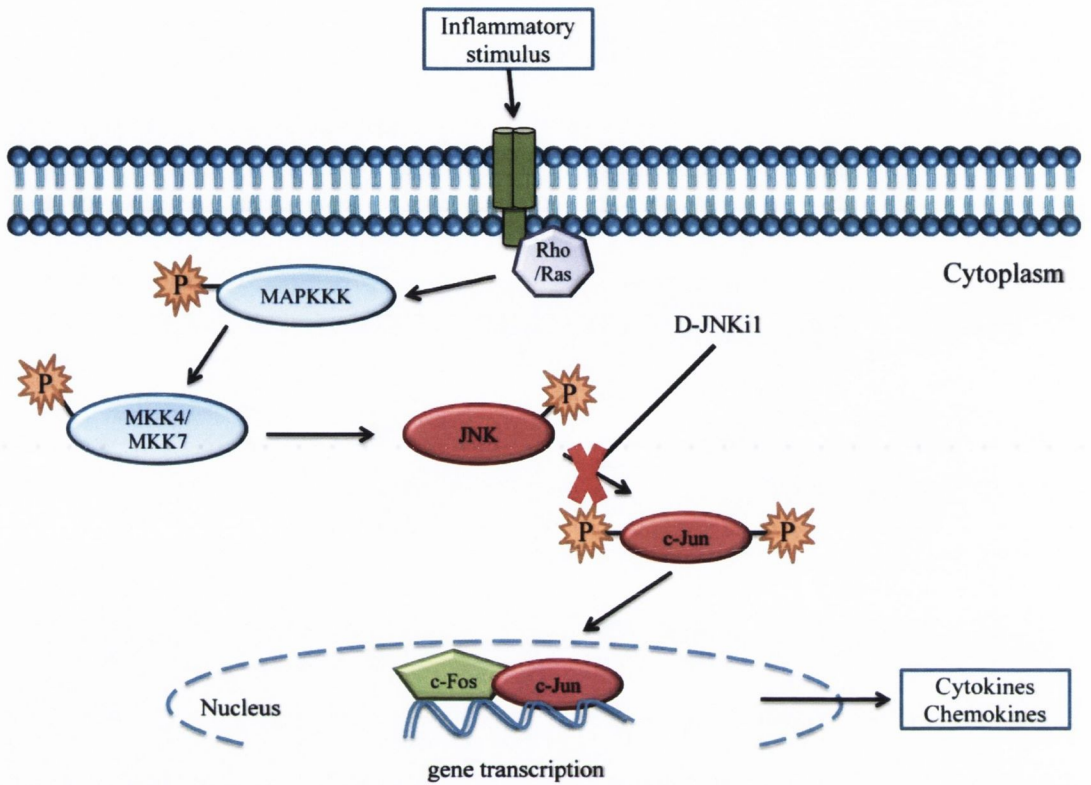
Figure 4.2 D-JNKi1 effect on JNK pathway.

D-JNKi1 is an inhibitor of the JNK signalling pathway which acts preventing the interaction of JNK with its substrates thus impeding gene transcription.
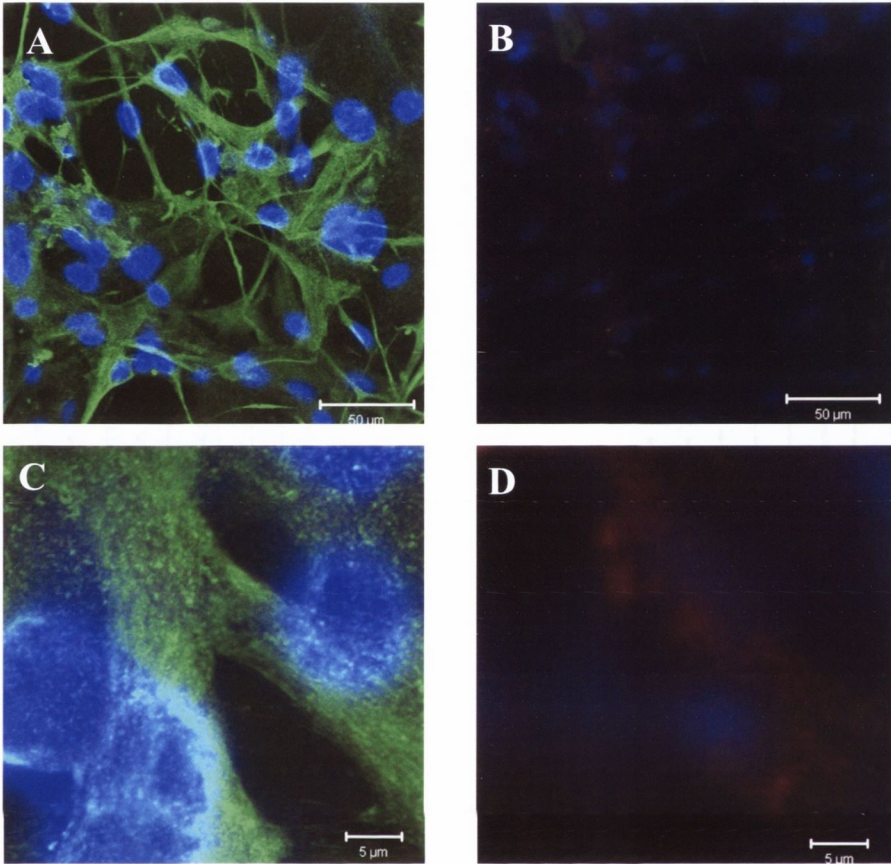
Figure 4.3 Characterization of cultured isolated astrocytes

Astrocytes and microglia obtained from the cortices of neonatal Wistar rats and plated into coverslips were prepared for confocal microscopy and co-stained with GFAP and CD11b. Images show immunofluorescence for GFAP (green), CD11b (red) and DAPI (blue), used as a counterstain, in isolated astrocytes.

A) Isolated astrocytes co-stained for GFAP and CD11b (DAPI counterstain; 40x, scale bar 50µm).

B) Isolated microglia co-stained for GFAP and CD11b (DAPI counterstain; 40x, scale bar 50µm).

C) Magnification of isolated astrocyte co-stained with GFAP and CD11b (DAPI counterstain; 40x; optical zoom x6, scale bar 5µm).

D) Magnification of isolated microglia co-stained with GFAP and CD11b (DAPI counterstain; 40x; optical zoom x6, scale bar 5µm).
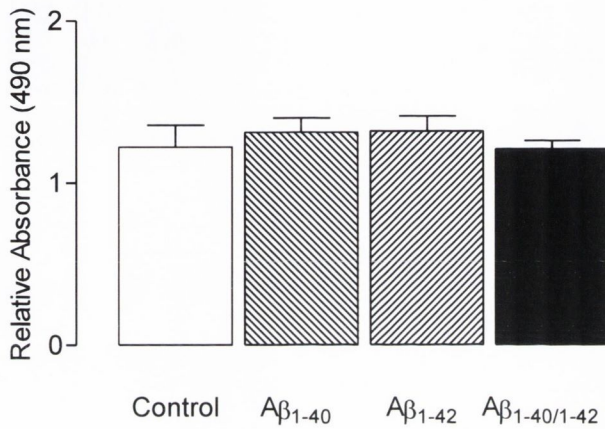
Figure 4.4 MTS assay to determine cell viability of Aβ treated isolated astrocytes

Astrocytes obtained from the cortices of neonatal Wistar rats were cultured with DMEM, $A\beta_{1-40}$ (4.2 µM), $A\beta_{1-42}$ (5.6µM) or a cocktail composed of both $A\beta_{1-40}$ and $A\beta_{1-42}$ (hereafter referred to as Aβ cocktail) for 24 hours. Cell viability was determined by the addition of MTS and assessment of absorbance at 490nm.

No significant differences in the relative absorbance of MTS were found between the Aβ–treated astrocytes and the controls (ANOVA $F_{(3,12)}$ =0.676, p<0.583; n=5). Data are presented as means ± SEM.
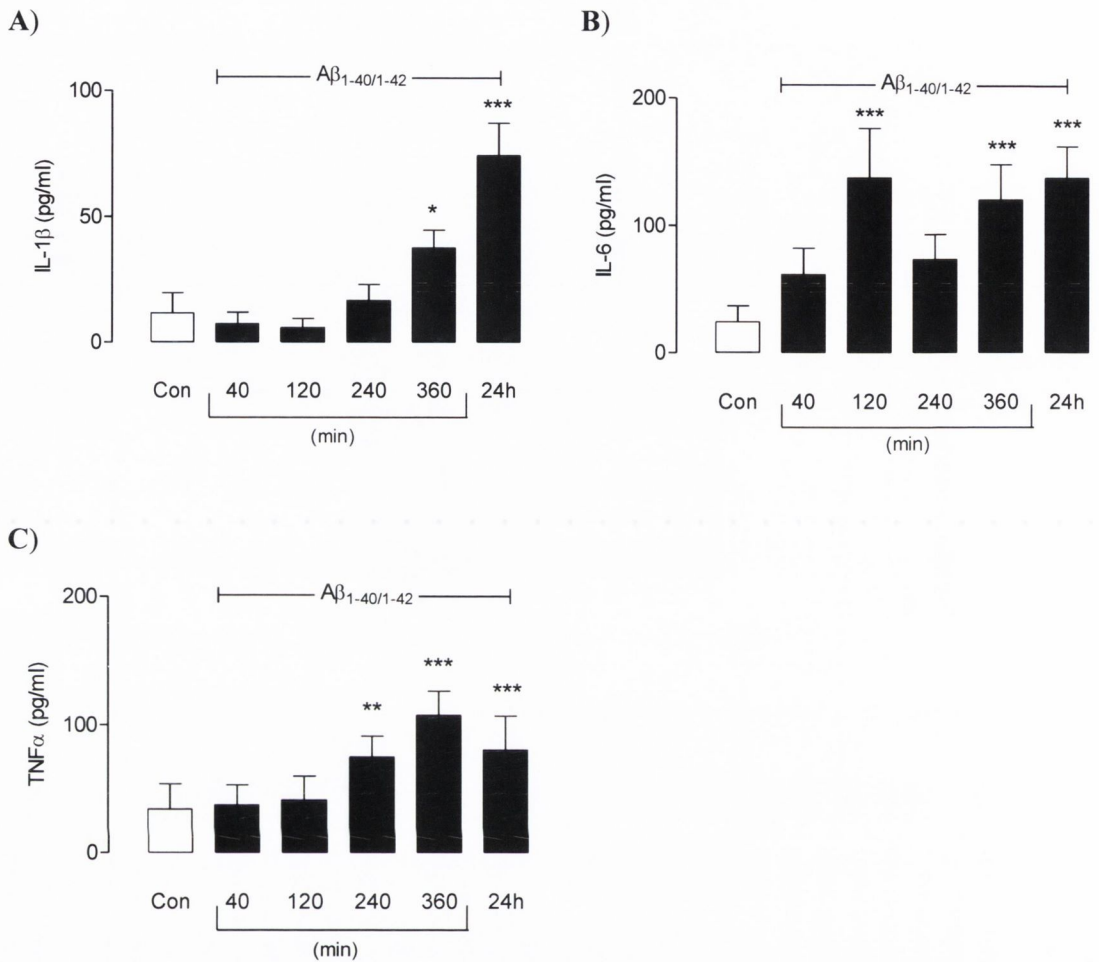
Figure 4.5 Treatment with Aβ stimulated the release of pro-inflammatory cytokines from isolated astrocytes

Astrocytes were incubated in the presence of Aβ or DMEM for 40 min, 120 min, 240 min, 360 min or 24 hours. Concentrations of IL-1β, IL-6 and TNFα were assessed in supernatants by ELISA. Data are presented as means ± SEM.

A) Aβ significantly increased IL-1β at 360 min (*p<0.05 vs. controls) and 24 hours (***p<0.001 vs. controls) compared with controls. ANOVA $F_{(5,20)}$ =21.16, p<0.0001; n=5.

B) Aβ significantly increased IL-6 at 120 min (***p<0.001 vs. controls), 360 min (*p<0.05 vs. controls) and 24 hours (***p<0.001 vs. controls) compared with controls. ANOVA $F_{(5,45)}$ =8.10, p<0.0001; n=10.

C) Aβ significantly increased TNFα at 240 min (**p<0.01 vs. controls), 360 min (***p<0.001 vs. controls) and 24 hours (***p<0.001 vs. controls) compared with controls. ANOVA $F_{(5,15)}$ =20.17, p<0.0001; n=4.
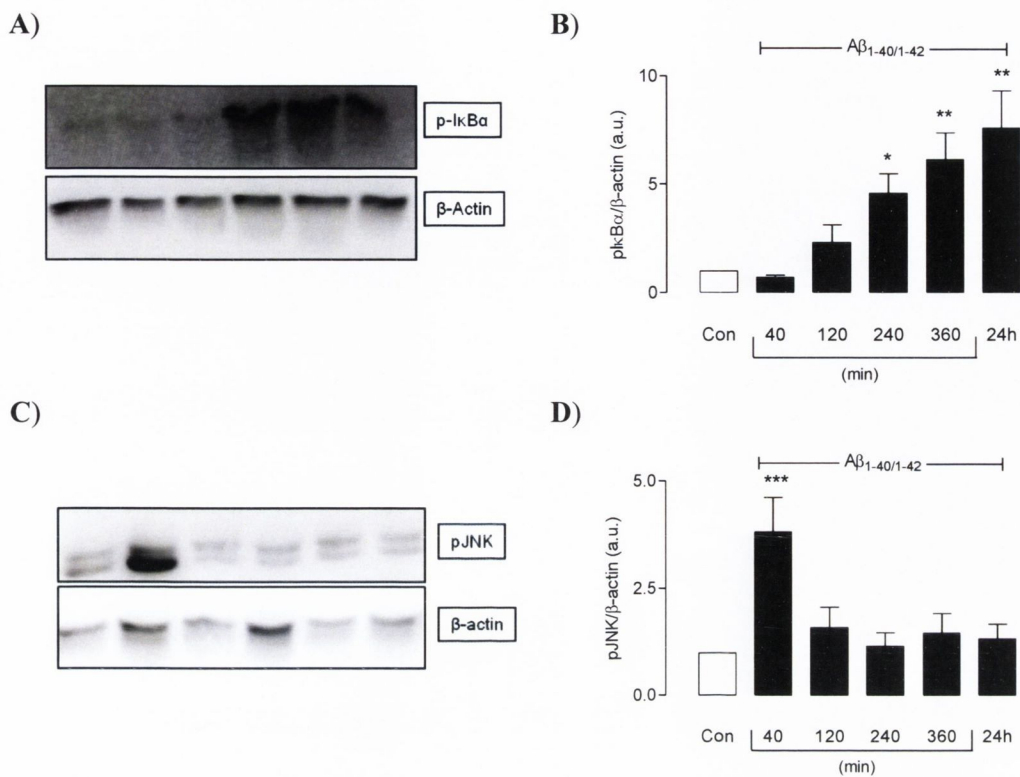
Figure 4.6 Treatment with Aβ stimulated phosphorylation of IκBα and JNK in isolated astrocytes

Astrocytes were incubated in the presence of Aβ or DMEM for 40 min, 120 min, 240 min, 360 min or 24 hours and IκBα and JNK phosphorylation were determined by western immunoblotting. Data are presented as means ± SEM.

A) Sample immunoblots indicating density of p-IκBα (40kDa) and β-actin (42kDa). **B**) Aβ significantly increased p-IκBα at 240 min (*$p < 0.05$ vs. controls), 360 min (**$p < 0.01$ vs. controls) and 24 hours (**$p < 0.01$ vs. controls) compared with controls. ANOVA $F_{(5,51)} = 8.306$, $p < 0.0001$; n=10. Values are expressed in arbitrary units (a.u.) obtained from calculating the ratio of p-IκBα to β-actin provided by densitometric analysis.

C) Sample immunoblots indicating density of p-JNK (upper band: 54kDa; lower band: 46kDa) and β-actin (42kDa). **D**) Aβ significantly increased p-JNK at 40 min compared with controls (***$p < 0.001$ vs. controls; ANOVA $F_{(5,40)} = 7.276$, $p < 0.0001$; n=9). Values are expressed in arbitrary units (a.u.) obtained from calculating the ratio of p-JNK to β-actin provided by densitometric analysis.

A)
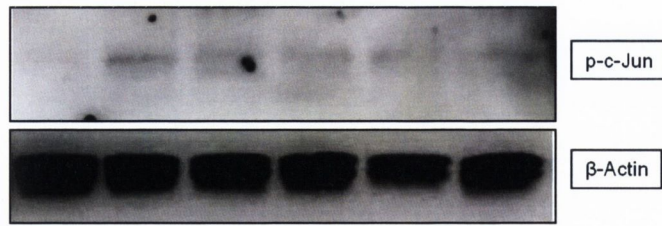
B)
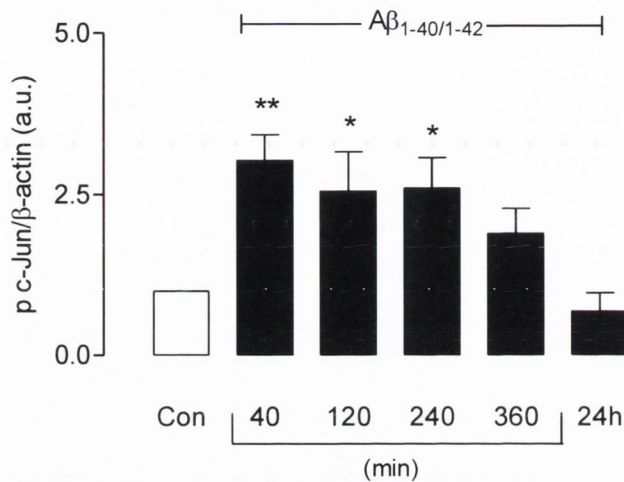
Figure 4.7 Treatment with Aβ stimulated phosphorylation of c-Jun in isolated astrocytes

Astrocytes were incubated in the presence of Aβ or DMEM for 40 min, 120 min, 240 min, 360 min or 24 hours and c-Jun phosphorylation was determined by western immunoblotting. Data are presented as means ± SEM.

A) Sample immunoblots indicating density of p-c-Jun (48kDa) and β-actin (42kDa).

B) Aβ significantly increased p-c-Jun at 40 min (**p<0.01 vs. controls), 120 min (*p<0.05 vs. controls) and 240 min (*p<0.05 vs. controls) compared with controls. ANOVA $F_{(5,34)}$ =5.167, p=0.0012; n=7. Values are expressed in arbitrary units (a.u.) obtained from calculating the ratio of p-c-Jun to β-actin provided by densitometric analysis.

128

A)

B)
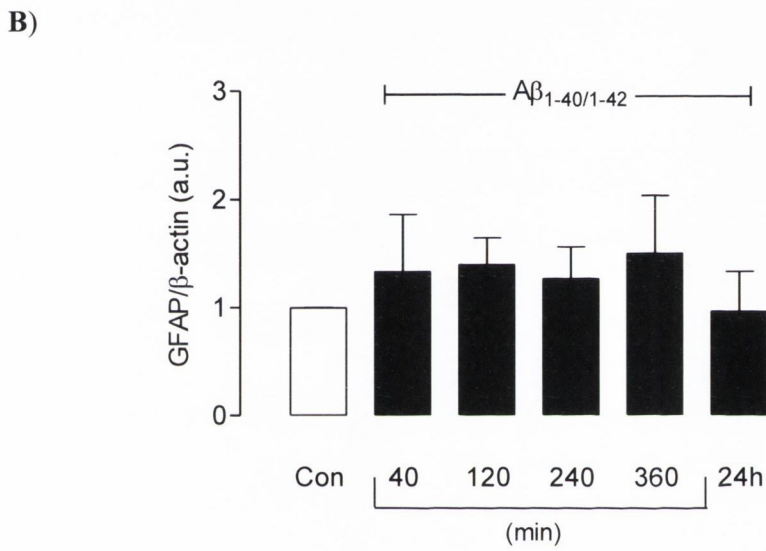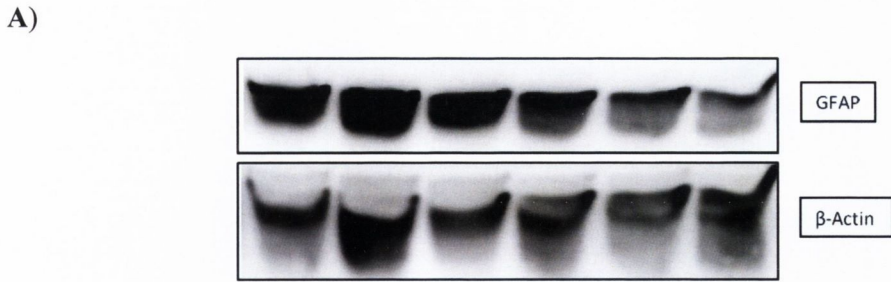
Figure 4.8 Treatment with Aβ did not affect GFAP in isolated astrocytes

Astrocytes were incubated in the presence of Aβ or DMEM for 40 min, 120 min, 240 min, 360 min or 24 hours, and GFAP was determined by western immunoblotting. Data are presented as means ± SEM.

A) Sample immunoblots indicating density of GFAP (55kDa) and β-actin (42kDa).

B) Aβ had no effect on GFAP (ANOVA $F_{(5,15)}$ =0.710, p=0.624; n=4). Values are expressed in arbitrary units (a.u.) obtained from calculating the ratio of GFAP to β-actin provided by densitometric analysis.

A)
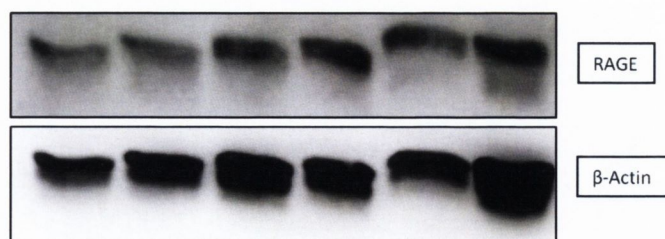
B)
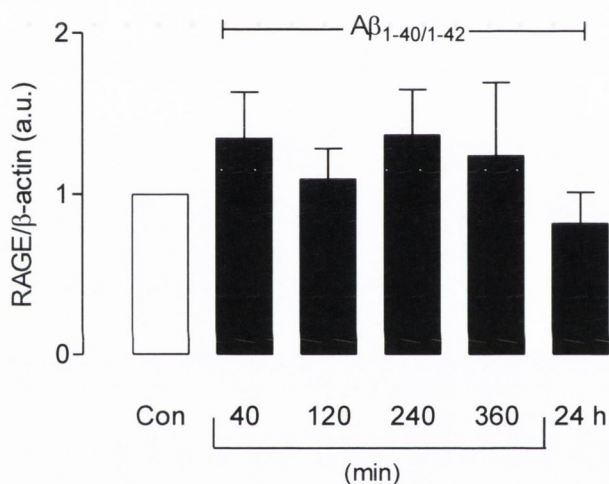
Figure 4.9 Treatment with Aβ did not affect RAGE in isolated astrocytes

Astrocytes were incubated in the presence of Aβ or DMEM for 40 min, 120 min, 240 min, 360 min or 24 hours, and RAGE was determined by western immunoblotting. Data are presented as means ± SEM.

A) Sample immunoblots indicating density of RAGE (42kDa) and β-actin (42kDa).

B) Aβ had no effect on RAGE (ANOVA $F_{(5,30)}$ =1.089, p=0.386; n=7). Values are expressed in arbitrary units (a.u.) obtained from calculating the ratio of RAGE to β-actin provided by densitometric analysis.
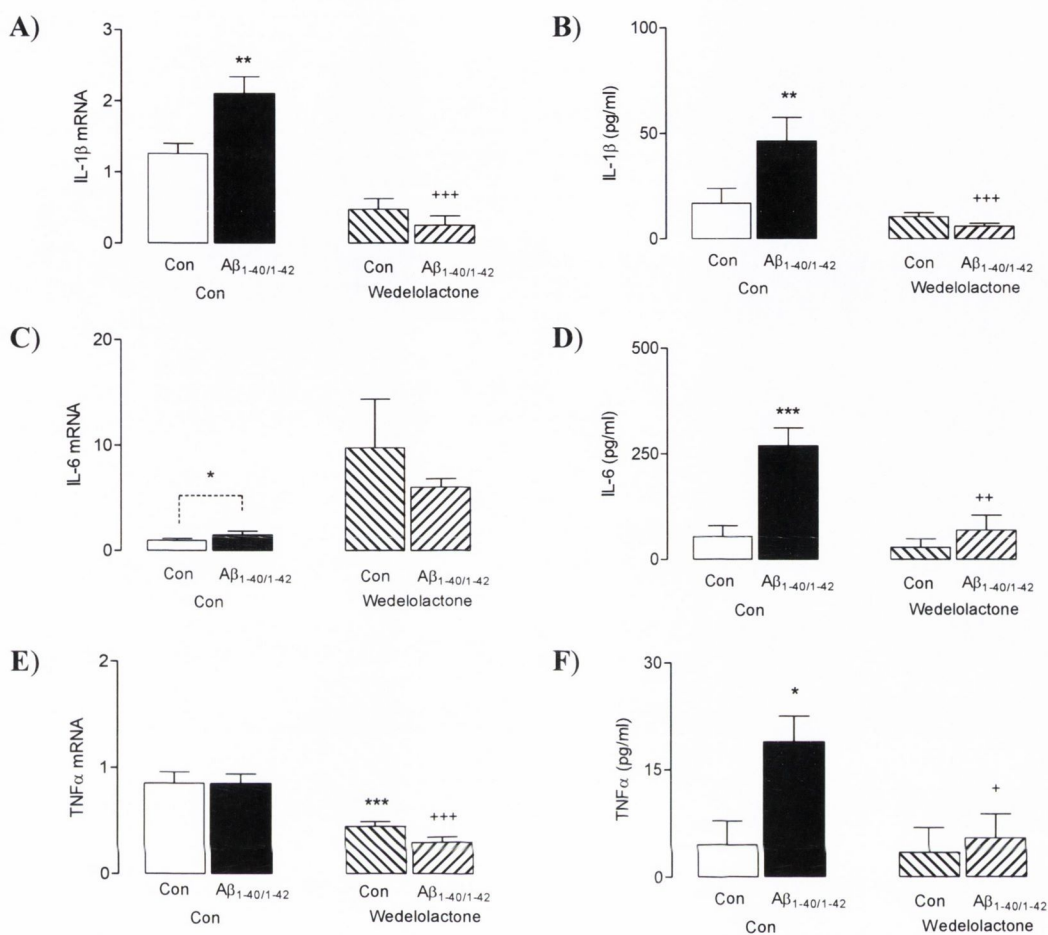
Figure 4.10 Wedelolactone attenuated Aβ-induced increase in IL-1β, IL-6 and TNFα in isolated astrocytes

Astrocytes were incubated in the presence/absence of Aβ following a 1 hour pre-treatment with wedelolactone (50μM). After 24 hours, IL-1β, IL-6 and TNFα mRNA, prepared from harvested cells and supernatant concentration of IL-1β, IL-6 and TNFα were determined by PCR and ELISA, respectively. Data are presented as means ± SEM.

A) Mean IL-1β mRNA was significantly increased in Aβ-treated isolated astrocytes compared with controls (**p<0.01 vs. controls). Pre-treatment with wedelolactone (+++p<0.001 vs. Aβ controls) significantly attenuated the Aβ-induced increase in IL-1β mRNA in astrocytes. ANOVA $F_{(3,15)}$ =45.12, p<0.0001; n=6. B) Mean IL-1β concentration was significantly increased in supernatant prepared from Aβ-treated astrocytes compared with controls (**p<0.01 vs. controls). Pre-treatment with wedelolactone (+++p<0.001 vs. Aβ controls) significantly attenuated the Aβ-induced increase in IL-1β concentration in astrocytes. ANOVA $F_{(3,15)}$ =11.68, p=0.0003; n=6.

C) Mean IL-6 mRNA was increased in Aβ-treated isolated astrocytes compared with controls (*p<0.05 vs. controls; Student t-test for dependent means; n=5). Dotted line represents the Student t-test analysis. D) Mean IL-6 concentration was significantly increased in supernatant prepared from Aβ-treated astrocytes compared with controls (***p<0.001 vs. controls). Pre-treatment with wedelolactone (++p<0.01 vs. Aβ controls) significantly attenuated the Aβ-induced increase in IL-6 concentration in isolated astrocytes. ANOVA $F_{(3,15)}$ =10.36, p=0.0006; n=6.

E) Mean TNFα mRNA was not affected with Aβ-treatment in isolated astrocytes. Astrocytes treated exclusively with wedelolactone showed a significant decrease in TNFα mRNA compared with controls (***p<0.001 vs. controls). Pre-treatment with wedelolactone (+++p<0.001 vs. Aβ controls) significantly decreased the TNFα mRNA in isolated astrocytes. ANOVA $F_{(3,15)}$ =25.14, p<0.0001; n=6. F) Mean TNFα concentration was significantly increased in supernatant prepared from Aβ-treated astrocytes compared with controls (*p<0.05 vs. controls). Pre-treatment with wedelolactone (+p<0.05 vs. Aβ controls) significantly attenuated the Aβ-induced increase in TNFα concentration in isolated astrocytes. ANOVA $F_{(3,12)}$ =4.093, p=0.032; n=6.

131

A)
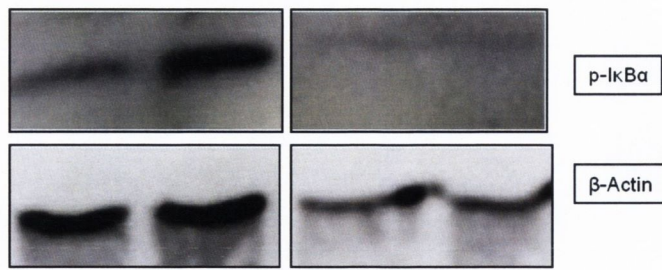
B)
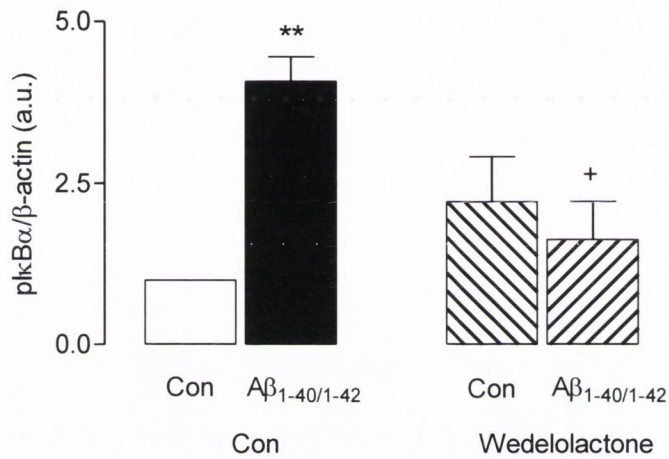
Figure 4.11 Wedelolactone attenuated the Aβ-induced increase in p-IκBα in isolated astrocytes

Astrocytes were incubated in the presence/absence of Aβ following a 1 hour pre-treatment with wedelolactone (50μM). IκBα phosphorylation was determined by western immunoblotting in cell lysates. Data are presented as means ± SEM.

A) Sample immunoblots indicating density of p-IκBα (40kDa) and β-actin (42kDa).

B) p-IκBα was significantly increased in Aβ-treated isolated astrocytes compared with controls (**p<0.01 vs. controls). Pre-treatment with wedelolactone ($^+$p<0.05 vs. Aβ controls) significantly attenuated the Aβ-induced increase in p-IκBα in astrocytes. ANOVA $F_{(3,9)}$ =6.732, p=0.011; n=4. Values are expressed in arbitrary units (a.u.) obtained from calculating the ratio of p-IκBα to β-actin provided by densitometric analysis.

132
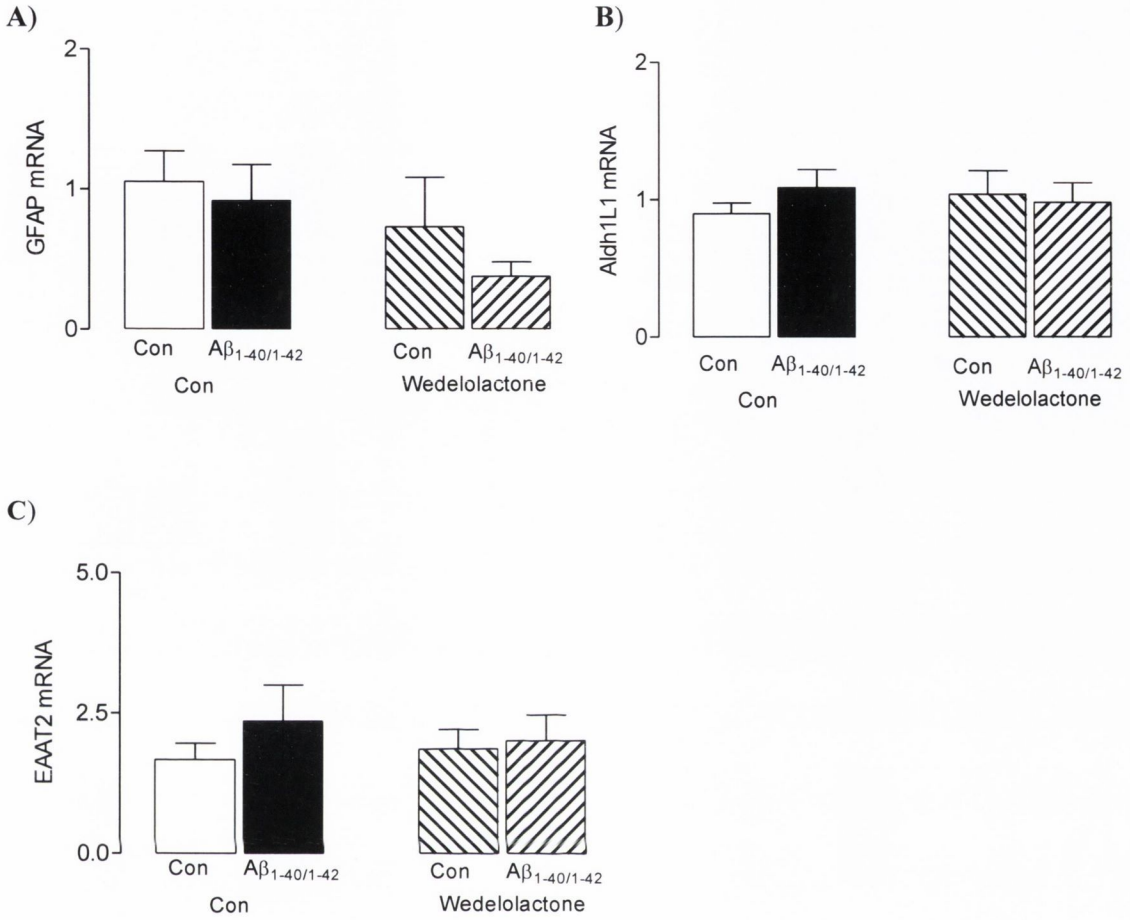
Figure 4.12 GFAP, Aldh1L1 and EAAT2 mRNA were not affected by treatment with wedelolactone or Aβ in isolated astrocytes

Astrocytes were incubated in the presence/absence of Aβ following a 1 hour pre-treatment with wedelolactone (50µM). After 24 hours, GFAP, Aldh1L1 and EAAT2 mRNA prepared from harvested cells were determined by PCR. Data are presented as means ± SEM.

Aβ exerted no significant effect on GFAP mRNA (**A**), Aldh1L1 mRNA (**B**) or EAAT2 mRNA (**C**) in isolated astrocytes and no significant effect of wedelolactone was observed.
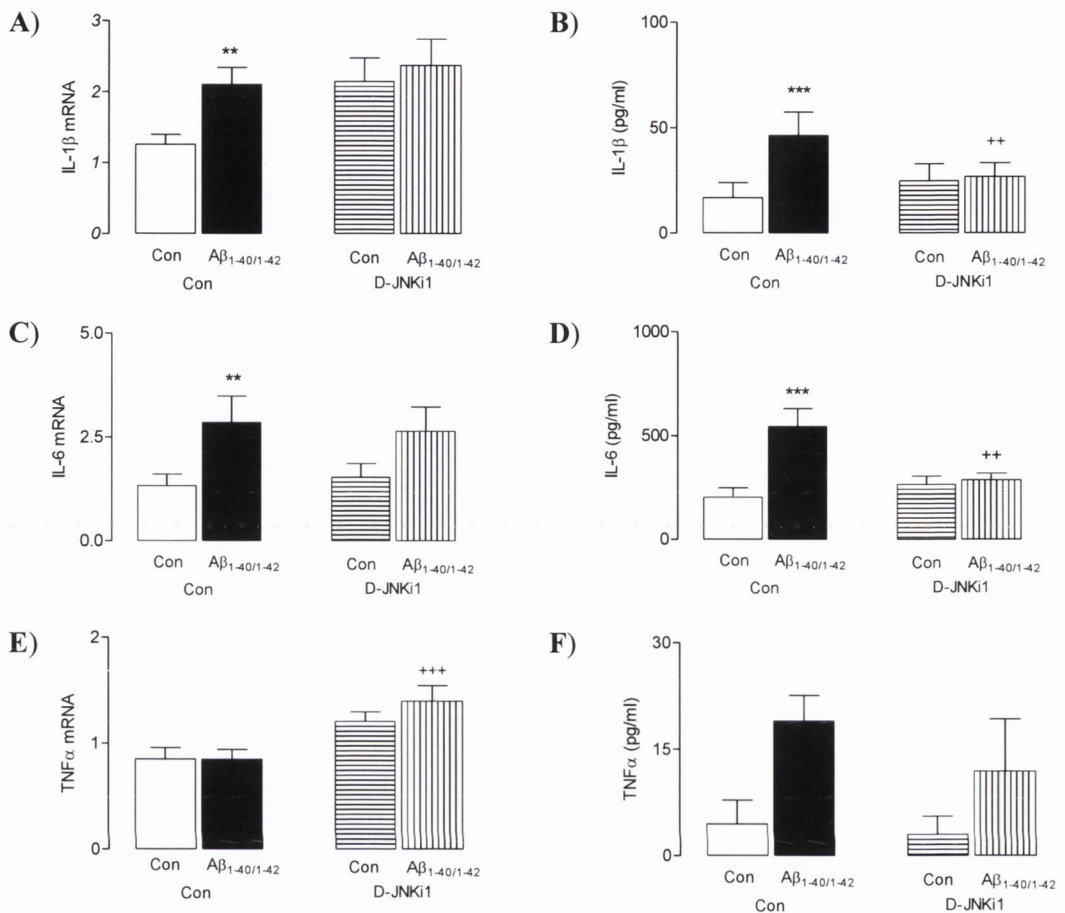
Figure 4.13 D-JNKi1 attenuated Aβ-induced increase in IL-1β and IL-6 in isolated astrocytes

Astrocytes were incubated in the presence/absence of Aβ following a 1 hour pre-treatment with D-JNKi1 (2μM). After 24 hours, IL-1β, IL-6 and TNFα mRNA, prepared from harvested cells and supernatant concentration of IL-1β, IL-6 and TNFα were determined by PCR and ELISA, respectively. Data are presented as means ± SEM.

A) Mean IL-1β mRNA was significantly increased in Aβ-treated isolated astrocytes compared with controls (**p<0.01 vs. controls). Pre-treatment with D-JNKi1 failed to attenuate the Aβ-induced increase in IL-1β mRNA in isolated astrocytes. ANOVA $F_{(3,15)}$ =10.37, p=0.0006; n=6. **B)** Mean IL-1β concentration was significantly increased in supernatant prepared from Aβ-treated astrocytes compared with controls (***p<0.001 vs. controls). Pre-treatment with D-JNKi1 ($^{++}$p<0.01 vs. Aβ controls) significantly attenuated the Aβ-induced increase in IL-1β concentration in isolated astrocytes. ANOVA $F_{(3,15)}$ =14.18, p=0.0001; n=6.

C) Mean IL-6 mRNA was significantly increased in Aβ-treated isolated astrocytes compared with controls (**p<0.01 vs. controls). Pre-treatment with D-JNKi1failed to attenuated the Aβ-induced increase in IL-6 mRNA in isolated astrocytes. ANOVA $F_{(3,15)}$ =7.481, p=0.0027; n=6. **D)** Mean IL-6 concentration was significantly increased in supernatant prepared from Aβ-treated astrocytes compared with controls (***p<0.001 vs. controls). Pre-treatment with D-JNKi1 ($^{++}$p<0.01 vs. Aβ controls) significantly attenuated the Aβ-induced increase in IL-6 concentration in isolated astrocytes. ANOVA $F_{(3,15)}$ =11.02, p=0.0004; n=6.

E) Mean TNFα mRNA was not affected with Aβ-treatment in isolated astrocytes. Pre-treatment with D-JNKi1 significantly increased TNFα mRNA in astrocytes ($^{+++}$p<0.001 vs. Aβ controls; ANOVA $F_{(3,15)}$ =16.42, p<0.0001; n=6). **F)** No Aβ or D-JNKi1 effects were observed in mean TNFα supernatant concentration in isolated astrocytes (ANOVA $F_{(3,12)}$ =2.081, p=0.156; n=5).
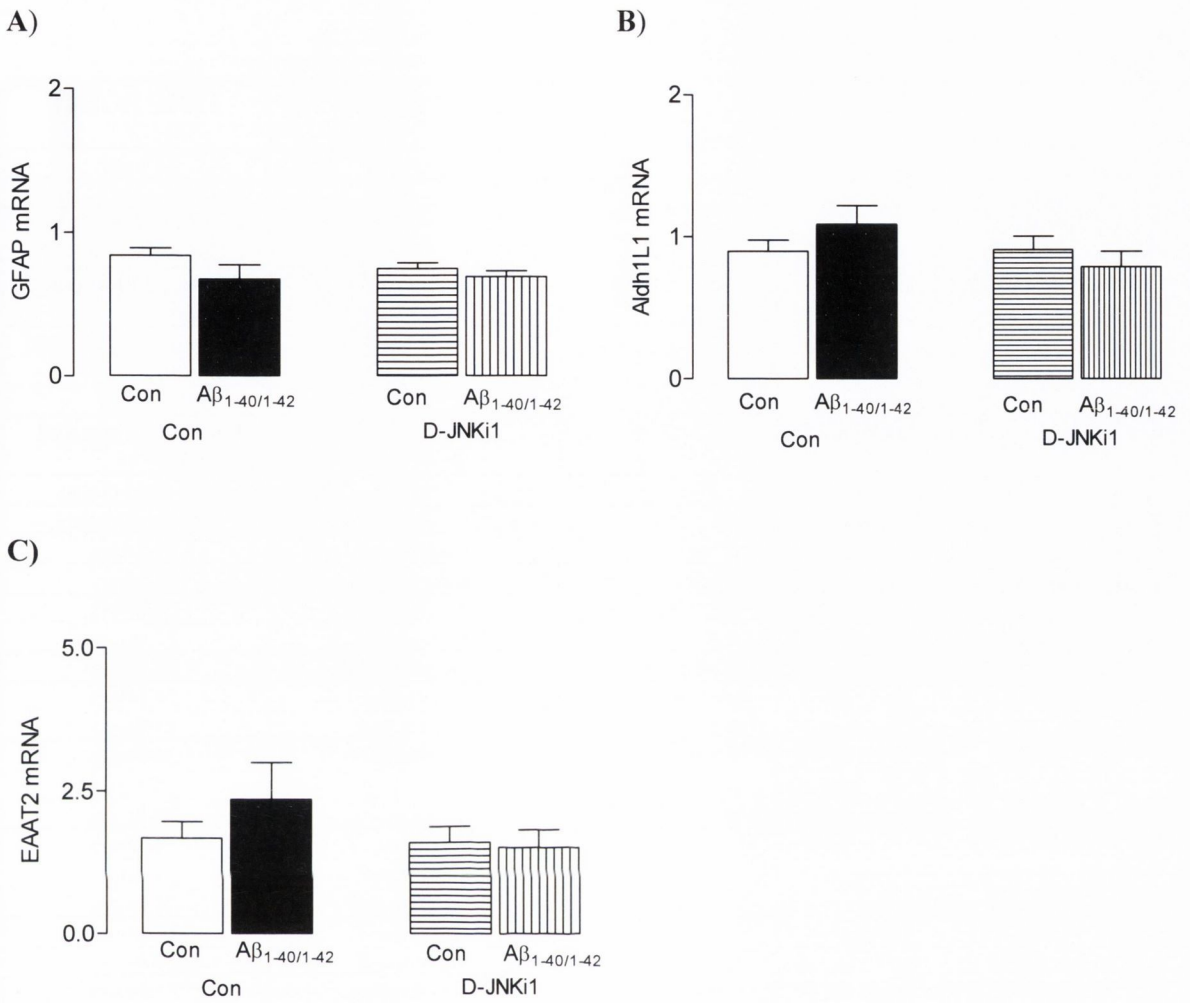
Figure 4.14 mRNA expression of GFAP, Aldh1L1 and EAAT2 were not affected by treatment with D-JNKi1 or Aβ in isolated astrocytes

Astrocytes were incubated in the presence/absence of Aβ following a 1 hour pre-treatment with D-JNKi1 (2μM). After 24 hours, GFAP, Aldh1L1 and EAAT2 mRNA prepared from harvested cells were determined by PCR. Data are presented as means ± SEM.

Aβ exerted no significant effect on GFAP mRNA (**A**), Aldh1L1 mRNA (**B**) or EAAT2 mRNA (**C**) in isolated astrocytes and no significant effect of D-JNKi1 was observed.

	Aβ	TREATMENT	TREATMENT + Aβ	TIME POINT
MTS assay	No changes	———	———	24 hours
IL-1β protein	**Increased**	———	———	360 min and 24 hours
IL-6 protein	**Increased**	———	———	120 min, 360 min and 24 hours
TNFα protein	**Increased**	———	———	240 min, 360 min and 24 hours
p-IκBα	**Increased**	———	———	240 min, 360 min and 24 hours
p-JNK	**Increased**	———	———	40 min
p-c-Jun	**Increased**	———	———	40 min, 120 min and 240 min
GFAP	No changes	———	———	All time points
RAGE	No changes	———	———	All time points
IL-1β mRNA	**Increased**	Wedelolactone	**Decreased**	24 hours
IL-1β protein	**Increased**	Wedelolactone	**Decreased**	24 hours
IL-6 mRNA	**Increased**	Wedelolactone	No changes	24 hours
IL-6 protein	**Increased**	Wedelolactone	**Decreased**	24 hours
TNFα mRNA	No changes	Wedelolactone	**Decreased**	24 hours
TNFα protein	**Increased**	Wedelolactone	**Decreased**	24 hours
p-IκBα	**Increased**	Wedelolactone	**Decreased**	24 hours
GFAP mRNA	No changes	Wedelolactone	No changes	24 hours
Aldh1L1 mRNA	No changes	Wedelolactone	No changes	24 hours
EAAT2 mRNA	No changes	Wedelolactone	No changes	24 hours
IL-1β mRNA	**Increased**	D-JNKi1	No changes	24 hours
IL-1β protein	**Increased**	D-JNKi1	**Decreased**	24 hours
IL-6 mRNA	**Increased**	D-JNKi1	No changes	24 hours
IL-6 protein	**Increased**	D-JNKi1	**Decreased**	24 hours
TNFα mRNA	No changes	D-JNKi1	**Increased**	24 hours
TNFα protein	No changes	D-JNKi1	No changes	24 hours
GFAP mRNA	No changes	D-JNKi1	No changes	24 hours
Aldh1L1 mRNA	No changes	D-JNKi1	No changes	24 hours
EAAT2 mRNA	No changes	D-JNKi1	No changes	24 hours

Table 4.1. Summary of results Chapter 4.

Summary of the data presented in this chapter. Highlighted in bold are results which reached a statistically significant difference.
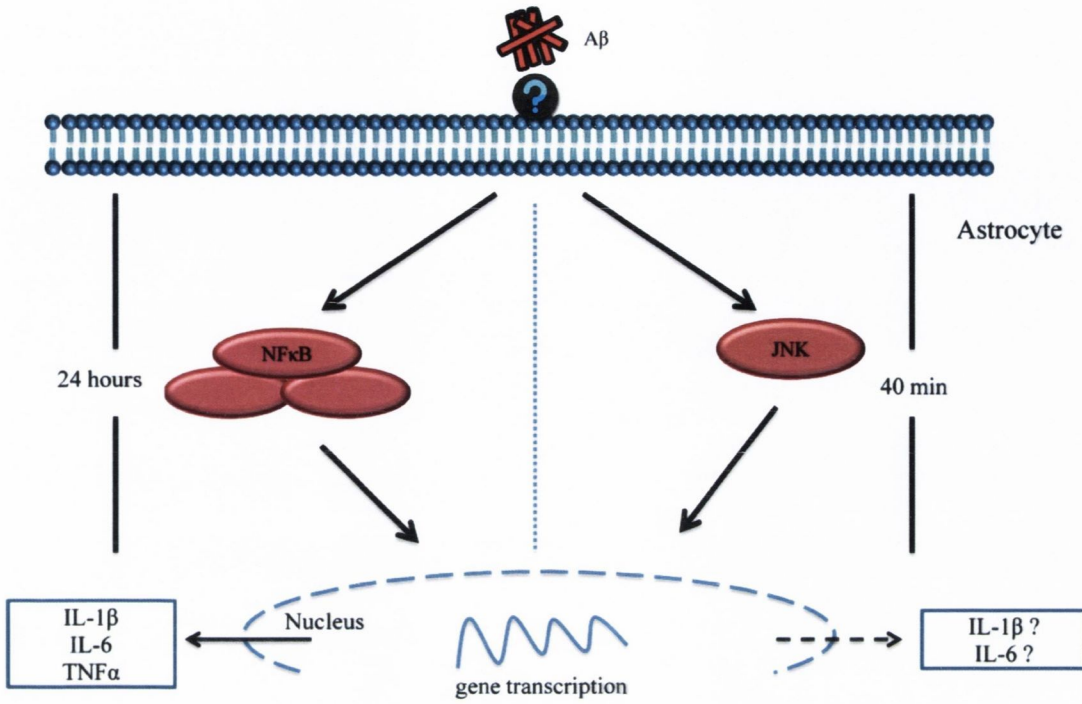
Figure 4.15 Mechanistic figure of Chapter 4

The interaction of Aβ with astrocytes induced the activation of NFκB and JNK signalling pathways. NFκB activation was present at 24 hours and induced an increase in pro-inflammatory cytokines. JNK activation was only present at 40 min and is not clear the role it plays in Aβ-induced astrocytic activation. A possible receptor through which Aβ interacts with astrocytes will be explored in Chapter 5.

Chapter 5

5.1. Introduction

There is clear evidence indicating that astrocytes react to the presence of Aβ. Astrocytes are known to migrate and localize in the proximity of amyloid plaques in AD (Nagele et al., 2004) and Aβ-containing astrocytes have been observed in the human entorhinal cortex (Thal et al., 2000). Moreover, it has also been reported that Aβ activates (Garcia-Matas et al., 2010) and is degraded (Wyss-Coray et al., 2003) by astrocytes *in vivo* and *in vitro*.

Numerous proteins expressed on the cell surface of astroglial cells have been proposed to be involved in Aβ binding (Farfara et al., 2008). RAGE binds to both monomeric and fibrillar forms of Aβ, while CD36 and CD47 are reported to bind only to fibrils (Verdier et al., 2004) (Figure 5.1).

RAGE is a transmembrane protein and a member of the immunoglobulin superfamily. RAGE identifies 3-dimensional structures of proteins rather than specific amino acid sequences explaining why it has multiple ligands which include S100 proteins, Aβ and amphoterin (Han et al., 2011). S100β, in particular, has been linked to pathological changes in AD (Mori et al., 2010).

Another receptor present on astrocytes that has been considered to be involved in the pathophysiology of AD is CD47. CD47 is a transmembrane protein, a member of the immunoglobulin superfamily, and the ligand for the extracellular region of SIRPα. The interaction between CD47 and SIRPα is important for the regulation of migration and phagocytosis (Matozaki et al., 2009).

CD36 is a glycoprotein member of the family of scavenger receptors with diverse functions which include modulation of behaviour, immunity and metabolism (Silverstein and Febbraio, 2009). CD36 has been reported to form a complex with CD47 and $\alpha_6\beta_1$ integrin that interacts with fibrillar Aβ (Koenigsknecht and Landreth, 2004), but CD36 has also been shown to bind Aβ on its own, activating microglia and inducing the production of cytokines (Wilkinson et al., 2011).

The aim of the study was to investigate the possible receptor through which Aβ interacts with astrocytes and explore the signalling pathways and cytokines involved in this process.

5.2. Methods

Isolated astrocytes were obtained from the cortices of neonatal rats and plated into 24-well plates following the protocol detailed in section 2.6.3. Astrocytes were pre-treated with an anti-RAGE antibody (αRAGE; 2.5μg/ml) or with S100β peptide (0.001μM) for 1 hour and then were incubated in the presence of Aβ or DMEM for 24 hours. Also, anti-CD47 (αCD47; 2μg/ml), anti-SIRPα (αSIRPα; 2.5μg/ml) and anti-CD36 (αCD36; 2μg/ml) antibodies were incubated for 1 hour followed by Aβ or DMEM for 24 hours. IL-1β, IL-6, TNFα, MCP-1, RAGE, S100β, CD47 and SIRPα mRNA prepared from the cell lysate were measured by PCR (see section 2.7. for details). The supernatant concentration of the cytokines was determined by ELISA (see section 2.8. for details). The phosphorylated forms of IκBα and JNK were determined by western immunoblotting (see section 2.10. for details).

5.3. Results

5.3. Effects of Aβ on cell-surface receptors in isolated rat cortical astrocytes

5.3.1. *Effect of Aβ on RAGE in isolated rat cortical astrocytes*

Aβ has been shown to bind to several cell surface proteins; one of these is RAGE. To study the possibility that Aβ exerts its effects by interacting with RAGE, isolated astrocytes were pre-treated with αRAGE (2.5μg/ml) for 1 hour and incubated in the presence of Aβ or DMEM for 24 hours. IL-1β, IL-6 and TNFα concentrations were measured in the supernatants and IL-1β, IL-6, TNFα and S100β mRNA were assessed in harvested cells. The phosphorylated form of IκBα and JNK were determined by western immunoblotting in samples of cell lysate.

IL-1β mRNA was significantly increased in Aβ-treated astrocytes compared with controls ($p < 0.01$; ANOVA; Figure 5.2A); pre-treatment with αRAGE did not affect the Aβ-induced increase in IL-1β mRNA (ANOVA; Figure 5.2A). IL-1β concentration was significantly increased in supernatants prepared from Aβ-treated astrocytes (52.48 ± 4.5pg/ml) compared with control astrocytes (24.46 ± 3.45pg/ml; $p < 0.001$; ANOVA; Figure 5.2B); pre-treatment with αRAGE significantly attenuated the Aβ-induced increase in IL-1β (32.23 ± 2.32pg/ml; $p < 0.01$; ANOVA; Figure 5.2B).

IL-6 mRNA was significantly increased in Aβ-treated astrocytes compared with controls ($p < 0.05$; ANOVA; Figure 5.2C); pre-treatment with αRAGE did not affect the Aβ-induced increase in IL-6 mRNA (ANOVA; Figure 5.2C). IL-6 concentration was significantly increased in supernatants prepared from Aβ-treated astrocytes (377.3 ± 53.78pg/ml) compared with control astrocytes (127.7 ± 44.27pg/ml; $p < 0.01$; ANOVA; Figure 5.2D); pre-treatment with αRAGE significantly attenuated the Aβ-induced increase in IL-6 concentration (179.1 ± 51.66pg/ml; $p < 0.05$; ANOVA; Figure 5.2D).

TNFα mRNA was increased in Aβ-treated astrocytes but failed to reach statistical significance (ANOVA; Figure 5.2E); pre-treatment with αRAGE had no effect on TNFα mRNA (ANOVA; Figure 5.2E). TNFα concentration was significantly increased in supernatants prepared from Aβ-treated astrocytes (34.47 ± 6.86pg/ml) compared with control astrocytes (10.59 ± 2.57pg/ml; $p < 0.01$; ANOVA; Figure 5.2F); pre-treatment with

αRAGE did not to attenuate the Aβ-induced increase in TNFα concentration (26.74 ± 7.51pg/ml; ANOVA; Figure 5.2F).

Neither Aβ nor α-RAGE affected S100β mRNA expression in isolated astrocytes (ANOVA; Figure 5.3).

IκBα phosphorylation was significantly increased in Aβ-treated astrocytes compared with controls (p<0.001; ANOVA; Figure 5.4B); pre-treatment with αRAGE significantly attenuated the Aβ-induced increase in p-IκBα (p<0.05; ANOVA; Figure 5.4B).

JNK phosphorylation was similar in Aβ-treated astrocytes compared with controls (ANOVA; Figure 5.5B) and pre-treatment with αRAGE had no significant effect on p-JNK in Aβ-treated astrocytes (ANOVA; Figure 5.5B).

5.3.2. *Effect of S100β peptide in isolated rat cortical astrocytes treated with Aβ*

S100β is a calcium-binding protein that acts as one of the natural ligands of RAGE. To study the relationship of Aβ with RAGE and RAGE intracellular pathways, isolated astrocytes were pre-treated with S100β peptide (0.001μM) for 1 hour and incubated in the presence of Aβ or DMEM for 24 hours. IL-1β, IL-6 and TNFα concentrations were measured in the supernatants and IL-1β, IL-6, TNFα and RAGE mRNA were assessed in harvested cells. The phosphorylated form of IκBα and JNK were determined by western immunoblotting in samples of cells lysate.

IL-1β mRNA was significantly increased in Aβ-treated astrocytes compared with controls (p<0.001; ANOVA; Figure 5.6A); pre-treatment with S100β significantly attenuated the Aβ-induced increase in IL-1β mRNA (p<0.05; ANOVA; Figure 5.6A). IL-1β concentration was significantly increased in supernatants prepared from Aβ-treated astrocytes (59.45 ± 13.97pg/ml) compared with control astrocytes (0 ± 0pg/ml; p<0.001; ANOVA; Figure 5.6B); pre-treatment with S100β significantly attenuated the Aβ-induced increase in IL-1β concentration (32.56 ± 6.57pg/ml; p<0.05; ANOVA; Figure 5.6B).

IL-6 mRNA was significantly increased in Aβ-treated astrocytes compared with controls (p<0.01; ANOVA; Figure 5.6C); pre-treatment with S100β did not affect the Aβ-induced increase in IL-6 mRNA (ANOVA; Figure 5.6C). IL-6 concentration was significantly

increased in supernatants prepared from Aβ-treated astrocytes (1481 ± 447.8pg/ml) compared with control astrocytes (135 ± 30.62pg/ml; $p<0.01$; ANOVA; Figure 5.6D); pre-treatment with S100β significantly attenuated the Aβ-induced increase in IL-6 concentration (642.5 ± 219.2pg/ml; $p<0.05$; ANOVA; Figure 5.6D).

TNFα mRNA was not significantly changed in Aβ-treated astrocytes (ANOVA; Figure 5.6E); pre-treatment with S100β had no effect on TNFα mRNA (ANOVA; Figure 5.6E). TNFα concentration was increased in supernatants prepared from Aβ-treated astrocytes (28.9 ± 14.52pg/ml) compared with control astrocytes (2.23 ± 1.48pg/ml) but the difference failed to reach statistical significance (ANOVA; Figure 5.6F); pre-treatment with S100β exerted no effect on TNFα concentration (32.96 ± 13.42pg/ml; ANOVA; Figure 5.6F).

Neither Aβ nor S100β affected RAGE expression in astrocytes (ANOVA; Figure 5.7).

IκBα phosphorylation was significantly increased in Aβ-treated astrocytes compared with controls ($p<0.01$; ANOVA); pre-treatment with S100β attenuated the Aβ-induced increase in p-IκBα but the difference failed to reach statistical significance.

5.3.3. *Effect of Aβ on CD47 in isolated rat cortical astrocytes*

CD47 is a transmembrane glycoprotein that interacts with integrins and CD36. To study the possibility that CD47 might mediate the effects of Aβ, isolated astrocytes were pre-treated with an anti-CD47 antibody (αCD47; 2μg/ml) for 1 hour and incubated in the presence of Aβ or DMEM for 24 hours. IL-1β, IL-6 and TNFα concentrations were measured in the supernatants and IL-1β, IL-6, TNFα and MCP-1 mRNA were assessed in harvested cells.

IL-1β mRNA was increased in Aβ-treated astrocytes compared with controls ($p<0.01$; Student t-test for dependent means; Figure 5.8A); the analysis by ANOVA failed to identify a significant change but a Student t-test comparison between Aβ-treated astrocytes and controls achieved statistical significance. Aβ-induced increase in IL-1β mRNA was further increased when astrocytes were pre-treated with αCD47 ($p<0.05$; ANOVA; Figure 5.8A). IL-1β concentration was increased in supernatants prepared from Aβ-treated astrocytes (57.79 ± 17.41pg/ml) compared with control astrocytes (19.56 ±

9.72pg/ml; p<0.01; Student t-test for dependent means; Figure 5.8B); Aβ-induced increase in IL-1β concentration was further increased when isolated astrocytes were pre-treated with αCD47 (162.4 ± 11.43pg/ml; p<0.001; ANOVA; Figure 5.8B).

IL-6 mRNA was significantly increased in Aβ-treated astrocytes compared with controls (p<0.01; Student t-test for dependent means; Figure 5.8C); Aβ-induced increase in IL-6 mRNA was further increased when astrocytes were pre-treated with αCD47 (p<0.001; ANOVA; Figure 5.8C). IL-6 concentration was significantly increased in supernatants prepared from Aβ-treated astrocytes (95.28 ± 19.95pg/ml) compared with control astrocytes (48.56 ± 16.4pg/ml; p<0.01; Student t-test for dependent means; Figure 5.8D); Aβ-induced increase in IL-6 concentration was further increased when astrocytes were pre-treated with αCD47 (550.9 ± 51.15pg/ml; p<0.001; ANOVA; Figure 5.8D).

TNFα mRNA was not affected in Aβ-treated astrocytes (ANOVA; Figure 5.8E); pre-treatment with αCD47 significantly increased TNFα mRNA in Aβ-treated astrocytes (ANOVA; Figure 5.8E). TNFα concentration was increased in supernatants prepared from Aβ-treated astrocytes (55.26 ± 22.75pg/ml) compared with control astrocytes (32.96 ± 13.42pg/ml) but the difference failed to reach statistical significance (ANOVA; Figure 5.14B); pre-treatment with αCD47 exerted no significant effect on TNFα concentration (96.56 ± 27.09pg/ml; ANOVA; Figure 5.8F).

MCP-1 mRNA was significantly increased in Aβ-treated isolated astrocytes compared with controls (p<0.001; Student t-test for dependent means; Figure 5.9); the Aβ-induced increase in MCP-1 mRNA was further increased when astrocytes were pre-treated with αCD47 (p<0.001; ANOVA; Figure 5.9).

5.3.4. *Effect of Aβ on SIRPα in isolated rat cortical astrocytes*

SIRPα is a signal-regulatory protein, member of the immunoglobulin superfamily capable of binding to CD47. To investigate the possibility that SIRPα may mediate the effects of Aβ, isolated astrocytes were pre-treated with an anti-SIRPα antibody (αSIRPα; 2.5μg/ml) for 1 hour and incubated in the presence of Aβ or DMEM for 24 hours. IL-1β, IL-6 and TNFα concentrations were measured from the supernatants and IL-1β, IL-6, TNFα and MCP-1 mRNA were assessed in harvested cells.

144

IL-1β mRNA was significantly increased in Aβ-treated astrocytes compared with controls (p<0.001; ANOVA; Figure 5.10A); pre-treatment with αSIRPα did not affect the Aβ-induced increase in IL-1β mRNA (ANOVA; Figure 5.10A). IL-1β concentration was significantly increased in supernatant prepared from Aβ-treated astrocytes (81.14 ± 14.21pg/ml) compared with control astrocytes (11.13 ± 4.94pg/ml; p<0.001; ANOVA; Figure 5.10B); pre-treatment with αSIRPα significantly attenuated the Aβ-induced increase in IL-1β concentration (47.0 ± 10.53pg/ml; p<0.05; ANOVA; Figure 5.10B).

IL-6 mRNA was significantly increased in Aβ-treated astrocytes compared with controls (p<0.001; ANOVA; Figure 5.10C); pre-treatment with αSIRPα did not affect the Aβ-induced increase in IL-6 mRNA (ANOVA; Figure 5.10C). IL-6 concentration was significantly increased in supernatant prepared from Aβ-treated astrocytes (105.5 ± 23.64pg/ml) compared with control astrocytes (3.40 ± 3.14pg/ml; p<0.001; ANOVA; Figure 5.10D); pre-treatment with αSIRPα attenuated the Aβ-induced increase in IL-6 concentration (79.33 ± 11.8pg/ml) but the difference failed to reach statistical significance (ANOVA; Figure 5.10D).

TNFα mRNA was significantly increased in Aβ-treated astrocytes compared with controls (p<0.05; ANOVA; Figure 5.10E); pre-treatment with αSIRPα failed to attenuate the Aβ-induced increase in TNFα mRNA in Aβ-treated astrocytes (ANOVA; Figure 5.10E). TNFα concentration was increased in supernatant prepared from Aβ-treated astrocytes (40.89 ± 12.24pg/ml) compared with control astrocytes (7.96 ± 6.45pg/ml) but the difference failed to reach statistical significance (ANOVA; Figure 5.10F); pre-treatment with αSIRPα exerted no significant effect on the Aβ-induced increase in TNFα concentration (24.83 ± 14.72pg/ml; ANOVA; Figure 5.10F).

Neither Aβ nor αSIRPα affected the expression of CD47 in astrocytes (ANOVA; Figure 5.11).

5.3.5. *Effect of Aβ on CD36 in isolated rat cortical astrocytes*

CD36 is a glycoprotein member of the family of scavenger receptors with signal transduction and cell adhesion functions. To investigate the possibility that CD36 may mediate the effects of Aβ, isolated astrocytes were pre-treated with an anti-CD36 antibody (αCD36; 2μg/ml) for 1 hour and incubated in the presence of Aβ or DMEM for 24 hours. IL-1β, IL-6 and TNFα concentrations were measured from the supernatants and IL-1β, IL-6, TNFα, CD47 and SIRPα mRNA were assessed in harvested cells.

IL-1β mRNA was significantly increased in αCD36-treated but not in Aβ-treated astrocytes compared with controls ($p < 0.001$; ANOVA; Figure 5.12A); pre-treatment with αCD36 significantly increased IL-1β mRNA in Aβ-treated astrocytes ($p < 0.001$; ANOVA; Figure 5.12A). IL-1β concentration was significantly increased in supernatants prepared from Aβ-treated astrocytes (11.63 ± 4.06pg/ml) compared with control astrocytes (0.11 ± 0.11pg/ml; $p < 0.05$; Student t-test for dependent means; Figure 5.12B); the Aβ-induced increase in IL-1β concentration was further increased when astrocytes were pre-treated with αCD36 (78.01 ± 19.63pg/ml; $p < 0.01$; ANOVA; Figure 5.12B).

IL-6 mRNA was significantly increased in αCD36-treated but not in Aβ-treated astrocytes compared with controls ($p < 0.01$; ANOVA; Figure 5.12C); pre-treatment with αCD36 significantly increased IL-6 mRNA in Aβ-treated astrocytes ($p < 0.01$; ANOVA; Figure 5.12C). IL-6 concentration was significantly increased in supernatants prepared from Aβ-treated (140.3 ± 7.3pg/ml; $p < 0.01$; Student t-test for dependent means; Figure 5.21B) and αCD36-treated (1450 ± 45.83pg/ml; $p < 0.001$; ANOVA; Figure 5.12D) astrocytes compared with control astrocytes (50.87 ± 22.86pg/ml). Aβ-induced increase in IL-6 concentration was further increased when astrocytes were pre-treated with αCD36 (1843 ± 155.3pg/ml; $p < 0.001$; ANOVA; Figure 5.12D).

TNFα mRNA was significantly increased in αCD36-treated but not in Aβ-treated astrocytes compared with controls ($p < 0.05$; ANOVA; Figure 5.12E); TNFα mRNA was significantly attenuated in Aβ-treated astrocytes pre-treated with αCD36 compared with control Aβ-treated astrocytes ($p < 0.01$; ANOVA; Figure 5.12E). TNFα concentration was significantly increased in supernatants prepared from αCD36-treated (385.6 ± 41.47pg/ml; $p < 0.001$; ANOVA; Figure 5.12F) but not from Aβ-treated (4.04 ± 2.27pg/ml; ANOVA; Figure 5.12F) astrocytes compared with control astrocytes (0.12 ±

0.12pg/ml). Aβ-induced increase in TNFα concentration was further increased when astrocytes were pre-treated with αCD36 (378.6 ± 37.22pg/ml; p<0.001; ANOVA; Figure 5.12F).

CD47 mRNA was significantly increased in αCD36-treated but not in Aβ-treated astrocytes compared with controls (p<0.05; ANOVA; Figure 5.13A). Neither Aβ nor αCD36 affected the mRNA expression of SIRPα in astrocytes (ANOVA; Figure 5.13B).

5.3.6. *Effects of simultaneous addition of αCD36 and αCD47 on Aβ-treated isolated rat cortical astrocytes*

To further study the relationship of Aβ with the CD36/CD47 complex, isolated astrocytes were pre-treated simultaneously with αCD36 (2μg/ml) and αCD47 (2μg/ml) for 1 hour and incubated in the presence of Aβ or DMEM for 24 hours. IL-6 and TNFα concentration was measured in the supernatants.

IL-6 concentration was significantly increased in supernatants prepared from Aβ-treated astrocytes (400.6 ± 81.39pg/ml; p<0.05; ANOVA; Figure 5.14A) and astrocytes incubated in the presence of αCD36+αCD47 (586.9 ± 54.04pg/ml; p<0.001; ANOVA; Figure 5.14A) compared with non-stimulated controls (222.2 ± 68.13pg/ml). Aβ-induced increase in IL-6 concentration was further increased when astrocytes were pre-treated with αCD36+αCD47 (738.8 ± 62.83pg/ml; p<0.001; ANOVA; Figure 5.14A).

TNFα concentration was significantly increased in supernatants prepared from Aβ-treated astrocytes (75.07 ± 9.51pg/ml; p<0.001; Student t-test for dependent means; Figure 5.14B) and astrocytes incubated in the presence of αCD36+αCD47 (481.9 ± 34.28pg/ml; p<0.001; ANOVA; Figure 5.14B) compared with non-stimulated controls (0.0 ± 0.0pg/ml). Aβ-induced increase in TNFα concentration was further increased when isolated astrocytes were pre-treated with αCD36+αCD47 (514.3 ± 36.85pg/ml; p<0.001; ANOVA; Figure 5.14B).

5.4. Discussion

The objective of this study was to explore the interaction of Aβ with different membrane receptors present in astrocytes. The data show that incubation in the presence of an anti-RAGE antibody significantly attenuated the Aβ-induced increase in IL-1β, IL-6 and IκBα phosphorylation. Incubation of astrocytes with anti-CD36 or anti-CD47 antibodies induced a pro-inflammatory response and augmented the Aβ-induced increase in cytokines (Table 5.1).

One of the most interesting findings in this study is that treatment with an anti-RAGE antibody significantly attenuated the Aβ-induced increase in pro-inflammatory cytokines released from cultured astrocytes. RAGE is a transmembrane receptor, member of the immunoglobulin superfamily, present in the nervous system on astrocytes, microglia, neurons, endothelial cells and smooth muscle cells (Yan et al., 2009). It has been shown that RAGE binds to Aβ resulting in cellular oxidative stress, chemotaxis and cytokine production (Yan et al., 1996). In human brain tissue, individuals with AD presented astrocytes containing co-localized AGE-, RAGE- and Aβ- positive granules as opposed to brains from control individuals and diabetes mellitus individuals which not (Sasaki et al., 2001). The results obtained in this work are consistent with these previously-reported observations which indicate that RAGE is a binding site for Aβ. Interestingly, RAGE has been suggested to work as a transporter of Aβ into the brain, while LRP transports it out (Donahue et al., 2006). Additionally, RAGE has been reported to be involved in the production of Aβ as shown by Cho and colleagues (2009) in an AD mouse model, where it stimulated the expression of BACE1 through activation of nuclear factor of activated T-cells 1 (NFAT1), resulting in increased production and deposition of Aβ in the brain (Cho et al., 2009).

In the present work, IL-1β and IL-6, but not TNFα mRNA were increased by Aβ and release of IL-1β and IL-6 were consistently observed, though release of TNFα was not. The data indicate that the effect of Aβ on release of IL-1β and IL-6 was inhibited by anti-RAGE though mRNA was not affected. This suggests that RAGE mediates the Aβ-induced effect on release rather than on transcription. Production and release of cytokines and pro-inflammatory agents through activation of RAGE has been reported before; in

plasma obtained from aged humans, elevated endogenous secretory RAGE concentrations were associated with elevated IL-6 and reduced IL-1 receptor antagonist (Crasto et al., 2011). Kokkola and colleagues (2005), reported that HMGB1 induced the production of TNFα and NO through RAGE activation in rat macrophages and that RAGE$^{-/-}$ mice, stimulated with HMGB1, had a 70% reduction in the production of IL-1β, IL-6 and TNFα compared with HMGB1-stimulated wild type mice, but still significantly higher than non-stimulated controls (Kokkola et al., 2005). Yan and colleagues (2000), showed that treatment with an anti-RAGE antibody inhibited the accumulation of serum amyloid A and decreased IL-6 in *in vivo* and *in vitro* mouse models (Yan et al., 2000). Functional inactivation of RAGE and deficiency of RAGE signalling in mouse microglia significantly suppressed Aβ-induced IL-1β production (Origlia et al., 2010). Although the investigations previously mentioned were not done in astroglia, the findings are consistent with and can be extrapolated to the results presented in this study regarding cytokine production through stimulation of RAGE in astrocytes. In the present work, IL-1β and IL-6 showed differences in expression and release compared with TNFα, this could be explained by evidence that indicates TNFα may have different activation pathways from other cytokines, such as IL-6, when induced through RAGE. Treatment of microglial mouse cells, stimulated with chicken albumin, with an anti-RAGE antibody, showed downregulation of NO, TNFα and IL-6, reporting differential pathways for TNFα and IL-6 since NOS inhibitors did not decreased TNFα secretion but reduced significantly IL-6 secretion (Dukic-Stefanovic et al., 2003). Another possible explanation involves the time of production and release of cytokines, as it has been shown that TNFα is induced at an earlier time than IL-1β or IL-6 (Kim et al., 2002); is possible that TNFα values are already in decline at 24 hours explaining why changes in TNFα induced by Aβ stimulation observed in this study are not reliable. Microglial cells, not astrocytes, are regarded as the main source of TNFα and NO within the brain (Delgado et al., 1998).

Treatment with an anti-RAGE antibody significantly attenuated the Aβ-induced increase in phosphorylated IκBα while, as expected in this study, neither Aβ nor αRAGE had any effect on phosphorylated JNK. RAGE activation of the NFκB pathway has been reported before; Du Yan and colleagues (1997) shown that Aβ binds to RAGE inducing M-CSF expression through NFκB-dependent pathway activation in human neuroblastoma cells

(Du Yan et al., 1997). Moreover, it has been observed that oxidative stress induces activation of the RAGE-NFκB pathway in muscle biopsy samples from patients with facioscapulohumeral muscular dystrophy (Macaione et al., 2007). In diabetic neuropathy, RAGE-dependent sustained activation of NFκB contributed to reduced nociception (Lukic et al., 2008). Additionally, the use of an anti-RAGE antibody inhibited NFκB activation in microglial mouse cells and down-regulated the production of NO, IL-6 and TNF-α (Dukic-Stefanovic et al., 2003). As both RAGE and NFκB are present in astrocytes, is reasonable to suggest that the Aβ-induced pro-inflammatory effects observed in this study involved activation of the RAGE-NFκB pathway.

In this study, astrocytes were treated with S100β, which is a ligand for RAGE, in order to compare its effects on RAGE and cytokine production with those of Aβ. S100β peptide, in contrast to Aβ, did not induce a pro-inflammatory response, as IL-1β, IL-6 and TNFα were not changed in S100β-treated astrocytes compared with controls. In fact, treatment with S100β peptide significantly attenuated the Aβ-induced increase in IL-1β and IL-6 and also reduced the Aβ-induced increase in phosphorylated IκBα but without reaching statistical significance. S100β is a calcium-binding protein abundant in glial cells, including astrocytes, and implicated in a diverse range of intracellular functions involving protein phosphorylation, regulation of cytoskeleton constituents, protection form oxidative damage, inflammation and cell proliferation (Donato, 1999). S100β is also one of the described ligands for RAGE and has been shown to activate NFκB pathway through RAGE (Huttunen et al., 2000). In this study, S100β and Aβ showed different effects when activating RAGE and its subsequent intracellular cascades; this may be explained by the following observations. RAGE is a multi-ligand receptor that binds ligands through different mechanisms making it a promiscuous receptor; S100β is recognized by RAGE through an entropic process involving hydrophobic interaction dependent on Ca^{2+} while RAGE interaction with advanced glycation end products (AGE) is dependent on negative charges recognition of AGE-proteins (Park et al., 2010). The particular structural characteristics of RAGE and the varied nature of its ligands may help explain why RAGE can activate numerous signalling cascades which include NFκB, MAP kinase and Jak/STAT among others (Han et al., 2011). It has been suggested that specific signalling cascades activated by ligand-RAGE interaction reflect both cell type

150

and duration of cellular stimulation and that the "form" in which ligands are presented to the receptor may impact on the specific pathways triggered through RAGE activation (Clynes et al., 2007). Moreover, it has been reported that S100β and Aβ have different binding sites in RAGE, with S100β, AGEs, Aβ oligomers and transthyretin binding to the V domain while Aβ aggregates bind to the C1 domain (Leclerc et al., 2010). S100β induces different cellular responses through RAGE that can vary from trophic to toxic according to the concentration. It has been shown that S100β at nM concentrations stimulates astrocyte proliferation (Selinfreund et al., 1991) and neurite outgrowth (Haglid et al., 1997), while at μM concentrations becomes toxic to neurons (Hu et al., 1997) and astrocytes (Hu et al., 1996). Businaro and colleagues (2006), showed that S100β at nM concentration protects human LAN-5 neuroblastoma cells from Aβ, while at μM concentrations not only S100β was cytotoxic by itself, but it also was additive to the negative effects of Aβ (Businaro et al., 2006). Furthermore, incubation of cultured astrocytes with S100β induced an increase in IL-6 and TNFα secretion in a concentration- and time- dependent manner, with IL-6 reaching peak levels at 32 hours while TNFα did so earlier at 6 hours (Ponath et al., 2007). In the present study, astrocytes were incubated with S100β at nM concentrations and consistent with the literature, S100β attenuated the Aβ-induced inflammation possibly indicating a protective response. This may also help explain why RAGE-mediated cellular responses can vary from pro-inflammatory (Aβ) to anti-inflammatory (S100β).

In this study, blocking CD47 receptor in astrocytes with an anti-CD47 antibody, significantly augmented the Aβ-induced increase in IL-1β, IL-6 and MCP-1, but not in TNFα. CD47 has been implicated in the pathophysiology of AD as a consequence of its capacity to bind Aβ (Verdier et al., 2004). CD47, a transmembrane protein present in astrocytes (Junker et al., 2009), is also a ligand for the extracellular region of SIRPα (Jiang et al., 1999) and associates with different integrins (Brown and Frazier, 2001). Sick and colleagues (2011), reported that activation of CD47 with 4N1, a CD47 agonist derived from the C-terminal domain of thrombospondin-1 (TSP-1), caused increased proliferation of human U87 and U373 astrocytoma cells but not normal astrocytes, although expression levels were similar in the three cell types (Sick et al., 2011). Ligation of CD47 by TSP-1, 4N1 and 1F7 (another CD47 binding partner) induced $G_{i\alpha}$-dependent,

151

but caspase-independent, apoptosis in activated T cells (Manna and Frazier, 2003). Red blood cells lacking CD47 were phagocytosed by splenic macrophages while the binding of CD47 to SIRPα prevented the removal of red blood cells, indicating CD47 as a "marker of self" in these cells (Oldenborg et al., 2000). Interestingly, suppression in the production of pro-inflammatory cytokines in dendritic cells, including IL-6 and TNFα, and prevention of the phenotypic and functional changes associated with dendritic cell maturation has been reported after ligation of CD47 to TSP (Demeure et al., 2000). It was suggested in microglial cells that CD47 interaction with Aβ involves the constitution of a multireceptor complex including CD36, CD47 and $\alpha_6\beta_1$-integrin which mediate the binding of Aβ fibrils and the activation of intracellular signalling pathways (Bamberger et al., 2003). A more recent study by Miller and colleagues (2010) using bovine, murine and human cells, proposed that Aβ inhibition of cGMP-dependent signalling requires the presence of CD47; however, it was suggested that CD36 is the receptor which interacts directly with Aβ instead of CD47, as Aβ was unable to displace the SIRPα/CD47 ligation (Miller et al., 2010). A similar finding was reported by Persaud-Sawin and colleagues (2009), where recruitment of CD36, but not CD47, to lipids rafts which are considered to be necessary for microglial phagocytosis of $A\beta_{1-42}$, suggests that CD47, if involved, may act mainly as a negative regulator of microglial phagocytosis (Persaud-Sawin et al., 2009). These previous reports indicate that CD47 possess a mainly regulatory function and that the nature of its response is highly dependent on its binding partnership. This agrees with the data of the present study where CD47 seems to be exerting a modulatory effect on astrocytic inflammatory cytokine production.

In this study, treatment of astrocytes with an anti-SIRPα antibody showed a significant reduction in the Aβ-induced increase in IL-1β and a moderate decrease in IL-6 and TNFα but had no effect on CD47 expression. As mentioned previously, the association of SIRPα with CD47 is critical in the recognition and clearance of red blood cells (Oldenborg et al., 2000), but this is not the only regulatory function ascribed to this partnership as CD47-SIRPα interaction was observed to regulate the homeostasis of human NK cells, T cells and eosinophils (Legrand et al., 2011, Verjan Garcia et al., 2011). CD47 and SIRPα interact with each other through their extracellular regions and are thought to initiate intracellular signalling in a bidirectional manner (Kusakari et al.,

2008). SIRPα cytoplasmic region binds to SHP initiating intracellular responses stimulated by different factors such as CD47 ligation or cytokines (van Beek et al., 2005). SIRPα is considered a negative regulator of cellular signalling but evidence in the literature indicates it is involved in the activation of certain effector functions as shown in macrophages where SIRPα promoted the production of NO via SIRPα-associated JAK2 (Alblas et al., 2005). Additionally, it has been reported that SIRPα can be a positive regulator for the development of Th17-related autoimmune pathologies and the development of dendritic cells (Matozaki et al., 2009). Data from the present study suggest that SIRPα may be involved in a pro-inflammatory reaction increasing primarily IL-1β when astrocytes are stimulated with Aβ.

The data presented here indicated that blocking CD36 receptor in astrocytes with an anti-CD36 antibody significantly increased the production of pro-inflammatory cytokines and augmented the Aβ-induced increase in IL-1β, IL-6 and TNFα. Moreover, αCD36-treatment increased CD47 expression but not SIRPα expression. SIRPα (also known as CD172a) has been found to be expressed in neural progenitor cells (Vogel et al., 2003), neurons and in astrocytes (Sergent-Tanguy et al., 2006). There is significant evidence indicating CD36 as a receptor for Aβ fibrils and its participation in initiation of intracellular signalling cascades in microglia and macrophages (Moore et al., 2002). CD36 expression correlated with the presence of amyloid plaques but not with AD in brain samples taken from human frontal cortices of cognitively normal individuals with diffuse amyloid plaques and of AD patients (Ricciarelli et al., 2004). Apart from the already-mentioned CD36/CD47/$\alpha_6\beta_1$-integrin complex, CD36 has been associated with another heterotrimeric complex involving TLR4 and TLR6 that signals through NFκB and induces a pro-inflammatory response when in the presence of Aβ in macrophages (Stewart et al., 2010). Ursolic acid has been reported to inhibit the association of Aβ with CD36 attenuating microglial Aβ-induced activation evidenced by a reduction in the production of ROS (Wilkinson et al., 2011). Pre-treatment of microglial cells with antibodies against CD36 or the CD36 ligand TSP-1 blocks the interaction between CD36 and fibrillar Aβ resulting in inhibition of ROS and hydrogen peroxide production (Coraci et al., 2002). In addition, CD36 seems to be critical in the regulation of NADPH oxidase-dependent vascular oxidative stress and neurovascular dysfunction induced by $A\beta_{1-40}$ in

153

mice (Park et al., 2011). Although most reports in the literature associate CD36 with pro-inflammatory activation, there is evidence indicating that CD36 may have immune modulatory actions as well. Bottcher and colleagues (2006) reported that when macrophages are engaged in phagocytosis CD36 can suppress proinflammatory cytokine signalling in human apoptotic cells (Bottcher et al., 2006). PPARγ agonists are known to inhibit production of monocytes inflammatory cytokines (Jiang et al., 1998a) and also PPARγ has been shown to regulate the expression of CD36 (Tontonoz et al., 1998). Asada and colleagues (2004), showed that activation of PPARγ expressed in human alveolar macrophage, led to inhibition of LPS-induced TNF-α production and induction of CD36 expression (Asada et al., 2004). Moreover, a link between the anti-inflammatory cytokine IL-10 and CD36 has been proposed as CD36 may directly induce the production of IL-10 (Parsons et al., 2008). In this study, CD36 seems to behave in a similar manner to CD47, exerting a modulatory effect on the production of pro-inflammatory cytokines.

It is concluded from the present data that the interaction of Aβ with RAGE triggers the NFκB pathway in astrocytes and increases the production of pro-inflammatory cytokines IL-1β and IL-6 but not TNFα. The Aβ-induced response was partially mimicked when astrocytes were incubated with S100β peptide, suggesting that the interaction of S100β at nM concentration with RAGE exerts a modulatory response indicating a possible protective role. In contrast, CD36 and CD47 interact with Aβ in a similar way, pointing to a shared modulatory effect of these surface proteins on the production of inflammatory cytokines in astrocytes. This was supported with the increase in IL-6 and TNFα observed when Aβ–stimulated astrocytes were simultaneously pre-treated with α-CD36 and αCD47. Crosstalk between RAGE pro-inflammatory signalling and CD36 and CD47 modulatory signalling in Aβ-treated astrocytes requires further exploration (Figure 5.15).
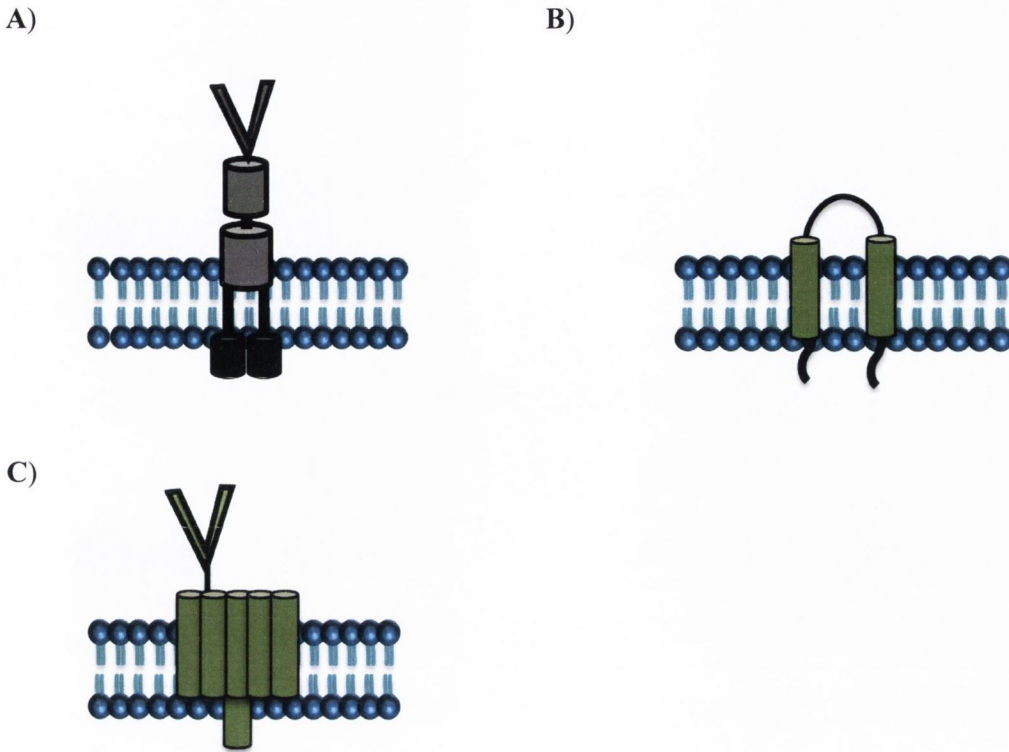
Figure 5.1 RAGE, CD36 and CD47 receptors.

Numerous astrocytic receptors have been proposed to bind Aβ. RAGE, CD36 and CD47 were explored in this study.

A) RAGE is a 45kDa transmembrane protein member of the immunoglobulin superfamily. It structure consists of an extracellular variable V-domain, two extracellular constant C type domains, a single transmembrane region and a short C-terminal cytoplasmic tail.

B) CD36 is an 88kDa glycoprotein member of the family of scavenger receptors. It is composed of a large extracellular loop and two transmembrane α-helices, one at the amino and the other at the carboxi termini.

C) CD47 is a 47-52kDa transmembrane protein member of the immunoglobulin superfamily. It possesses a single IgV-like domain at its N-terminus, a hydrophobic stretch with five membrane-spanning segments and an alternatively-spliced cytoplasmic C-terminus.
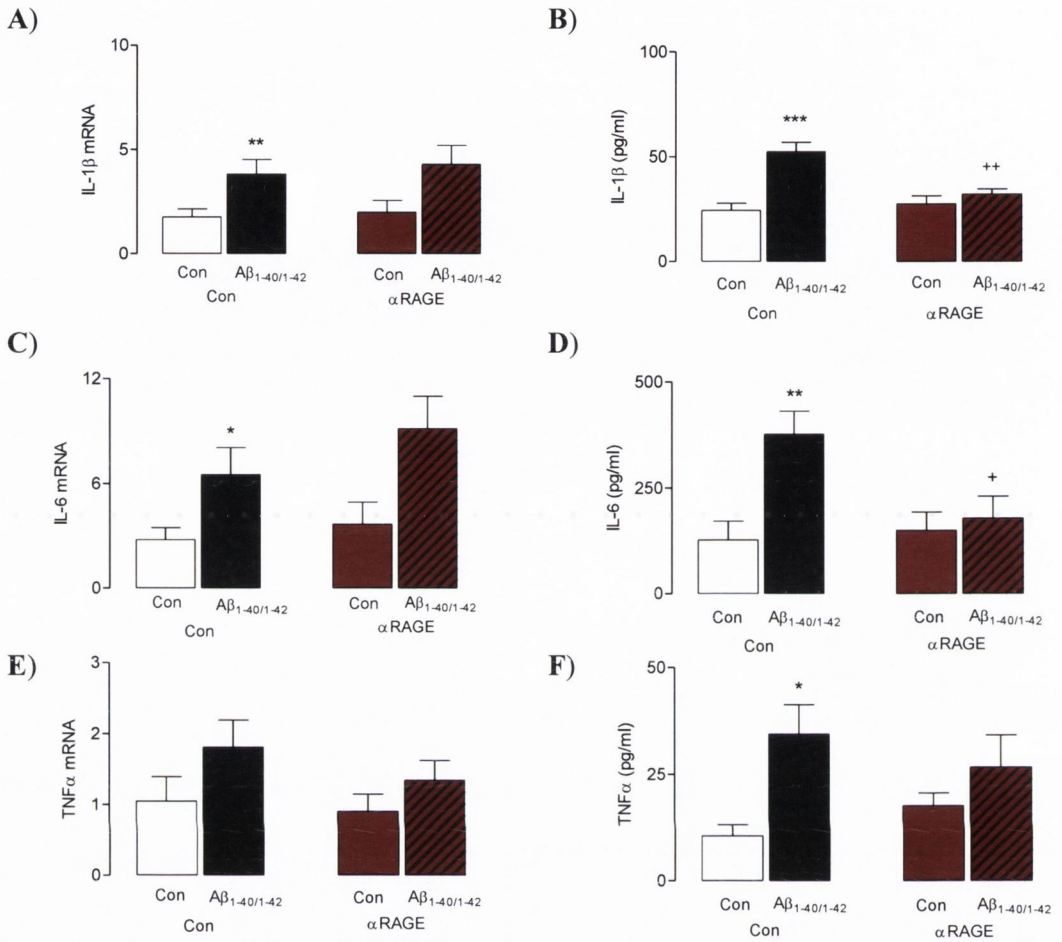
Figure 5.2 Anti-RAGE antibody attenuated the Aβ-induced increase in IL-1β and IL-6 in isolated astrocytes

Astrocytes obtained from the cortices of neonatal Wistar rats were cultured in the presence of a cocktail of $Aβ_{1-40}$ (4.2μM) and $Aβ_{1-42}$ (5.6μM) following 1 hour pre-treatment with an anti-RAGE antibody (αRAGE; 2.5μg/ml). After 24 hours, IL-1β, IL-6 and TNFα mRNA and supernatant concentration of IL-1β, IL-6 and TNFα were determined by PCR and ELISA, respectively. Data are presented as means ± SEM.

A) Mean IL-1β mRNA was significantly increased in Aβ-treated astrocytes compared with controls (**p<0.01 vs. controls). Pre-treatment with αRAGE failed to attenuate the Aβ-induced increase in IL-1β mRNA (ANOVA $F_{(3,12)}$ =18.13, p<0.0001; n=5). **B**) Mean IL-1β concentration was significantly increased in supernatant obtained from Aβ-treated astrocytes compared with controls (***p<0.001 vs. controls). Pre-treatment with αRAGE significantly attenuated the Aβ-induced increase in IL-1β concentration (++p<0.01 vs. Aβ controls; ANOVA $F_{(3,12)}$ =17.31, p=0.0001; n=5).
C) Mean IL-6 mRNA was significantly increased in Aβ-treated astrocytes compared with controls (*p<0.05 vs. controls). Pre-treatment with αRAGE failed to attenuate the Aβ-induced increase in IL-6 mRNA (ANOVA $F_{(3,9)}$ =10.10, p=0.0031; n=4). **D**) Mean IL-6 concentration was significantly increased in supernatant obtained from Aβ-treated astrocytes compared with controls (**p<0.01 vs. controls). Pre-treatment with αRAGE significantly attenuated the Aβ-induced increase in IL-6 concentration (+p<0.05 vs. Aβ controls; ANOVA $F_{(3,15)}$ =7.404, p=0.0029; n=6).
E) Mean TNFα mRNA was not affected by treatment with Aβ or αRAGE in astrocytes (ANOVA $F_{(3,12)}$ =3.752, p=0.041; n=5). **F**) Mean TNFα concentration was significantly increased in supernatant obtained from Aβ-treated astrocytes compared with controls (*p<0.05 vs. controls). Pre-treatment with αRAGE failed to attenuate the Aβ-induced increase in TNFα concentration (ANOVA $F_{(3,19)}$ =3.514, p=0.035; n=6).

156
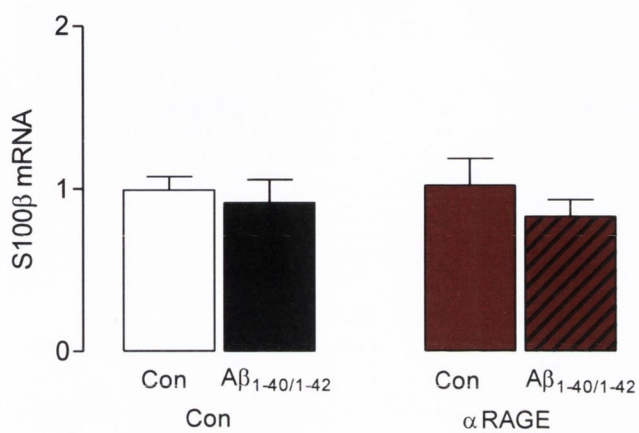
Figure 5.3 Anti-RAGE antibody had no effect on S100β mRNA expression in Aβ-treated isolated astrocytes

Astrocytes were incubated in the presence of Aβ following 1 hour pre-treatment with αRAGE antibody (2.5µg/ml). After 24 hours, S100β mRNA prepared from harvested cells was determined by PCR. Data are presented as means ± SEM.

Mean S100β mRNA was not affected by treatment with Aβ or αRAGE in astrocytes (ANOVA $F_{(3,12)}$ =0.802, p=0.516; n=5).

A)
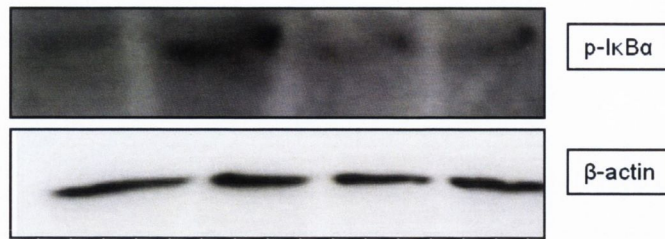
B)

Figure 5.4 Anti-RAGE antibody attenuated the Aβ-induced increase in pIκBα in isolated astrocytes

Astrocytes were incubated in the presence of Aβ following 1 hour pre-treatment with αRAGE antibody (2.5μg/ml). IκBα phosphorylation was determined by western immunoblotting. Data are presented as means ± SEM.

A) Sample immunoblots indicating density of p-IκBα (40kDa) and β-actin (42kDa).

B) p-IκBα was significantly increased in cell lysates prepared from Aβ-treated astrocytes compared with controls (***p<0.001 vs. controls). Pre-treatment with αRAGE significantly attenuated the Aβ-induced increase in p-IκBα ([+]p<0.05 vs. Aβ controls; ANOVA $F_{(3,9)}$ =26.03, p<0.0001; n=4). Values are expressed in arbitrary units (a.u.) obtained from calculating the ratio of p-IκBα to β-actin provided by densitometric analysis.

A)

B)
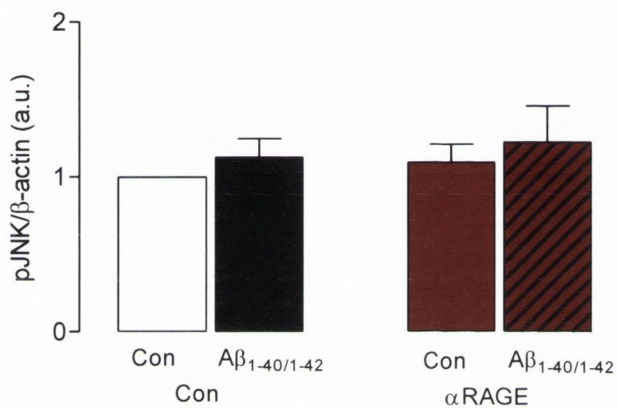
Figure 5.5 Anti-RAGE antibody had no effect on pJNK in Aβ-treated isolated astrocytes

Astrocytes were incubated in the presence of Aβ following 1 hour pre-treatment with αRAGE antibody (2.5μg/ml). JNK phosphorylation was determined by western immunoblotting. Data are presented as means ± SEM.

A) Sample immunoblots indicating density of p-JNK (upper band: 54kDa; lower band: 46kDa) and β-actin (42kDa).

B) p-JNK was not affected by treatment with Aβ or αRAGE in Aβ-treated astrocytes (ANOVA $F_{(3,35)}$ =0.449, p=0.719; n=10. Values are expressed in arbitrary units (a.u.) obtained from calculating the ratio of p-JNK to β-actin provided by densitometric analysis.

Figure 5.6 S100β attenuated the Aβ-induced increase in IL-1β and IL-6 in isolated astrocytes

Astrocytes were incubated in the presence of Aβ following 1 hour pre-treatment with S100β peptide (0.001μM). After 24 hours, IL-1β, IL-6 and TNFα mRNA, prepared from harvested cells and supernatant concentration of IL-1β, IL-6 and TNFα were determined by PCR and ELISA, respectively. Data are presented as means ± SEM.

A) Mean IL-1β mRNA was significantly increased in Aβ-treated astrocytes compared with controls (***$p < 0.001$ vs. controls). Pre-treatment with S100β significantly attenuated the Aβ-induced increase in IL-1β mRNA ([+]$p < 0.05$ vs. Aβ controls; ANOVA $F_{(3,12)}$ =15.89, $p = 0.0002$; n=5). **B)** Mean IL-1β concentration was significantly increased in supernatant obtained from Aβ-treated astrocytes compared with controls (***$p < 0.001$ vs. controls). Pre-treatment with S100β significantly attenuated the Aβ-induced increase in IL-1β concentration ([+]$p < 0.05$ vs. Aβ controls; ANOVA $F_{(3,15)}$ =12.30, $p = 0.0003$; n=5).

C) Mean IL-6 mRNA was significantly increased in Aβ-treated astrocytes compared with controls (**$p < 0.01$ vs. controls). Pre-treatment with S100β attenuated the Aβ-induced increase in IL-6 mRNA but the difference failed to reach statistical significance (ANOVA $F_{(3,12)}$ =10.87, $p = 0.001$; n=5). **D)** Mean IL-6 concentration was significantly increased in supernatant obtained from Aβ-treated astrocytes compared with controls (**$p < 0.01$ vs. controls). Pre-treatment with S100β significantly attenuated the Aβ-induced increase in IL-6 concentration ([+]$p < 0.05$ vs. Aβ controls; ANOVA $F_{(3,12)}$ =9.107, $p = 0.002$; n=5).

E) Mean TNFα mRNA was not affected by treatment with Aβ or S100β in Aβ-treated astrocytes (ANOVA $F_{(3,12)}$ =1.433, $p = 0.281$; n=5). **F)** Mean TNFα concentration was increased in supernatant obtained from Aβ-treated astrocytes compared with controls but the difference failed to reach statistical significance. Pre-treatment with S100β had no effect on TNFα concentration. ANOVA $F_{(3,9)}$ =5.546, $p = 0.0019$; n=4.

Figure 5.7 S100β had no effect on RAGE mRNA in Aβ-treated isolated astrocytes

Astrocytes were incubated In the presence of Aβ following 1 hour pre-treatment with S100β (0.001μM). After 24 hours, RAGE mRNA prepared from harvested cells was determined by PCR. Data are presented as means ± SEM.

Mean RAGE mRNA was not affected by treatment with Aβ or S100β in astrocytes (ANOVA $F_{(3,12)}$ =1.812, p=0.198; n=5).
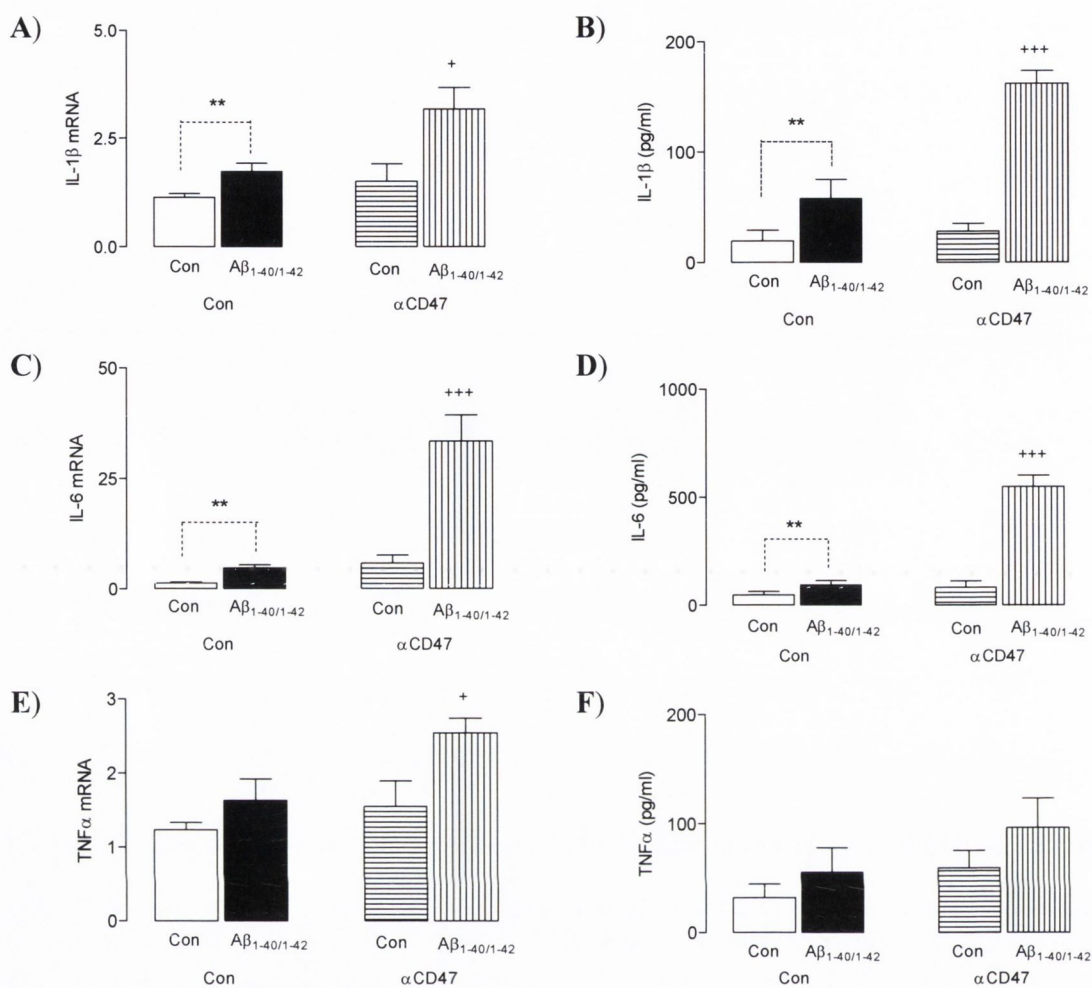
Figure 5.8 Anti-CD47 antibody augmented the Aβ-induced increase in IL-1β and IL-6 in isolated astrocytes

Astrocytes were incubated in the presence of Aβ following 1 hour pre-treatment with an anti-CD47 antibody (αCD47; 2.5μg/ml). After 24 hours, IL-1β, IL-6 and TNFα mRNA, prepared from harvested cells and supernatant concentration of IL-1β, IL-6 and TNFα were determined by PCR and ELISA, respectively. Data are presented as means ± SEM. Dotted line represents the Student t-test analysis.
A) Mean IL-1β mRNA was significantly increased in Aβ-treated astrocytes compared with controls (**$p<0.01$ vs. controls; Student t-test for dependent means). Pre-treatment with αCD47 augmented the Aβ-induced increase in IL-1β mRNA ([+]$p<0.05$ vs. Aβ controls; ANOVA $F_{(3,15)}$ =8.871, p=0.013; n=6). **B)** Mean IL-1β concentration was significantly increased in supernatant obtained from Aβ-treated astrocytes compared with controls (**$p<0.01$ vs. controls; Student t-test for dependent means). Pre-treatment with αCD47 augmented the Aβ-induced increase in IL-1β concentration ([+++]$p<0.001$ vs. Aβ controls; ANOVA $F_{(3,16)}$ =36.58, p<0.0001; n=5).
C) Mean IL-6 mRNA was significantly increased in Aβ-treated astrocytes compared with controls (**$p<0.01$ vs. controls; Student t-test for dependent means). Pre-treatment with αCD47 augmented the Aβ-induced increase in IL-6 mRNA ([+++]$p<0.001$ vs. Aβ controls; ANOVA $F_{(3,12)}$ =26.01, p<0.0001; n=5). **D)** Mean IL-6 concentration was significantly increased in supernatant obtained from Aβ-treated astrocytes compared with controls (**$p<0.01$ vs. controls; Student t-test for dependent means). Pre-treatment with αCD47 augmented the Aβ-induced increase in IL-6 concentration ([+++]$p<0.001$ vs. Aβ controls; ANOVA $F_{(3,15)}$ =97.85, p<0.0001; n=6).
E) Mean TNFα mRNA was not affected by treatment with Aβ. Pre-treatment with αCD47 significantly increased TNFα mRNA in Aβ-treated astrocytes ([+]$p<0.05$ vs. Aβ controls; ANOVA $F_{(3,15)}$ =9.932, p=0.0007; n=6). **F)** Mean TNFα concentration was increased in supernatant obtained from Aβ-treated astrocytes compared with controls but the difference failed to reach statistical significance. Pre-treatment with S100β had no significant effect on TNFα concentration (ANOVA $F_{(3,15)}$ =3.691, p=0.0035; n=6).
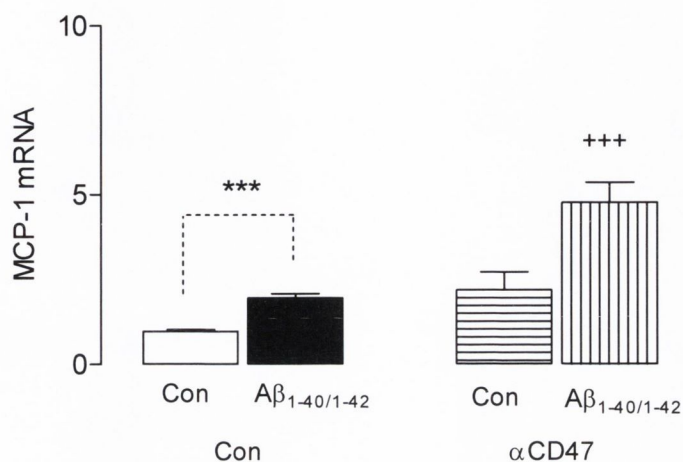
Figure 5.9 Anti-CD47 antibody augmented the Aβ-induced increase in MCP-1 mRNA expression in isolated astrocytes
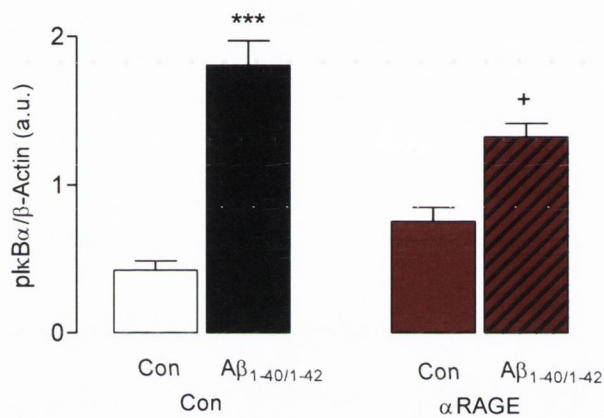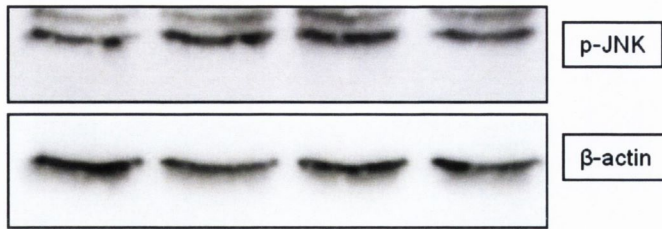
Astrocytes were incubated in the presence of Aβ following 1 hour pre-treatment with αCD47 antibody (2.5μg/ml). After 24 hours, MCP-1 mRNA prepared from harvested cells was determined by PCR. Data are presented as means ± SEM.

Mean MCP-1 mRNA was significantly increased in Aβ-treated astrocytes compared with controls (***$p < 0.001$ vs. controls; Student t-test for dependent means). Pre-treatment with αCD47 augmented the Aβ-induced increase in MCP-1 mRNA ([+++]$p < 0.001$ vs. Aβ controls; ANOVA $F_{(3,12)} = 19.31$, $p < 0.0001$; n=5). Dotted line represents the Student t-test analysis.

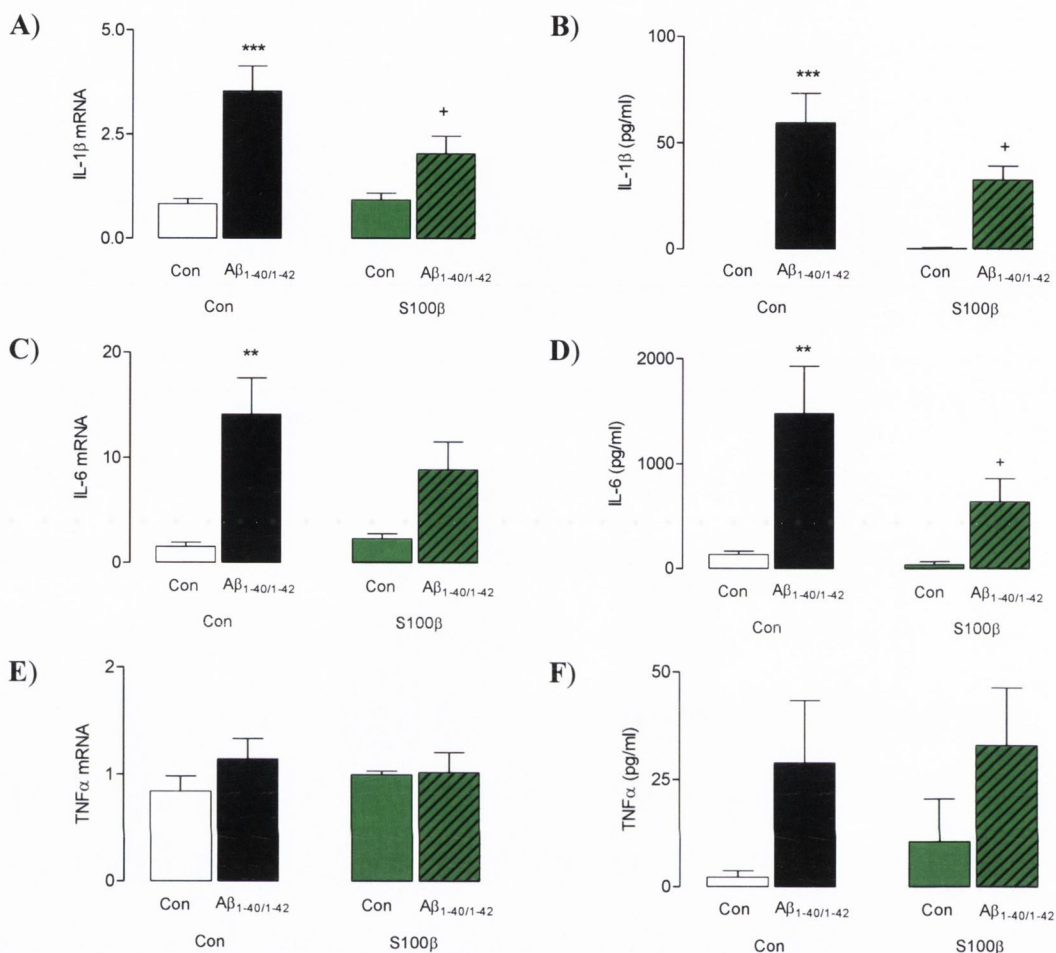**Figure 5.10 Anti-SIRPα antibody attenuated the Aβ-induced increase in IL-1β in isolated astrocytes**

Astrocytes were incubated in the presence of Aβ following 1 hour pre-treatment with an anti-SIRPα antibody (αSIRPα; 2.5μg/ml). After 24 hours, IL-1β, IL-6 and TNFα mRNA prepared from harvested cells and supernatant concentration of IL-1β, IL-6 and TNFα were determined by PCR and ELISA, respectively. Data are presented as means ± SEM.

A) Mean IL-1β mRNA was significantly increased in Aβ-treated astrocytes compared with controls (***$p < 0.001$ vs. controls). Pre-treatment with αSIRPα failed to attenuate the Aβ-induced increase in IL-1β mRNA (ANOVA $F_{(3,15)}$ =17.17, $p < 0.0001$; n=6). **B)** Mean IL-1β concentration was significantly increased in supernatant obtained from Aβ-treated astrocytes compared with controls (***$p < 0.001$ vs. controls). Pre-treatment with αSIRPα significantly attenuated the Aβ-induced increase in IL-1β concentration (+$p < 0.05$ vs. Aβ controls; ANOVA $F_{(3,15)}$ =24.52, $p < 0.0001$; n=6).
C) Mean IL-6 mRNA was significantly increased in Aβ-treated astrocytes compared with controls (***$p < 0.001$ vs. controls). Pre-treatment with αSIRPα failed to attenuate the Aβ-induced increase in IL-6 mRNA (ANOVA $F_{(3,15)}$ =18.18, $p < 0.0001$; n=6). **D)** Mean IL-6 concentration was significantly increased in supernatant obtained from Aβ-treated astrocytes compared with controls (***$p < 0.001$ vs. controls; ANOVA). Pre-treatment with αSIRPα attenuated the Aβ-induced increase in IL-6 concentration but the difference failed to reach statistical significance (ANOVA $F_{(3,12)}$ =18.79, $p < 0.0001$; n=5).
E) Mean TNFα mRNA was significantly increased in Aβ-treated astrocytes compared with controls (**$p < 0.01$ vs. controls). Pre-treatment with αSIRPα failed to attenuate the Aβ-induced increase in TNFα mRNA (ANOVA $F_{(3,15)}$ =11.26, $p = 0.0004$; n=6). **F)** Mean TNFα concentration was increased in supernatant obtained from Aβ-treated astrocytes compared with controls but the difference failed to reach statistical significance. Pre-treatment with αSIRPα had no effect on the TNFα concentration (ANOVA $F_{(3,15)}$ =3.981, $p = 0.028$; n=6).

164
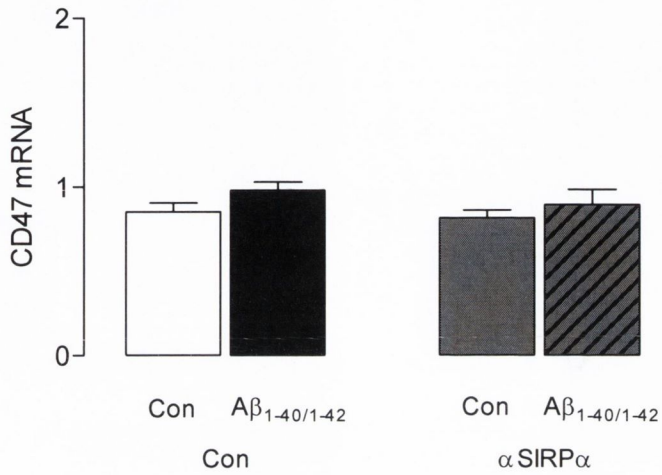
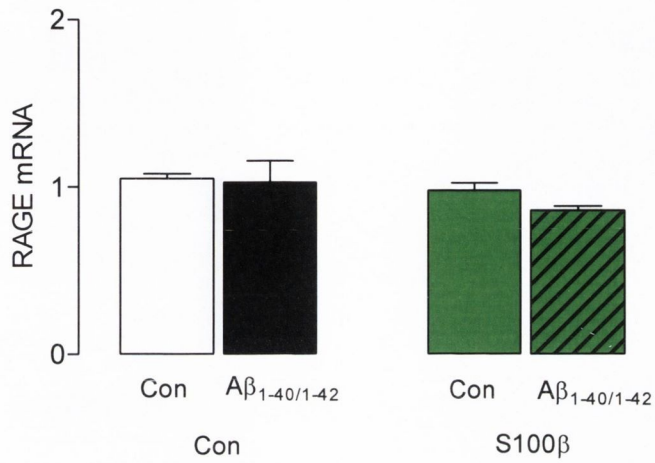**Figure 5.11 Anti-SIRPα antibody had no effect on CD47 mRNA in Aβ-treated isolated astrocytes**

Astrocytes were incubated in the presence of Aβ following 1 hour pre-treatment with αSIRPα antibody (2.5µg/ml). After 24 hours, CD47 mRNA prepared from harvested cells was determined by PCR. Data are presented as means ± SEM.

Mean CD47 mRNA was not affected by treatment with Aβ or αSIRPα in astrocytes (ANOVA $F_{(3,15)}$ =1.442, p=0.27; n=6).
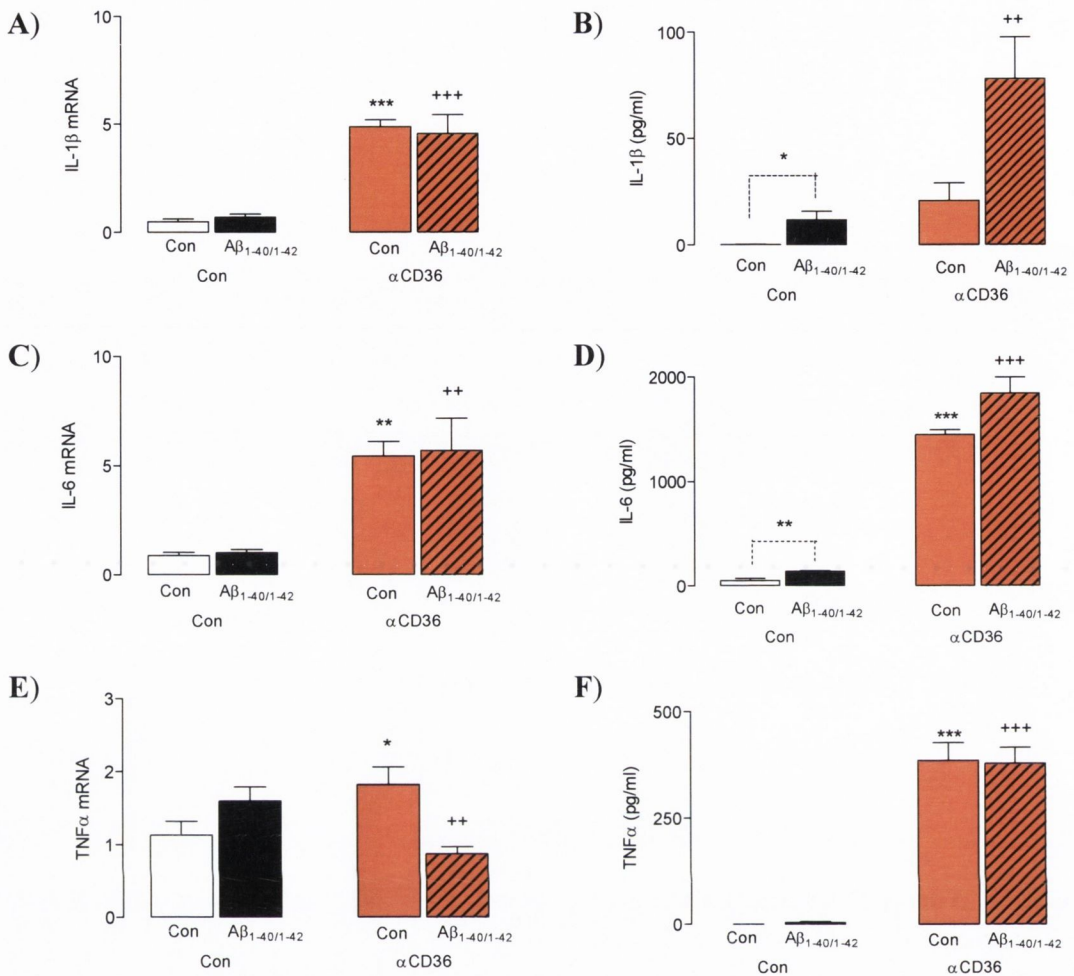
Figure 5.12 Anti-CD36 antibody augmented the Aβ-induced increase in IL-1β in isolated astrocytes

Astrocytes were incubated in the presence of Aβ following 1 hour pre-treatment with an anti-CD36 antibody (αCD36; 2µg/ml). After 24 hours, IL-1β mRNA prepared from harvested cells and supernatant concentration of IL-1β were determined by PCR and ELISA, respectively. Data are presented as means ± SEM. Dotted line represents the Student t-test analysis.

A) Mean IL-1β mRNA was not affected by treatment with Aβ, but was significantly increased in αCD36-treated astrocytes compared with controls (***$p < 0.001$ vs. controls). Pre-treatment with αCD36 showed a significant increase in the IL-1β mRNA (+++$p < 0.001$ vs. Aβ controls; ANOVA $F_{(3,15)}$ =28.62, $p < 0.0001$; n=6). **B)** Mean IL-1β concentration was significantly increased in supernatant obtained from Aβ-treated astrocytes compared with controls (*$p < 0.05$ vs. controls; Student t-test for dependent means). Pre-treatment with αCD36 augmented the Aβ-induced increase in IL-1β concentration (+++$p < 0.001$ vs. Aβ controls; ANOVA $F_{(3,15)}$ =11.65, $p = 0.0003$; n=6).

C) Mean IL-6 mRNA was not affected by treatment with Aβ, but was significantly increased in αCD36-treated astrocytes compared with controls (**$p < 0.01$ vs. controls). Pre-treatment with αCD36 showed a significant increase in the IL-6 mRNA (++$p < 0.01$ vs. Aβ controls; ANOVA $F_{(3,15)}$ =13.49, $p = 0.0002$; n=6). **D)** Mean IL-6 concentration was significantly increased in supernatant obtained from Aβ-treated (**$p < 0.01$ vs. controls; Student t-test for dependent means) and αCD36-treated (***$p < 0.001$ vs. controls; ANOVA) astrocytes compared with controls. Pre-treatment with αCD36 augmented the Aβ-induced increase in IL-6 concentration (+++$p < 0.001$ vs. Aβ controls; ANOVA $F_{(3,16)}$ =123.3, $p < 0.0001$; n=6).

E) Mean TNFα mRNA was not affected by treatment with Aβ, but was significantly increased in αCD36-treated astrocytes compared with controls (*$p < 0.05$ vs. controls). Pre-treatment with αCD36 showed a significant decrease in TNFα mRNA of Aβ-treated astrocytes (++$p < 0.01$ vs. Aβ controls; ANOVA $F_{(3,15)}$ =10.37, $p = 0.0006$; n=6). **F)** Mean TNFα supernatant concentration was not affected by treatment with Aβ, but was significantly increased in αCD36-treated astrocytes compared with controls (***$p < 0.001$ vs. controls). Pre-treatment with αCD36 significantly increased TNFα concentration in Aβ-treated astrocytes (+++$p < 0.001$ vs. Aβ controls; ANOVA $F_{(3,12)}$ =48.3, $p < 0.0001$; n=5).
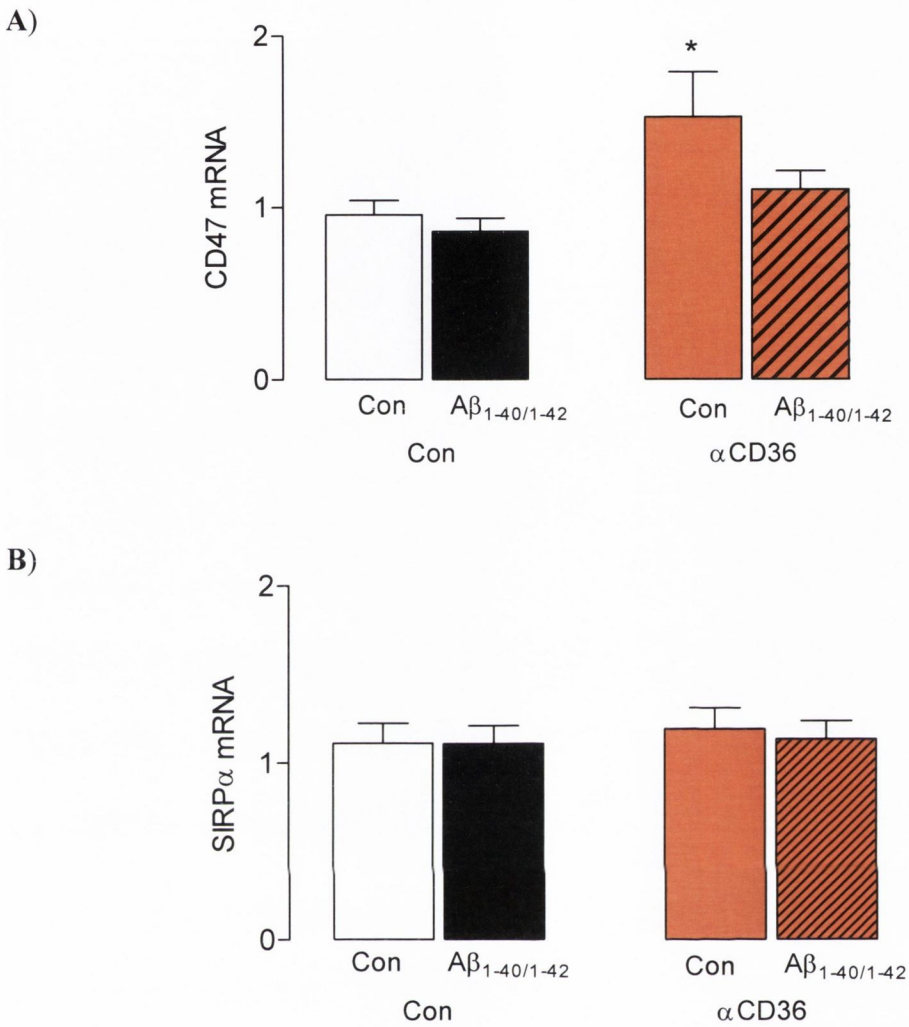
Figure 5.13 Anti-CD36 antibody increased CD47 mRNA expression in isolated astrocytes

Astrocytes were incubated in the presence of Aβ following 1 hour pre-treatment with αCD36 antibody (2μg/ml). After 24 hours, CD47 mRNA and SIRPα mRNA prepared from harvested cells was determined by PCR. Data are presented as means ± SEM.

A) Mean CD47 mRNA was not affected by treatment with Aβ, but was significantly increased in αCD36-treated astrocytes compared with controls (*$p < 0.05$ vs. controls; ANOVA $F_{(3,15)} = 5.26$, $p = 0.011$; n=6).

B) Mean SIRPα mRNA was not affected by treatment with Aβ or αCD36 in astrocytes (ANOVA $F_{(3,15)} = 0.649$, $p = 0.595$; n=6).
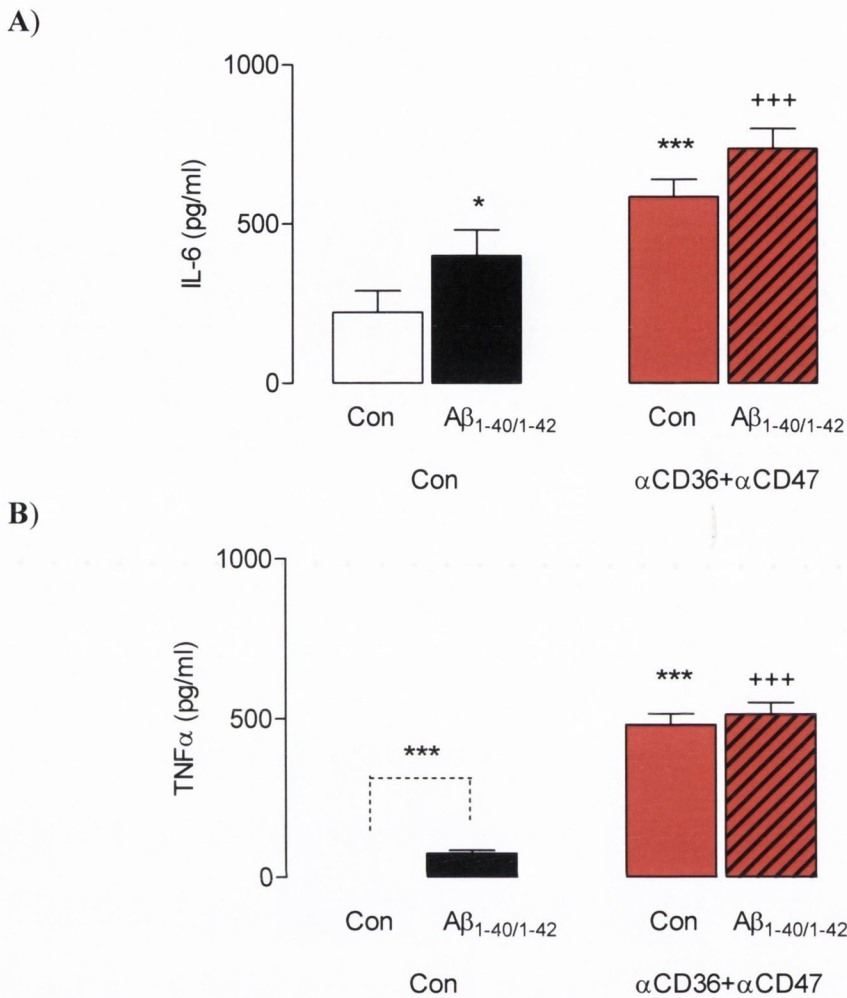
Figure 5.14 Anti-CD36 antibody in combination with anti-CD47 antibody increased the concentration of IL-6 and TNFα in Aβ-treated isolated astrocytes

Astrocytes were incubated in the presence of Aβ following 1 hour pre-treatment with αCD36 (2μg/ml) and αCD47 (2.5μg/ml) antibodies. After 24 hours, supernatant concentration of IL-6 and TNFα were determined by ELISA. Data are presented as means ± SEM.

A) Mean IL-6 concentration was significantly increased in supernatant obtained from Aβ-treated (*$p<0.05$ vs. controls) and αCD36+αCD47-treated (***$p<0.001$ vs. controls) astrocytes compared with controls. Pre-treatment with αCD36+αCD47 augmented the Aβ-induced increase in IL-6 concentration ([+++]$p<0.001$ vs. Aβ controls; ANOVA $F_{(3,15)}$ =27.56, $p<0.0001$; n=6).

B) Mean TNFα concentration was significantly increased in supernatant obtained from Aβ-treated (***$p<0.001$ vs. controls; Student t-test for dependent means) and αCD36+αCD47-treated (***$p<0.001$ vs. controls; ANOVA) astrocytes compared with controls. Pre-treatment with αCD36+αCD47-treated augmented the Aβ-induced increase in TNFα concentration ([+++]$p<0.001$ vs. Aβ controls; ANOVA $F_{(3,15)}$ =124, $p<0.0001$; n=6). Dotted line represents the Student t-test analysis.

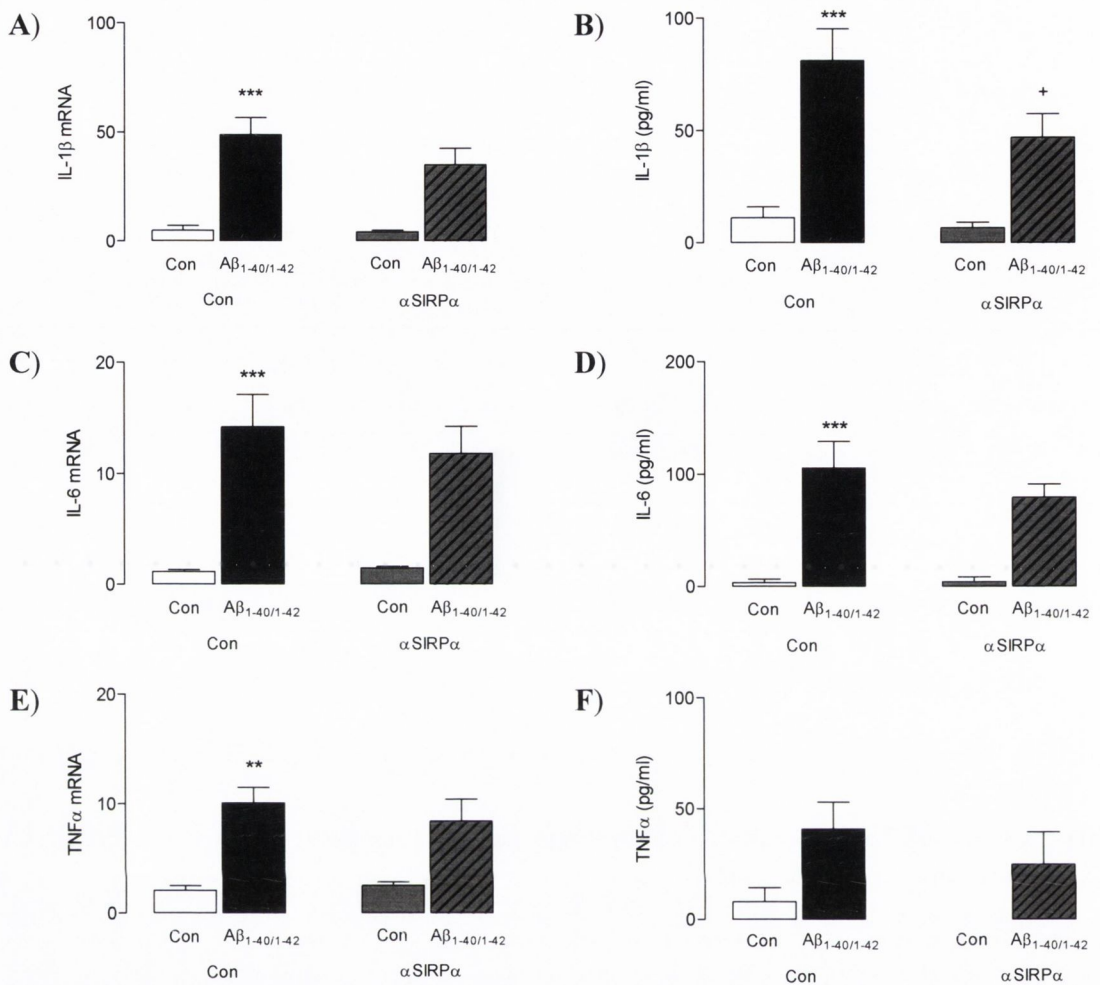|	Aβ	TREATMENT	TREATMENT + Aβ
IL-1β mRNA	**Increased**	αRAGE	No changes
IL-1β protein	**Increased**	αRAGE	**Decreased**
IL-6 mRNA	**Increased**	αRAGE	No changes
IL-6 protein	**Increased**	αRAGE	**Decreased**
TNFα mRNA	No changes	αRAGE	No changes
TNFα protein	**Increased**	αRAGE	No changes
S100β mRNA	No changes	αRAGE	No changes
p-IκBα	**Increased**	αRAGE	**Decreased**
p-JNK	No changes	αRAGE	No changes
IL-1β mRNA	**Increased**	S100β	**Decreased**
IL-1β protein	**Increased**	S100β	**Decreased**
IL-6 mRNA	**Increased**	S100β	No changes
IL-6 protein	**Increased**	S100β	**Decreased**
TNFα mRNA	No changes	S100β	No changes
TNFα protein	No changes	S100β	No changes
RAGE mRNA	No changes	S100β	No changes
IL-1β mRNA	**Increased**	αCD47	**Increased**
IL-1β protein	**Increased**	αCD47	**Increased**
IL-6 mRNA	**Increased**	αCD47	**Increased**
IL-6 protein	**Increased**	αCD47	**Increased**
TNFα mRNA	No changes	αCD47	**Increased**
TNFα protein	No changes	αCD47	No changes
MCP-1 mRNA	**Increased**	αCD47	**Increased**
IL-1β mRNA	**Increased**	αSIRPα	No changes
IL-1β protein	**Increased**	αSIRPα	**Decreased**
IL-6 mRNA	**Increased**	αSIRPα	No changes
IL-6 protein	**Increased**	αSIRPα	No changes
TNFα mRNA	**Increased**	αSIRPα	No changes
TNFα protein	No changes	αSIRPα	No changes
CD47 mRNA	No changes	αSIRPα	No changes
IL-1β mRNA	No changes	αCD36	**Increased**
IL-1β protein	**Increased**	αCD36	**Increased**
IL-6 mRNA	No changes	αCD36	**Increased**
IL-6 protein	**Increased**	αCD36	**Increased**
TNFα mRNA	No changes	αCD36	**Decreased**
TNFα protein	No changes	αCD36	**Increased**
CD47 mRNA	No changes	αCD36	No changes
SIRPα mRNA	No changes	αCD36	No changes
IL-6 protein	**Increased**	αCD36 + αCD47	**Increased**
TNFα protein	**Increased**	αCD36 + αCD47	**Increased**

Table 5.1. Summary of results Chapter 5.

Summary of the data presented in this chapter. Highlighted in bold are results which reached a statistically significant difference. The time point for all experiments shown in this chapter was 24 hours.
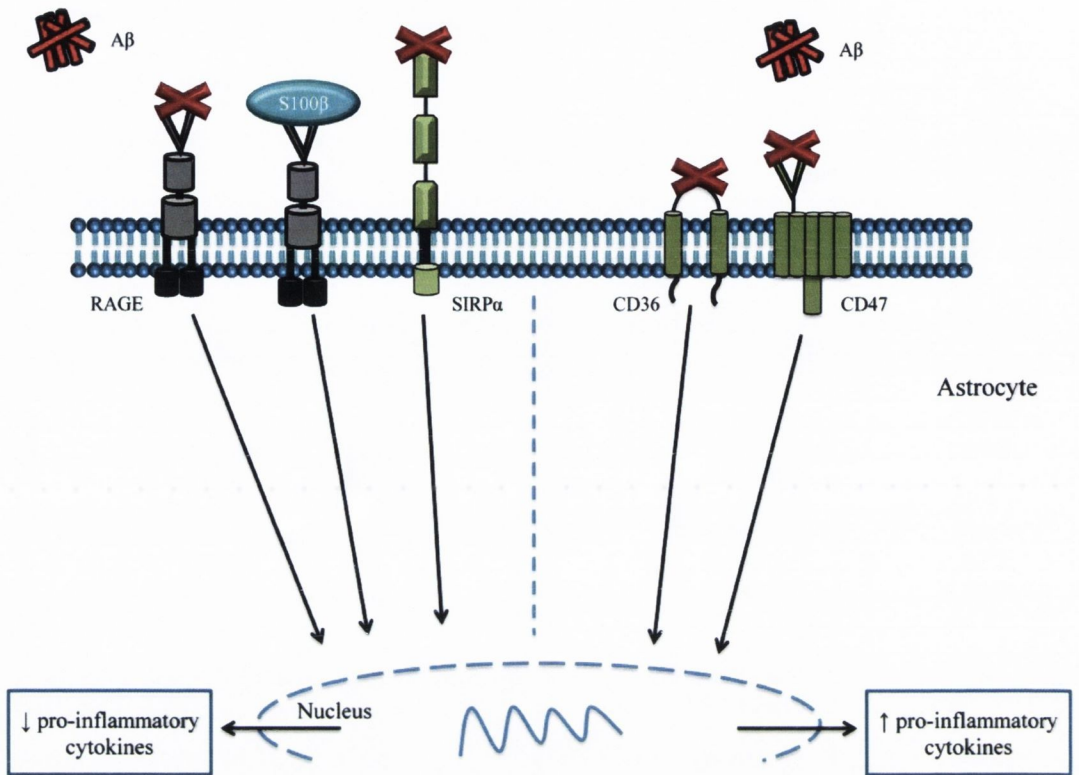
Figure 5.15 Mechanistic figure of Chapter 5

RAGE and its ligand S100β, CD47 and its ligand SIRPα and CD36, were studied in isolated astrocytes incubated in the presence of Aβ for 24 hours. Treatment with an antibody anti-RAGE, S100β peptide and an antibody anti-SIRPα showed a reduction in the production of pro-inflammatory cytokines while treatment with an antibody anti-CD47 and an antibody anti-CD36 induced an increase in the production of pro-inflammatory cytokines. The data presented in this chapter suggests that the interaction of Aβ with RAGE induces a pro-inflammatory response while S100β, CD47 and CD36 may exert modulatory responses.

Chapter 6 General Discussion

The objectives of this study were to determine, *in vivo*, the effects chronic icv treatment with Aβ has in the brains of aged and young rats and to explore age-related changes, and, *in vitro*, to examine the effects Aβ treatment has on cytokine production and release and to investigate the signalling pathways and membrane receptors involved in this process, in rat isolated astrocytes. The data showed that icv treatment with Aβ induced the appearance of immunoreactive structures accompanied by increased GFAP and decreased CD11b in the brains of aged, but not young rats; no changes were observed in other markers of microglial activation, spatial learning or in pro-inflammatory cytokines. The data obtained *in vitro* showed that Aβ induced a time-related increase in pro-inflammatory cytokines paralleled with IκBα phosphorylation, which indicates activation of NFκB signalling pathway and this process was mediated by RAGE. Interestingly, incubation of astrocytes with anti-CD36 or anti-CD47 antibodies induced a pro-inflammatory response and augmented the Aβ-induced increase in pro-inflammatory cytokines (Figure 6.1).

A rodent model of chronic delivery of Aβ into the brain via icv administration was used in this study. The results indicate that Aβ was successfully pumped into the CSF and then transported into the brain stimulating the formation of Aβ-positive immunoreactive structures in aged (18-22 months) but not young (2-4 months), rats. Similarly, treatment with Aβ resulted in an increase in the hippocampal concentration of soluble $Aβ_{1-40}$ and insoluble $Aβ_{1-42}$ in aged but not in young, rats. In spite of this increase in Aβ accumulation following Aβ treatment, no effect on the escape latency in the Morris water maze was observed, although young animals performed better than the aged animals. Treatment with Aβ also reduced the age-related increase in CD11b, although it increased the hippocampal expression of GFAP and GFAP immunostaining in cortex and hippocampus of aged rats. In this study, the only Aβ-induced changes present in young rats were observed in LTP, where a significant attenuation in mean epsp was observed. All these results combined indicate that an age-related difference is present in the brain mechanisms involving Aβ transport and clearance between aged and young rats. Expression of GFAP, RANTES, CD11b and CD68 in the hippocampus as well as fluorescent intensity of MHC-II and expression of GFAP in the cortex showed an age-related increase in control-treated rats. Age-related increase in markers of astrocytic and

microglial activity including GFAP (Amenta et al., 1998), RANTES (Mello Coelho et al., 2009), CD11b (Horrillo et al., 2011), CD68 (Wong et al., 2005) and MHC II (Sheffield and Berman, 1998) have been reported in the literature, indicating that astrocytes and microglia adopt a reactive conformation with aging.

A major question is why young rats cope better with an icv Aβ challenge than aged rats or why the aging brain seem more susceptible to Aβ-induced changes. The choroid plexus cells show age-related morphological changes that include epithelium flattening, basement membrane thickening and lipofuscin deposits, all these changes are not only present but also significantly increased in AD (Preston, 2001). Alterations in CSF hydrodynamics have been observed in aging and in AD (Stivaros and Jackson, 2007). A decrease in CSF secretion rates and turnover, accompanied by increased levels of albumin in CSF are observed with age (Chen et al., 2010). Furthermore, it has been observed that individuals with AD have increased concentrations of CSF proteins such as α-1-antichymotrypsin (ACT) suggesting the CSF system is not fully functional (Porcellini et al., 2008). A study done by Eriksson and colleagues (1995) showed that *in vitro* ACT binds to Aβ and affects the rate of amyloid fibril formation (Eriksson et al., 1995). Rats perfused icv with a ^{125}I-labelled Aβ peptide showed that the choroid plexus uptake of Aβ was almost 3 times higher in 9 month-old rats compared with 3 month-old rats and 17 times higher in 30 month-old rats compared with 3 month-old rats (Preston, 2001). Additionally, it has been reported that aging increases the susceptibility of the brain to Aβ neurotoxicity (Geula et al., 1998) and that leukocyte infiltration and loss of cortical volume after traumatic brain injury are increased with age (Claus et al., 2010). It is still not clear which transporter or specific mechanism enables Aβ to cross from the CSF into the brain. An important question is how Aβ moves through the interstitial brain fluids as it may reflect the way Aβ accumulation spreads in AD.

Lee and colleagues (2007) using rats chronically infused with Aβ$_{1-40}$ reported a significant decrease in the water maze escape latency of Aβ-treated rats compared with control-treated rats (Lee et al., 2007). Additionally, Li and colleagues (2010) observed behavioural deficits in rats which received a single intrahippocampal injection of Aβ$_{1-42}$ (Li et al., 2010). These behavioural changes may be explained by different experimental

procedures such as a reduction in the number of trials in the study by Lee and colleagues (2007) compared with this study, or by the use of an acute and higher dose of Aβ in a different brain area (hippocampus as opposed to lateral ventricles used in this study) as Li and colleagues (2010) reported.

In aged animals glial cells responded differently to chronic infusion with Aβ. Astrocytes showed an increase in both expression of GFAP and GFAP immunoreactivity while Aβ infusion in aged rats resulted in decreased CD11b mRNA. Similarly, treatment with Aβ exerted no changes in the expression and release of IL-1β, IL-6 or TNFα in hippocampus of aged rats. Microglia could offer an explanation for these results, as microglia are considered to be the main produces of pro-inflammatory cytokines in the brain (Aloisi, 2001). This lack of inflammatory response may also be partially explained by the absence of tau in this animal model, as it has been shown that the presence of truncated tau protein induces an increase in the release and expression of IL-1β, IL-6, TNFα and NO (Kovac et al., 2011). It has been shown that formation and maintenance of Aβ plaques in transgenic mice occurs independently of the presence of microglia (Grathwohl et al., 2009). Furthermore, the literature indicates that microglia can phagocyte Aβ *in vitro*, although the ability to do so is diminished in the presence of fibrillar Aβ (Floden and Combs, 2006). It is still not clear if microglia are the main cells responsible for Aβ clearance in the brain, as the results reported in the literature in AD and in *in vivo* animal models are controversial (Jucker and Heppner, 2008). On the other hand, data from this study suggest that astrocytes, not microglia, are the cells that interact primarily with Aβ. It is known that astrocytic expression of GFAP is upregulated in response to brain injury or toxic stimuli (Eng et al., 2000) and that GFAP is increased in the brains of individuals with AD (Korolainen et al., 2005). Astrocytes accumulate Aβ in AD (Nagele et al., 2003) and are able to bind and internalize Aβ$_{1-42}$ *in vitro* (Nielsen et al., 2009). Furthermore, ACT overexpression, driven by the GFAP promoter in astrocytes, induces increased Aβ deposition and plaque formation in the brain of transgenic mice, suggesting that ACT interferes with Aβ clearance (Abraham, 2001). A recent report demonstrated the presence of Aβ annular protofibrils associated with activated astrocytes in the brains of individuals with AD (Lasagna-Reeves and Kayed, 2011).

The results obtained in this study prompted a more detailed exploration of the relationship between astrocytes and Aβ and this was conducted *in vitro*. Incubation of astrocytes with Aβ induced a time-dependent increase in the supernatant concentration of cytokines, peaking between 360 min and 24 hours. Phosphorylation of IκBα increased in a time-dependent manner in Aβ-stimulated astrocytes with significant increases observed at 240 min, 360 min and 24 hours, resembling the Aβ-induced time-dependent change in cytokine production. Additionally, pre-treatment with the NFκB pathway inhibitor wedelolactone, attenuated the Aβ-induced increase in p-IκBα and also significantly reduced the expression of IL-1β and the supernatant concentration of IL-1β, IL-6 and TNFα. Interestingly, treatment with an anti-RAGE antibody significantly attenuated the Aβ-induced increase in pro-inflammatory cytokines and in phosphorylated IκBα but had no effect on phosphorylated JNK. These results indicate that astrocytes stimulated with Aβ increase the production of inflammatory cytokines through activation of the RAGE-NFκB pathway. The JNK pathway was also analyzed in this study but, although p-JNK and p-c-Jun were increased in the presence of Aβ, the time relationship of the activation did not parallel the time-related change in cytokine production. Furthermore, treatment with D-JNKi1, an inhibitor of the JNK pathway, showed no effect on IL-1β or IL-6 expression but significantly reduced the supernatant concentration of both cytokines. These results suggest that JNK may be more involved in astrocytic regulation of cytokine release than in production and may indicate a complementary role to the more steady NFκB inflammatory response. This results are in agreement with the work of Alves and colleagues (2005) which showed that RAGE leads to activation of NFκB pathway inducing sustained oxidative stress and pro-inflammatory cytokine expression in lacrimal glands of diabetic rats (Alves et al., 2005). NFκB pathway activation via up-regulated RAGE has been suggested to produce the constant inflammatory and oxidative stress state frequently observed in patients with end-stage renal disease which require haemodialysis (Rodriguez-Ayala et al., 2005). Additionally, the use of an anti-RAGE antibody inhibited NFκB activation in microglial mouse cells and down-regulated the production of NO, IL-6 and TNF-α (Dukic-Stefanovic et al., 2003). Furthermore, it has been shown in endothelial cells that Aβ induces activation of NFκB pathway and that addition of an anti-RAGE antibody impedes the binding of Aβ to RAGE reducing NFκB

175

activation (Yan et al., 1996). As far as I know, this is the first study that reports Aβ-induced activation of RAGE-NFκB pathway and increased pro-inflammatory cytokines in astrocytes.

In this study the effects of antibodies to CD36 and CD47 showed similar modulatory effects on the production of pro-inflammatory cytokines in astrocytes as opposed to SIRPα which seems to be more involved in a pro-inflammatory role. Blocking of the CD36 receptor with an anti-CD36 antibody significantly increased the production of pro-inflammatory cytokines and augmented the Aβ-induced increase in IL-1β, IL-6 and TNFα. Similarly, blocking the CD47 receptor with an anti-CD47 antibody significantly augmented the Aβ-induced increase in IL-1β, IL-6 and MCP-1, but not TNFα. Furthermore, the data showed that incubation of astrocytes with an anti-CD36 antibody increased CD47 expression but not SIRPα expression. In contrast, blocking of SIRPα receptor with an anti-SIRPα antibody significantly attenuated the Aβ-induced increase in IL-1β and showed a moderate decrease in IL-6 and TNFα but had no effect on CD47 expression. These results suggest that CD36 and CD47 may play a role in the regulation of Aβ-induced pro-inflammatory cytokines production or release as opposed to SIRPα. It has been shown that CD36 and CD47 receptors possess similar binding sites for ligands such as TSP-1 (Kaur et al., 2010) and Aβ (Park et al., 2011, Koenigsknecht and Landreth, 2004). In microglia, CD36, CD47 and $\alpha_6\beta_1$-integrin, form a multireceptor complex which mediates the binding of Aβ fibrils and the activation of intracellular signalling pathways (Bamberger et al., 2003). In macrophages, CD36 has also been reported to form a multiple functional complex with TLR2 and TLR4 which signals through NFκB pathway inducing pro-inflammatory responses in the presence of Aβ (Stewart et al., 2010). CD36 has been suggested to be a better ligand for Aβ than CD47 as Aβ is not strong enough to break the ligation of CD47 with SIRPα (Miller et al., 2010). To my knowledge these CD36, CD47 and SIRPα responses are novel and have not been described before in astrocytes incubated in the presence of Aβ.

RAGE has been reported to interact with CD36 but not with CD47. Similar to RAGE, CD36, as well as other members of the scavenger receptor family, recognize AGE proteins mediating endocytic uptake and subsequent intracellular degradation (Ohgami et al., 2001). In a rat model for diabetes type 2, RAGE, NFκB and CD36 were found to be

increased compared with nondiabetic rats; it was suggested that the overexpression of CD36 was, in part, a response related to AGEs stimulation of RAGE and NFκB (de Oliveira Silva et al., 2008). It has been shown that the soluble form of RAGE (sRAGE) binds selectively to CD36, preventing lipid accumulation and foam cell formation (Marsche et al., 2007). In human monocytes, RAGE expression was blocked using siRNA resulting in significant inhibition of CD36 expression and ROS production, suggesting a positive interaction between RAGE, CD36 and ROS in monocytes (Xanthis et al., 2009). A crosstalk between RAGE pro-inflammatory signalling and CD36 and CD47 modulatory signalling may be present with Aβ stimulation, this concept will require further exploration.

The complex balance of the neuronal-glial relation can be altered by different processes such as aging or the development of neuropathological disorders including AD. Astrocytes in the aged brain are in an activated state and respond more profoundly to challenges, perhaps contributing to the development of neurodegenerative changes. Astrocytic interaction with Aβ induces the activation of diverse signalling cascades but the pathophysiological meaning of these responses remains unknown. However, glial cells may also offer protective effects and a greater understanding of their function may identify potential therapeutic targets in the future.

The results obtained in this work are encouraging for future experiments both *in vitro* and *in vivo* that will further explore the relation of Aβ with astrocytes. *In vitro*, it would be interesting to explore, if present, a crosstalk between RAGE and CD36 or CD47. Also, a similar set of experiments could be done using soluble Aβ instead of aggregated Aβ to explore how astrocytes interact with different presentations of Aβ. The impact of Aβ-induced activation of JNK signalling pathway in astrocytes and the possible interaction of JNK with other signalling pathways could also be further explored. *In vivo*, a transgenic mouse model with AD-related mutations such as APP and which lacks expression of RAGE, CD36 or CD47 could be developed to help understand the dynamics of Aβ and its interaction with astrocytes. Additionally, drugs that interact with RAGE, CD36 or CD47 could also be tested in *in vivo* animal models.
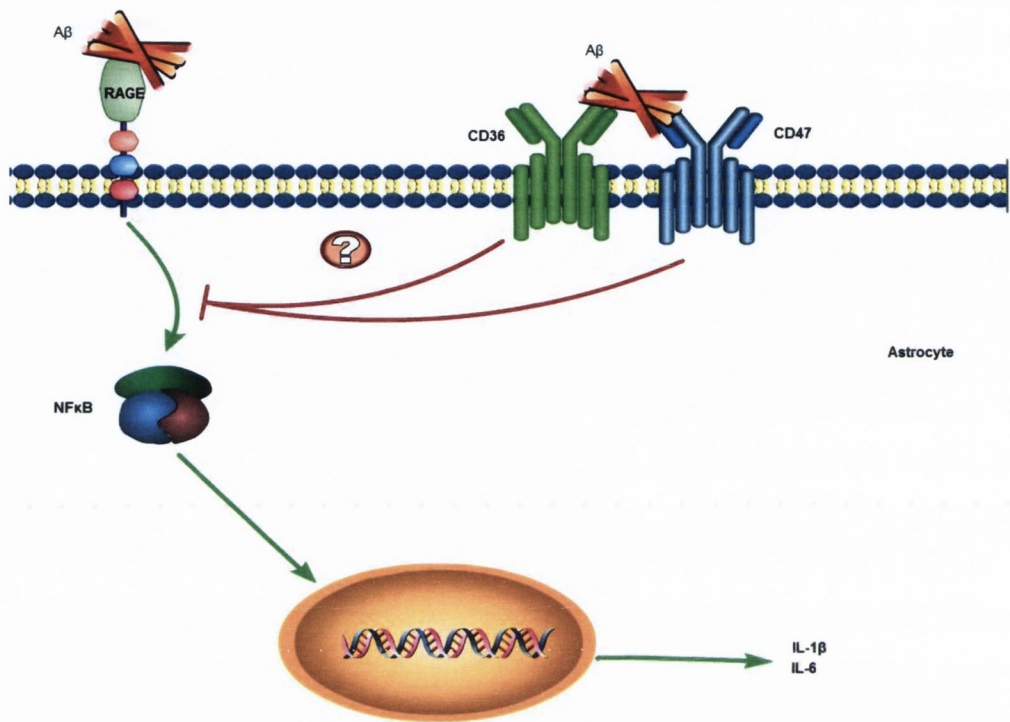
Figure 6.1. Mechanistic figure of the interaction between astrocytes and Aβ.

The data in this study showed that Aβ interacts with astrocytes inducing a pro-inflammatory response. Aβ activates diverse astrocytic receptors including RAGE, CD36 and CD47. RAGE activates the NFκB signalling pathway and induces the production of IL-1β and IL-6 while CD36 and CD47 seem to play a regulatory role in the process, suggesting a possible signalling crosstalk between these astrocytic receptors.

Bibliography

ABBOTT, A. 2011. Dementia: a problem for our age. *Nature,* 475, S2-4.

ABRAHAM, C. R. 2001. Reactive astrocytes and alpha1-antichymotrypsin in Alzheimer's disease. *Neurobiology of aging,* 22, 931-6.

AIZENSTEIN, H. J., NEBES, R. D., SAXTON, J. A., PRICE, J. C., MATHIS, C. A., TSOPELAS, N. D., ZIOLKO, S. K., JAMES, J. A., SNITZ, B. E., HOUCK, P. R., BI, W., COHEN, A. D., LOPRESTI, B. J., DEKOSKY, S. T., HALLIGAN, E. M. & KLUNK, W. E. 2008. Frequent amyloid deposition without significant cognitive impairment among the elderly. *Archives of neurology,* 65, 1509-17.

AKAMA, K. T., ALBANESE, C., PESTELL, R. G. & VAN ELDIK, L. J. 1998. Amyloid beta-peptide stimulates nitric oxide production in astrocytes through an NFkappaB-dependent mechanism. *Proceedings of the National Academy of Sciences of the United States of America,* 95, 5795-800.

AKHISAROGLU, M., MANEV, R., AKHISAROGLU, E., UZ, T. & MANEV, H. 2003. Both aging and chronic fluoxetine increase S100B content in the mouse hippocampus. *Neuroreport,* 14, 1471-3.

AKIYAMA, H., BARGER, S., BARNUM, S., BRADT, B., BAUER, J., COLE, G. M., COOPER, N. R., EIKELENBOOM, P., EMMERLING, M., FIEBICH, B. L., FINCH, C. E., FRAUTSCHY, S., GRIFFIN, W. S., HAMPEL, H., HULL, M., LANDRETH, G., LUE, L., MRAK, R., MACKENZIE, I. R., MCGEER, P. L., O'BANION, M. K., PACHTER, J., PASINETTI, G., PLATA-SALAMAN, C., ROGERS, J., RYDEL, R., SHEN, Y., STREIT, W., STROHMEYER, R., TOOYOMA, I., VAN MUISWINKEL, F. L., VEERHUIS, R., WALKER, D., WEBSTER, S., WEGRZYNIAK, B., WENK, G. & WYSS-CORAY, T. 2000. Inflammation and Alzheimer's disease. *Neurobiology of aging,* 21, 383-421.

ALBLAS, J., HONING, H., DE LAVALETTE, C. R., BROWN, M. H., DIJKSTRA, C. D. & VAN DEN BERG, T. K. 2005. Signal regulatory protein alpha ligation induces macrophage nitric oxide production through JAK/STAT- and phosphatidylinositol 3-kinase/Rac1/NAPDH oxidase/H2O2-dependent pathways. *Molecular and cellular biology,* 25, 7181-92.

ALEARDI, A. M., BENARD, G., AUGEREAU, O., MALGAT, M., TALBOT, J. C., MAZAT, J. P., LETELLIER, T., DACHARY-PRIGENT, J., SOLAINI, G. C. & ROSSIGNOL, R. 2005. Gradual alteration of mitochondrial structure and function by beta-amyloids: importance of membrane viscosity changes, energy deprivation, reactive oxygen species production, and cytochrome c release. *Journal of bioenergetics and biomembranes,* 37, 207-25.

ALLEN, S. J., CROWN, S. E. & HANDEL, T. M. 2007. Chemokine: receptor structure, interactions, and antagonism. *Annual review of immunology,* 25, 787-820.

ALOISI, F. 2001. Immune function of microglia. *Glia,* 36, 165-79.

ALVES, M., CALEGARI, V. C., CUNHA, D. A., SAAD, M. J., VELLOSO, L. A. & ROCHA, E. M. 2005. Increased expression of advanced glycation end-products and their receptor, and activation of nuclear factor kappa-B in lacrimal glands of diabetic rats. *Diabetologia,* 48, 2675-81.

ALZHEIMER, A., STELZMANN, R. A., SCHNITZLEIN, H. N. & MURTAGH, F. R. 1995. An English translation of Alzheimer's 1907 paper, "Uber eine eigenartige Erkankung der Hirnrinde". *Clinical anatomy,* 8, 429-31.

AMENTA, F., BRONZETTI, E., SABBATINI, M. & VEGA, J. A. 1998. Astrocyte changes in aging cerebral cortex and hippocampus: a quantitative immunohistochemical study. *Microscopy research and technique,* 43, 29-33.

ANDERSON, A. J., CUMMINGS, B. J. & COTMAN, C. W. 1994. Increased immunoreactivity for Jun- and Fos-related proteins in Alzheimer's disease: association with pathology. *Experimental neurology,* 125, 286-95.

ANTHONY, T. E. & HEINTZ, N. 2007. The folate metabolic enzyme ALDH1L1 is restricted to the midline of the early CNS, suggesting a role in human neural tube defects. *The Journal of comparative neurology,* 500, 368-83.

ASADA, K., SASAKI, S., SUDA, T., CHIDA, K. & NAKAMURA, H. 2004. Antiinflammatory roles of peroxisome proliferator-activated receptor gamma in human alveolar macrophages. *American journal of respiratory and critical care medicine,* 169, 195-200.

AUTILIO-GAMBETTI, L., MORANDI, A., TABATON, M., SCHAETZLE, B., KOVACS, D., PERRY, G., SHARMA, S., CORNETTE, J., GREENBERG, B. & GAMBETTI, P. 1988. The amyloid percursor protein of Alzheimer disease is expressed as a 130 kDa polypeptide in various cultured cell types. *FEBS letters,* 241, 94-8.

AVDOSHINA, V., BIGGIO, F., PALCHIK, G., CAMPBELL, L. A. & MOCCHETTI, I. 2010. Morphine induces the release of CCL5 from astrocytes: potential neuroprotective mechanism against the HIV protein gp120. *Glia,* 58, 1630-9.

AZEVEDO, F. A., CARVALHO, L. R., GRINBERG, L. T., FARFEL, J. M., FERRETTI, R. E., LEITE, R. E., JACOB FILHO, W., LENT, R. & HERCULANO-HOUZEL, S. 2009. Equal numbers of neuronal and nonneuronal cells make the human brain an isometrically scaled-up primate brain. *The Journal of comparative neurology,* 513, 532-41.

BALDUCCI, C., BEEG, M., STRAVALACI, M., BASTONE, A., SCLIP, A., BIASINI, E., TAPELLA, L., COLOMBO, L., MANZONI, C., BORSELLO, T., CHIESA, R., GOBBI, M., SALMONA, M. & FORLONI, G. 2010. Synthetic amyloid-beta oligomers impair long-term memory independently of cellular prion protein. *Proceedings of the National Academy of Sciences of the United States of America,* 107, 2295-300.

BALLARD, C., GAUTHIER, S., CORBETT, A., BRAYNE, C., AARSLAND, D. & JONES, E. 2011. Alzheimer's disease. *Lancet,* 377, 1019-31.

BAMBERGER, M. E., HARRIS, M. E., MCDONALD, D. R., HUSEMANN, J. & LANDRETH, G. E. 2003. A cell surface receptor complex for fibrillar beta-amyloid mediates microglial activation. *The Journal of neuroscience : the official journal of the Society for Neuroscience,* 23, 2665-74.

BANISADR, G., ROSTENE, W., KITABGI, P. & PARSADANIANTZ, S. M. 2005. Chemokines and brain functions. *Current drug targets. Inflammation and allergy,* 4, 387-99.

BARCLAY, A. N. 2009. Signal regulatory protein alpha (SIRPalpha)/CD47 interaction and function. *Current opinion in immunology,* 21, 47-52.

BARCLAY, A. N. & BROWN, M. H. 2006. The SIRP family of receptors and immune regulation. *Nature reviews. Immunology,* 6, 457-64.

BARNES, C. A. 2003. Long-term potentiation and the ageing brain. *Philosophical transactions of the Royal Society of London. Series B, Biological sciences,* 358, 765-72.

BARNES, C. A., RAO, G. & ORR, G. 2000. Age-related decrease in the Schaffer collateral-evoked EPSP in awake, freely behaving rats. *Neural plasticity,* 7, 167-78.

BARNES, T. C., ANDERSON, M. E. & MOOTS, R. J. 2011. The Many Faces of Interleukin-6: The Role of IL-6 in Inflammation, Vasculopathy, and Fibrosis in Systemic Sclerosis. *International journal of rheumatology,* 2011, 721608.

BEHL, C., DAVIS, J. B., LESLEY, R. & SCHUBERT, D. 1994. Hydrogen peroxide mediates amyloid beta protein toxicity. *Cell,* 77, 817-27.

BEKRIS, L. M., GALLOWAY, N. M., MILLARD, S., LOCKHART, D., LI, G., GALASKO, D. R., FARLOW, M. R., CLARK, C. M., QUINN, J. F., KAYE, J. A., SCHELLENBERG, G. D., LEVERENZ, J. B., SEUBERT, P., TSUANG, D. W., PESKIND, E. R. & YU, C. E. 2011. Amyloid precursor protein (APP) processing genes and cerebrospinal fluid APP cleavage product levels in Alzheimer's disease. *Neurobiology of aging,* 32, 556 e13-23.

BETTELLI, E., CARRIER, Y., GAO, W., KORN, T., STROM, T. B., OUKKA, M., WEINER, H. L. & KUCHROO, V. K. 2006. Reciprocal developmental pathways for the generation of pathogenic effector TH17 and regulatory T cells. *Nature,* 441, 235-8.

BITAN, G., KIRKITADZE, M. D., LOMAKIN, A., VOLLERS, S. S., BENEDEK, G. B. & TEPLOW, D. B. 2003. Amyloid beta -protein (Abeta) assembly: Abeta 40 and Abeta 42 oligomerize through distinct pathways. *Proceedings of the National Academy of Sciences of the United States of America,* 100, 330-5.

BODLES, A. M. & BARGER, S. W. 2004. Cytokines and the aging brain - what we don't know might help us. *Trends in neurosciences,* 27, 621-6.

BOER, K., SPLIET, W. G., VAN RIJEN, P. C., REDEKER, S., TROOST, D. & ARONICA, E. 2006. Evidence of activated microglia in focal cortical dysplasia. *Journal of neuroimmunology,* 173, 188-95.

BOGOYEVITCH, M. A., NGOEI, K. R., ZHAO, T. T., YEAP, Y. Y. & NG, D. C. 2010. c-Jun N-terminal kinase (JNK) signaling: recent advances and challenges. *Biochimica et biophysica acta,* 1804, 463-75.

BOLLER, F. & FORBES, M. M. 1998. History of dementia and dementia in history: an overview. *Journal of the neurological sciences,* 158, 125-33.

BOOM, A., POCHET, R., AUTHELET, M., PRADIER, L., BORGHGRAEF, P., VAN LEUVEN, F., HEIZMANN, C. W. & BRION, J. P. 2004. Astrocytic calcium/zinc binding protein S100A6 over expression in Alzheimer's disease and in PS1/APP transgenic mice models. *Biochimica et biophysica acta,* 1742, 161-8.

BORSELLO, T., CLARKE, P. G., HIRT, L., VERCELLI, A., REPICI, M., SCHORDERET, D. F., BOGOUSSLAVSKY, J. & BONNY, C. 2003. A peptide inhibitor of c-Jun N-terminal kinase protects against excitotoxicity and cerebral ischemia. *Nature medicine,* 9, 1180-6.

BOTTCHER, A., GAIPL, U. S., FURNROHR, B. G., HERRMANN, M., GIRKONTAITE, I., KALDEN, J. R. & VOLL, R. E. 2006. Involvement of phosphatidylserine, alphavbeta3, CD14, CD36, and complement C1q in the

phagocytosis of primary necrotic lymphocytes by macrophages. *Arthritis and rheumatism,* 54, 927-38.

BRAHMACHARI, S., FUNG, Y. K. & PAHAN, K. 2006. Induction of glial fibrillary acidic protein expression in astrocytes by nitric oxide. *The Journal of neuroscience : the official journal of the Society for Neuroscience,* 26, 4930-9.

BRAND-SCHIEBER, E., WERNER, P., IACOBAS, D. A., IACOBAS, S., BEELITZ, M., LOWERY, S. L., SPRAY, D. C. & SCEMES, E. 2005. Connexin43, the major gap junction protein of astrocytes, is down-regulated in inflamed white matter in an animal model of multiple sclerosis. *Journal of neuroscience research,* 80, 798-808.

BROOKMEYER, R., CORRADA, M. M., CURRIERO, F. C. & KAWAS, C. 2002. Survival following a diagnosis of Alzheimer disease. *Archives of neurology,* 59, 1764-7.

BROWN, E., HOOPER, L., HO, T. & GRESHAM, H. 1990. Integrin-associated protein: a 50-kD plasma membrane antigen physically and functionally associated with integrins. *The Journal of cell biology,* 111, 2785-94.

BROWN, E. J. & FRAZIER, W. A. 2001. Integrin-associated protein (CD47) and its ligands. *Trends in cell biology,* 11, 130-5.

BUEE, L., BUSSIERE, T., BUEE-SCHERRER, V., DELACOURTE, A. & HOF, P. R. 2000. Tau protein isoforms, phosphorylation and role in neurodegenerative disorders. *Brain research. Brain research reviews,* 33, 95-130.

BUSINARO, R., LEONE, S., FABRIZI, C., SORCI, G., DONATO, R., LAURO, G. M. & FUMAGALLI, L. 2006. S100B protects LAN-5 neuroblastoma cells against Abeta amyloid-induced neurotoxicity via RAGE engagement at low doses but increases Abeta amyloid neurotoxicity at high doses. *Journal of neuroscience research,* 83, 897-906.

BUTOVSKY, O., TALPALAR, A. E., BEN-YAAKOV, K. & SCHWARTZ, M. 2005. Activation of microglia by aggregated beta-amyloid or lipopolysaccharide impairs MHC-II expression and renders them cytotoxic whereas IFN-gamma and IL-4 render them protective. *Molecular and cellular neurosciences,* 29, 381-93.

BUTTERFIELD, D. A. 2002. Amyloid beta-peptide (1-42)-induced oxidative stress and neurotoxicity: implications for neurodegeneration in Alzheimer's disease brain. A review. *Free radical research,* 36, 1307-13.

CAGNIN, A., BROOKS, D. J., KENNEDY, A. M., GUNN, R. N., MYERS, R., TURKHEIMER, F. E., JONES, T. & BANATI, R. B. 2001. In-vivo measurement of activated microglia in dementia. *Lancet,* 358, 461-7.

CAHOY, J. D., EMERY, B., KAUSHAL, A., FOO, L. C., ZAMANIAN, J. L., CHRISTOPHERSON, K. S., XING, Y., LUBISCHER, J. L., KRIEG, P. A., KRUPENKO, S. A., THOMPSON, W. J. & BARRES, B. A. 2008. A transcriptome database for astrocytes, neurons, and oligodendrocytes: a new resource for understanding brain development and function. *The Journal of neuroscience : the official journal of the Society for Neuroscience,* 28, 264-78.

CAMBIEN, B., POMERANZ, M., MILLET, M. A., ROSSI, B. & SCHMID-ALLIANA, A. 2001. Signal transduction involved in MCP-1-mediated monocytic transendothelial migration. *Blood,* 97, 359-66.

CAMERON, B. & LANDRETH, G. E. 2010. Inflammation, microglia, and Alzheimer's disease. *Neurobiology of disease,* 37, 503-9.

CARGNELLO, M. & ROUX, P. P. 2011. Activation and function of the MAPKs and their substrates, the MAPK-activated protein kinases. *Microbiology and molecular biology reviews : MMBR,* 75, 50-83.

CERPA, W., DINAMARCA, M. C. & INESTROSA, N. C. 2008. Structure-function implications in Alzheimer's disease: effect of Abeta oligomers at central synapses. *Current Alzheimer research,* 5, 233-43.

CHAN, F. K., CHUN, H. J., ZHENG, L., SIEGEL, R. M., BUI, K. L. & LENARDO, M. J. 2000. A domain in TNF receptors that mediates ligand-independent receptor assembly and signaling. *Science,* 288, 2351-4.

CHAN, W. Y., KOHSAKA, S. & REZAIE, P. 2007. The origin and cell lineage of microglia: new concepts. *Brain research reviews,* 53, 344-54.

CHEN, C. J., OU, Y. C., CHANG, C. Y., PAN, H. C., LIAO, S. L., RAUNG, S. L. & CHEN, S. Y. 2011. TNF-alpha and IL-1beta mediate Japanese encephalitis virus-induced RANTES gene expression in astrocytes. *Neurochemistry international,* 58, 234-42.

CHEN, C. P., CHEN, R. L. & PRESTON, J. E. 2010. The influence of cerebrospinal fluid turnover on age-related changes in cerebrospinal fluid protein concentrations. *Neuroscience letters,* 476, 138-41.

CHEN, G., CHEN, K. S., KNOX, J., INGLIS, J., BERNARD, A., MARTIN, S. J., JUSTICE, A., MCCONLOGUE, L., GAMES, D., FREEDMAN, S. B. & MORRIS, R. G. 2000a. A learning deficit related to age and beta-amyloid plaques in a mouse model of Alzheimer's disease. *Nature,* 408, 975-9.

CHEN, Q. S., KAGAN, B. L., HIRAKURA, Y. & XIE, C. W. 2000b. Impairment of hippocampal long-term potentiation by Alzheimer amyloid beta-peptides. *Journal of neuroscience research,* 60, 65-72.

CHEN, R. L. & PRESTON, J. E. 2010. Changes in kinetics of amino acid uptake at the ageing ovine blood-cerebrospinal fluid barrier. *Neurobiology of aging.*

CHEN, S. Y., WRIGHT, J. W. & BARNES, C. D. 1996. The neurochemical and behavioral effects of beta-amyloid peptide(25-35). *Brain research,* 720, 54-60.

CHO, H. J., SON, S. M., JIN, S. M., HONG, H. S., SHIN, D. H., KIM, S. J., HUH, K. & MOOK-JUNG, I. 2009. RAGE regulates BACE1 and Abeta generation via NFAT1 activation in Alzheimer's disease animal model. *The FASEB journal : official publication of the Federation of American Societies for Experimental Biology,* 23, 2639-49.

CHOUCAIR-JAAFAR, N., LAPORTE, V., LEVY, R., POINDRON, P., LOMBARD, Y. & GIES, J. P. 2011. Complement receptor 3 (CD11b/CD18) is implicated in the elimination of beta-amyloid peptides. *Fundamental & clinical pharmacology,* 25, 115-22.

CHOW, S. K., YU, D., MACDONALD, C. L., BUIBAS, M. & SILVA, G. A. 2010a. Amyloid beta-peptide directly induces spontaneous calcium transients, delayed intercellular calcium waves and gliosis in rat cortical astrocytes. *ASN neuro,* 2, e00026.

CHOW, V. W., MATTSON, M. P., WONG, P. C. & GLEICHMANN, M. 2010b. An overview of APP processing enzymes and products. *Neuromolecular medicine,* 12, 1-12.

CLAUS, C. P., TSURU-AOYAGI, K., ADWANIKAR, H., WALKER, B., MANVELYAN, H., WHETSTONE, W. & NOBLE-HAEUSSLEIN, L. J. 2010. Age is a determinant of leukocyte infiltration and loss of cortical volume after traumatic brain injury. *Developmental neuroscience,* 32, 454-65.

CLEARY, J. P., WALSH, D. M., HOFMEISTER, J. J., SHANKAR, G. M., KUSKOWSKI, M. A., SELKOE, D. J. & ASHE, K. H. 2005. Natural oligomers of the amyloid-beta protein specifically disrupt cognitive function. *Nature neuroscience,* 8, 79-84.

CLYNES, R., MOSER, B., YAN, S. F., RAMASAMY, R., HEROLD, K. & SCHMIDT, A. M. 2007. Receptor for AGE (RAGE): weaving tangled webs within the inflammatory response. *Current molecular medicine,* 7, 743-51.

COLOMBO, A., REPICI, M., PESARESI, M., SANTAMBROGIO, S., FORLONI, G. & BORSELLO, T. 2007. The TAT-JNK inhibitor peptide interferes with beta amyloid protein stability. *Cell death and differentiation,* 14, 1845-8.

COLOTTA, F., RE, F., MUZIO, M., BERTINI, R., POLENTARUTTI, N., SIRONI, M., GIRI, J. G., DOWER, S. K., SIMS, J. E. & MANTOVANI, A. 1993. Interleukin-1 type II receptor: a decoy target for IL-1 that is regulated by IL-4. *Science,* 261, 472-5.

COMBS, C. K. 2009. Inflammation and microglia actions in Alzheimer's disease. *Journal of neuroimmune pharmacology : the official journal of the Society on NeuroImmune Pharmacology,* 4, 380-8.

COOK, R. J., LLOYD, R. S. & WAGNER, C. 1991. Isolation and characterization of cDNA clones for rat liver 10-formyltetrahydrofolate dehydrogenase. *The Journal of biological chemistry,* 266, 4965-73.

CORACI, I. S., HUSEMANN, J., BERMAN, J. W., HULETTE, C., DUFOUR, J. H., CAMPANELLA, G. K., LUSTER, A. D., SILVERSTEIN, S. C. & EL-KHOURY, J. B. 2002. CD36, a class B scavenger receptor, is expressed on microglia in Alzheimer's disease brains and can mediate production of reactive oxygen species in response to beta-amyloid fibrils. *The American journal of pathology,* 160, 101-12.

COSKUN, P., WYREMBAK, J., SCHRINER, S., CHEN, H. W., MARCINIACK, C., LAFERLA, F. & WALLACE, D. C. 2011. A mitochondrial etiology of Alzheimer and Parkinson disease. *Biochimica et biophysica acta.*

COTRINA, M. L. & NEDERGAARD, M. 2002. Astrocytes in the aging brain. *Journal of neuroscience research,* 67, 1-10.

COWLEY, T. R., O'SULLIVAN, J., BLAU, C., DEIGHAN, B. F., JONES, R., KERSKENS, C., RICHARDSON, J. C., VIRLEY, D., UPTON, N. & LYNCH, M. A. 2010. Rosiglitazone attenuates the age-related changes in astrocytosis and the deficit in LTP. *Neurobiology of aging.*

CRASTO, C. L., SEMBA, R. D., SUN, K., DALAL, M., CORSI, A. M., BANDINELLI, S., GURALNIK, J. M. & FERRUCCI, L. 2011. Endogenous secretory receptor for advanced glycation end products is associated with low serum interleukin-1 receptor antagonist and elevated IL-6 in older community-dwelling adults. *The*

journals of gerontology. Series A, Biological sciences and medical sciences, 66, 437-43.

CROFT, M. 2009. The role of TNF superfamily members in T-cell function and diseases. *Nature reviews. Immunology,* 9, 271-85.

CUMMINGS, J. L. 2004. Alzheimer's disease. *The New England journal of medicine,* 351, 56-67.

DALLAS, M., BOYCOTT, H. E., ATKINSON, L., MILLER, A., BOYLE, J. P., PEARSON, H. A. & PEERS, C. 2007. Hypoxia suppresses glutamate transport in astrocytes. *The Journal of neuroscience : the official journal of the Society for Neuroscience,* 27, 3946-55.

DE OLIVEIRA SILVA, C., DELBOSC, S., ARAIS, C., MONNIER, L., CRISTOL, J. P. & PARES-HERBUTE, N. 2008. Modulation of CD36 protein expression by AGEs and insulin in aortic VSMCs from diabetic and non-diabetic rats. *Nutrition, metabolism, and cardiovascular diseases : NMCD,* 18, 23-30.

DE TOLEDO-MORRELL, L. & MORRELL, F. 1985. Electrophysiological markers of aging and memory loss in rats. *Annals of the New York Academy of Sciences,* 444, 296-311.

DECKER, H., LO, K. Y., UNGER, S. M., FERREIRA, S. T. & SILVERMAN, M. A. 2010. Amyloid-beta peptide oligomers disrupt axonal transport through an NMDA receptor-dependent mechanism that is mediated by glycogen synthase kinase 3beta in primary cultured hippocampal neurons. *The Journal of neuroscience : the official journal of the Society for Neuroscience,* 30, 9166-71.

DELGADO, R., CARLIN, A., AIRAGHI, L., DEMITRI, M. T., MEDA, L., GALIMBERTI, D., BARON, P., LIPTON, J. M. & CATANIA, A. 1998. Melanocortin peptides inhibit production of proinflammatory cytokines and nitric oxide by activated microglia. *Journal of leukocyte biology,* 63, 740-5.

DEMEURE, C. E., TANAKA, H., MATEO, V., RUBIO, M., DELESPESSE, G. & SARFATI, M. 2000. CD47 engagement inhibits cytokine production and maturation of human dendritic cells. *Journal of immunology,* 164, 2193-9.

DESHMANE, S. L., KREMLEV, S., AMINI, S. & SAWAYA, B. E. 2009. Monocyte chemoattractant protein-1 (MCP-1): an overview. *Journal of interferon & cytokine research : the official journal of the International Society for Interferon and Cytokine Research,* 29, 313-26.

DESIKAN, R. S., MCEVOY, L. K., THOMPSON, W. K., HOLLAND, D., RODDEY, J. C., BLENNOW, K., AISEN, P. S., BREWER, J. B., HYMAN, B. T. & DALE, A. M. 2011. Amyloid-beta associated volume loss occurs only in the presence of phospho-tau. *Annals of neurology,* 70, 657-61.

DI CASTRO, M. A., CHUQUET, J., LIAUDET, N., BHAUKAURALLY, K., SANTELLO, M., BOUVIER, D., TIRET, P. & VOLTERRA, A. 2011. Local Ca(2+) detection and modulation of synaptic release by astrocytes. *Nature neuroscience.*

DI SANTO, E., ALONZI, T., POLI, V., FATTORI, E., TONIATTI, C., SIRONI, M., RICCIARDI-CASTAGNOLI, P. & GHEZZI, P. 1997. Differential effects of IL-6 on systemic and central production of TNF: a study with IL-6-deficient mice. *Cytokine,* 9, 300-6.

DIAS-SANTAGATA, D., FULGA, T. A., DUTTAROY, A. & FEANY, M. B. 2007. Oxidative stress mediates tau-induced neurodegeneration in Drosophila. *The Journal of clinical investigation,* 117, 236-45.

DINARELLO, C. A. 2009. Immunological and inflammatory functions of the interleukin-1 family. *Annual review of immunology,* 27, 519-50.

DINARELLO, C. A., IKEJIMA, T., WARNER, S. J., ORENCOLE, S. F., LONNEMANN, G., CANNON, J. G. & LIBBY, P. 1987. Interleukin 1 induces interleukin 1. I. Induction of circulating interleukin 1 in rabbits in vivo and in human mononuclear cells in vitro. *Journal of immunology,* 139, 1902-10.

DINELEY, K. E., SCANLON, J. M., KRESS, G. J., STOUT, A. K. & REYNOLDS, I. J. 2000. Astrocytes are more resistant than neurons to the cytotoxic effects of increased [Zn(2+)](i). *Neurobiology of disease,* 7, 310-20.

DONAHUE, J. E., FLAHERTY, S. L., JOHANSON, C. E., DUNCAN, J. A., 3RD, SILVERBERG, G. D., MILLER, M. C., TAVARES, R., YANG, W., WU, Q., SABO, E., HOVANESIAN, V. & STOPA, E. G. 2006. RAGE, LRP-1, and amyloid-beta protein in Alzheimer's disease. *Acta neuropathologica,* 112, 405-15.

DONATO, R. 1999. Functional roles of S100 proteins, calcium-binding proteins of the EF-hand type. *Biochimica et biophysica acta,* 1450, 191-231.

DONATO, R., SORCI, G., RIUZZI, F., ARCURI, C., BIANCHI, R., BROZZI, F., TUBARO, C. & GIAMBANCO, I. 2009. S100B's double life: intracellular regulator and extracellular signal. *Biochimica et biophysica acta,* 1793, 1008-22.

DOODY, R. S., GAVRILOVA, S. I., SANO, M., THOMAS, R. G., AISEN, P. S., BACHURIN, S. O., SEELY, L. & HUNG, D. 2008. Effect of dimebon on cognition, activities of daily living, behaviour, and global function in patients with mild-to-moderate Alzheimer's disease: a randomised, double-blind, placebo-controlled study. *Lancet,* 372, 207-15.

DU, F., QIAN, Z. M., ZHU, L., WU, X. M., QIAN, C., CHAN, R. & KE, Y. 2010. Purity, cell viability, expression of GFAP and bystin in astrocytes cultured by different procedures. *Journal of cellular biochemistry,* 109, 30-7.

DU YAN, S., ZHU, H., FU, J., YAN, S. F., ROHER, A., TOURTELLOTTE, W. W., RAJAVASHISTH, T., CHEN, X., GODMAN, G. C., STERN, D. & SCHMIDT, A. M. 1997. Amyloid-beta peptide-receptor for advanced glycation endproduct interaction elicits neuronal expression of macrophage-colony stimulating factor: a proinflammatory pathway in Alzheimer disease. *Proceedings of the National Academy of Sciences of the United States of America,* 94, 5296-301.

DUFFY, P. E., RAPPORT, M. & GRAF, L. 1980. Glial fibrillary acidic protein and Alzheimer-type senile dementia. *Neurology,* 30, 778-82.

DUKIC-STEFANOVIC, S., GASIC-MILENKOVIC, J., DEUTHER-CONRAD, W. & MUNCH, G. 2003. Signal transduction pathways in mouse microglia N-11 cells activated by advanced glycation endproducts (AGEs). *Journal of neurochemistry,* 87, 44-55.

DUYCKAERTS, C., DELATOUR, B. & POTIER, M. C. 2009. Classification and basic pathology of Alzheimer disease. *Acta neuropathologica,* 118, 5-36.

EDWARDS, M. M. & ROBINSON, S. R. 2006. TNF alpha affects the expression of GFAP and S100B: implications for Alzheimer's disease. *Journal of neural transmission,* 113, 1709-15.

EID, T., LEE, T. S., THOMAS, M. J., AMIRY-MOGHADDAM, M., BJORNSEN, L. P., SPENCER, D. D., AGRE, P., OTTERSEN, O. P. & DE LANEROLLE, N. C. 2005. Loss of perivascular aquaporin 4 may underlie deficient water and K+ homeostasis in the human epileptogenic hippocampus. *Proceedings of the National Academy of Sciences of the United States of America,* 102, 1193-8.

EMERY, V. O. 2011. Alzheimer disease: are we intervening too late? *Journal of neural transmission,* 118, 1361-78.

ENG, L. F., GHIRNIKAR, R. S. & LEE, Y. L. 2000. Glial fibrillary acidic protein: GFAP-thirty-one years (1969-2000). *Neurochemical research,* 25, 1439-51.

ENGSTROM, W., WARD, A. & MOORWOOD, K. 2010. The role of scaffold proteins in JNK signalling. *Cell proliferation,* 43, 56-66.

ERIKSSON, S., JANCIAUSKIENE, S. & LANNFELT, L. 1995. Alpha 1-antichymotrypsin regulates Alzheimer beta-amyloid peptide fibril formation. *Proceedings of the National Academy of Sciences of the United States of America,* 92, 2313-7.

FAGAN, A. M. & HOLTZMAN, D. M. 2000. Astrocyte lipoproteins, effects of apoE on neuronal function, and role of apoE in amyloid-beta deposition in vivo. *Microscopy research and technique,* 50, 297-304.

FAN, L. W., MITCHELL, H. J., TIEN, L. T., RHODES, P. G. & CAI, Z. 2009. Interleukin-1beta-induced brain injury in the neonatal rat can be ameliorated by alpha-phenyl-n-tert-butyl-nitrone. *Exp Neurol,* 220, 143-53.

FANG, D., LI, Z., ZHONG-MING, Q., MEI, W. X., HO, Y. W., YUAN, X. W. & YA, K. 2008. Expression of bystin in reactive astrocytes induced by ischemia/reperfusion and chemical hypoxia in vitro. *Biochimica et biophysica acta,* 1782, 658-63.

FARBER, K. & KETTENMANN, H. 2005. Physiology of microglial cells. *Brain research. Brain research reviews,* 48, 133-43.

FARFARA, D., LIFSHITZ, V. & FRENKEL, D. 2008. Neuroprotective and neurotoxic properties of glial cells in the pathogenesis of Alzheimer's disease. *Journal of cellular and molecular medicine,* 12, 762-80.

FEBBRAIO, M. & SILVERSTEIN, R. L. 2007. CD36: implications in cardiovascular disease. *The international journal of biochemistry & cell biology,* 39, 2012-30.

FERNANDEZ-RUIZ, E., ARMESILLA, A. L., SANCHEZ-MADRID, F. & VEGA, M. A. 1993. Gene encoding the collagen type I and thrombospondin receptor CD36 is located on chromosome 7q11.2. *Genomics,* 17, 759-61.

FERRER, I., BLANCO, R., CARMONA, M. & PUIG, B. 2001. Phosphorylated mitogen-activated protein kinase (MAPK/ERK-P), protein kinase of 38 kDa (p38-P), stress-activated protein kinase (SAPK/JNK-P), and calcium/calmodulin-dependent kinase II (CaM kinase II) are differentially expressed in tau deposits in neurons and glial cells in tauopathies. *Journal of neural transmission,* 108, 1397-415.

FLODEN, A. M. & COMBS, C. K. 2006. Beta-amyloid stimulates murine postnatal and adult microglia cultures in a unique manner. *The Journal of neuroscience : the official journal of the Society for Neuroscience,* 26, 4644-8.

FOSTER, J. K., VERDILE, G., BATES, K. A. & MARTINS, R. N. 2009. Immunization in Alzheimer's disease: naive hope or realistic clinical potential? *Molecular psychiatry,* 14, 239-51.

FRAUTSCHY, S. A., BAIRD, A. & COLE, G. M. 1991. Effects of injected Alzheimer beta-amyloid cores in rat brain. *Proceedings of the National Academy of Sciences of the United States of America,* 88, 8362-6.

FRAUTSCHY, S. A., YANG, F., CALDERON, L. & COLE, G. M. 1996. Rodent models of Alzheimer's disease: rat A beta infusion approaches to amyloid deposits. *Neurobiology of aging,* 17, 311-21.

GARCIA-MARIN, V., GARCIA-LOPEZ, P. & FREIRE, M. 2007. Cajal's contributions to glia research. *Trends in neurosciences,* 30, 479-87.

GARCIA-MATAS, S., DE VERA, N., AZNAR, A. O., MARIMON, J. M., ADELL, A., PLANAS, A. M., CRISTOFOL, R. & SANFELIU, C. 2010. In vitro and in vivo activation of astrocytes by amyloid-beta is potentiated by pro-oxidant agents. *Journal of Alzheimer's disease : JAD,* 20, 229-45.

GARZON, D. J. & FAHNESTOCK, M. 2007. Oligomeric amyloid decreases basal levels of brain-derived neurotrophic factor (BDNF) mRNA via specific downregulation of BDNF transcripts IV and V in differentiated human neuroblastoma cells. *The Journal of neuroscience : the official journal of the Society for Neuroscience,* 27, 2628-35.

GERLI, R., MONTI, D., BISTONI, O., MAZZONE, A. M., PERI, G., COSSARIZZA, A., DI GIOACCHINO, M., CESAROTTI, M. E., DONI, A., MANTOVANI, A., FRANCESCHI, C. & PAGANELLI, R. 2000. Chemokines, sTNF-Rs and sCD30 serum levels in healthy aged people and centenarians. *Mechanisms of ageing and development,* 121, 37-46.

GEULA, C., WU, C. K., SAROFF, D., LORENZO, A., YUAN, M. & YANKNER, B. A. 1998. Aging renders the brain vulnerable to amyloid beta-protein neurotoxicity. *Nature medicine,* 4, 827-31.

GIBBS, M. E., HUTCHINSON, D. & HERTZ, L. 2008. Astrocytic involvement in learning and memory consolidation. *Neuroscience and biobehavioral reviews,* 32, 927-44.

GLASS, C. K., SAIJO, K., WINNER, B., MARCHETTO, M. C. & GAGE, F. H. 2010. Mechanisms underlying inflammation in neurodegeneration. *Cell,* 140, 918-34.

GOLDE, T. E., SCHNEIDER, L. S. & KOO, E. H. 2011. Anti-abeta therapeutics in Alzheimer's disease: the need for a paradigm shift. *Neuron,* 69, 203-13.

GRACE, E. A., RABINER, C. A. & BUSCIGLIO, J. 2002. Characterization of neuronal dystrophy induced by fibrillar amyloid beta: implications for Alzheimer's disease. *Neuroscience,* 114, 265-73.

GRAEBER, M. B. & STREIT, W. J. 2010. Microglia: biology and pathology. *Acta neuropathologica,* 119, 89-105.

GRANIC, I., DOLGA, A. M., NIJHOLT, I. M., VAN DIJK, G. & EISEL, U. L. 2009. Inflammation and NF-kappaB in Alzheimer's disease and diabetes. *Journal of Alzheimer's disease : JAD,* 16, 809-21.

GRATHWOHL, S. A., KALIN, R. E., BOLMONT, T., PROKOP, S., WINKELMANN, G., KAESER, S. A., ODENTHAL, J., RADDE, R., ELDH, T., GANDY, S., AGUZZI, A., STAUFENBIEL, M., MATHEWS, P. M., WOLBURG, H.,

HEPPNER, F. L. & JUCKER, M. 2009. Formation and maintenance of Alzheimer's disease beta-amyloid plaques in the absence of microglia. *Nature neuroscience,* 12, 1361-3.

GRAVINA, S. A., HO, L., ECKMAN, C. B., LONG, K. E., OTVOS, L., JR., YOUNKIN, L. H., SUZUKI, N. & YOUNKIN, S. G. 1995. Amyloid beta protein (A beta) in Alzheimer's disease brain. Biochemical and immunocytochemical analysis with antibodies specific for forms ending at A beta 40 or A beta 42(43). *The Journal of biological chemistry,* 270, 7013-6.

GREENFEDER, S. A., NUNES, P., KWEE, L., LABOW, M., CHIZZONITE, R. A. & JU, G. 1995. Molecular cloning and characterization of a second subunit of the interleukin 1 receptor complex. *The Journal of biological chemistry,* 270, 13757-65.

GRIFFIN, R., NALLY, R., NOLAN, Y., MCCARTNEY, Y., LINDEN, J. & LYNCH, M. A. 2006. The age-related attenuation in long-term potentiation is associated with microglial activation. *Journal of neurochemistry,* 99, 1263-72.

GRIFFIN, W. S., SHENG, J. G., ROBERTS, G. W. & MRAK, R. E. 1995. Interleukin-1 expression in different plaque types in Alzheimer's disease: significance in plaque evolution. *Journal of neuropathology and experimental neurology,* 54, 276-81.

GRIMMER, T., RIEMENSCHNEIDER, M., FORSTL, H., HENRIKSEN, G., KLUNK, W. E., MATHIS, C. A., SHIGA, T., WESTER, H. J., KURZ, A. & DRZEZGA, A. 2009. Beta amyloid in Alzheimer's disease: increased deposition in brain is reflected in reduced concentration in cerebrospinal fluid. *Biological psychiatry,* 65, 927-34.

GUGLIELMOTTO, M., ARAGNO, M., AUTELLI, R., GILIBERTO, L., NOVO, E., COLOMBATTO, S., DANNI, O., PAROLA, M., SMITH, M. A., PERRY, G., TAMAGNO, E. & TABATON, M. 2009. The up-regulation of BACE1 mediated by hypoxia and ischemic injury: role of oxidative stress and HIF1alpha. *Journal of neurochemistry,* 108, 1045-56.

GUIZZETTI, M., KAVANAGH, T. J. & COSTA, L. G. 2011. Measurements of astrocyte proliferation. *Methods in molecular biology,* 758, 349-59.

GURER, G., GURSOY-OZDEMIR, Y., ERDEMLI, E., CAN, A. & DALKARA, T. 2009. Astrocytes are more resistant to focal cerebral ischemia than neurons and die by a delayed necrosis. *Brain pathology,* 19, 630-41.

HAASS, C., SCHLOSSMACHER, M. G., HUNG, A. Y., VIGO-PELFREY, C., MELLON, A., OSTASZEWSKI, B. L., LIEBERBURG, I., KOO, E. H., SCHENK, D., TEPLOW, D. B. & ET AL. 1992. Amyloid beta-peptide is produced by cultured cells during normal metabolism. *Nature,* 359, 322-5.

HAGEMANN, T. L., CONNOR, J. X. & MESSING, A. 2006. Alexander disease-associated glial fibrillary acidic protein mutations in mice induce Rosenthal fiber formation and a white matter stress response. *The Journal of neuroscience : the official journal of the Society for Neuroscience,* 26, 11162-73.

HAGLID, K. G., YANG, Q., HAMBERGER, A., BERGMAN, S., WIDERBERG, A. & DANIELSEN, N. 1997. S-100beta stimulates neurite outgrowth in the rat sciatic nerve grafted with acellular muscle transplants. *Brain research,* 753, 196-201.

HAMO, L., STOHLMAN, S. A., OTTO-DUESSEL, M. & BERGMANN, C. C. 2007. Distinct regulation of MHC molecule expression on astrocytes and microglia during viral encephalomyelitis. *Glia,* 55, 1169-77.

HAN, S. H., KIM, Y. H. & MOOK-JUNG, I. 2011. RAGE: the beneficial and deleterious effects by diverse mechanisms of actions. *Molecules and cells,* 31, 91-7.

HAUGETO, O., ULLENSVANG, K., LEVY, L. M., CHAUDHRY, F. A., HONORE, T., NIELSEN, M., LEHRE, K. P. & DANBOLT, N. C. 1996. Brain glutamate transporter proteins form homomultimers. *The Journal of biological chemistry,* 271, 27715-22.

HAYDEN, M. S. & GHOSH, S. 2008. Shared principles in NF-kappaB signaling. *Cell,* 132, 344-62.

HAYDEN, M. S., WEST, A. P. & GHOSH, S. 2006. NF-kappaB and the immune response. *Oncogene,* 25, 6758-80.

HE, J., CHEN, Y., FARZAN, M., CHOE, H., OHAGEN, A., GARTNER, S., BUSCIGLIO, J., YANG, X., HOFMANN, W., NEWMAN, W., MACKAY, C. R., SODROSKI, J. & GABUZDA, D. 1997. CCR3 and CCR5 are co-receptors for HIV-1 infection of microglia. *Nature,* 385, 645-9.

HERNANDEZ, F., GOMEZ DE BARREDA, E., FUSTER-MATANZO, A., LUCAS, J. J. & AVILA, J. 2010. GSK3: a possible link between beta amyloid peptide and tau protein. *Experimental neurology,* 223, 322-5.

HIBI, M., MURAKAMI, M., SAITO, M., HIRANO, T., TAGA, T. & KISHIMOTO, T. 1990. Molecular cloning and expression of an IL-6 signal transducer, gp130. *Cell,* 63, 1149-57.

HIRT, L., BADAUT, J., THEVENET, J., GRANZIERA, C., REGLI, L., MAURER, F., BONNY, C. & BOGOUSSLAVSKY, J. 2004. D-JNKI1, a cell-penetrating c-Jun-N-terminal kinase inhibitor, protects against cell death in severe cerebral ischemia. *Stroke; a journal of cerebral circulation,* 35, 1738-43.

HIRTZ, D., THURMAN, D. J., GWINN-HARDY, K., MOHAMED, M., CHAUDHURI, A. R. & ZALUTSKY, R. 2007. How common are the "common" neurologic disorders? *Neurology,* 68, 326-37.

HOFMAN, F. M., HINTON, D. R., JOHNSON, K. & MERRILL, J. E. 1989. Tumor necrosis factor identified in multiple sclerosis brain. *The Journal of experimental medicine,* 170, 607-12.

HOFMANN, M. A., DRURY, S., FU, C., QU, W., TAGUCHI, A., LU, Y., AVILA, C., KAMBHAM, N., BIERHAUS, A., NAWROTH, P., NEURATH, M. F., SLATTERY, T., BEACH, D., MCCLARY, J., NAGASHIMA, M., MORSER, J., STERN, D. & SCHMIDT, A. M. 1999. RAGE mediates a novel proinflammatory axis: a central cell surface receptor for S100/calgranulin polypeptides. *Cell,* 97, 889-901.

HOLLINGWORTH, P., HAROLD, D., SIMS, R., GERRISH, A., LAMBERT, J. C., CARRASQUILLO, M. M., ABRAHAM, R., HAMSHERE, M. L., PAHWA, J. S., MOSKVINA, V., DOWZELL, K., JONES, N., STRETTON, A., THOMAS, C., RICHARDS, A., IVANOV, D., WIDDOWSON, C., CHAPMAN, J., LOVESTONE, S., POWELL, J., PROITSI, P., LUPTON, M. K., BRAYNE, C., RUBINSZTEIN, D. C., GILL, M., LAWLOR, B., LYNCH, A., BROWN, K. S., PASSMORE, P. A., CRAIG, D., MCGUINNESS, B., TODD, S., HOLMES, C.,

MANN, D., SMITH, A. D., BEAUMONT, H., WARDEN, D., WILCOCK, G., LOVE, S., KEHOE, P. G., HOOPER, N. M., VARDY, E. R., HARDY, J., MEAD, S., FOX, N. C., ROSSOR, M., COLLINGE, J., MAIER, W., JESSEN, F., RUTHER, E., SCHURMANN, B., HEUN, R., KOLSCH, H., VAN DEN BUSSCHE, H., HEUSER, I., KORNHUBER, J., WILTFANG, J., DICHGANS, M., FROLICH, L., HAMPEL, H., GALLACHER, J., HULL, M., RUJESCU, D., GIEGLING, I., GOATE, A. M., KAUWE, J. S., CRUCHAGA, C., NOWOTNY, P., MORRIS, J. C., MAYO, K., SLEEGERS, K., BETTENS, K., ENGELBORGHS, S., DE DEYN, P. P., VAN BROECKHOVEN, C., LIVINGSTON, G., BASS, N. J., GURLING, H., MCQUILLIN, A., GWILLIAM, R., DELOUKAS, P., AL-CHALABI, A., SHAW, C. E., TSOLAKI, M., SINGLETON, A. B., GUERREIRO, R., MUHLEISEN, T. W., NOTHEN, M. M., MOEBUS, S., JOCKEL, K. H., KLOPP, N., WICHMANN, H. E., PANKRATZ, V. S., SANDO, S. B., AASLY, J. O., BARCIKOWSKA, M., WSZOLEK, Z. K., DICKSON, D. W., GRAFF-RADFORD, N. R., PETERSEN, R. C., et al. 2011. Common variants at ABCA7, MS4A6A/MS4A4E, EPHA1, CD33 and CD2AP are associated with Alzheimer's disease. *Nature genetics,* 43, 429-35.

HONG, H. S., HWANG, E. M., SIM, H. J., CHO, H. J., BOO, J. H., OH, S. S., KIM, S. U. & MOOK-JUNG, I. 2003. Interferon gamma stimulates beta-secretase expression and sAPPbeta production in astrocytes. *Biochem Biophys Res Commun,* 307, 922-7.

HOOK, V., TONEFF, T., BOGYO, M., GREENBAUM, D., MEDZIHRADSZKY, K. F., NEVEU, J., LANE, W., HOOK, G. & REISINE, T. 2005. Inhibition of cathepsin B reduces beta-amyloid production in regulated secretory vesicles of neuronal chromaffin cells: evidence for cathepsin B as a candidate beta-secretase of Alzheimer's disease. *Biological chemistry,* 386, 931-40.

HORRILLO, D., SIERRA, J., ARRIBAS, C., GARCIA-SAN FRUTOS, M., CARRASCOSA, J. M., LAUZURICA, N., FERNANDEZ-AGULLO, T. & ROS, M. 2011. Age-associated development of inflammation in Wistar rats: Effects of caloric restriction. *Archives of physiology and biochemistry,* 117, 140-50.

HOWLETT, D. R., BATE, S. T., COLLIER, S., LAWMAN, A., CHAPMAN, T., ASHMEADE, T., MARSHALL, I., ANDERSON, P. J., PHILPOTT, K. L., RICHARDSON, J. C. & HILLE, C. J. 2011. Characterisation of amyloid-induced inflammatory responses in the rat retina. *Experimental brain research. Experimentelle Hirnforschung. Experimentation cerebrale.*

HSIEH, H., BOEHM, J., SATO, C., IWATSUBO, T., TOMITA, T., SISODIA, S. & MALINOW, R. 2006. AMPAR removal underlies Abeta-induced synaptic depression and dendritic spine loss. *Neuron,* 52, 831-43.

HU, J., AKAMA, K. T., KRAFFT, G. A., CHROMY, B. A. & VAN ELDIK, L. J. 1998. Amyloid-beta peptide activates cultured astrocytes: morphological alterations, cytokine induction and nitric oxide release. *Brain research,* 785, 195-206.

HU, J., CASTETS, F., GUEVARA, J. L. & VAN ELDIK, L. J. 1996. S100 beta stimulates inducible nitric oxide synthase activity and mRNA levels in rat cortical astrocytes. *The Journal of biological chemistry,* 271, 2543-7.

HU, J., FERREIRA, A. & VAN ELDIK, L. J. 1997. S100beta induces neuronal cell death through nitric oxide release from astrocytes. *Journal of neurochemistry,* 69, 2294-301.

HU, S., MARTELLA, A., ANDERSON, W. R. & CHAO, C. C. 1994. Role of cytokines in lipopolysaccharide-induced functional and structural abnormalities of astrocytes. *Glia,* 10, 227-34.

HUA, L. L., ZHAO, M. L., COSENZA, M., KIM, M. O., HUANG, H., TANOWITZ, H. B., BROSNAN, C. F. & LEE, S. C. 2002. Role of mitogen-activated protein kinases in inducible nitric oxide synthase and TNFalpha expression in human fetal astrocytes. *Journal of neuroimmunology,* 126, 180-9.

HUANG, G., SHI, L. Z. & CHI, H. 2009. Regulation of JNK and p38 MAPK in the immune system: signal integration, propagation and termination. *Cytokine,* 48, 161-9.

HUSEMANN, J., LOIKE, J. D., ANANKOV, R., FEBBRAIO, M. & SILVERSTEIN, S. C. 2002. Scavenger receptors in neurobiology and neuropathology: their role on microglia and other cells of the nervous system. *Glia,* 40, 195-205.

HUTTUNEN, H. J., KUJA-PANULA, J., SORCI, G., AGNELETTI, A. L., DONATO, R. & RAUVALA, H. 2000. Coregulation of neurite outgrowth and cell survival by amphoterin and S100 proteins through receptor for advanced glycation end products (RAGE) activation. *The Journal of biological chemistry,* 275, 40096-105.

IQBAL, K., LIU, F., GONG, C. X. & GRUNDKE-IQBAL, I. 2010. Tau in Alzheimer disease and related tauopathies. *Current Alzheimer research,* 7, 656-64.

ISAACS, A., BAKER, M., WAVRANT-DE VRIEZE, F. & HUTTON, M. 1998. Determination of the gene structure of human GFAP and absence of coding region mutations associated with frontotemporal dementia with parkinsonism linked to chromosome 17. *Genomics,* 51, 152-4.

ISENBERG, J. S., ROBERTS, D. D. & FRAZIER, W. A. 2008. CD47: a new target in cardiovascular therapy. *Arteriosclerosis, thrombosis, and vascular biology,* 28, 615-21.

JACK, C. R., JR., ALBERT, M. S., KNOPMAN, D. S., MCKHANN, G. M., SPERLING, R. A., CARRILLO, M. C., THIES, B. & PHELPS, C. H. 2011. Introduction to the recommendations from the National Institute on Aging-Alzheimer's Association workgroups on diagnostic guidelines for Alzheimer's disease. *Alzheimer's & dementia : the journal of the Alzheimer's Association,* 7, 257-62.

JAEGER, L. B., DOHGU, S., SULTANA, R., LYNCH, J. L., OWEN, J. B., ERICKSON, M. A., SHAH, G. N., PRICE, T. O., FLEEGAL-DEMOTTA, M. A., BUTTERFILED, D. A. & BANKS, W. A. 2009. Lipopolysaccharide alters the blood-brain barrier transport of amyloid beta protein: a mechanism for inflammation in the progression of Alzheimer's disease. *Brain, behavior, and immunity,* 23, 507-17.

JANA, M., JANA, A., PAL, U. & PAHAN, K. 2007. A simplified method for isolating highly purified neurons, oligodendrocytes, astrocytes, and microglia from the same human fetal brain tissue. *Neurochemical research,* 32, 2015-22.

JAYAKUMAR, A. R., PANICKAR, K. S., MURTHY CH, R. & NORENBERG, M. D. 2006. Oxidative stress and mitogen-activated protein kinase phosphorylation mediate ammonia-induced cell swelling and glutamate uptake inhibition in cultured astrocytes. *The Journal of neuroscience : the official journal of the Society for Neuroscience,* 26, 4774-84.

JIANG, C., TING, A. T. & SEED, B. 1998a. PPAR-gamma agonists inhibit production of monocyte inflammatory cytokines. *Nature,* 391, 82-6.

JIANG, P., LAGENAUR, C. F. & NARAYANAN, V. 1999. Integrin-associated protein is a ligand for the P84 neural adhesion molecule. *The Journal of biological chemistry,* 274, 559-62.

JIANG, Z., SHIH, D. M., XIA, Y. R., LUSIS, A. J., DE BEER, F. C., DE VILLIERS, W. J., VAN DER WESTHUYZEN, D. R. & DE BEER, M. C. 1998b. Structure, organization, and chromosomal mapping of the gene encoding macrosialin, a macrophage-restricted protein. *Genomics,* 50, 199-205.

JIMENEZ, S., BAGLIETTO-VARGAS, D., CABALLERO, C., MORENO-GONZALEZ, I., TORRES, M., SANCHEZ-VARO, R., RUANO, D., VIZUETE, M., GUTIERREZ, A. & VITORICA, J. 2008. Inflammatory response in the hippocampus of PS1M146L/APP751SL mouse model of Alzheimer's disease: age-dependent switch in the microglial phenotype from alternative to classic. *The Journal of neuroscience : the official journal of the Society for Neuroscience,* 28, 11650-61.

JOHNSON, G. L. & NAKAMURA, K. 2007. The c-jun kinase/stress-activated pathway: regulation, function and role in human disease. *Biochimica et biophysica acta,* 1773, 1341-8.

JOHNSTON, M. & PAPAICONOMOU, C. 2002. Cerebrospinal fluid transport: a lymphatic perspective. *News in physiological sciences : an international journal of physiology produced jointly by the International Union of Physiological Sciences and the American Physiological Society,* 17, 227-30.

JOHNSTONE, M., GEARING, A. J. & MILLER, K. M. 1999. A central role for astrocytes in the inflammatory response to beta-amyloid; chemokines, cytokines and reactive oxygen species are produced. *Journal of neuroimmunology,* 93, 182-93.

JONES, R. W. 2010. Dimebon disappointment. *Alzheimer's research & therapy,* 2, 25.

JUCKER, M. & HEPPNER, F. L. 2008. Cerebral and peripheral amyloid phagocytes--an old liaison with a new twist. *Neuron,* 59, 8-10.

JUNKER, A., KRUMBHOLZ, M., EISELE, S., MOHAN, H., AUGSTEIN, F., BITTNER, R., LASSMANN, H., WEKERLE, H., HOHLFELD, R. & MEINL, E. 2009. MicroRNA profiling of multiple sclerosis lesions identifies modulators of the regulatory protein CD47. *Brain : a journal of neurology,* 132, 3342-52.

KANEMITSU, H., TOMIYAMA, T. & MORI, H. 2003. Human neprilysin is capable of degrading amyloid beta peptide not only in the monomeric form but also the pathological oligomeric form. *Neuroscience letters,* 350, 113-6.

KAPOOR, K. G., KATZ, S. E., GRZYBOWSKI, D. M. & LUBOW, M. 2008. Cerebrospinal fluid outflow: an evolving perspective. *Brain research bulletin,* 77, 327-34.

KAUR, C., HAO, A. J., WU, C. H. & LING, E. A. 2001. Origin of microglia. *Microscopy research and technique,* 54, 2-9.

KAUR, S., MARTIN-MANSO, G., PENDRAK, M. L., GARFIELD, S. H., ISENBERG, J. S. & ROBERTS, D. D. 2010. Thrombospondin-1 inhibits VEGF receptor-2 signaling by disrupting its association with CD47. *The Journal of biological chemistry,* 285, 38923-32.

KAYED, R., SOKOLOV, Y., EDMONDS, B., MCINTIRE, T. M., MILTON, S. C., HALL, J. E. & GLABE, C. G. 2004. Permeabilization of lipid bilayers is a common conformation-dependent activity of soluble amyloid oligomers in protein misfolding diseases. *The Journal of biological chemistry,* 279, 46363-6.

KELLY, P. H., BONDOLFI, L., HUNZIKER, D., SCHLECHT, H. P., CARVER, K., MAGUIRE, E., ABRAMOWSKI, D., WIEDERHOLD, K. H., STURCHLER-PIERRAT, C., JUCKER, M., BERGMANN, R., STAUFENBIEL, M. & SOMMER, B. 2003. Progressive age-related impairment of cognitive behavior in APP23 transgenic mice. *Neurobiology of aging,* 24, 365-78.

KEROKOSKI, P., SOININEN, H. & PIRTTILA, T. 2001. Beta-amyloid (1-42) affects MTT reduction in astrocytes: implications for vesicular trafficking and cell functionality. *Neurochemistry international,* 38, 127-34.

KIM, J. I., JU, W. K., CHOI, J. H., CHOI, E., CARP, R. I., WISNIEWSKI, H. M. & KIM, Y. S. 1999. Expression of cytokine genes and increased nuclear factor-kappa B activity in the brains of scrapie-infected mice. *Brain research. Molecular brain research,* 73, 17-27.

KIM, M. S., SUNG, M. J., SEO, S. B., YOO, S. J., LIM, W. K. & KIM, H. M. 2002. Water-soluble chitosan inhibits the production of pro-inflammatory cytokine in human astrocytoma cells activated by amyloid beta peptide and interleukin-1beta. *Neuroscience letters,* 321, 105-9.

KIMBERLY, W. T., LAVOIE, M. J., OSTASZEWSKI, B. L., YE, W., WOLFE, M. S. & SELKOE, D. J. 2003. Gamma-secretase is a membrane protein complex comprised of presenilin, nicastrin, Aph-1, and Pen-2. *Proceedings of the National Academy of Sciences of the United States of America,* 100, 6382-7.

KIMURA, A., NAKA, T., NAKAHAMA, T., CHINEN, I., MASUDA, K., NOHARA, K., FUJII-KURIYAMA, Y. & KISHIMOTO, T. 2009. Aryl hydrocarbon receptor in combination with Stat1 regulates LPS-induced inflammatory responses. *The Journal of experimental medicine,* 206, 2027-35.

KISHIMOTO, T. 2010. IL-6: from its discovery to clinical applications. *International immunology,* 22, 347-52.

KLYUBIN, I., WANG, Q., REED, M. N., IRVING, E. A., UPTON, N., HOFMEISTER, J., CLEARY, J. P., ANWYL, R. & ROWAN, M. J. 2011. Protection against Abeta-mediated rapid disruption of synaptic plasticity and memory by memantine. *Neurobiology of aging,* 32, 614-23.

KOBORI, M., YANG, Z., GONG, D., HEISSMEYER, V., ZHU, H., JUNG, Y. K., GAKIDIS, M. A., RAO, A., SEKINE, T., IKEGAMI, F., YUAN, C. & YUAN, J. 2004. Wedelolactone suppresses LPS-induced caspase-11 expression by directly inhibiting the IKK complex. *Cell death and differentiation,* 11, 123-30.

KOENIGSKNECHT, J. & LANDRETH, G. 2004. Microglial phagocytosis of fibrillar beta-amyloid through a beta1 integrin-dependent mechanism. *The Journal of neuroscience : the official journal of the Society for Neuroscience,* 24, 9838-46.

KOISTINAHO, M., LIN, S., WU, X., ESTERMAN, M., KOGER, D., HANSON, J., HIGGS, R., LIU, F., MALKANI, S., BALES, K. R. & PAUL, S. M. 2004. Apolipoprotein E promotes astrocyte colocalization and degradation of deposited amyloid-beta peptides. *Nature medicine,* 10, 719-26.

KOKKOLA, R., ANDERSSON, A., MULLINS, G., OSTBERG, T., TREUTIGER, C. J., ARNOLD, B., NAWROTH, P., ANDERSSON, U., HARRIS, R. A. & HARRIS, H. E. 2005. RAGE is the major receptor for the proinflammatory activity of HMGB1 in rodent macrophages. *Scandinavian journal of immunology,* 61, 1-9.

KOROLAINEN, M. A., AURIOLA, S., NYMAN, T. A., ALAFUZOFF, I. & PIRTTILA, T. 2005. Proteomic analysis of glial fibrillary acidic protein in Alzheimer's disease and aging brain. *Neurobiology of disease,* 20, 858-70.

KOVAC, A., ZILKA, N., KAZMEROVA, Z., CENTE, M., ZILKOVA, M. & NOVAK, M. 2011. Misfolded Truncated Protein {tau} Induces Innate Immune Response via MAPK Pathway. *Journal of immunology,* 187, 2732-9.

KRUPENKO, S. A. 2009. FDH: an aldehyde dehydrogenase fusion enzyme in folate metabolism. *Chemico-biological interactions,* 178, 84-93.

KUKULL, W. A., HIGDON, R., BOWEN, J. D., MCCORMICK, W. C., TERI, L., SCHELLENBERG, G. D., VAN BELLE, G., JOLLEY, L. & LARSON, E. B. 2002. Dementia and Alzheimer disease incidence: a prospective cohort study. *Archives of neurology,* 59, 1737-46.

KUMANOGOH, A. & OGATA, M. 2010. The study of cytokines by Japanese researchers: a historical perspective. *International immunology,* 22, 341-5.

KUMAR, V. & ROBBINS, S. L. 2007. *Robbins basic pathology,* Philadelphia, PA, Saunders/Elsevier.

KUSAKARI, S., OHNISHI, H., JIN, F. J., KANEKO, Y., MURATA, T., MURATA, Y., OKAZAWA, H. & MATOZAKI, T. 2008. Trans-endocytosis of CD47 and SHPS-1 and its role in regulation of the CD47-SHPS-1 system. *Journal of cell science,* 121, 1213-23.

KYRIAKIS, J. M. & AVRUCH, J. 2001. Mammalian mitogen-activated protein kinase signal transduction pathways activated by stress and inflammation. *Physiological reviews,* 81, 807-69.

LADU, M. J., SHAH, J. A., REARDON, C. A., GETZ, G. S., BU, G., HU, J., GUO, L. & VAN ELDIK, L. J. 2000. Apolipoprotein E receptors mediate the effects of beta-amyloid on astrocyte cultures. *The Journal of biological chemistry,* 275, 33974-80.

LAMBERT, M. P., BARLOW, A. K., CHROMY, B. A., EDWARDS, C., FREED, R., LIOSATOS, M., MORGAN, T. E., ROZOVSKY, I., TROMMER, B., VIOLA, K. L., WALS, P., ZHANG, C., FINCH, C. E., KRAFFT, G. A. & KLEIN, W. L. 1998. Diffusible, nonfibrillar ligands derived from Abeta1-42 are potent central nervous system neurotoxins. *Proceedings of the National Academy of Sciences of the United States of America,* 95, 6448-53.

LAMY, L., FOUSSAT, A., BROWN, E. J., BORNSTEIN, P., TICCHIONI, M. & BERNARD, A. 2007. Interactions between CD47 and thrombospondin reduce inflammation. *Journal of immunology,* 178, 5930-9.

LASAGNA-REEVES, C. A. & KAYED, R. 2011. Astrocytes contain amyloid-beta annular protofibrils in Alzheimer's disease brains. *FEBS letters.*

LATOUR, S., TANAKA, H., DEMEURE, C., MATEO, V., RUBIO, M., BROWN, E. J., MALISZEWSKI, C., LINDBERG, F. P., OLDENBORG, A., ULLRICH, A., DELESPESSE, G. & SARFATI, M. 2001. Bidirectional negative regulation of human T and dendritic cells by CD47 and its cognate receptor signal-regulator protein-alpha: down-regulation of IL-12 responsiveness and inhibition of dendritic cell activation. *Journal of immunology,* 167, 2547-54.

LAURIAT, T. L. & MCINNES, L. A. 2007. EAAT2 regulation and splicing: relevance to psychiatric and neurological disorders. *Molecular psychiatry,* 12, 1065-78.

LEBOUVIER, T., SCALES, T. M., WILLIAMSON, R., NOBLE, W., DUYCKAERTS, C., HANGER, D. P., REYNOLDS, C. H., ANDERTON, B. H. & DERKINDEREN, P. 2009. The microtubule-associated protein tau is also phosphorylated on tyrosine. *Journal of Alzheimer's disease : JAD,* 18, 1-9.

LECLERC, E., FRITZ, G., VETTER, S. W. & HEIZMANN, C. W. 2009. Binding of S100 proteins to RAGE: an update. *Biochimica et biophysica acta,* 1793, 993-1007.

LECLERC, E., STURCHLER, E. & VETTER, S. W. 2010. The S100B/RAGE Axis in Alzheimer's Disease. *Cardiovascular psychiatry and neurology,* 2010, 539581.

LEE, C. L., KUO, T. F., WANG, J. J. & PAN, T. M. 2007. Red mold rice ameliorates impairment of memory and learning ability in intracerebroventricular amyloid beta-infused rat by repressing amyloid beta accumulation. *Journal of neuroscience research,* 85, 3171-82.

LEGRAND, N., HUNTINGTON, N. D., NAGASAWA, M., BAKKER, A. Q., SCHOTTE, R., STRICK-MARCHAND, H., DE GEUS, S. J., POUW, S. M., BOHNE, M., VOORDOUW, A., WEIJER, K., DI SANTO, J. P. & SPITS, H. 2011. Functional CD47/signal regulatory protein alpha (SIRP{alpha}) interaction is required for optimal human T- and natural killer- (NK) cell homeostasis in vivo. *Proceedings of the National Academy of Sciences of the United States of America,* 108, 13224-9.

LEVY, J. A. 2009. The unexpected pleiotropic activities of RANTES. *Journal of immunology,* 182, 3945-6.

LI, C., ZHAO, R., GAO, K., WEI, Z., YIN, M. Y., LAU, L. T., CHUI, D. & HOI YU, A. C. 2011a. Astrocytes: implications for neuroinflammatory pathogenesis of Alzheimer's disease. *Current Alzheimer research,* 8, 67-80.

LI, J. & SCHMIDT, A. M. 1997. Characterization and functional analysis of the promoter of RAGE, the receptor for advanced glycation end products. *The Journal of biological chemistry,* 272, 16498-506.

LI, J., WANG, G., LIU, J., ZHOU, L., DONG, M., WANG, R., LI, X., LIN, C. & NIU, Y. 2010. Puerarin attenuates amyloid-beta-induced cognitive impairment through suppression of apoptosis in rat hippocampus in vivo. *European journal of pharmacology,* 649, 195-201.

LI, S., HONG, S., SHEPARDSON, N. E., WALSH, D. M., SHANKAR, G. M. & SELKOE, D. 2009. Soluble oligomers of amyloid Beta protein facilitate hippocampal long-term depression by disrupting neuronal glutamate uptake. *Neuron,* 62, 788-801.

LI, S., MALLORY, M., ALFORD, M., TANAKA, S. & MASLIAH, E. 1997. Glutamate transporter alterations in Alzheimer disease are possibly associated with abnormal APP expression. *Journal of neuropathology and experimental neurology,* 56, 901-11.

LI, X. H., LV, B. L., XIE, J. Z., LIU, J., ZHOU, X. W. & WANG, J. Z. 2011b. AGEs induce Alzheimer-like tau pathology and memory deficit via RAGE-mediated GSK-3 activation. *Neurobiology of aging.*

LI, Y. M., XU, M., LAI, M. T., HUANG, Q., CASTRO, J. L., DIMUZIO-MOWER, J., HARRISON, T., LELLIS, C., NADIN, A., NEDUVELIL, J. G., REGISTER, R. B., SARDANA, M. K., SHEARMAN, M. S., SMITH, A. L., SHI, X. P., YIN, K. C., SHAFER, J. A. & GARDELL, S. J. 2000. Photoactivated gamma-secretase inhibitors directed to the active site covalently label presenilin 1. *Nature,* 405, 689-94.

LIEBERMAN, A. P., PITHA, P. M., SHIN, H. S. & SHIN, M. L. 1989. Production of tumor necrosis factor and other cytokines by astrocytes stimulated with lipopolysaccharide or a neurotropic virus. *Proceedings of the National Academy of Sciences of the United States of America,* 86, 6348-52.

LIU, G. J., NAGARAJAH, R., BANATI, R. B. & BENNETT, M. R. 2009. Glutamate induces directed chemotaxis of microglia. *The European journal of neuroscience,* 29, 1108-18.

LIU, X., BOLTEUS, A. J., BALKIN, D. M., HENSCHEL, O. & BORDEY, A. 2006. GFAP-expressing cells in the postnatal subventricular zone display a unique glial phenotype intermediate between radial glia and astrocytes. *Glia,* 54, 394-410.

LU, L., MAK, Y. T., FANG, M. & YEW, D. T. 2009. The difference in gliosis induced by beta-amyloid and Tau treatments in astrocyte cultures derived from senescence accelerated and normal mouse strains. *Biogerontology,* 10, 695-710.

LUE, L. F., KUO, Y. M., ROHER, A. E., BRACHOVA, L., SHEN, Y., SUE, L., BEACH, T., KURTH, J. H., RYDEL, R. E. & ROGERS, J. 1999. Soluble amyloid beta peptide concentration as a predictor of synaptic change in Alzheimer's disease. *The American journal of pathology,* 155, 853-62.

LUE, L. F., WALKER, D. G., JACOBSON, S. & SABBAGH, M. 2009. Receptor for advanced glycation end products: its role in Alzheimer's disease and other neurological diseases. *Future neurology,* 4, 167-177.

LUHRS, T., RITTER, C., ADRIAN, M., RIEK-LOHER, D., BOHRMANN, B., DOBELI, H., SCHUBERT, D. & RIEK, R. 2005. 3D structure of Alzheimer's amyloid-beta(1-42) fibrils. *Proceedings of the National Academy of Sciences of the United States of America,* 102, 17342-7.

LUKIC, I. K., HUMPERT, P. M., NAWROTH, P. P. & BIERHAUS, A. 2008. The RAGE pathway: activation and perpetuation in the pathogenesis of diabetic neuropathy. *Annals of the New York Academy of Sciences,* 1126, 76-80.

LYNCH, M. A. 2004. Long-term potentiation and memory. *Physiological reviews,* 84, 87-136.

LYONS, A., GRIFFIN, R. J., COSTELLOE, C. E., CLARKE, R. M. & LYNCH, M. A. 2007. IL-4 attenuates the neuroinflammation induced by amyloid-beta in vivo and in vitro. *Journal of neurochemistry,* 101, 771-81.

MA, X., REYNOLDS, S. L., BAKER, B. J., LI, X., BENVENISTE, E. N. & QIN, H. 2010. IL-17 enhancement of the IL-6 signaling cascade in astrocytes. *Journal of immunology,* 184, 4898-906.

MACAIONE, V., AGUENNOUZ, M., RODOLICO, C., MAZZEO, A., PATTI, A., CANNISTRACI, E., COLANTONE, L., DI GIORGIO, R. M., DE LUCA, G. & VITA, G. 2007. RAGE-NF-kappaB pathway activation in response to oxidative stress in facioscapulohumeral muscular dystrophy. *Acta neurologica Scandinavica,* 115, 115-21.

MAJUMDAR, A., CAPETILLO-ZARATE, E., CRUZ, D., GOURAS, G. K. & MAXFIELD, F. R. 2011. Degradation of Alzheimer's amyloid fibrils by microglia requires delivery of ClC-7 to lysosomes. *Molecular biology of the cell,* 22, 1664-76.

MAJUMDAR, A., CRUZ, D., ASAMOAH, N., BUXBAUM, A., SOHAR, I., LOBEL, P. & MAXFIELD, F. R. 2007. Activation of microglia acidifies lysosomes and leads to degradation of Alzheimer amyloid fibrils. *Molecular biology of the cell,* 18, 1490-6.

MANDELKOW, E. M., SCHWEERS, O., DREWES, G., BIERNAT, J., GUSTKE, N., TRINCZEK, B. & MANDELKOW, E. 1996. Structure, microtubule interactions, and phosphorylation of tau protein. *Annals of the New York Academy of Sciences,* 777, 96-106.

MANDREKAR, S., JIANG, Q., LEE, C. Y., KOENIGSKNECHT-TALBOO, J., HOLTZMAN, D. M. & LANDRETH, G. E. 2009. Microglia mediate the clearance of soluble Abeta through fluid phase macropinocytosis. *The Journal of neuroscience : the official journal of the Society for Neuroscience,* 29, 4252-62.

MANNA, P. P. & FRAZIER, W. A. 2003. The mechanism of CD47-dependent killing of T cells: heterotrimeric Gi-dependent inhibition of protein kinase A. *Journal of immunology,* 170, 3544-53.

MARIANI, E., CATTINI, L., NERI, S., MALAVOLTA, M., MOCCHEGIANI, E., RAVAGLIA, G. & FACCHINI, A. 2006. Simultaneous evaluation of circulating chemokine and cytokine profiles in elderly subjects by multiplex technology: relationship with zinc status. *Biogerontology,* 7, 449-59.

MARSCHE, G., WEIGLE, B., SATTLER, W. & MALLE, E. 2007. Soluble RAGE blocks scavenger receptor CD36-mediated uptake of hypochlorite-modified low-density lipoprotein. *The FASEB journal : official publication of the Federation of American Societies for Experimental Biology,* 21, 3075-82.

MARTIN, C. A., LONGMAN, E., WOODING, C., HOOSDALLY, S. J., ALI, S., AITMAN, T. J., GUTMANN, D. A., FREEMONT, P. S., BYRNE, B. & LINTON, K. J. 2007. Cd36, a class B scavenger receptor, functions as a monomer to bind acetylated and oxidized low-density lipoproteins. *Protein science : a publication of the Protein Society,* 16, 2531-41.

MARTIN, L., LATYPOVA, X. & TERRO, F. 2011. Post-translational modifications of tau protein: implications for Alzheimer's disease. *Neurochemistry international,* 58, 458-71.

MARTINON, F., MAYOR, A. & TSCHOPP, J. 2009. The inflammasomes: guardians of the body. *Annual review of immunology,* 27, 229-65.

MATOS, M., AUGUSTO, E., OLIVEIRA, C. R. & AGOSTINHO, P. 2008. Amyloid-beta peptide decreases glutamate uptake in cultured astrocytes: involvement of oxidative stress and mitogen-activated protein kinase cascades. *Neuroscience,* 156, 898-910.

MATOZAKI, T., MURATA, Y., OKAZAWA, H. & OHNISHI, H. 2009. Functions and molecular mechanisms of the CD47-SIRPalpha signalling pathway. *Trends in cell biology,* 19, 72-80.

MATTSSON, N., BLENNOW, K. & ZETTERBERG, H. 2009. CSF biomarkers: pinpointing Alzheimer pathogenesis. *Annals of the New York Academy of Sciences,* 1180, 28-35.

MCCARTHY, K. D. & DE VELLIS, J. 1980. Preparation of separate astroglial and oligodendroglial cell cultures from rat cerebral tissue. *The Journal of cell biology,* 85, 890-902.

MCCOY, M. K. & TANSEY, M. G. 2008. TNF signaling inhibition in the CNS: implications for normal brain function and neurodegenerative disease. *Journal of neuroinflammation,* 5, 45.

MCKHANN, G. M., KNOPMAN, D. S., CHERTKOW, H., HYMAN, B. T., JACK, C. R., JR., KAWAS, C. H., KLUNK, W. E., KOROSHETZ, W. J., MANLY, J. J., MAYEUX, R., MOHS, R. C., MORRIS, J. C., ROSSOR, M. N., SCHELTENS, P., CARRILLO, M. C., THIES, B., WEINTRAUB, S. & PHELPS, C. H. 2011. The diagnosis of dementia due to Alzheimer's disease: recommendations from the National Institute on Aging-Alzheimer's Association workgroups on diagnostic guidelines for Alzheimer's disease. *Alzheimer's & dementia : the journal of the Alzheimer's Association,* 7, 263-9.

MEGA, M. S., CUMMINGS, J. L., FIORELLO, T. & GORNBEIN, J. 1996. The spectrum of behavioral changes in Alzheimer's disease. *Neurology,* 46, 130-5.

MEHAN, S., MEENA, H., SHARMA, D. & SANKHLA, R. 2011. JNK: a stress-activated protein kinase therapeutic strategies and involvement in Alzheimer's and various neurodegenerative abnormalities. *Journal of molecular neuroscience : MN,* 43, 376-90.

MELLO COELHO, V., BUNBURY, A., RANGEL, L. B., GIRI, B., WEERARATNA, A., MORIN, P. J., BERNIER, M. & TAUB, D. D. 2009. Fat-storing multilocular cells expressing CCR5 increase in the thymus with advancing age: potential role for CCR5 ligands on the differentiation and migration of preadipocytes. *International journal of medical sciences,* 7, 1-14.

MESSIER, C. & TEUTENBERG, K. 2005. The role of insulin, insulin growth factor, and insulin-degrading enzyme in brain aging and Alzheimer's disease. *Neural plasticity,* 12, 311-28.

MESSING, A., HEAD, M. W., GALLES, K., GALBREATH, E. J., GOLDMAN, J. E. & BRENNER, M. 1998. Fatal encephalopathy with astrocyte inclusions in GFAP transgenic mice. *The American journal of pathology,* 152, 391-8.

METCALFE, M. J. & FIGUEIREDO-PEREIRA, M. E. 2010. Relationship between tau pathology and neuroinflammation in Alzheimer's disease. *The Mount Sinai journal of medicine, New York,* 77, 50-8.

MIGNOT, E., LIN, L., ROGERS, W., HONDA, Y., QIU, X., LIN, X., OKUN, M., HOHJOH, H., MIKI, T., HSU, S., LEFFELL, M., GRUMET, F., FERNANDEZ-VINA, M., HONDA, M. & RISCH, N. 2001. Complex HLA-DR and -DQ interactions confer risk of narcolepsy-cataplexy in three ethnic groups. *American journal of human genetics,* **68,** 686-99.

MILLER, T. W., ISENBERG, J. S., SHIH, H. B., WANG, Y. & ROBERTS, D. D. 2010. Amyloid-beta inhibits No-cGMP signaling in a CD36- and CD47-dependent manner. *PloS one,* **5,** e15686.

MINOGUE, A. M., LYNCH, A. M., LOANE, D. J., HERRON, C. E. & LYNCH, M. A. 2007. Modulation of amyloid-beta-induced and age-associated changes in rat hippocampus by eicosapentaenoic acid. *Journal of neurochemistry,* **103,** 914-26.

MINOGUE, A. M., SCHMID, A. W., FOGARTY, M. P., MOORE, A. C., CAMPBELL, V. A., HERRON, C. E. & LYNCH, M. A. 2003. Activation of the c-Jun N-terminal kinase signaling cascade mediates the effect of amyloid-beta on long term potentiation and cell death in hippocampus: a role for interleukin-1beta? *The Journal of biological chemistry,* **278,** 27971-80.

MOBBERLEY-SCHUMAN, P. S. & WEISS, A. A. 2005. Influence of CR3 (CD11b/CD18) expression on phagocytosis of Bordetella pertussis by human neutrophils. *Infection and immunity,* **73,** 7317-23.

MOGI, M., TOGARI, A., KONDO, T., MIZUNO, Y., KOMURE, O., KUNO, S., ICHINOSE, H. & NAGATSU, T. 2000. Caspase activities and tumor necrosis factor receptor R1 (p55) level are elevated in the substantia nigra from parkinsonian brain. *Journal of neural transmission,* **107,** 335-41.

MOORE, K. J., EL KHOURY, J., MEDEIROS, L. A., TERADA, K., GEULA, C., LUSTER, A. D. & FREEMAN, M. W. 2002. A CD36-initiated signaling cascade mediates inflammatory effects of beta-amyloid. *The Journal of biological chemistry,* **277,** 47373-9.

MORGANTI-KOSSMAN, M. C., LENZLINGER, P. M., HANS, V., STAHEL, P., CSUKA, E., AMMANN, E., STOCKER, R., TRENTZ, O. & KOSSMANN, T. 1997. Production of cytokines following brain injury: beneficial and deleterious for the damaged tissue. *Molecular psychiatry,* **2,** 133-6.

MORI, F., ROSSI, S., SANCESARIO, G., CODECA, C., MATALUNI, G., MONTELEONE, F., BUTTARI, F., KUSAYANAGI, H., CASTELLI, M., MOTTA, C., STUDER, V., BERNARDI, G., KOCH, G., BERNARDINI, S. & CENTONZE, D. 2011. Cognitive and Cortical Plasticity Deficits Correlate with Altered Amyloid-beta CSF Levels in Multiple Sclerosis. *Neuropsychopharmacology,* **36,** 559-68.

MORI, T., KOYAMA, N., ARENDASH, G. W., HORIKOSHI-SAKURABA, Y., TAN, J. & TOWN, T. 2010. Overexpression of human S100B exacerbates cerebral amyloidosis and gliosis in the Tg2576 mouse model of Alzheimer's disease. *Glia,* **58,** 300-14.

MORRIS, M., MAEDA, S., VOSSEL, K. & MUCKE, L. 2011. The many faces of tau. *Neuron,* **70,** 410-26.

MORRIS, R. G., GARRUD, P., RAWLINS, J. N. & O'KEEFE, J. 1982. Place navigation impaired in rats with hippocampal lesions. *Nature,* **297,** 681-3.

MRAK, R. E. & GRIFFINBC, W. S. 2001. The role of activated astrocytes and of the neurotrophic cytokine S100B in the pathogenesis of Alzheimer's disease. *Neurobiology of aging,* 22, 915-22.

MRAK, R. E., SHENG, J. G. & GRIFFIN, W. S. 1996. Correlation of astrocytic S100 beta expression with dystrophic neurites in amyloid plaques of Alzheimer's disease. *Journal of neuropathology and experimental neurology,* 55, 273-9.

MULDER, S. D., VAN DER FLIER, W. M., VERHEIJEN, J. H., MULDER, C., SCHELTENS, P., BLANKENSTEIN, M. A., HACK, C. E. & VEERHUIS, R. 2010. BACE1 activity in cerebrospinal fluid and its relation to markers of AD pathology. *J Alzheimers Dis,* 20, 253-60.

MUNCH, G., APELT, J., ROSEMARIE KIENTSCH, E., STAHL, P., LUTH, H. J. & SCHLIEBS, R. 2003. Advanced glycation endproducts and pro-inflammatory cytokines in transgenic Tg2576 mice with amyloid plaque pathology. *Journal of neurochemistry,* 86, 283-9.

MURAMORI, F., KOBAYASHI, K. & NAKAMURA, I. 1998. A quantitative study of neurofibrillary tangles, senile plaques and astrocytes in the hippocampal subdivisions and entorhinal cortex in Alzheimer's disease, normal controls and non-Alzheimer neuropsychiatric diseases. *Psychiatry and clinical neurosciences,* 52, 593-9.

MUROOKA, T. T., WONG, M. M., RAHBAR, R., MAJCHRZAK-KITA, B., PROUDFOOT, A. E. & FISH, E. N. 2006. CCL5-CCR5-mediated apoptosis in T cells: Requirement for glycosaminoglycan binding and CCL5 aggregation. *The Journal of biological chemistry,* 281, 25184-94.

MURPHY, M. P. & LEVINE, H., 3RD 2010. Alzheimer's disease and the amyloid-beta peptide. *Journal of Alzheimer's disease : JAD,* 19, 311-23.

NAGATA, T., TOMIYAMA, T., MORI, H., YAGUCHI, T. & NISHIZAKI, T. 2010. DCP-LA neutralizes mutant amyloid beta peptide-induced impairment of long-term potentiation and spatial learning. *Behavioural brain research,* 206, 151-4.

NAGELE, R. G., D'ANDREA, M. R., LEE, H., VENKATARAMAN, V. & WANG, H. Y. 2003. Astrocytes accumulate A beta 42 and give rise to astrocytic amyloid plaques in Alzheimer disease brains. *Brain research,* 971, 197-209.

NAGELE, R. G., WEGIEL, J., VENKATARAMAN, V., IMAKI, H. & WANG, K. C. 2004. Contribution of glial cells to the development of amyloid plaques in Alzheimer's disease. *Neurobiology of aging,* 25, 663-74.

NAGY, J. I., LI, W., HERTZBERG, E. L. & MAROTTA, C. A. 1996. Elevated connexin43 immunoreactivity at sites of amyloid plaques in Alzheimer's disease. *Brain research,* 717, 173-8.

NAKAYAMA, K., NAGASE, H., KOH, C. S. & OHKAWARA, T. 2011. γ-secretase-regulated mechanisms similar to Notch signaling may play a role in signaling events, including APP signaling, which leads to Alzheimer's disease. *Cellular and molecular neurobiology,* 31, 887-900.

NARUSE, K., UENO, M., SATOH, T., NOMIYAMA, H., TEI, H., TAKEDA, M., LEDBETTER, D. H., COILLIE, E. V., OPDENAKKER, G., GUNGE, N., SAKAKI, Y., IIO, M. & MIURA, R. 1996. A YAC contig of the human CC chemokine genes clustered on chromosome 17q11.2. *Genomics,* 34, 236-40.

NEEPER, M., SCHMIDT, A. M., BRETT, J., YAN, S. D., WANG, F., PAN, Y. C., ELLISTON, K., STERN, D. & SHAW, A. 1992. Cloning and expression of a cell surface receptor for advanced glycosylation end products of proteins. *J Biol Chem,* 267, 14998-5004.

NI, Y., MALARKEY, E. B. & PARPURA, V. 2007. Vesicular release of glutamate mediates bidirectional signaling between astrocytes and neurons. *Journal of neurochemistry,* 103, 1273-84.

NIEDERHOFFER, N., LEVY, R., SICK, E., ANDRE, P., COUPIN, G., LOMBARD, Y. & GIES, J. P. 2009. Amyloid beta peptides trigger CD47-dependent mast cell secretory and phagocytic responses. *International journal of immunopathology and pharmacology,* 22, 473-83.

NIELSEN, H. M., VEERHUIS, R., HOLMQVIST, B. & JANCIAUSKIENE, S. 2009. Binding and uptake of A beta1-42 by primary human astrocytes in vitro. *Glia,* 57, 978-88.

NIELSEN, M., LUND, O., BUUS, S. & LUNDEGAARD, C. 2010. MHC class II epitope predictive algorithms. *Immunology,* 130, 319-28.

NOGUEIRA, M. I., ABBAS, S. Y., CAMPOS, L. G., ALLEMANDI, W., LAWSON, P., TAKADA, S. H. & AZMITIA, E. C. 2009. S100beta protein expression: gender- and age-related daily changes. *Neurochemical research,* 34, 1355-62.

O'NEILL, L. A. 2008. The interleukin-1 receptor/Toll-like receptor superfamily: 10 years of progress. *Immunological reviews,* 226, 10-8.

OHGAMI, N., NAGAI, R., IKEMOTO, M., ARAI, H., KUNIYASU, A., HORIUCHI, S. & NAKAYAMA, H. 2001. CD36, a member of class B scavenger receptor family, is a receptor for advanced glycation end products. *Annals of the New York Academy of Sciences,* 947, 350-5.

OLABARRIA, M., NORISTANI, H. N., VERKHRATSKY, A. & RODRIGUEZ, J. J. 2010. Concomitant astroglial atrophy and astrogliosis in a triple transgenic animal model of Alzheimer's disease. *Glia,* 58, 831-8.

OLDENBORG, P. A., ZHELEZNYAK, A., FANG, Y. F., LAGENAUR, C. F., GRESHAM, H. D. & LINDBERG, F. P. 2000. Role of CD47 as a marker of self on red blood cells. *Science,* 288, 2051-4.

ORIGLIA, N., BONADONNA, C., ROSELLINI, A., LEZNIK, E., ARANCIO, O., YAN, S. S. & DOMENICI, L. 2010. Microglial receptor for advanced glycation end product-dependent signal pathway drives beta-amyloid-induced synaptic depression and long-term depression impairment in entorhinal cortex. *The Journal of neuroscience : the official journal of the Society for Neuroscience,* 30, 11414-25.

OSTENDORP, T., DIEZ, J., HEIZMANN, C. W. & FRITZ, G. 2011. The crystal structures of human S100B in the zinc- and calcium-loaded state at three pH values reveal zinc ligand swapping. *Biochimica et biophysica acta,* 1813, 1083-91.

OSTENDORP, T., HEIZMANN, C. W., KRONECK, P. M. & FRITZ, G. 2005. Purification, crystallization and preliminary X-ray diffraction studies on human Ca2+-binding protein S100B. *Acta crystallographica. Section F, Structural biology and crystallization communications,* 61, 673-5.

OSTENDORP, T., LECLERC, E., GALICHET, A., KOCH, M., DEMLING, N., WEIGLE, B., HEIZMANN, C. W., KRONECK, P. M. & FRITZ, G. 2007. Structural and functional insights into RAGE activation by multimeric S100B. *The EMBO journal,* 26, 3868-78.

OVANESOV, M. V., AYHAN, Y., WOLBERT, C., MOLDOVAN, K., SAUDER, C. & PLETNIKOV, M. V. 2008. Astrocytes play a key role in activation of microglia by persistent Borna disease virus infection. *Journal of neuroinflammation,* 5, 50.

PAIETTA, E., ANDERSEN, J., YUNIS, J., ROWE, J. M., CASSILETH, P. A., TALLMAN, M. S., BENNETT, J. M. & WIERNIK, P. H. 1998. Acute myeloid leukaemia expressing the leucocyte integrin CD11b-a new leukaemic syndrome with poor prognosis: result of an ECOG database analysis. Eastern Cooperative Oncology Group. *British journal of haematology,* 100, 265-72.

PALMER, A. M. 2011. Neuroprotective therapeutics for Alzheimer's disease: progress and prospects. *Trends in pharmacological sciences,* 32, 141-7.

PARADISI, S., SACCHETTI, B., BALDUZZI, M., GAUDI, S. & MALCHIODI-ALBEDI, F. 2004. Astrocyte modulation of in vitro beta-amyloid neurotoxicity. *Glia,* 46, 252-60.

PARK, H., ADSIT, F. G. & BOYINGTON, J. C. 2010. The 1.5 A crystal structure of human receptor for advanced glycation endproducts (RAGE) ectodomains reveals unique features determining ligand binding. *The Journal of biological chemistry,* 285, 40762-70.

PARK, H. & BOYINGTON, J. C. 2010. The 1.5 A crystal structure of human receptor for advanced glycation endproducts (RAGE) ectodomains reveals unique features determining ligand binding. *J Biol Chem,* 285, 40762-70.

PARK, I. H., YEON, S. I., YOUN, J. H., CHOI, J. E., SASAKI, N., CHOI, I. H. & SHIN, J. S. 2004. Expression of a novel secreted splice variant of the receptor for advanced glycation end products (RAGE) in human brain astrocytes and peripheral blood mononuclear cells. *Molecular immunology,* 40, 1203-11.

PARK, J., KWON, D., CHOI, C., OH, J. W. & BENVENISTE, E. N. 2003. Chloroquine induces activation of nuclear factor-kappaB and subsequent expression of pro-inflammatory cytokines by human astroglial cells. *Journal of neurochemistry,* 84, 1266-74.

PARK, L., WANG, G., ZHOU, P., ZHOU, J., PITSTICK, R., PREVITI, M. L., YOUNKIN, L., YOUNKIN, S. G., VAN NOSTRAND, W. E., CHO, S., ANRATHER, J., CARLSON, G. A. & IADECOLA, C. 2011. Scavenger receptor CD36 is essential for the cerebrovascular oxidative stress and neurovascular dysfunction induced by amyloid-beta. *Proceedings of the National Academy of Sciences of the United States of America,* 108, 5063-8.

PARK, M. H., LEE, Y. K., LEE, Y. H., KIM, Y. B., YUN, Y. W., NAM, S. Y., HWANG, S. J., HAN, S. B., KIM, S. U. & HONG, J. T. 2009. Chemokines released from astrocytes promote chemokine receptor 5-mediated neuronal cell differentiation. *Experimental cell research,* 315, 2715-26.

PARKHURST, C. N. & GAN, W. B. 2010. Microglia dynamics and function in the CNS. *Current opinion in neurobiology,* 20, 595-600.

PARSONS, M. S., BARRETT, L., LITTLE, C. & GRANT, M. D. 2008. Harnessing CD36 to rein in inflammation. *Endocrine, metabolic & immune disorders drug targets,* 8, 184-91.

PASPARAKIS, M. 2009. Regulation of tissue homeostasis by NF-kappaB signalling: implications for inflammatory diseases. *Nature reviews. Immunology,* 9, 778-88.

PEKNY, M. & PEKNA, M. 2004. Astrocyte intermediate filaments in CNS pathologies and regeneration. *The Journal of pathology,* 204, 428-37.

PELLICANO, M., BULATI, M., BUFFA, S., BARBAGALLO, M., DI PRIMA, A., MISIANO, G., PICONE, P., DI CARLO, M., NUZZO, D., CANDORE, G., VASTO, S., LIO, D., CARUSO, C. & COLONNA-ROMANO, G. 2010. Systemic immune responses in Alzheimer's disease: in vitro mononuclear cell activation and cytokine production. *Journal of Alzheimer's disease : JAD,* 21, 181-92.

PERLMUTTER, L. S., SCOTT, S. A., BARRON, E. & CHUI, H. C. 1992. MHC class II-positive microglia in human brain: association with Alzheimer lesions. *Journal of neuroscience research,* 33, 549-58.

PERSAUD-SAWIN, D. A., BANACH, L. & HARRY, G. J. 2009. Raft aggregation with specific receptor recruitment is required for microglial phagocytosis of Abeta42. *Glia,* 57, 320-35.

PHAM, C. G., BUBICI, C., ZAZZERONI, F., PAPA, S., JONES, J., ALVAREZ, K., JAYAWARDENA, S., DE SMAELE, E., CONG, R., BEAUMONT, C., TORTI, F. M., TORTI, S. V. & FRANZOSO, G. 2004. Ferritin heavy chain upregulation by NF-kappaB inhibits TNFalpha-induced apoptosis by suppressing reactive oxygen species. *Cell,* 119, 529-42.

PHILIPSON, O., LORD, A., GUMUCIO, A., O'CALLAGHAN, P., LANNFELT, L. & NILSSON, L. N. 2010. Animal models of amyloid-beta-related pathologies in Alzheimer's disease. *The FEBS journal,* 277, 1389-409.

PICONE, P., CARROTTA, R., MONTANA, G., NOBILE, M. R., SAN BIAGIO, P. L. & DI CARLO, M. 2009. Abeta oligomers and fibrillar aggregates induce different apoptotic pathways in LAN5 neuroblastoma cell cultures. *Biophysical journal,* 96, 4200-11.

PIHLAJA, R., KOISTINAHO, J., MALM, T., SIKKILA, H., VAINIO, S. & KOISTINAHO, M. 2008. Transplanted astrocytes internalize deposited beta-amyloid peptides in a transgenic mouse model of Alzheimer's disease. *Glia,* 56, 154-63.

PIKE, C. J., CUMMINGS, B. J. & COTMAN, C. W. 1995. Early association of reactive astrocytes with senile plaques in Alzheimer's disease. *Experimental neurology,* 132, 172-9.

PONATH, G., SCHETTLER, C., KAESTNER, F., VOIGT, B., WENTKER, D., AROLT, V. & ROTHERMUNDT, M. 2007. Autocrine S100B effects on astrocytes are mediated via RAGE. *Journal of neuroimmunology,* 184, 214-22.

PORCELLINI, E., DAVIS, E. J., CHIAPPELLI, M., IANNI, E., DI STEFANO, G., FORTI, P., RAVAGLIA, G. & LICASTRO, F. 2008. Elevated plasma levels of alpha-1-anti-chymotrypsin in age-related cognitive decline and Alzheimer's disease: a potential therapeutic target. *Current pharmaceutical design,* 14, 2659-64.

PRESTON, J. E. 2001. Ageing choroid plexus-cerebrospinal fluid system. *Microscopy research and technique,* 52, 31-7.

PROUDFOOT, A. E. 2002. Chemokine receptors: multifaceted therapeutic targets. *Nature reviews. Immunology,* 2, 106-15.

PULVERER, B. J., KYRIAKIS, J. M., AVRUCH, J., NIKOLAKAKI, E. & WOODGETT, J. R. 1991. Phosphorylation of c-jun mediated by MAP kinases. *Nature,* 353, 670-4.

QIN, H., WILSON, C. A., LEE, S. J., ZHAO, X. & BENVENISTE, E. N. 2005. LPS induces CD40 gene expression through the activation of NF-kappaB and STAT-1alpha in macrophages and microglia. *Blood,* 106, 3114-22.

QIU, W. Q. & FOLSTEIN, M. F. 2006. Insulin, insulin-degrading enzyme and amyloid-beta peptide in Alzheimer's disease: review and hypothesis. *Neurobiology of aging,* 27, 190-8.

QUERFURTH, H. W. & LAFERLA, F. M. 2010. Alzheimer's disease. *The New England journal of medicine,* 362, 329-44.

RADDASSI, K., KENT, S. C., YANG, J., BOURCIER, K., BRADSHAW, E. M., SEYFERT-MARGOLIS, V., NEPOM, G. T., KWOK, W. W. & HAFLER, D. A. 2011. Increased frequencies of myelin oligodendrocyte glycoprotein/MHC class II-binding CD4 cells in patients with multiple sclerosis. *Journal of immunology,* 187, 1039-46.

REINHOLD, M. I., LINDBERG, F. P., PLAS, D., REYNOLDS, S., PETERS, M. G. & BROWN, E. J. 1995. In vivo expression of alternatively spliced forms of integrin-associated protein (CD47). *Journal of cell science,* 108 (Pt 11), 3419-25.

REINKE, A. A. & GESTWICKI, J. E. 2011. Insight into amyloid structure using chemical probes. *Chemical biology & drug design,* 77, 399-411.

REITZ, C., HONIG, L., VONSATTEL, J. P., TANG, M. X. & MAYEUX, R. 2009. Memory performance is related to amyloid and tau pathology in the hippocampus. *Journal of neurology, neurosurgery, and psychiatry,* 80, 715-21.

RESTON, J. T., HU, X. L., MACINA, R. A., SPAIS, C. & RIETHMAN, H. C. 1995. Structure of the terminal 300 kb of DNA from human chromosome 21q. *Genomics,* 26, 31-8.

REYES, J. F., REYNOLDS, M. R., HOROWITZ, P. M., FU, Y., GUILLOZET-BONGAARTS, A. L., BERRY, R. & BINDER, L. I. 2008. A possible link between astrocyte activation and tau nitration in Alzheimer's disease. *Neurobiology of disease,* 31, 198-208.

REZAEI-GHALEH, N., GILLER, K., BECKER, S. & ZWECKSTETTER, M. 2011. Effect of Zinc Binding on beta-Amyloid Structure and Dynamics: Implications for Abeta Aggregation. *Biophysical journal,* 101, 1202-11.

RICCIARELLI, R., D'ABRAMO, C., ZINGG, J. M., GILIBERTO, L., MARKESBERY, W., AZZI, A., MARINARI, U. M., PRONZATO, M. A. & TABATON, M. 2004. CD36 overexpression in human brain correlates with beta-amyloid deposition but not with Alzheimer's disease. *Free radical biology & medicine,* 36, 1018-24.

RIDET, J. L., MALHOTRA, S. K., PRIVAT, A. & GAGE, F. H. 1997. Reactive astrocytes: cellular and molecular cues to biological function. *Trends in neurosciences,* 20, 570-7.

RIEK, R., GUNTERT, P., DOBELI, H., WIPF, B. & WUTHRICH, K. 2001. NMR studies in aqueous solution fail to identify significant conformational differences between the monomeric forms of two Alzheimer peptides with widely different plaque-competence, A beta(1-40)(ox) and A beta(1-42)(ox). *European journal of biochemistry / FEBS,* 268, 5930-6.

RODRIGUEZ-AYALA, E., ANDERSTAM, B., SULIMAN, M. E., SEEBERGER, A., HEIMBURGER, O., LINDHOLM, B. & STENVINKEL, P. 2005. Enhanced RAGE-mediated NFkappaB stimulation in inflamed hemodialysis patients. *Atherosclerosis,* 180, 333-40.

RODRIGUEZ-KERN, A., GEGELASHVILI, M., SCHOUSBOE, A., ZHANG, J., SUNG, L. & GEGELASHVILI, G. 2003. Beta-amyloid and brain-derived neurotrophic factor, BDNF, up-regulate the expression of glutamate transporter GLT-1/EAAT2 via different signaling pathways utilizing transcription factor NF-kappaB. *Neurochemistry international,* 43, 363-70.

RODRIGUEZ, J. J., OLABARRIA, M., CHVATAL, A. & VERKHRATSKY, A. 2009. Astroglia in dementia and Alzheimer's disease. *Cell death and differentiation,* 16, 378-85.

ROLTSCH, E., HOLCOMB, L., YOUNG, K. A., MARKS, A. & ZIMMER, D. B. 2010. PSAPP mice exhibit regionally selective reductions in gliosis and plaque deposition in response to S100B ablation. *Journal of neuroinflammation,* 7, 78.

ROPPER, A. H., ADAMS, R. D., VICTOR, M. & BROWN, R. H. 2005. *Adams and Victor's principles of neurology,* New York, McGraw-Hill, Medical Pub. Division.

ROSAS-BALLINA, M. & TRACEY, K. J. 2009. The neurology of the immune system: neural reflexes regulate immunity. *Neuron,* 64, 28-32.

ROSS, G. D. 2002. Role of the lectin domain of Mac-1/CR3 (CD11b/CD18) in regulating intercellular adhesion. *Immunologic research,* 25, 219-27.

ROSS, G. W., O'CALLAGHAN, J. P., SHARP, D. S., PETROVITCH, H., MILLER, D. B., ABBOTT, R. D., NELSON, J., LAUNER, L. J., FOLEY, D. J., BURCHFIEL, C. M., HARDMAN, J. & WHITE, L. R. 2003. Quantification of regional glial fibrillary acidic protein levels in Alzheimer's disease. *Acta neurologica Scandinavica,* 107, 318-23.

ROY, A., FUNG, Y. K., LIU, X. & PAHAN, K. 2006. Up-regulation of microglial CD11b expression by nitric oxide. *The Journal of biological chemistry,* 281, 14971-80.

ROY, A., JANA, A., YATISH, K., FREIDT, M. B., FUNG, Y. K., MARTINSON, J. A. & PAHAN, K. 2008. Reactive oxygen species up-regulate CD11b in microglia via nitric oxide: Implications for neurodegenerative diseases. *Free radical biology & medicine,* 45, 686-99.

RUAN, L., KANG, Z., PEI, G. & LE, Y. 2009. Amyloid deposition and inflammation in APPswe/PS1dE9 mouse model of Alzheimer's disease. *Current Alzheimer research,* 6, 531-40.

RUITENBERG, A., OTT, A., VAN SWIETEN, J. C., HOFMAN, A. & BRETELER, M. M. 2001. Incidence of dementia: does gender make a difference? *Neurobiology of aging,* 22, 575-80.

SAHIN, E. & DEPINHO, R. A. 2010. Linking functional decline of telomeres, mitochondria and stem cells during ageing. *Nature,* 464, 520-8.

SAIJO, K., WINNER, B., CARSON, C. T., COLLIER, J. G., BOYER, L., ROSENFELD, M. G., GAGE, F. H. & GLASS, C. K. 2009. A Nurr1/CoREST pathway in microglia and astrocytes protects dopaminergic neurons from inflammation-induced death. *Cell,* 137, 47-59.

SALINERO, O., MORENO-FLORES, M. T., CEBALLOS, M. L. & WANDOSELL, F. 1997. beta-Amyloid peptide induced cytoskeletal reorganization in cultured astrocytes. *Journal of neuroscience research,* 47, 216-23.

SANZ, J. M., CHIOZZI, P., FERRARI, D., COLAIANNA, M., IDZKO, M., FALZONI, S., FELLIN, R., TRABACE, L. & DI VIRGILIO, F. 2009. Activation of microglia by amyloid {beta} requires P2X7 receptor expression. *Journal of immunology,* 182, 4378-85.

SASAKI, N., TOKI, S., CHOWEI, H., SAITO, T., NAKANO, N., HAYASHI, Y., TAKEUCHI, M. & MAKITA, Z. 2001. Immunohistochemical distribution of the receptor for advanced glycation end products in neurons and astrocytes in Alzheimer's disease. *Brain research,* 888, 256-262.

SASTRE, M., KLOCKGETHER, T. & HENEKA, M. T. 2006. Contribution of inflammatory processes to Alzheimer's disease: molecular mechanisms. *International journal of developmental neuroscience : the official journal of the International Society for Developmental Neuroscience,* 24, 167-76.

SAURA, J. 2007. Microglial cells in astroglial cultures: a cautionary note. *Journal of neuroinflammation,* 4, 26.

SAURA, J., TUSELL, J. M. & SERRATOSA, J. 2003. High-yield isolation of murine microglia by mild trypsinization. *Glia,* 44, 183-9.

SAWAISHI, Y. 2009. Review of Alexander disease: beyond the classical concept of leukodystrophy. *Brain & development,* 31, 493-8.

SCHMID, C. D., MELCHIOR, B., MASEK, K., PUNTAMBEKAR, S. S., DANIELSON, P. E., LO, D. D., SUTCLIFFE, J. G. & CARSON, M. J. 2009. Differential gene expression in LPS/IFNgamma activated microglia and macrophages: in vitro versus in vivo. *Journal of neurochemistry,* 109 Suppl 1, 117-25.

SCHWANINGER, M., SALLMANN, S., PETERSEN, N., SCHNEIDER, A., PRINZ, S., LIBERMANN, T. A. & SPRANGER, M. 1999. Bradykinin induces interleukin-6 expression in astrocytes through activation of nuclear factor-kappaB. *Journal of neurochemistry,* 73, 1461-6.

SCHWEICKART, V. L., EPP, A., RAPORT, C. J. & GRAY, P. W. 2000. CCR11 is a functional receptor for the monocyte chemoattractant protein family of chemokines. *The Journal of biological chemistry,* 275, 9550-6.

SCOTTO, C., DELOULME, J. C., ROUSSEAU, D., CHAMBAZ, E. & BAUDIER, J. 1998. Calcium and S100B regulation of p53-dependent cell growth arrest and apoptosis. *Molecular and cellular biology,* 18, 4272-81.

SELINFREUND, R. H., BARGER, S. W., PLEDGER, W. J. & VAN ELDIK, L. J. 1991. Neurotrophic protein S100 beta stimulates glial cell proliferation. *Proceedings of the National Academy of Sciences of the United States of America,* 88, 3554-8.

SELKOE, D. J. 2001. Alzheimer's disease: genes, proteins, and therapy. *Physiological reviews,* 81, 741-66.

SELKOE, D. J. & WOLFE, M. S. 2007. Presenilin: running with scissors in the membrane. *Cell,* 131, 215-21.

SERGENT-TANGUY, S., VEZIERS, J., BONNAMAIN, V., BOUDIN, H., NEVEU, I. & NAVEILHAN, P. 2006. Cell surface antigens on rat neural progenitors and characterization of the CD3 (+)/CD3 (-) cell populations. *Differentiation; research in biological diversity,* 74, 530-41.

SETH, P. & KOUL, N. 2008. Astrocyte, the star avatar: redefined. *Journal of biosciences,* 33, 405-21.

SHAFFER, L. M., DORITY, M. D., GUPTA-BANSAL, R., FREDERICKSON, R. C., YOUNKIN, S. G. & BRUNDEN, K. R. 1995. Amyloid beta protein (A beta) removal by neuroglial cells in culture. *Neurobiology of aging,* 16, 737-45.

SHAH, S., LEE, S. F., TABUCHI, K., HAO, Y. H., YU, C., LAPLANT, Q., BALL, H., DANN, C. E., 3RD, SUDHOF, T. & YU, G. 2005. Nicastrin functions as a gamma-secretase-substrate receptor. *Cell,* 122, 435-47.

SHANKAR, G. M., LI, S., MEHTA, T. H., GARCIA-MUNOZ, A., SHEPARDSON, N. E., SMITH, I., BRETT, F. M., FARRELL, M. A., ROWAN, M. J., LEMERE, C. A., REGAN, C. M., WALSH, D. M., SABATINI, B. L. & SELKOE, D. J. 2008. Amyloid-beta protein dimers isolated directly from Alzheimer's brains impair synaptic plasticity and memory. *Nature medicine,* 14, 837-42.

SHAO, B., LI, C., YANG, H., SHEN, A., WU, X., YUAN, Q., KANG, L., LIU, Z., ZHANG, G., LU, X. & CHENG, C. 2011. The Relationship Between Src-Suppressed C Kinase Substrate and beta-1,4 Galactosyltransferase-I in the Process of Lipopolysaccharide-Induced TNF-alpha Secretion in Rat Primary Astrocytes. *Cellular and molecular neurobiology.*

SHEFFIELD, L. G. & BERMAN, N. E. 1998. Microglial expression of MHC class II increases in normal aging of nonhuman primates. *Neurobiology of aging,* 19, 47-55.

SHEIKINE, Y. & HANSSON, G. K. 2004. Chemokines and atherosclerosis. *Annals of medicine,* 36, 98-118.

SHENG, J. G., MRAK, R. E. & GRIFFIN, W. S. 1997. Glial-neuronal interactions in Alzheimer disease: progressive association of IL-1alpha+ microglia and S100beta+ astrocytes with neurofibrillary tangle stages. *Journal of neuropathology and experimental neurology,* 56, 285-90.

SHI, J. Q., CHEN, J., WANG, B. R., ZHU, Y. W., XU, Y., WANG, J., XIAO, H., SHI, J. P., ZHANG, Y. D. & XU, J. 2011. Short amyloid-beta immunogens show strong immunogenicity and avoid stimulating pro-inflammatory pathways in bone marrow-derived dendritic cells from C57BL/6J mice in vitro. *Peptides,* 32, 1617-25.

SICK, E., BOUKHARI, A., DERAMAUDT, T., RONDE, P., BUCHER, B., ANDRE, P., GIES, J. P. & TAKEDA, K. 2011. Activation of CD47 receptors causes proliferation of human astrocytoma but not normal astrocytes via an Akt-dependent pathway. *Glia,* 59, 308-19.

SILVERSTEIN, R. L. & FEBBRAIO, M. 2009. CD36, a scavenger receptor involved in immunity, metabolism, angiogenesis, and behavior. *Science signaling,* 2, re3.

SIMARD, M., ARCUINO, G., TAKANO, T., LIU, Q. S. & NEDERGAARD, M. 2003. Signaling at the gliovascular interface. *The Journal of neuroscience : the official journal of the Society for Neuroscience,* 23, 9254-62.

SIMS, J. E. & SMITH, D. E. 2010. The IL-1 family: regulators of immunity. *Nature reviews. Immunology,* 10, 89-102.

SMALE, S. T. 2010. Selective transcription in response to an inflammatory stimulus. *Cell,* 140, 833-44.

SMALL, D. H. & CAPPAI, R. 2006. Alois Alzheimer and Alzheimer's disease: a centennial perspective. *Journal of neurochemistry,* 99, 708-10.

SMITH, J. P., LAL, V., BOWSER, D., CAPPAI, R., MASTERS, C. L. & CICCOTOSTO, G. D. 2009. Stimulus pattern dependence of the Alzheimer's disease amyloid-beta 42 peptide's inhibition of long term potentiation in mouse hippocampal slices. *Brain research,* 1269, 176-84.

SNYDER, E. M., NONG, Y., ALMEIDA, C. G., PAUL, S., MORAN, T., CHOI, E. Y., NAIRN, A. C., SALTER, M. W., LOMBROSO, P. J., GOURAS, G. K. & GREENGARD, P. 2005. Regulation of NMDA receptor trafficking by amyloid-beta. *Nature neuroscience,* 8, 1051-8.

SOFRONIEW, M. V. & VINTERS, H. V. 2010. Astrocytes: biology and pathology. *Acta neuropathologica,* 119, 7-35.

SOKOLOV, Y., KOZAK, J. A., KAYED, R., CHANTURIYA, A., GLABE, C. & HALL, J. E. 2006. Soluble amyloid oligomers increase bilayer conductance by altering dielectric structure. *The Journal of general physiology,* 128, 637-47.

SOKOLOVA, A., HILL, M. D., RAHIMI, F., WARDEN, L. A., HALLIDAY, G. M. & SHEPHERD, C. E. 2009. Monocyte chemoattractant protein-1 plays a dominant role in the chronic inflammation observed in Alzheimer's disease. *Brain pathology,* 19, 392-8.

SOMJEN, G. G. 1988. Nervenkitt: notes on the history of the concept of neuroglia. *Glia,* 1, 2-9.

SONDAG, C. M., DHAWAN, G. & COMBS, C. K. 2009. Beta amyloid oligomers and fibrils stimulate differential activation of primary microglia. *Journal of neuroinflammation,* 6, 1.

SPECTOR, R. 2010. Nature and consequences of mammalian brain and CSF efflux transporters: four decades of progress. *Journal of neurochemistry,* 112, 13-23.

SPERLING, R. A., LAVIOLETTE, P. S., O'KEEFE, K., O'BRIEN, J., RENTZ, D. M., PIHLAJAMAKI, M., MARSHALL, G., HYMAN, B. T., SELKOE, D. J., HEDDEN, T., BUCKNER, R. L., BECKER, J. A. & JOHNSON, K. A. 2009. Amyloid deposition is associated with impaired default network function in older persons without dementia. *Neuron,* 63, 178-88.

SPRINGER, T. A. 1997. Folding of the N-terminal, ligand-binding region of integrin alpha-subunits into a beta-propeller domain. *Proceedings of the National Academy of Sciences of the United States of America,* 94, 65-72.

STANIMIROVIC, D., ZHANG, W., HOWLETT, C., LEMIEUX, P. & SMITH, C. 2001. Inflammatory gene transcription in human astrocytes exposed to hypoxia: roles of the nuclear factor-kappaB and autocrine stimulation. *Journal of neuroimmunology,* 119, 365-76.

STARK, A. K., PELVIG, D. P., JORGENSEN, A. M., ANDERSEN, B. B. & PAKKENBERG, B. 2005. Measuring morphological and cellular changes in Alzheimer's dementia: a review emphasizing stereology. *Current Alzheimer research*, 2, 449-81.

STARR, R., WILLSON, T. A., VINEY, E. M., MURRAY, L. J., RAYNER, J. R., JENKINS, B. J., GONDA, T. J., ALEXANDER, W. S., METCALF, D., NICOLA, N. A. & HILTON, D. J. 1997. A family of cytokine-inducible inhibitors of signalling. *Nature*, 387, 917-21.

STEINER, J., BERNSTEIN, H. G., BIELAU, H., BERNDT, A., BRISCH, R., MAWRIN, C., KEILHOFF, G. & BOGERTS, B. 2007. Evidence for a wide extra-astrocytic distribution of S100B in human brain. *BMC neuroscience*, 8, 2.

STERN, L. J., BROWN, J. H., JARDETZKY, T. S., GORGA, J. C., URBAN, R. G., STROMINGER, J. L. & WILEY, D. C. 1994. Crystal structure of the human class II MHC protein HLA-DR1 complexed with an influenza virus peptide. *Nature*, 368, 215-21.

STEWART, C. R., STUART, L. M., WILKINSON, K., VAN GILS, J. M., DENG, J., HALLE, A., RAYNER, K. J., BOYER, L., ZHONG, R., FRAZIER, W. A., LACY-HULBERT, A., EL KHOURY, J., GOLENBOCK, D. T. & MOORE, K. J. 2010. CD36 ligands promote sterile inflammation through assembly of a Toll-like receptor 4 and 6 heterodimer. *Nature immunology*, 11, 155-61.

STIVAROS, S. M. & JACKSON, A. 2007. Changing concepts of cerebrospinal fluid hydrodynamics: role of phase-contrast magnetic resonance imaging and implications for cerebral microvascular disease. *Neurotherapeutics : the journal of the American Society for Experimental NeuroTherapeutics*, 4, 511-22.

STREIT, W. J., BRAAK, H., XUE, Q. S. & BECHMANN, I. 2009. Dystrophic (senescent) rather than activated microglial cells are associated with tau pathology and likely precede neurodegeneration in Alzheimer's disease. *Acta neuropathologica*, 118, 475-85.

STREIT, W. J., CONDE, J. R. & HARRISON, J. K. 2001. Chemokines and Alzheimer's disease. *Neurobiology of aging*, 22, 909-13.

STREIT, W. J. & XUE, Q.-S. 2010. The Brain's Aging Immune System. *Aging and disease*, 1, 254-261.

STRITTMATTER, W. J. & ROSES, A. D. 1996. Apolipoprotein E and Alzheimer's disease. *Annual review of neuroscience*, 19, 53-77.

SUGAMA, S., TAKENOUCHI, T., FUJITA, M., CONTI, B. & HASHIMOTO, M. 2009. Differential microglial activation between acute stress and lipopolysaccharide treatment. *Journal of neuroimmunology*, 207, 24-31.

SUTTON, C., BRERETON, C., KEOGH, B., MILLS, K. H. & LAVELLE, E. C. 2006. A crucial role for interleukin (IL)-1 in the induction of IL-17-producing T cells that mediate autoimmune encephalomyelitis. *The Journal of experimental medicine*, 203, 1685-91.

SUZUMURA, A., TAKEUCHI, H., ZHANG, G., KUNO, R. & MIZUNO, T. 2006. Roles of glia-derived cytokines on neuronal degeneration and regeneration. *Annals of the New York Academy of Sciences*, 1088, 219-29.

SWARDFAGER, W., LANCTOT, K., ROTHENBURG, L., WONG, A., CAPPELL, J. & HERRMANN, N. 2010. A meta-analysis of cytokines in Alzheimer's disease. *Biological psychiatry,* 68, 930-41.

SZAINGURTEN-SOLODKIN, I., HADAD, N. & LEVY, R. 2009. Regulatory role of cytosolic phospholipase A2alpha in NADPH oxidase activity and in inducible nitric oxide synthase induction by aggregated Abeta1-42 in microglia. *Glia,* 57, 1727-40.

SZMYDYNGER-CHODOBSKA, J., FOX, L. M., LYNCH, K. M., ZINK, B. J. & CHODOBSKI, A. 2010. Vasopressin amplifies the production of proinflammatory mediators in traumatic brain injury. *Journal of neurotrauma,* 27, 1449-61.

TAFT, J. R., VERTES, R. P. & PERRY, G. W. 2005. Distribution of GFAP+ astrocytes in adult and neonatal rat brain. *The International journal of neuroscience,* 115, 1333-43.

TANAKA, H., KATOH, A., OGURO, K., SHIMAZAKI, K., GOMI, H., ITOHARA, S., MASUZAWA, T. & KAWAI, N. 2002. Disturbance of hippocampal long-term potentiation after transient ischemia in GFAP deficient mice. *Journal of neuroscience research,* 67, 11-20.

TANSEY, M. G. & GOLDBERG, M. S. 2010. Neuroinflammation in Parkinson's disease: its role in neuronal death and implications for therapeutic intervention. *Neurobiology of disease,* 37, 510-8.

TANUMA, N., SAKUMA, H., SASAKI, A. & MATSUMOTO, Y. 2006. Chemokine expression by astrocytes plays a role in microglia/macrophage activation and subsequent neurodegeneration in secondary progressive multiple sclerosis. *Acta neuropathologica,* 112, 195-204.

TERAI, K., MATSUO, A. & MCGEER, P. L. 1996. Enhancement of immunoreactivity for NF-kappa B in the hippocampal formation and cerebral cortex of Alzheimer's disease. *Brain research,* 735, 159-68.

TERWEL, D., STEFFENSEN, K. R., VERGHESE, P. B., KUMMER, M. P., GUSTAFSSON, J. A., HOLTZMAN, D. M. & HENEKA, M. T. 2011. Critical role of astroglial apolipoprotein E and liver X receptor-alpha expression for microglial Abeta phagocytosis. *The Journal of neuroscience : the official journal of the Society for Neuroscience,* 31, 7049-59.

THAL, D. R., SCHULTZ, C., DEHGHANI, F., YAMAGUCHI, H., BRAAK, H. & BRAAK, E. 2000. Amyloid beta-protein (Abeta)-containing astrocytes are located preferentially near N-terminal-truncated Abeta deposits in the human entorhinal cortex. *Acta neuropathologica,* 100, 608-17.

THOMPSON, P. M., HAYASHI, K. M., DE ZUBICARAY, G., JANKE, A. L., ROSE, S. E., SEMPLE, J., HERMAN, D., HONG, M. S., DITTMER, S. S., DODDRELL, D. M. & TOGA, A. W. 2003. Dynamics of gray matter loss in Alzheimer's disease. *The Journal of neuroscience : the official journal of the Society for Neuroscience,* 23, 994-1005.

THOMPSON, W. L. & VAN ELDIK, L. J. 2009. Inflammatory cytokines stimulate the chemokines CCL2/MCP-1 and CCL7/MCP-3 through NFkB and MAPK dependent pathways in rat astrocytes [corrected]. *Brain research,* 1287, 47-57.

THORNE, R. F., LAW, E. G., ELITH, C. A., RALSTON, K. J., BATES, R. C. & BURNS, G. F. 2006. The association between CD36 and Lyn protein tyrosine kinase is mediated by lipid. *Biochemical and biophysical research communications,* 351, 51-6.

TONTONOZ, P., NAGY, L., ALVAREZ, J. G., THOMAZY, V. A. & EVANS, R. M. 1998. PPARgamma promotes monocyte/macrophage differentiation and uptake of oxidized LDL. *Cell,* 93, 241-52.

TRACEY, K. J. 2007. Physiology and immunology of the cholinergic antiinflammatory pathway. *The Journal of clinical investigation,* 117, 289-96.

TRIPATHY, D., THIRUMANGALAKUDI, L. & GRAMMAS, P. 2010. RANTES upregulation in the Alzheimer's disease brain: a possible neuroprotective role. *Neurobiology of aging,* 31, 8-16.

TSAI, J., GRUTZENDLER, J., DUFF, K. & GAN, W. B. 2004. Fibrillar amyloid deposition leads to local synaptic abnormalities and breakage of neuronal branches. *Nature neuroscience,* 7, 1181-3.

TSYBOVSKY, Y. & KRUPENKO, S. A. 2011. Conserved catalytic residues of the ALDH1L1 aldehyde dehydrogenase domain control binding and discharging of the coenzyme. *The Journal of biological chemistry,* 286, 23357-67.

VALLABHAPURAPU, S. & KARIN, M. 2009. Regulation and function of NF-kappaB transcription factors in the immune system. *Annual review of immunology,* 27, 693-733.

VALLERIE, S. N. & HOTAMISLIGIL, G. S. 2010. The role of JNK proteins in metabolism. *Science translational medicine,* 2, 60rv5.

VAN BEEK, E. M., COCHRANE, F., BARCLAY, A. N. & VAN DEN BERG, T. K. 2005. Signal regulatory proteins in the immune system. *Journal of immunology,* 175, 7781-7.

VAN WAGONER, N. J. & BENVENISTE, E. N. 1999. Interleukin-6 expression and regulation in astrocytes. *Journal of neuroimmunology,* 100, 124-39.

VERDIER, Y., ZARANDI, M. & PENKE, B. 2004. Amyloid beta-peptide interactions with neuronal and glial cell plasma membrane: binding sites and implications for Alzheimer's disease. *Journal of peptide science : an official publication of the European Peptide Society,* 10, 229-48.

VERJAN GARCIA, N., UMEMOTO, E., SAITO, Y., YAMASAKI, M., HATA, E., MATOZAKI, T., MURAKAMI, M., JUNG, Y. J., WOO, S. Y., SEOH, J. Y., JANG, M. H., AOZASA, K. & MIYASAKA, M. 2011. SIRP{alpha}/CD172a Regulates Eosinophil Homeostasis. *Journal of immunology,* 187, 2268-77.

VIDYADARAN, S., OOI, Y. Y., SUBRAMAIAM, H., BADIEI, A., ABDULLAH, M., RAMASAMY, R. & SEOW, H. F. 2009. Effects of macrophage colony-stimulating factor on microglial responses to lipopolysaccharide and beta amyloid. *Cellular immunology,* 259, 105-10.

VIVES, V., ALONSO, G., SOLAL, A. C., JOUBERT, D. & LEGRAVEREND, C. 2003. Visualization of S100B-positive neurons and glia in the central nervous system of EGFP transgenic mice. *The Journal of comparative neurology,* 457, 404-19.

VOGEL, W., GRUNEBACH, F., MESSAM, C. A., KANZ, L., BRUGGER, W. & BUHRING, H. J. 2003. Heterogeneity among human bone marrow-derived mesenchymal stem cells and neural progenitor cells. *Haematologica,* 88, 126-33.

VOLTERRA, A. & MELDOLESI, J. 2005. Astrocytes, from brain glue to communication elements: the revolution continues. *Nature reviews. Neuroscience,* 6, 626-40.

WALSH, D. M., KLYUBIN, I., FADEEVA, J. V., CULLEN, W. K., ANWYL, R., WOLFE, M. S., ROWAN, M. J. & SELKOE, D. J. 2002. Naturally secreted oligomers of amyloid beta protein potently inhibit hippocampal long-term potentiation in vivo. *Nature,* 416, 535-9.

WALSH, D. M. & SELKOE, D. J. 2007. A beta oligomers - a decade of discovery. *Journal of neurochemistry,* 101, 1172-84.

WALZ, W. & LANG, M. K. 1998. Immunocytochemical evidence for a distinct GFAP-negative subpopulation of astrocytes in the adult rat hippocampus. *Neuroscience letters,* 257, 127-30.

WANG, C. Y., MAYO, M. W., KORNELUK, R. G., GOEDDEL, D. V. & BALDWIN, A. S., JR. 1998. NF-kappaB antiapoptosis: induction of TRAF1 and TRAF2 and c-IAP1 and c-IAP2 to suppress caspase-8 activation. *Science,* 281, 1680-3.

WANG, D. & HAZELL, A. S. 2010. Microglial activation is a major contributor to neurologic dysfunction in thiamine deficiency. *Biochemical and biophysical research communications,* 402, 123-8.

WANG, D. D. & BORDEY, A. 2008. The astrocyte odyssey. *Progress in neurobiology,* 86, 342-67.

WANG, H. W., PASTERNAK, J. F., KUO, H., RISTIC, H., LAMBERT, M. P., CHROMY, B., VIOLA, K. L., KLEIN, W. L., STINE, W. B., KRAFFT, G. A. & TROMMER, B. L. 2002. Soluble oligomers of beta amyloid (1-42) inhibit long-term potentiation but not long-term depression in rat dentate gyrus. *Brain research,* 924, 133-40.

WANG, H. Y., LEE, D. H., D'ANDREA, M. R., PETERSON, P. A., SHANK, R. P. & REITZ, A. B. 2000. beta-Amyloid(1-42) binds to alpha7 nicotinic acetylcholine receptor with high affinity. Implications for Alzheimer's disease pathology. *The Journal of biological chemistry,* 275, 5626-32.

WANG, X., WATSON, C., SHARP, J. S., HANDEL, T. M. & PRESTEGARD, J. H. 2011a. Oligomeric structure of the chemokine CCL5/RANTES from NMR, MS, and SAXS data. *Structure,* 19, 1138-48.

WANG, Y., LI, M., TANG, J., SONG, M., XU, X., XIONG, J., LI, J. & BAI, Y. 2011b. Glucocorticoids facilitate astrocytic amyloid-beta peptide deposition by increasing the expression of APP and BACE1 and decreasing the expression of amyloid-beta-degrading proteases. *Endocrinology,* 152, 2704-15.

WEN, L. L., CHIU, C. T., HUANG, Y. N., CHANG, C. F. & WANG, J. Y. 2007. Rapid glia expression and release of proinflammatory cytokines in experimental Klebsiella pneumoniae meningoencephalitis. *Experimental neurology,* 205, 270-8.

WESTON, C. R. & DAVIS, R. J. 2002. The JNK signal transduction pathway. *Current opinion in genetics & development,* 12, 14-21.

WHITE, J. A., MANELLI, A. M., HOLMBERG, K. H., VAN ELDIK, L. J. & LADU, M. J. 2005. Differential effects of oligomeric and fibrillar amyloid-beta 1-42 on astrocyte-mediated inflammation. *Neurobiology of disease,* 18, 459-65.

WILCOCK, D. M., GORDON, M. N. & MORGAN, D. 2006. Quantification of cerebral amyloid angiopathy and parenchymal amyloid plaques with Congo red histochemical stain. *Nature protocols,* 1, 1591-5.

WILHELMUS, M. M., OTTE-HOLLER, I., VAN TRIEL, J. J., VEERHUIS, R., MAAT-SCHIEMAN, M. L., BU, G., DE WAAL, R. M. & VERBEEK, M. M. 2007. Lipoprotein receptor-related protein-1 mediates amyloid-beta-mediated cell death of cerebrovascular cells. *The American journal of pathology,* 171, 1989-99.

WILKINSON, J., RADKOWSKI, M., ESCHBACHER, J. M. & LASKUS, T. 2010. Activation of brain macrophages/microglia cells in hepatitis C infection. *Gut,* 59, 1394-400.

WILKINSON, K., BOYD, J. D., GLICKSMAN, M., MOORE, K. J. & EL KHOURY, J. 2011. A high-content drug screen identifies ursolic acid as an inhibitor of amyloid-{beta} interactions with its receptor CD36. *The Journal of biological chemistry.*

WIMO, A. & PRINCE, M. 2010. World Alzheimer Report 2010. The global economic impact of dementia: Alzheimer's Disease International. Alzheimer's Disease International.

WIRAK, D. O., BAYNEY, R., RAMABHADRAN, T. V., FRACASSO, R. P., HART, J. T., HAUER, P. E., HSIAU, P., PEKAR, S. K., SCANGOS, G. A., TRAPP, B. D. & ET AL. 1991. Deposits of amyloid beta protein in the central nervous system of transgenic mice. *Science,* 253, 323-5.

WIRENFELDT, M., BABCOCK, A. A. & VINTERS, H. V. 2011. Microglia - insights into immune system structure, function, and reactivity in the central nervous system. *Histology and histopathology,* 26, 519-30.

WIRTHS, O., BREYHAN, H., MARCELLO, A., COTEL, M. C., BRUCK, W. & BAYER, T. A. 2010. Inflammatory changes are tightly associated with neurodegeneration in the brain and spinal cord of the APP/PS1KI mouse model of Alzheimer's disease. *Neurobiology of aging,* 31, 747-57.

WONG, A. M., PATEL, N. V., PATEL, N. K., WEI, M., MORGAN, T. E., DE BEER, M. C., DE VILLIERS, W. J. & FINCH, C. E. 2005. Macrosialin increases during normal brain aging are attenuated by caloric restriction. *Neuroscience letters,* 390, 76-80.

WU, J., ANWYL, R. & ROWAN, M. J. 1995. beta-Amyloid-(1-40) increases long-term potentiation in rat hippocampus in vitro. *European journal of pharmacology,* 284, R1-3.

WYSS-CORAY, T., LOIKE, J. D., BRIONNE, T. C., LU, E., ANANKOV, R., YAN, F., SILVERSTEIN, S. C. & HUSEMANN, J. 2003. Adult mouse astrocytes degrade amyloid-beta in vitro and in situ. *Nature medicine,* 9, 453-7.

WYSS, J. M., CHAMBLESS, B. D., KADISH, I. & VAN GROEN, T. 2000. Age-related decline in water maze learning and memory in rats: strain differences. *Neurobiology of aging,* 21, 671-81.

XANTHIS, A., HATZITOLIOS, A., FIDANI, S., BEFANI, C., GIANNAKOULAS, G. & KOLIAKOS, G. 2009. Receptor of advanced glycation end products (RAGE) positively regulates CD36 expression and reactive oxygen species production in human monocytes in diabetes. *Angiology,* 60, 772-9.

Solutions

Complete Lysis Buffer (pH 9.5)

Tris-HCl	10mM
NaCl	50mM
$Na_4P_2O_7\cdot10H_2O$	10mM
NaF	50mM
IGEPAL	1%
Na_3VO_4	1mM
PMSF	1mM
PIC	1/1000 dilution

Krebs buffer with CaCl₂ (pH 7.5)

NaCl	136mM
KCl	2.54mM
KH_2PO_4	1.18mM
Mg_2SO_4	1.18mM
$NaHCO_3$	16mM
Glucose	10mM
$CaCl_2$	1.13mM

Phosphate buffered saline (pH 7.5)

NaCl	137mM
KCl	2.7mM
Na_2HPO_4	8.1mM
KH_2PO_4	1.5mM

PHEM buffer (pH 6.9)

PIPES	60mM
HEPES	25mM
EDTA	10mM
$MgCl_2$	2mM

Artificial CSF

NaCl	296mM
K	3mM
Ca	1.4mM
Mg	0.8mM
P	1mM

TBS-T (pH 7.4)

Tris-HCl	20mM
NaCl	150mM
Tween-20	0.05%

Tris-glycine sample buffer (pH 6.8)

Tris-HCl	0.03125M
Glycerol	12.5%
SDS	1%
β-mercaptoethanol	2.5%
Bromophenol blue powder	

Gel buffer + SDS (SPA; pH 8.8)

Tris base	1.5M
SDS	0.2%

Stacking buffer (pH 6.8)

Tris base	0.5M
SDS	0.4%
Bromophenol blue powder	

10x Electrode running buffer

Tris base	25mM
Glycine	192mM
SDS	0.1%

10x Transfer buffer (pH 8.3)

Tris base	25mM
Glycine	192mM
Methanol	20%